
Electronic Thesis and Dissertation Repository

7-29-2015 12:00 AM

Strategies for Photochemical and Thermal Modification of Materials

Sara Ghiassian
The University of Western Ontario

Supervisor
Prof. Mark S. Workentin
The University of Western Ontario

Graduate Program in Chemistry
A thesis submitted in partial fulfillment of the requirements for the degree in Doctor of Philosophy
© Sara Ghiassian 2015

Follow this and additional works at: <https://ir.lib.uwo.ca/etd>

 Part of the [Materials Chemistry Commons](#), and the [Organic Chemistry Commons](#)

Recommended Citation

Ghiassian, Sara, "Strategies for Photochemical and Thermal Modification of Materials" (2015). *Electronic Thesis and Dissertation Repository*. 3009.
<https://ir.lib.uwo.ca/etd/3009>

This Dissertation/Thesis is brought to you for free and open access by Scholarship@Western. It has been accepted for inclusion in Electronic Thesis and Dissertation Repository by an authorized administrator of Scholarship@Western. For more information, please contact wlsadmin@uwo.ca.

STRATEGIES FOR PHOTOCHEMICAL AND THERMAL
MODIFICATION OF MATERIALS

(Thesis format: Integrated Article)

by

Sara Ghiassian

Graduate Program in Chemistry

A thesis submitted in partial fulfillment
of the requirements for the degree of
Doctor of Philosophy

The School of Graduate and Postdoctoral Studies
The University of Western Ontario
London, Ontario, Canada

© Sara Ghiassian 2015

Abstract

The modification of materials/surfaces is central to numerous applications ranging from opto-electronic devices to biomedical implants and drug delivery. Thus, there exists a high motivation for improving the methodologies which can be employed in order to modify surfaces in a selective and efficient fashion. One of the major goals of surface engineering is to control the chemical composition at the material interface. The fine control of the surface properties is a field of intense research as the performance of functional materials is strongly related to the processes and interactions that are occurring at the materials' interface.

In general, the modification or transformation of surfaces can be achieved via various chemical and physical methods. Although there is a general need for simple and convenient methods to covalently conjugate a molecule of interest to a surface, no single coupling strategy has been broadly adopted. Instead, numerous strategies have been reported in the literature. In an attempt to develop novel strategies to prepare functional materials via surface modifications we examined the potential of a series of photochemical and thermal reactions for such purposes. Methods described in this thesis are divided into two categories: Photochemical and Thermal. In the first chapter, these strategies are introduced. Since many of the modification methods deal with gold nanoparticles (AuNPs), a review of their properties and synthesis methods are also included. Two chapters (chapter 2 and 3) are devoted to the potential of diazirine for photochemical modification of materials and nanomaterials. In chapter 2, diazirine is employed to prepare robust hydrophobic cotton and paper surfaces by coating them with

a highly fluorinated phosphonium salt using diazirine as the tether. In chapter 3, the same photochemical modification strategy is extended to nanomaterials by incorporating diazirine onto the surface of water soluble AuNPs. The synthesis and characterization of diazirine-AuNPs is described and it is demonstrated that upon irradiation, the photo generated carbene can be used for the insertion reaction which leads to interfacially modified AuNPs.

Starting with chapter 4, we focus on “click-type” and more biologically friendly reactions for surface modification of water soluble AuNPs. Chapter 4 reports our efforts towards modification of small water soluble AuNPs using maleimide interfacial functionality. Both 1,3-dipolar cycloaddition and Diels Alder reactions are studied. In chapter 5, a novel strategy for modification of AuNPs via strain-promoted alkyne-nitrone cycloaddition (SPANC) is introduced. Nitrone functionalized AuNPs are synthesized and characterized. It is demonstrated in this chapter that one can take advantage of the nitrone moiety for interfacial SPANC (i-SPANC) reaction to prepare ^{18}F -radiolabeled AuNPs with potential applications in positron emission tomography (PET). In the second part of chapter 5, the i-SPANC method is further extended to material chemistry by preparing AuNP-carbon nanotube (AuNP-CNT) hybrid nanomaterials.

Keywords: Surface modification, Gold nanoparticles, Photochemistry, Diazirine, Click-type reactions, Diels Alder, 1,3-Dipolar cycloaddition, Strain-promoted alkyne-nitrone Cycloaddition.

Acknowledgments

I would like to express my gratitude to my supervisor, Dr. Mark S. Workentin, for his support, patience and supervision during the past five years. I thank him for challenging me and providing me with opportunities that have made my graduate school experience very rewarding.

I am grateful to all of my colleagues within the Workentin group for their help and support. I would also like to thank our collaborators Professors Ragogna, Luyt, and Gillies. Special thanks goes to Dr. Ali Nazemi for the opportunity to work on a great project during the last year of my PhD by introducing me to the concept of alkyne-nitrone cycloadditions. Many thanks to all the staff at UWO without whom this thesis would not have been possible; in particular I would like to thank Mathew Willans, Mark Biesinger, and Dr. Richard Gardiner.

I am thankful to my thesis examiners Professors Wisner, Ding, Flynn, and Leigh for taking the time out of their busy schedules and reading through my thesis.

I am deeply grateful to my father, mother, and brother for all their encouragement, support, and unconditional love throughout my life. Thanks for believing in me and my abilities. I am the person I am today because of your love and motivation.

Finally I thank my best friend and my husband, Siavash, who is last in my acknowledgements, but first in my life. You are always there for me, to talk about science or anything else. It just would not have been the same without you.

Table of Contents

Abstract	ii
Acknowledgments.....	iv
Table of Contents	v
List of Tables	viii
List of Figures	ix
List of Figures for Supporting Information	xiii
List of Schemes.....	xvii
List of Abbreviations	xx
Chapter 1: Introduction.....	1
1.1 Material Surface Modification.....	1
1.2 Robust and Efficient Methods for Material Surface Modification	4
1.2.1 Photochemical Reactions	4
1.2.2 Thermal Reactions	8
1.3 Gold Nanoparticles (AuNPs).....	29
1.3.1 AuNPs and their properties.....	29
1.3.2 Synthesis of AuNPs	31
1.3.3 Approaches towards Preparation of Functionalized AuNPs.....	35
1.3.4 Photochemical and Thermal Interfacial Reactions on the Surface of AuNPs.....	38
1.3.5 Characterization of AuNPs	42
1.4 Thesis objectives.....	46
1.5 References.....	51

Chapter 2: Photoinduced Carbene Generation from Diazirine Modified Task Specific Phosphonium Salts to Prepare Robust Hydrophobic Coatings	67
2.1 Introduction.....	68
2.2 Results and Discussion	71
2.3 Conclusion	85
2.4 Experimental.....	86
2.5 References.....	96
2.6 Supporting Information.....	100
Chapter 3: Synthesis of Small Water-Soluble Diazirine-Functionalized Gold Nanoparticles and Their Photochemical Modification	103
3.1 Introduction.....	104
3.2 Results and Discussion	108
3.3 Conclusion	122
3.4 Experimental.....	123
3.5 References.....	129
3.6 Supporting Information.....	132
Chapter 4: Water Soluble Maleimide Modified Gold Nanoparticles (AuNPs) as a Platform for Cycloaddition Reactions	140
4.1 Introduction.....	141
4.2 Results and Discussion	145
4.3 Conclusion	162
4.4 Experimental.....	163
4.5 References.....	170
4.6 Supporting Information.....	173

Chapter 5: Nitron Modified Gold Nanoparticles: Synthesis, Characterization and Their Potential for the Development of ¹⁸F-Labeled PET Probes and Hybrid Nanomaterials	181
5.1 Introduction.....	182
5.2 Results and Discussion	187
5.3 Conclusion	209
5.4 Experimental.....	211
5.5 References.....	230
5.6 Supporting Information.....	236
Chapter 6: Contributions of the Studies	250
Appendix-List of Permissions.....	259
CurriculumVitae	296

List of Tables

Table 4.1. Time for completion of 1,3-dipolar cycloaddition reactions of Mal-EG ₄ -AuNPs and model compound 3 with nitrones A-E under ambient pressure and at 37 °C.	151
Table 4.2. Time for completion of Diels Alder reactions of Mal-EG ₄ -AuNPs and model compound 3 with dienes F-J under ambient pressure and at 37 °C.	157

List of Figures

Figure 1.1. A water droplet on a superhydrophobic silver surface coated with highly fluorinated phosphonium salt.....	3
Figure 1.2. Orbital correlation diagram illustrating the distinction between normal electron demand (left side) and inverse electron demand (right side) Diels-Alder reactions.....	12
Figure 1.3. Structures of <i>endo</i> and <i>exo</i> Diels-Alder products from reacting furan and a modified maleimide molecule.....	13
Figure 1.4. Strategy for the immobilization of ligands to SAMs via Diels–Alder cycloaddition. Cells attached to the patterned regions modified with RGD is shown on the right.....	14
Figure 1.5. A) Allyl anion type and B) Propargyl/Allenyl anion type 1,3-dipoles.....	17
Figure 1.6. Classification of 1,3-dipoles consisting of carbon, nitrogen, and oxygen centers.	18
Figure 1.7. The HOMO-LUMO interaction between 1,3-dipole (a-b-c) and dipolarophile (e-f) depends on the orbital energies of the 1,3-dipole: _____ strong and - - - weak interactions.....	20
Figure 1.8. Examples of cyclootyne derivatives investigated for strain-promoted cycloadditions.	26
Figure 1.9. A) Cartoon representation of a thiolate-stabilized AuNP, B) High-resolution transmission electron microscopy (HRTEM) image of an individual thiolate-protected gold particle..	30

Figure 1.10. ^1H NMR spectra of A) diazirine functionalized AuNPs and B) diazirine-EG ₃ -SH.	44
Figure 2.1. Variation in water contact angles as a function of irradiation time of 5 mg/ml samples (square, top scale) and as a function of the HFPS [I] concentration on both cotton (inverted triangle, bottom scale) and paper (circle, bottom scale).....	77
Figure 2.2. Pictures of colored water droplets (colored to aid visualization) placed on standard printer paper samples (left column) and cotton (right column): A and E untreated, B and F treated-dark sample (no irradiation), and C and G treated with HFPS and irradiated. D (paper) and H (cotton) are representative pictures of water contact angle measurements.....	80
Figure 2.3. XPS spectra of: treated, treated with no light (dark treated) and untreated cotton (left) and paper (right) with HFPS.	81
Figure 2.4. Change in the water contact angle (WCA) as a function of simulated wash cycles on treated cotton sample treated with HFPS [I], irradiated and washed.....	83
Figure 2.5. Cartoon of the macro-patterning and a photograph of the paper surface after patterning. Spot on the left, indicated by the penciled circle is where the mask let light through. The spot on the right is where the mask was dark.....	85
Figure 3.1. A: ^1H NMR spectrum of the Me-EG ₃ -AuNPs; B and D: ^1H and ^{19}F NMR spectra of the Diaz-EG ₄ -AuNP (recorded in D ₂ O). C and E: ^1H and ^{19}F NMR spectra of the Diaz-EG ₄ -SH (recorded in CDCl ₃)..	111
Figure 3.2. TGA graphs of Me-EG ₃ -AuNP (dashed line) and Diaz-EG ₄ -AuNP (solid line): Mass loss curves (left) and the first derivative of the mass loss curves (right).....	113
Figure 3.3. High resolution XPS spectra of Me-EG ₃ -AuNP and Diaz-EG ₄ -AuNP.....	115

Figure 3.4. ^{19}F NMR spectrum of Diaz-EG ₄ -AuNPs in methanol during photolysis at different times A) t = 0 B) t = 90 mins C) t = 12 h.	117
Figure 3.5. Cartoon representation of Diaz-EG ₄ -AuNP (A) and its carbene insertion products(left) and their ^{19}F NMR spectra (right): B) Methanol; C) Ethyl vinyl ether and D) Acetic acid.	119
Figure 3.6. Cartoon representation of photolysis of Diaz-EG ₄ -AuNP in the presence of mannose and the formation of the desired insertion product (right) and ^{19}F NMR spectra of the reaction products in different concentrations (left).	121
Figure 3.7. TEM images of A) Me-EG ₃ -AuNP B) Diaz-EG ₄ -AuNP and the insertion products of Diaz-EG ₄ -AuNP with C) Methanol D) Acetic Acid E) Ethyl vinyl ether. ..	122
Figure 4.1. Schematic representation of the synthetic approach towards preparation of Mal-EG ₄ -AuNPs and the ^1H NMR spectra of: A) Me-EG ₃ -AuNPs, B) FP-Mal-EG ₄ -AuNPs, and C) Mal-EG ₄ -AuNPs.....	148
Figure 4.2. ^1H NMR spectra in 5-9 ppm region for the reaction of compound 3 and nitrene D at different time intervals.....	153
Figure 4.3. Representative ^1H NMR spectra of: A) Mal-EG ₄ -AuNPs and products from 1,3-dipolar cycloaddition reaction of Mal-EG ₄ -AuNPs with nitrene D to yield B) 2D-AuNP as a mixture of diastereomers and compound 3 with nitrene D to yield C) 4D-exo and D) 4D-endo respectively..	155
Figure 4.4. ^1H NMR spectra for the reaction of compound 3 and diene H at different time intervals.....	159
Figure 4.5. Representative ^1H NMR spectra of products from Diels Alder reaction of: A) Mal-EG ₄ -AuNP with 2,3-dimethyl 1,3-butadiene to yield B) 3H-AuNP and 3 with 2,3-dimethyl 1,3-butadiene to yield C) 5H..	160

Figure 4.6. TEM images of A) FP-Ma-EG ₄ -AuNPs B) Mal-EG ₄ -AuNPs C) 2D-AuNPs D) 3H-AuNPs.....	161
Figure 5.1. ¹ H NMR spectra of A) Me-EG ₃ -AuNPs and B) Nitron-AuNPs in D ₂ O.....	189
Figure 5.2. Survey scan and high resolution XPS of Nitron-AuNPs.....	192
Figure 5.3. ¹ H NMR spectra of A) Nitron-AuNPs B) isoxazoline AuNP and C) model isoxazoline 14.	196
Figure 5.4. ¹ H NMR spectra of A) model isoxazoline 16, and B) F-isoxazoline AuNPs. ¹⁹ F NMR spectra of C) model isoxazoline 16, and D) F-isoxazoline AuNPs.	200
Figure 5.5. Survey scan and high resolution XPS spectra of F-isoxazoline AuNPs.	202
Figure 5.6. Survey scan and high resolution XPS spectra of SWCNT (left), SWCNT-BCN(middle), and SWCNT-AuNP hybrid (right).....	206
Figure 5.7. TEM images of A) SWCNT-BCN, B) SWCNT-AuNP hybrid, (C) control experiment (SWCNT-BCN + Me-EG ₃ -AuNP).	208

List of Figures for Supporting Information

Figure S2.1. SEM micrographs of: cotton samples (top column) and paper samples (bottom column): untreated (right) and treated (left) with HFPS [Br].	101
Figure S2.2. Pictures of water droplets A) placed on the treated and irradiated 100% cotton fabric and then B) drawn up with pipette to yield a C) dry surface modified substrate.	101
Figure S2.3. Representative pictures of water contact angle measurements using 5 μ L droplets on A) cotton and B) paper C) cotton when it is turned upside down D) paper at 20° tilt angle, all coated with HFPS [I], irradiated and washed.....	102
Figure S3.1. ^1H NMR spectrum of Me-EG ₃ -AuNP in D ₂ O.....	133
Figure S3.2. ^1H NMR spectrum of Diaz-EG ₄ -AuNP in CDCl ₃	133
Figure S3.3. ^1H NMR of the insertion product of Diaz-EG ₄ -AuNP into methanol, recorded in CD ₃ OD.....	134
Figure S3.4. ^{19}F NMR spectrum of the insertion product of Diaz-EG ₄ -AuNP into methanol, recorded in CD ₃ OD.....	134
Figure S3.5. ^1H NMR spectrum of the insertion product of Diaz-EG ₄ -AuNP into acetic acid, recorded in CD ₃ OD.....	135
Figure S3.6. ^{19}F NMR spectrum of the insertion product of Diaz-EG ₄ -AuNP into acetic acid, recorded in CD ₃ OD.....	135
Figure S3.7. ^1H NMR spectrum of the insertion product of Diaz-EG ₄ -AuNP into ethyl vinyl ether, recorded in CD ₃ OD.....	136
Figure S3.8. ^1H NMR spectrum of the insertion product of Diaz-EG ₄ -AuNP into ethyl vinyl ether, recorded in CD ₃ OD.....	136

Figure S3.9. ^{19}F NMR of the insertion product of Diaz-EG ₄ -AuNP into H ₂ O, recorded in CD ₃ OD.....	137
Figure S3.10. First derivative of the TGA graph of Diaz-EG ₄ -AuNPs (blue dashed line), fit 1 (purple), fit 2(red), fit 3 (green), sum of fits (blue solid line).	137
Figure S3.11. UV-Vis spectra of Diaz-EG ₄ -SH (orange), Me-EG ₃ -AuNP (dark blue), Diaz-EG ₄ -AuNP (red), and insertion products of Diaz-EG ₄ -AuNP with methanol (green), ethyl vinyl ether (purple), acetic acid (light blue).....	139
Figure S4.1. ^1H NMR spectra of: a) 2A-AuNPs, b) 4A-endo, c) 4A-exo recorded in CD ₃ CN.....	174
Figure S4.2. ^1H NMR spectra of: a) 2B-AuNPs, b) 4B-endo, c) 4B-exo recorded in CD ₃ CN.....	174
Figure S4.3. ^1H NMR spectra of: a) 2C-AuNPs and b) 4C recorded in CD ₃ CN.....	175
Figure S4.4. ^1H NMR spectra of: a) 2A-AuNPs, b) 4A-exo, c) 4A-endo recorded in CD ₃ CN.....	175
Figure S4.5. ^1H NMR spectra of: a) 2E-AuNPs, b) 4E-endo, c) 4E-exo recorded in CD ₃ CN.....	176
Figure S4.6. ^1H NMR spectra of: a) 3F-AuNPs and b) 5F recorded in CD ₃ CN.....	176
Figure S4.7. ^1H NMR spectra of: a) 3G-AuNPs and b) 5G recorded in CD ₃ CN.....	177
Figure S4.8. ^1H NMR spectra of: a) 3H-AuNPs and b) 5H recorded in CD ₃ CN.....	177
Figure S4.9. ^1H NMR spectra of: a) 3I-AuNPs and b) 5I recorded in CD ₃ CN.	178
Figure S4.10. ^1H NMR spectra of: a) 3J-AuNPs and b) 5J (inseparable mixture of endo/exo) recorded in CD ₃ CN.....	178

Figure S4.11. ^1H NMR spectrum of 5J with a close look at the <i>endo:exo</i> ratio which is 2:3	179
Figure S4.12. UV-Vis spectra of FP-Mal-AuNP, Mal-EG ₄ -AuNP and 2(A-E)-AuNPs.	180
Figure S4.13. UV-Vis spectra of FP-Mal-AuNP, Mal-EG ₄ -AuNP and 3(F-J)-AuNPs..	180
Figure S5.1. ^1H NMR spectrum of Nitron-AuNPs in D ₂ O.....	237
Figure S5.2. ^1H NMR spectrum of compound isoxazoline AuNPs in D ₂ O.....	237
Figure S5.3. ^1H NMR spectrum of compound F-isoxazoline AuNPs in D ₂ O.	238
Figure S5.4. ^{19}F { ^1H } NMR spectrum of compound F-isoxazoline AuNPs in D ₂ O.....	238
Figure S5.5. ^1H NMR spectra array for a representative kinetic study of SPACC reaction of nitron 6 and BCN 5 to prepare compound 14.	239
Figure S5.6. ^1H NMR spectra array for a representative kinetic study of SPAAC reaction of azide 7 and BCN 5 to prepare compound 15.....	240
Figure S5.7. TGA (top) and deconvolution of the TGA first derivative curve (bottom) of the Nitron-AuNPs.....	241
Figure S5.8. TEM images of Nitron-AuNPs (left) and F-isoxazoline AuNPs (right). .	243
Figure S5.9. UV-vis spectra of compound 6 (blue), Nitron-AuNPs (dark red), F-isoxazoline AuNPs (green)	243
Figure S5.10. Rate plots for the strain-promoted cycloaddition reaction of BCN-5 with nitron 6 (top) and azide 7 (bottom).	244
Figure S5.11. HPLC and flow count for compound 10/ [^{18}F] 10. UV detector: $\lambda_{\text{max}}=230$ nm (red curve); radioactive detector (blue curve).....	245

Figure S5.12. HPLC and flow count for compound 13/ [¹⁸ F] 13. UV detector: λ_{\max} =230 nm (red curve); radioactive detector (blue curve).....	245
Figure S5.13. High resolution XPS C 1s spectrum of SWCNT-AuNP.....	246
Figure S5.14. High resolution XPS O 1s spectrum of SWCNT-AuNP.....	246
Figure S5.15. High resolution XPS N 1s spectrum of SWCNT-AuNP.....	247
Figure S5.16. High resolution XPS Au 4f spectrum of SWCNT-AuNP.....	247
Figure S5.17. High resolution XPS S 1s spectrum of SWCNT-AuNP.	248
Figure S5.18. IR spectra of A) SWCNT starting material and B) SWCNT-BCN.....	248
Figure S5.19. TEM images of A) SWCNT-BCN, B) SWCNT-AuNP hybrid, C) control experiment (SWCNT-BCN + Me-EG ₃ -AuNP), D) SWCNT-AuNP hybrid after 1 hour sonication	249

List of Schemes

Scheme 1.1. Simplified scheme for the photoreaction of diazirines.....	6
Scheme 1.2. Cartoon representation of preparing AuNP-hybrid materials using diazirine as a tether..	8
Scheme 1.3. Step growth polymerization of a bis-nitrone with a bis-maleimide via a 1,3-dipolar cycloaddition reaction as reported by Vretik and Ritter.....	22
Scheme 1.4. Schematic representation of two strain-promoted cycloaddition reactions: SPAAC and SPANC.....	27
Scheme 1.5. N-terminal serine functionalization of IL-8 by SPANC..	28
Scheme 1.6. Cartoon representation of AuNPs using Turkevich method.	33
Scheme 1.7. Cartoon representation of Brust-Schiffrin two-phase synthesis of AuNPs..	34
Scheme 1.8. Functionalization of AuNP by a ligand exchange reaction where resulting AuNP contains a mixture of initial thiol groups and functionalized (incoming) thiols....	37
Scheme 1.9. Cartoon representation of interfacial reaction on AuNPs to introduce new functionality (R).....	38
Scheme 1.10. Examples of thermal interfacial reactions on AuNPs; left to right: esterification, S _N 2 substitution, amination reaction of C ₆₀ , Michael addition, maleimide Michael addition, Diels Alder, 1,3-dipolar cycloaddition, SPAAC reaction of DBCO, and Staudinger ligation.	41
Scheme 1.11. Illustration of the photochemical approach used for surface modification of cotton and paper to prepare hydrophobic surfaces.	47

Scheme 1.12. Cartoon representation of photo-induced carbene generation and reactivity of diazirine functionalized AuNPs for interfacial modification.	49
Scheme 1.13. Schematic representation of water soluble maleimide functionalize AuNPs and their interfacial reactions: Diels Alder (blue), and 1,3-dipolar cycloaddition (green).	50
Scheme 1.14. Schematic illustration of i-SPANC reaction using water-soluble AuNPs and a strained alkyne modified substrate.....	51
Scheme 2.1. Reaction pathway towards the synthesis HFPS and the model compound PMe_3S	72
Scheme 2.2. Illustration of photochemical reaction used for surface modification of cotton and paper using HFPS and PMe_3S	75
Scheme 2.3. Reaction pathway towards the preparation of diazirine 8.	88
Scheme 3.1. Cartoon representation of thiol exchange reaction for the preparation of Diaz-EG ₄ -AuNPs and their photo-induced carbene generation and reactivity for interfacial modification.	107
Scheme 3.2. Pathway towards the synthesis of Diaz-EG ₄ -SH (5).	108
Scheme 4.1. Cartoon representation of Mal-EG ₄ -AuNPs and their versatile interfacial reactions: Michael addition (red), Diels Alder (blue), and 1,3-dipolar cycloaddition (green).	142
Scheme 4.2. The 1,3-dipolar cycloaddition reaction of Mal-EG ₄ -AuNP and model compound 3 with nitrones A-E to form the corresponding isoxazolidine modified 2-AuNPs and model isoxazolidine products 4.	150

Scheme 4.3. Diels Alder reaction of Mal-EG ₄ -AuNP and model compound 3 with dienes F-J to form the corresponding modified 3-AuNPs and model Diels Alder cycloadducts 5.	157
Scheme 4.4. Pathway towards the synthesis of maleimide model compound 3.	165
Scheme 5.1. Cartoon representation towards preparation of Nitron-AuNPs and their corresponding i-SPANC reaction.	184
Scheme 5.2. Synthetic procedure towards the preparation of thiol 4.	188
Scheme 5.3. Reaction scheme for the SPANC reaction of Nitron-AuNPs and model nitron 6 with two BCN derivatives (5 and 13) to prepare the corresponding isoxazolines.	194
Scheme 5.4. Strain-promoted cycloaddition reactions of BCN endo 5 with nitron 6 and azide 7 to prepare isoxazoline 14 and triazole 15 respectively.	198
Scheme 5.5. Synthetic procedure towards the preparation of compound 13.	199
Scheme 5.6. Synthetic approach towards the preparation of SWCNT–AuNP through i-SPANC reaction at the Nitron-AuNP interface.	204
Scheme 5.7. Synthetic procedure towards the preparation of compound 5.	216
Scheme 5.8. Synthetic procedure towards the preparation of compound 6.	218
Scheme 5.9. Reaction pathway towards the synthesis of [¹⁸ F] 13 prosthetic group and their i-SPANC reaction to prepare [¹⁸ F] AuNPs.	227

List of Abbreviations

AuNPs	Gold nanoparticles
BARAC	Biarylazacyclooctynone
BBB	Blood-brain barrier
BCN	Bicyclononyne
BE	Binding energy
CNT	Carbon nanotubes
CuAAC	Copper-catalyzed azide-alkyne cycloaddition
DBCO	Dibenzocyclooctyne
DCM	Dichloromethane
DIBO	4-dibenzocyclooctynol
DIFO	Difluorinated cyclooctyne
DIPEA	N,N-Diisopropylethylamine
DMAP	4-dimethylamino pyridine
DMF	Dimethylformamide
DSA	Drop Shape Analysis
Edg	Electron donating group
ESI-MS	Electrospray ionization mass spectrometry
EtOH	Ethanol
Ewg	Electron withdrawing group
fcc	Face centered cubic
FMO	Frontier molecular orbital
FTIR	Fourier transform infrared

HBTU	O-(Benzotriazol-1-yl)-N,N,N',N'-tetramethyluronium hexafluorophosphate
HFPS	Highly fluorinated phosphonium salt
HOMO	Highest occupied molecular orbital
HRMS	High-resolution mass spectrometry
HRTEM	High-resolution transmission electron microscopy
IL-8	chemokine interleukin-8
I-SPANC	Interfacial strain-promoted alkyne-nitrone cycloaddition
LUMO	Lowest unoccupied molecular orbital
MeOH	Methanol
NMR	Nuclear magnetic resonance
NVOC	Nitroveratryloxycarbonyl
PEG	Polyethylene glycol
PET	Positron emission tomography
RCY	Radiochemical yield
SAM	Self-assembled monolayer
SEM	Scanning electron microscopy
SPAAC	Strain-promoted alkyne-azide cycloaddition
SPANC	Strain-promoted alkyne-nitrone cycloaddition
SPR	Surface plasmon resonance
SWCNT	Single-walled carbon nanotubes
T _d	Decomposition temperature
TEM	Transmission electron microscopy
TFA	Trifluoroacetic acid

T _g	Glass transition temperature
TGA	Thermogravimetric analysis
THF	Tetrahydrofuran
TIPS	Triisopropylsilane
TLC	Thin-layer chromatography
TOAB	Tetraoctylammonium bromide
UV	Ultra violet
WCA	Water contact angle
XPS	X-ray photoelectron spectroscopy

Chapter 1

Introduction

1.1 Material Surface Modification

Before considering specific surface modification techniques, it is useful to understand common objectives underlying the approach. Surface modification (engineering) techniques are oftentimes at the forefront of developments in biomedical and technological applications due to their unique ability to change surface properties without altering the bulk material. A surface functionalization technique makes the desired physical, thermal, electrical, and mechanical properties attainable. Meanwhile, it also serves as one of the most important key steps for further assembly process for the construction of novel devices and materials. Therefore, it is not only desirable but also vital to modify surface of materials, physically or chemically in order to control the subsequent surface interactions and responses which are required for any following application.

Demand in a range of industrial and research settings is increasing the necessity to construct material systems with precise control over architecture, functionality, polarity, solubility and reactivity. In addition to these materials and structural requirements, researchers have sought to prepare these systems *via* high yielding, simple covalent chemistry. Chemical modification techniques strive to alter the surface of the material in

order to enhance the functionality of that material. Surface modification and functionalization can be applied to a variety of different substrates and nanoparticles for their target properties by designing appropriate chemical reactions, resulting in a material with an improved surface and mostly unchanged bulk properties. The modification can be accomplished using different methods with a view to altering a wide range of characteristics including but not limited to: hydrophilicity, surface energy, biocompatibility, reactivity, or specific recognition. By incorporating thermally or photochemically reactive moieties onto the surface of interest, one can build robust and novel architectures for any desired application taking advantage of the interfacial reactions occurring on that surface.

A very familiar and readily observed surface property is controlled by the interaction of a liquid, often water, with the surface. Water spreads out evenly on a hydrophilic surface, since the interaction between the surface and water is stronger than the intermolecular interactions in bulk water. Hydrophobic surfaces, on the other hand, weakly attract or even repel water to produce droplets or beads of water on the surface due to much weaker surface interactions. An example of how the surface chemistry of a thin layer can dramatically alter wettability is shown in Figure 1.1, which shows a silver surface coated with highly fluorinated phosphonium salt, lowering the surface energy to an extent that the surface becomes superhydrophobic.¹ In chapter two we will discuss how we prepared hydrophobic cotton/paper surfaces using a photo-initiated surface modification strategy.

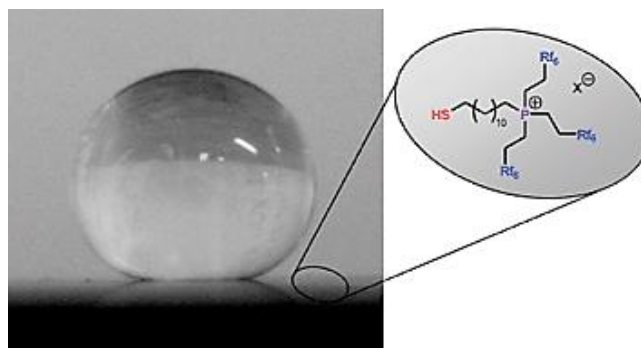


Figure 1.1. A water droplet on a superhydrophobic silver surface coated with highly fluorinated phosphonium salt. Reprinted with permission of reference 1.

There are many examples in the literature of a surface modification designed to enable a subsequent interaction between the surface and additional modification. For example, a monolayer of an organic compound bonded to a metal may completely change the chemical characteristics of the surface, depending on the identity of the terminal group of the organic modifier. The molecule can be terminated by a functional group that is hydrophilic, acidic, photoreactive, or that has other chemical properties which are quite different from those of the original metal. These terminal groups can then be exploited for further modification of that material as will be discussed in this dissertation.

1.2 Robust and Efficient Methods for Material Surface Modification

1.2.1 Photochemical Reactions

Photochemistry relies on the absorption of a photon by a molecule. Photochemical methods have proven to be advantageous from both chemical and surface engineering points of view. From the chemical point of view, the methods provide a clean and easy means for immobilization of the desired molecules in which only photons are required as a reagent. They give robust surfaces that ensure reproducible results and withstand storage. From the surface engineering point of view, the photochemical functionalization methods are versatile and thus can be applied to a range of substrate structures, and are easily adaptable to many state-of-the-art biotechnologies. Furthermore, surface patterning of such surfaces can be achieved by applying a photo-mask.

Photo-probes are stable reagents that generate highly reactive species when activated by UV light, often forming new covalent bonds between the photo-precursor and the target molecule/surface. Common photoactivatable functional groups include benzophenones,²⁻⁴ aryl azides,⁵⁻⁸ and diazirines,⁹⁻¹³ generating reactive intermediates such as ketyls, nitrenes, and carbenes respectively. The advantage in using benzophenones is a long wavelength of irradiation and their inertness towards the solvent. However, prolonged exposure to UV light is required for their photoactivation which can be detrimental to some applications. Aryl azides are easily prepared, however the short wavelengths at which they are excited may damage biological macromolecules.

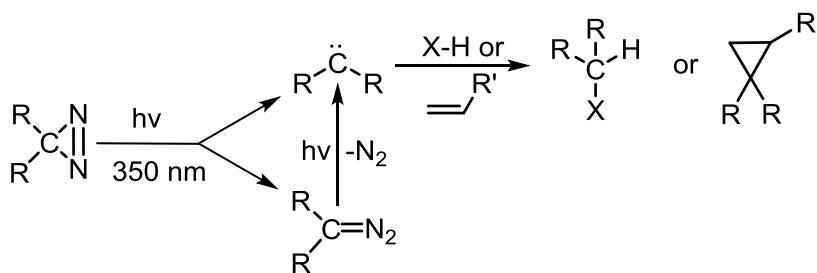
Since all the photochemical surface modification methods utilized in this dissertation are exclusive to a subgroup of diazirine photo-precursors, this family is discussed further in the following section, while more details on the other photochemical approaches are excluded.

1.2.1.1 Diazirine and their Corresponding Photo-Induced Insertion/Addition Reactions

Diazirines are strained three-membered heterocyclic ring systems that contain an sp^3 hybridized carbon atom bonded to an azo group. Diazirines readily form carbene species upon liberating molecular nitrogen, on exposure to stimuli such as light¹⁴ or heat.¹⁵ The synthesis and characterization of diazirine,¹⁶ dialkyl diazirines,^{17,18} alkyl diazirines,¹⁸ and 3-halodiazirines¹⁹ were first reported in the 1960s. However, the potential of diazirines as photoprobes was first revealed much later in the 1970s by Jeremy Knowles.²⁰⁻²² The potential of early diazirine compounds as synthetic reagents is rather limited. 3-Halodiazirines have an explosive nature (3-chloro-3-phenyldiazirine is more shock sensitive than nitroglycerine), while carbenes formed from dialkyl diazirines and alkyl 3H-diazirines have a tendency to self-react in both intramolecular and intermolecular reactions.^{23,24} Intramolecular carbene reactions such as 1,2-hydride and 1,3- hydride migrations have been reported to afford alkenes and cyclopropanes.²⁴ The formation of an azine from the corresponding diazirine via intermolecular carbene attack has also been reported.²³

Generally, upon photoirradiation diazirines release N_2 and generate carbenes, which are highly reactive species with lifetimes in the range of nanoseconds.²⁵ In addition to

generating carbenes, diazirines undergo isomerization generating linear diazo compounds. However, longer irradiation of the diazo isomer will lead to carbene generation. Out of the two reactive species formed upon diazirine photolysis, singlet carbene and diazo compounds, the insertion or addition reaction of the carbene forms covalent crosslinks to a variety of functionalities including O-H, N-H, C-H and C=C bonds (Scheme 1.1).²⁶⁻²⁸



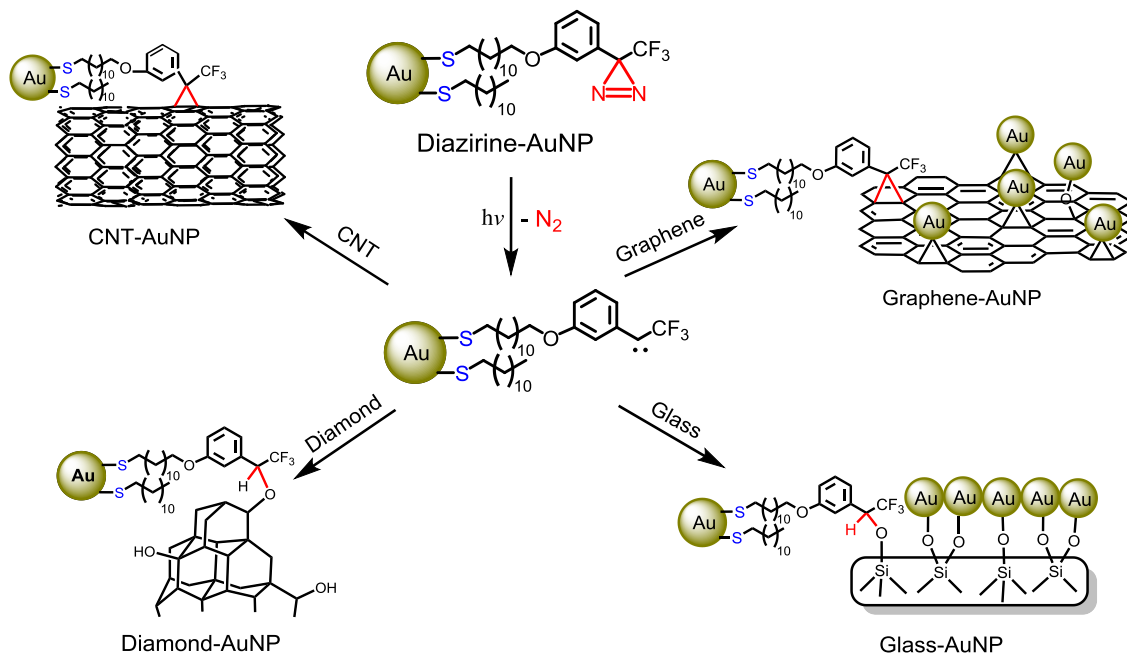
Scheme 1.1. Simplified scheme for the photoreaction of diazirines.

In 1980, Brunner *et al.*²⁹ introduced a trifluoromethyl group to the carbon of an aromatic diazirine and this discovery broadened their use as photophores. Today, the most widely used diazirine derivative is the 3-aryl-3-(trifluoromethyl)diazirine family. It has been reported that 3-(trifluoromethyl)-3-phenyldiazirine is stable in 1M HCl or NaOH solution for at least 2 h, and is also stable at 75 °C for at least 30 min if kept in darkness.²⁹ Moreover, because of strong carbon fluorine bonds in the CF₃ group,²⁶ rearrangement resulting from fluoride migration to the sp² carbon does not occur leaving

a stable carbene for insertion into O-H, N-H and C-H bonds or addition to C=C bonds.^{27,28}

The desirable properties of 3-aryl-3-(trifluoromethyl)diazirine as carbene precursors has led to their successful application for photoaffinity labeling, used to study ligand-protein complexes, and other biological applications.^{27,30,31} Besides the widely explored photoaffinity labeling, diazirines have found applications in surface modification and the synthesis of functional materials. For example, Blencowe *et al.* covalently modified nylon-6,6 powder by photolysis of a fluorenone-derived 3-(trifluoromethyl)diazirine compound.¹⁴ The generated carbene is believed to have inserted into the N-H and C-H bonds, and evidence that suggests the successful covalent modification of nylon-6,6 with the fluorenone moiety was obtained using UV-vis spectroscopy. Brooks *et al.* functionalized glassy carbon with biotin via photolysis of the biotin-derived 3-(trifluoromethyl)diazirine. They also performed the functionalization using an analogous nitrene approach.³² The covalently attached biotin was labeled with a fluorophore, and fluorescence imaging was employed to visualize the extent of surface coverage. The carbene (diazirine) approach demonstrated increased loading of biotin moieties onto the substrate surface compared to the analogous nitrene, which was unable to insert into C-H bonds. Workentin *et al.* have utilized the photochemistry of 3-aryl-3-(trifluoromethyl)diazirine modified AuNPs to prepare AuNP hybrids with a suite of materials including carbon nanotubes (CNTs), graphene, micro-diamond and glass via insertion into the native C=C or C-H, or O-H functionalities inherently present on the surface of these materials.¹¹⁻¹³ They demonstrated that the reactive carbene formed

covalent bonds with these materials simply and efficiently, modifying them with AuNPs (Scheme 1.2).



Scheme 1.2. Cartoon representation of preparing AuNP-hybrid materials using diazirine as a tether. Reproduced with permission of reference 11-13.

1.2.2 Thermal Reactions

All the thermal reactions utilized in this dissertation, fall into the category of click-type reactions. With respect to the modification of surfaces, click chemistry represents a strategy for the efficient coupling of chemical species to surfaces, thus allowing complex molecular architectures to be generated on materials. Examples of click reactions on

polymers and solid surfaces have been thoroughly reviewed.^{33,34} Numerous strategies are available to exploit these reactions enabling surface scientists to benefit from its high selectivity, high yields and remarkable tolerances to varying reaction conditions.

The click concept was first reported in 2001 by Sharpless³⁵ with the objective to establish an ideal set of efficient and highly selective reactions in synthetic chemistry. There are a number of criteria for reactions to fulfill in order to be labeled “click reactions” including : modular, wide in scope, high yielding, generating only inoffensive byproducts, stereospecific, simple to perform, insensitive to water and oxygen, based on readily available starting materials and reagents, run in a mild or easily removable solvent and easy to purify. Common examples of click-type reactions are:

- 1) Cycloaddition reactions, especially Diels-Alder and [3+2] cycloadditions.³⁶⁻³⁸
- 2) Nucleophilic substitution chemistry, particularly ring-opening reactions of strained heterocycles such as epoxides and aziridines.³⁹⁻⁴³
- 3) Carbonyl chemistry of non-aldol type reactions, such as the formation of ureas, thioureas, aromatic heterocycles, oxime ethers, hydrazones as well as amides.⁴⁴
- 4) Addition reactions to carbon-carbon multiple bonds, especially oxidative cases such as epoxidation,⁴⁵⁻⁴⁷ dihydroxylation,⁴⁸ or aziridination,⁴⁹ but also Michael addition reaction.

Click chemistry is widely employed to achieve efficient surface modifications of materials ranging from gold and silica nanoparticles, polymeric films and microspheres to fullerenes as well as CNTs. In addition, functionalization of surfaces with biomolecules is also possible via click chemistry. Out of the various reactions which fall under the click

criteria, cycloaddition reactions are one of the more common strategies used for surface modifications. The reason for the synthetic preference of pericyclic reactions over alternative click concepts may lie in the fact that alternative reactions do not reach the level of yield, simplicity and ease of product isolation that are often desired. In the following section, Diels-Alder reaction and [3+2] cycloadditions including 1,3-dipolar cycloadditions and strain-promoted cycloadditions, which are utilized in the current research work are discussed in more detail.

1.2.2.1 Diels-Alder Reaction

In the Diels-Alder reaction a six-membered ring is formed through fusion of a four- π component, usually a diene and a two- π component, which is commonly referred to as the dienophile. Ever since the Diels-Alder reaction was first reported by Otto Diels and Kurt Alder in 1928,⁵⁰ [4+2] cycloaddition chemistry has become one of the most powerful and widely used synthetic strategies in organic chemistry for its ability to construct two σ -bonds (carbon-carbon or carbon-heteroatom) simultaneously for preparation of six-membered rings.^{51,52} Diels Alder cycloaddition reaction forms not only carbon-carbon bonds but also heteroatom-heteroatom bonds (hetero-Diels-Alder). These bonds are thermally reversible at elevated temperatures.

The Diels Alder reaction is a concerted pericyclic reaction and its characteristics can be explained with the frontier molecular orbital (FMO) theory.⁵³ However, indications for a diradical or di-ion mechanism can only be found in certain cases.^{54,55} Noteworthy is that the concertedness does not imply that in the activated complex the

extent of formation of the two new σ -bonds is necessarily the same. Asymmetric substitution patterns on the diene and/or dienophile can lead to an asynchronous activation process.⁵⁶

Diels-Alder reactions can be divided into normal electron demand and inverse electron demand additions. Normal electron demand Diels-Alder reactions are promoted by electron donating substituents on the diene and electron withdrawing substituents on the dienophile. In contrast, inverse electron demand reactions are accelerated by electron withdrawing substituents on the diene and electron donating ones on the dienophile. The way the substituents affect the rate of the reaction can be rationalized with the aid of the FMO theory. The FMO theory states that a reaction between two compounds is controlled by the efficiency with which the molecular orbitals of the individual reaction partners interact. The interaction is most efficient for those orbitals that overlap best and are closest in energy. The FMO theory further assumes that the reactivity is completely determined by interactions of the electrons that are highest in energy of one of the reaction partners i.e. those in the Highest Occupied Molecular Orbital (HOMO) with the Lowest Unoccupied Molecular Orbital (LUMO) of the other partner. Applied to the Diels-Alder reactions, two modes of interaction are possible: the reaction can be controlled by the interaction of the $\text{HOMO}_{\text{diene}}$ and the $\text{LUMO}_{\text{dienophile}}$ (normal electron demand), or by the interaction between the $\text{LUMO}_{\text{diene}}$ and the $\text{HOMO}_{\text{dienophile}}$ (inverse electron demand), as illustrated in Figure 1.2, in the former case, a reduction of the $\text{HOMO}_{\text{diene}}$ and the $\text{LUMO}_{\text{dienophile}}$ energy gap can be realized by either raising the energy of the HOMO of the diene by introducing electron donating substituents or lowering the

energy of the LUMO of the dienophile by the introduction of electron withdrawing substituents.

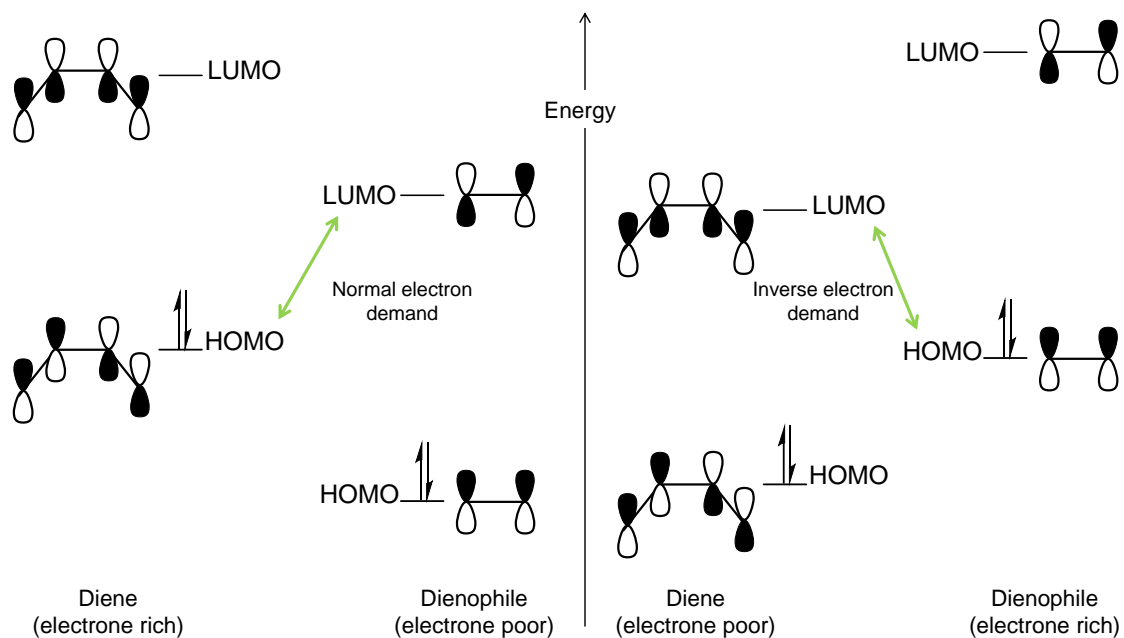


Figure 1.2. Orbital correlation diagram illustrating the distinction between normal electron demand (left side) and inverse electron demand (right side) Diels-Alder reactions.

Due to the concerted mechanism, Diels Alder reactions are stereospecific, i.e. the stereochemical conformation (*E* or *Z*) of the diene and the dienophile are fully retained in the configuration of the product. In addition, Diels Alder reactions show a high regioselectivity towards the ortho and para substituted product over the meta product. The regiochemical preferences of Diels Alder reactions can be determined by analyzing the FMO coefficients of the atoms forming the σ -bonds.⁵⁷

Another form of selectivity can arise when substituted dienes and dienophiles that are employed in the Diels-Alder reaction. Two different cycloadducts denoted as *endo* and *exo* can form (Figure 1.3). Under the usual conditions their ratio is kinetically controlled. Alder and Stein already discerned that there usually exists a preference for formation of the *endo* isomer.⁵⁸ Indeed, there are only very few examples of Diels-Alder reactions where the *exo* isomer is the major product.^{59,60} The interactions underlying this behavior have been subject of intensive research. The stereoselectivity is often explained with secondary orbital interactions but can also be explained with solvent effects, steric interactions, hydrogen bonds, electrostatic forces, and other effects.⁶¹

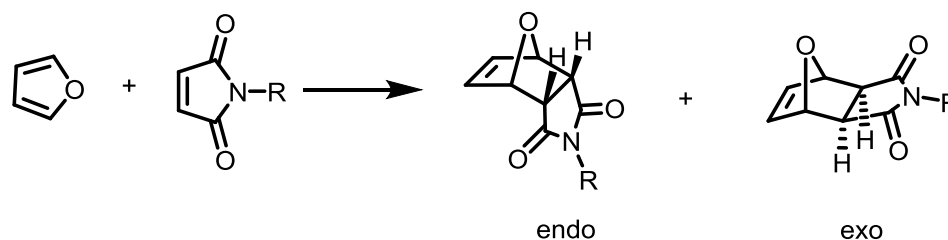


Figure 1.3. Structures of *endo* and *exo* Diels-Alder products from reacting furan and a modified maleimide molecule.

Because of their tolerance towards a wide range of unprotected chemical groups, Diels Alder cycloadditions have proven to be very successful in attaching proteins and cell-adhesion ligands and, consequently, attachment of cells.^{62,63} In a very elegant approach reported by Mrksich's group, hydroquinone groups on self-assembled

monolayers (SAMs) were electrochemically oxidized into quinone groups that, in turn, underwent Diels–Alder reaction.⁶⁴ The unique aspect of this approach is that these systems can react on demand, as they are turned “on” through the initial electrochemical reaction step. Alternatively, monolayers presenting nitroveratryloxycarbonyl (NVOC)-protected hydroquinones were photochemically cleaved to reveal the hydroquinone groups (Figure 1.4).⁶⁵ These activated groups were reversibly oxidized to the corresponding benzoquinones, which were then used to immobilize diene-functionalized ligands (such as cell adhesion peptides) via Diels–Alder reaction. Another approach used a Diels–Alder reaction for the immobilization of unsaturated DNA strands onto maleimide-coated AuNPs.⁶⁶ Self-assembled nanoparticles can be further used for biosensor applications or supramolecular assemblies.

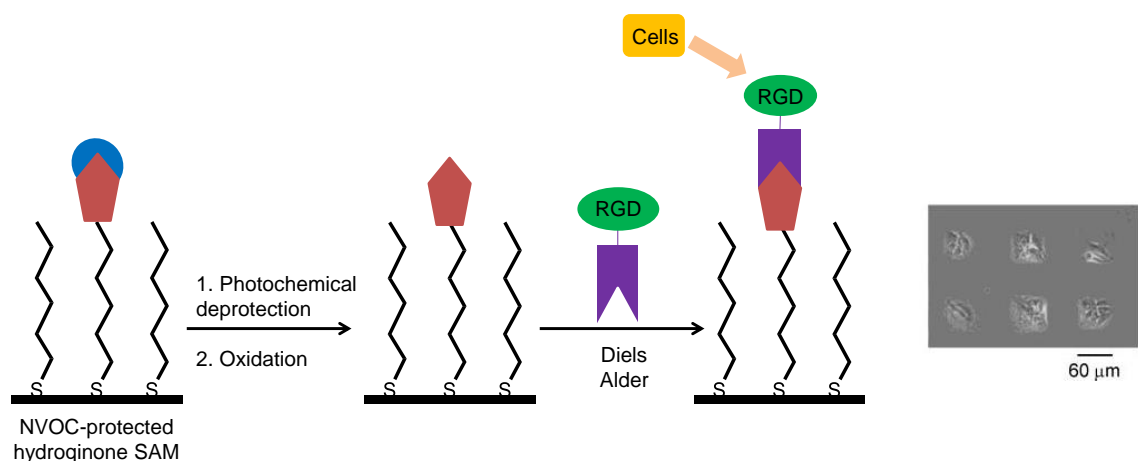


Figure 1.4. Strategy for the immobilization of ligands to SAMs via Diels–Alder cycloaddition. Cells attached to the patterned regions modified with RGD is shown on the right. Reproduced with permission from reference 65.

Diels–Alder cycloaddition reaction between anthracene and maleimide derivatives has proven to produce excellent results in the formation of dendrimers and dendronized polymers in a modular approach. First, McElhanon and co-workers reported the use of thermally reversible furan–maleimide Diels Alder cycloaddition reactions for a convergent approach towards benzyl aryl ether dendrimers up to the third generation.⁶⁷ This work was the first example of a new class of thermally reversible dendrimers taking advantage of the Diels-Alder/retro Diels-Alder approach. Later on, the same group reported a similar system with a bismaleimide core and fourth generation benzyl aryl ether based dendrons that contained furan moieties at their focal point to access the first fourth generation dendrimers through Diels Alder.⁶⁸ Diels Alder reactions between maleimide and anthracene functionalities were further employed for polymer end-group⁶⁹ and backbone functionalization^{70,71} as well as for the construction of complex macromolecular architectures.⁷²⁻⁷⁴ Selective modification of carbon black,⁷⁵ fullerenes,^{76,77} and CNTs⁷⁸⁻⁸⁰ have been achieved using Diels Alder strategy. For example, *O*-quinodimethane was directly coupled to single-walled carbon nanotubes (SWCNTs) with the help of microwave irradiation.⁸¹ These reactions open up possibilities for enhancing the solubility of CNTs, as needed in several technological applications.⁸¹

1.2.2.2 1,3-Dipolar Cycloaddition Reactions

Within the class of cycloaddition reactions, 1,3-dipolar cycloaddition reaction is widely used as a high yielding, efficient, regio- and stereoselective method for the synthesis of a variety of valuable five-membered heterocycles. 1,3-dipolar cycloaddition

reaction, where two organic molecules, a 1,3-dipole and a dipolarophile combine to give a five-membered heterocycle, is one of the typical reactions in synthetic organic chemistry. Starting from relatively simple and easily accessible molecules, this reaction can offer a wide variety of simple as well as complex heterocyclic compounds. The 1,3-dipolar cycloaddition has evolved for more than 100 years, and a variety of different 1,3-dipoles have been discovered. The history of 1,3-dipoles starts with Curtius, who discovered diazoacetic ester in 1883.⁸² Five years later Buchner from Curtius' group studied the reactions of diazoacetic ester with α,β -unsaturated esters and he described the first 1,3-dipolar cycloaddition reaction. Buchner discovered that when methyl diazoacetate reacts with methyl acrylate the product isolated is 2-pyrazoline which is formed after the rearrangement of the initially formed unstable 1-pyrazoline.⁸³ Shortly after, Beckmann discovered azomethine oxides/nitrones.⁸⁴ Nitrile oxides were discovered by Werner and Buss a few years after.⁸⁵ At the same time, 1,3-dipolar cycloaddition reaction of diazoalkanes⁸⁶ and alkyl azides⁸⁷ were also reported. The synthetic scope of 1,3-dipolar cycloaddition and its application in organic chemistry was first established by Huisgen in the 1960s.³⁸ He published a large number of research articles on 1,3-dipolar cycloaddition and gradually it became one of the standard methods for the preparation of five membered heterocycles. He classified 1,3-dipolar cycloaddition reactions and formulated the basic definitions.³⁸

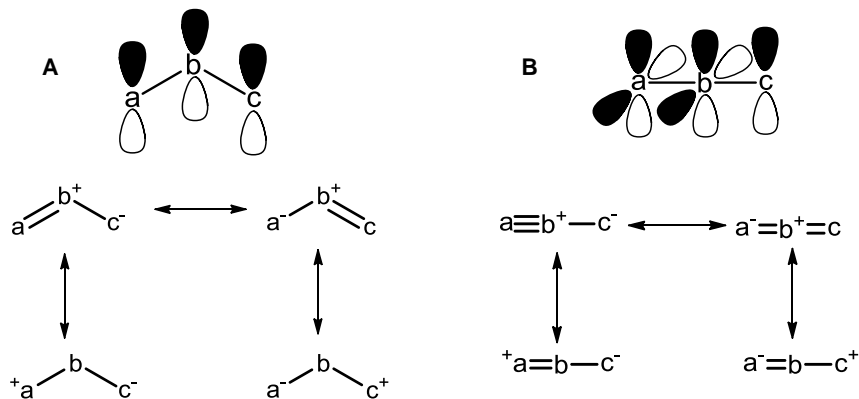


Figure 1.5. A) Allyl anion type and B) Propargyl/Allenyl anion type 1,3-dipoles.

The 1,3-dipole, also known as a ylide, is defined by Huisgen as an *a-b-c* structure, with a positive and a negative charge distributed over three atoms and has four π electrons.³⁸ Huisgen categorized 1,3-dipoles into two general classes namely, allyl anion type and propargyl/allenyl anion type 1,3-dipoles. The allyl anion type 1,3-dipoles are characterized by the presence of four π electrons in three parallel *p*-orbitals perpendicular to the plane of 1,3-dipole and possessing a bent structure. Two resonance structures in which three centers have an electron octet, and two structures in which *a* or *c* has an electron sextet, can be drawn. The central atom *b* can be nitrogen, oxygen or sulfur (Figure 1.5, A). The propargyl/allenyl anion type has an extra π bond in the plane perpendicular to allyl anion type molecular orbital and the former orbital is for that reason not directly involved in resonance structures as well as reactions of 1,3-dipoles. Usually, the occurrence of this extra π bond makes 1,3-dipoles of propargyl/allenyl anion type linear. Generally, the central atom *b* is limited to nitrogen (Figure 1.5, B). Examples of both types of 1,3-dipoles are displayed in Figure 1.6.

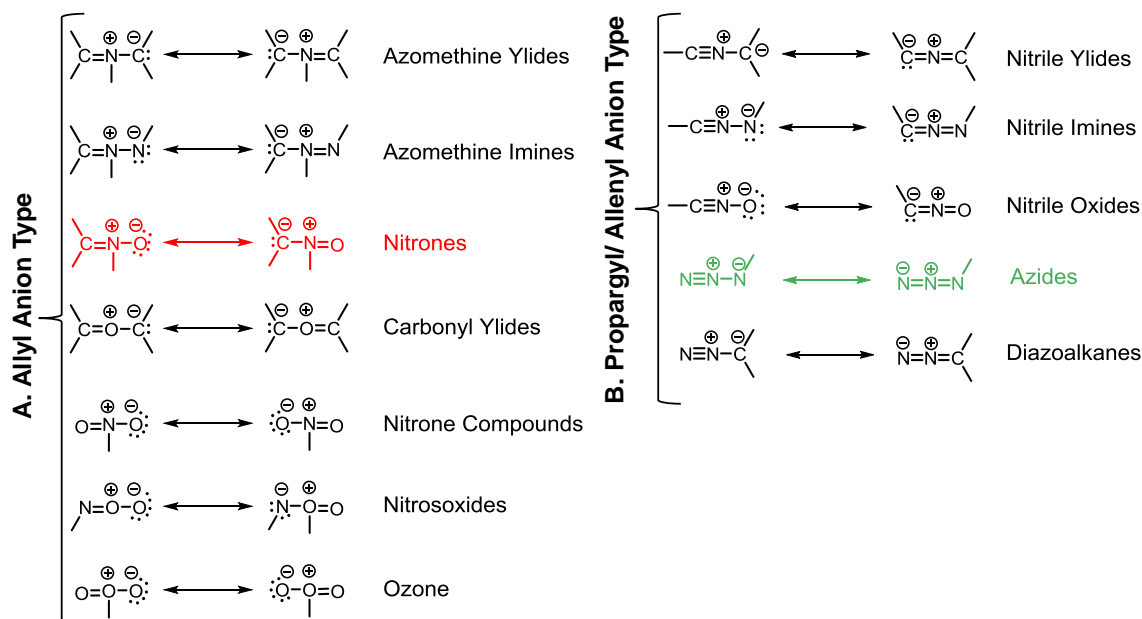


Figure 1.6. Classification of 1,3-dipoles consisting of carbon, nitrogen, and oxygen centers.

The mechanism of 1,3-dipolar cycloaddition has been investigated intensively. The first mechanistic study was reported by Huisgen in 1963.⁸⁸ Whether the reaction is concerted or stepwise is a fundamental question in 1,3-dipolar cycloaddition chemistry.⁸⁹⁻⁹¹ The conclusion of all the debates to date is that, these reactions are concerted but not synchronous.⁹² This means the degree to which each of the two new bonds formed in the transition state is not the same i.e. making of one σ bond may lag behind that of second σ bond in the transition state.⁹² According to quantum chemical calculations, concerted 1,3-dipolar cycloaddition reaction proceeds via “*early transition state*”.³⁸ Thus the transition state occurs early along the reaction coordinate of energy profile diagram. This has the effect of making the transition state “*reactant like*”, while a late transition state is referred to as “*product like*”. The transition state of the concerted 1,3-dipolar cycloaddition

reaction is controlled by the FMO of the substrates. The $LUMO_{\text{dipole}}$ can interact with the $HOMO_{\text{alkene}}$ and the $HOMO_{\text{dipole}}$ with the $LUMO_{\text{alkene}}$. According to the Sustmann classification, 1,3-dipolar cycloadditions can be placed in one of three groups with respect to the dominant HOMO-LUMO interaction.⁹³ The classification depends on the number and the nature of the heteroatoms, and on the electron donor/withdrawal properties of any substituents on the reactants.^{94,95} The classifications, represented in Figure 1.7, are as follows: in type-I, 1,3-dipolar cycloaddition reaction, the dominant FMO interaction is that of $HOMO_{\text{dipole}}$ with $LUMO_{\text{dipolarophile}}$. Generally this type of 1,3-dipolar cycloaddition reaction is referred to as “normal electron demand” or “HOMO controlled” reactions. Cycloadditions of 1,3-dipoles of type-I are accelerated by the presence of electron donating groups (edg) in 1,3-dipole. On the other hand, electron withdrawing groups (ewg) in the dipolarophile will lower the energy of the LUMO towards the HOMO of the dipole. In both cases HOMO-LUMO separation of the predominant interaction is diminished and the reaction proceeds faster. In type-II, since FMO energies of the dipole and alkene are similar, both HOMO-LUMO interactions are to be considered. Adding either an edg or ewg to the dipole or dipolarophile can accelerate these reactions. 1,3-Dipolar cycloaddition reaction of type-III is dominated by interaction between $LUMO_{\text{dipole}}$ and $HOMO_{\text{dipolarophile}}$. The term ‘inverse electron demand’ is used to refer to this type of 1,3-dipolar cycloaddition. This is also known as “LUMO controlled” reactions. Since the dominant interaction is between $LUMO_{\text{dipole}}$ and $HOMO_{\text{dipolarophile}}$, edgs on dipolarophile and ewgs on dipole will accelerate the reaction. 1,3-dipolar cycloaddition reactions of type I are typical for substrates such as azomethine

ylides and azomethine imines, while reactions of nitrones are normally classified as type II. Examples of type III interactions are 1,3-dipolar cycloaddition reactions of ozone and nitrous oxide. However, the introduction of electron-donating or electron-withdrawing substituents on the dipole or the alkene can alter the relative FMO energies, and therefore the reaction type dramatically.

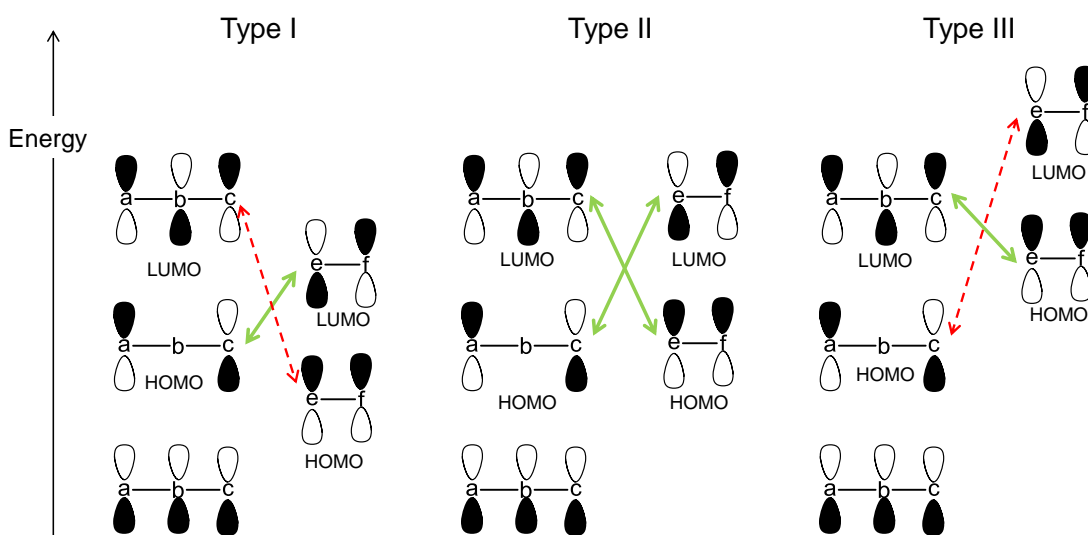
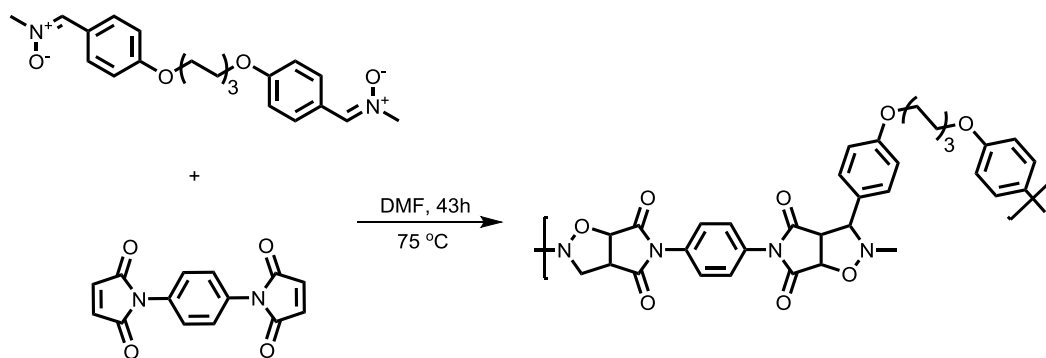


Figure 1.7. The HOMO-LUMO interaction between 1,3-dipole (a-b-c) and dipolarophile (e-f) depends on the orbital energies of the 1,3-dipole: _____ strong and - - - weak interactions.

Similar to Diels Alder reactions, formation of *endo* and *exo* isomers is possible in the reaction between an alkene and a 1,3-dipole. However, since the secondary orbital interactions are very weak compared to Diels Alder reaction, the *endo/exo* selectivity in 1,3-dipolar cycloaddition reaction is mainly controlled by the structure of substrates and the presence of catalysts.⁹⁶

Nowadays, 1,3-dipolar cycloaddition is extensively employed for the construction of heterocycles containing simple to complex ring systems.⁹⁷ The simplicity of reaction, possibility of creating polyfunctional structures in a fairly small molecular skeleton, high stereochemical control, and superior predictability of its regiochemistry have contributed to the popularity of 1,3-dipolar cycloaddition reaction in organic synthesis.⁹⁸⁻¹⁰³ The pretty complex heterocycles thus obtained can be readily transformed into a variety of other cyclic as well as acyclic functionalized organic molecules. 1,3-Dipolar cycloaddition reaction is for that reason generally described as the single most important method for the construction of five membered heterocyclic rings in the field of synthetic organic chemistry.⁹⁷

Besides the usefulness of 1,3-dipolar cycloadditions in synthetic organic chemistry, some of the major reported applications of 1,3-dipolar cycloaddition chemistry include polymer modification. Ritter and Vretik reported on a step growth mechanism via 1,3-dipolar cycloaddition reactions between bifunctional nitrones and bis-maleimide compounds forming polymers that are inter-connected by isoxazolidine rings (Scheme 1.3). These step-growth polymers were described to have good performance for coating formation on glass surfaces.¹⁰⁴ The main feature of the above work is undoubtedly the successful cycloaddition reaction involving nitrones on a macromolecular scale. It is worth noting that an analogous 1,3-dipolar cycloaddition reaction with nitrile oxides was also developed as a tool for end group polymer modifications.^{105,106}



Scheme 1.3. Step growth polymerization of a bis-nitrone with a bis-maleimide via a 1,3-dipolar cycloaddition reaction as reported by Vretik and Ritter. Reproduced with permission from reference 104.

Alternatively 1,3-dipolar cycloadditions can be utilized for material surface modification. Prato and co-workers modified CNTs via the in situ generation of azomethine ylides from the condensation of aldehydes and amino acids to form five-membered pyrrolidine tethers.^{107,108} A similar method was used by Callegari *et al.* to immobilize ferrocenyl moieties onto the surface of SWCNTs in the construction of an amperometric biosensor.¹⁰⁹ Other 1,3-dipolar cycloadditions using ozone as the reactive species have also been used to modify the surface of CNTs.^{110,111} 1,3-dipolar cycloaddition was also employed to immobilize azide-functionalized sugars (mannose, lactose, and galactose) onto alkyne-terminated SAMs on gold. It was found that these carbohydrate-based sensors maintained their specificity towards the corresponding proteins, which could lead to potential applications in high-throughput characterization of carbohydrate–protein interactions.¹¹²

1.2.2.3 Strain-Promoted Cycloaddition of 1,3-Dipoles to Alkynes

The [3+2] cycloaddition of azides with alkenes and alkynes was first reported at the end of 19th century.⁸⁷ However, the high temperatures or pressures required promoting cycloaddition of azides and most dipolarophiles are not compatible with living systems.¹¹³ Sharpless¹¹⁴ and Meldal¹¹⁵ independently demonstrated that the 1,3-dipolar cycloaddition of azides with terminal alkynes to produce 1,4-disubstituted 1,2,3-triazoles could be effectively catalyzed by Cu(I). This reaction, now termed the copper-catalyzed azide-alkyne 1,3-dipolar cycloaddition (CuAAC), takes advantage of Cu-acetylide formation to activate terminal alkynes toward reaction with azides. The result of Cu(I) catalysis is a reaction that proceeds roughly seven orders of magnitude faster than the uncatalyzed cycloaddition,¹¹⁶ and the reaction can be further accelerated by the use of specific ligands for Cu(I).^{117,118} The CuAAC reaction has all the properties of a click-type reaction (including efficiency, simplicity, and selectivity), as defined by Sharpless and coworkers.³⁵ In fact, it has become the quintessential click reaction and is often referred to simply as “click chemistry”. CuAAC has gained widespread use in organic synthesis, polymer chemistry, materials chemistry, and chemical biology.³³

In order to extend use of click chemistry to *in vivo* studies there was a need to overcome the detrimental effects of metal catalyst by introducing an alternative, more biologically friendly method to lower the activation energy of the azide-alkyne cycloaddition. Bertozzi *et al.* introduced an intriguing strategy by using ring strain to activate the alkyne for the azide-alkyne cycloadditions.¹¹⁹ It had been previously shown that the smallest stable cycloalkyne (i.e. cyclooctyne) reacts rapidly with azides to form a

single triazole product.¹²⁰ This reactivity is attributed to the destabilization of the triple bond due to bond angle distortion. Compared to the ideal acetylene angle of 180°, alkyne incorporated into an eight-membered ring has a bond angle estimated to be ~160°. ¹²¹ Such deformation accounts for a significant amount of ring strain energy of 18 kcal mol⁻¹ ¹²² or up to 19.9 kcal mol⁻¹ according to more recent studies. ¹²³ This ring strain energy is partially released upon reaction.

The first account of strain-promoted azide-alkyne cycloaddition (SPAAC) was reported by Bertozzi *et al.* on model reactions of biotinylated cyclooctyne with organic azides. ¹¹⁹ The second-order rate constant of model cycloaddition with benzyl azide was found to be $2.4 \times 10^{-3} \text{ M}^{-1}\text{s}^{-1}$. ¹²⁴ The cyclooctyne was also successfully applied in a biological labelling experiment, where cyclooctyne-biotin derivative was used to detect azides that had been metabolically incorporated into cell-surface glycans.

Over the years, a host of cyclooctyne derivatives have been evaluated in terms of their ability to undergo copper-free click chemistry reactions. The purpose of these studies is often focused on enhancing the rate of the cycloaddition reaction by making structural modifications to the cyclooctyne species (Figure 1.8). For example, it has been discovered that introducing one or more electron-withdrawing substituents (*e.g.* fluorine) in close proximity to the alkyne group leads to a substantial increase of rates of reaction. The difluorinated cyclooctyne (DIFO) ¹²⁵ reacts with azides approximately sixty times faster than unsubstituted cyclooctyne. Other modifications, such as one ¹²⁶ or two ^{127,128} adjacent aryl rings have also been found to improve reaction rates yet further. Boons and

coworkers reported that derivatives of 4-dibenzocyclooctynol (DIBO) and related analogues (DIBO1 and DIBO2) rapidly react with azido-containing saccharides and amino acids and can be employed for visualizing metabolically labeled glycans of living cells.¹²⁸ Furthermore, Delft *et al.* developed a novel cyclooctyne, bicyclononyne (BCN), in which the alkyne additional ring strain is derived from fusion of a cyclopropane ring in the backbone of the cyclooctyne as opposed to fused phenyl rings in DIBO. The rate constant for reaction of BCN with benzyl azide ($k_2 = 1.9\text{-}2.9 \times 10^{-1} \text{ M}^{-1}\text{s}^{-1}$) is comparable to that obtained for analogous reaction with DIBO.¹²⁹ Since the introduction of SPAAC in 2004, the structural features contributing to enhanced reactivity of the cyclooctyne reagents were all combined in the design of the most reactive cyclooctyne: biarylazacyclooctynone (BARAC).¹²⁷ The synthesis of BARAC has the advantages of being modular and scalable. The second-order rate constant for the reaction of BARAC with benzyl azide ($k_2 = 0.96 \text{ M}^{-1}\text{s}^{-1}$) is 800-fold greater than that of unsubstituted cyclooctyne.¹²⁷ However, a recent study has found evidence that BARAC itself is prone to rearrangement yielding tetracyclic products.¹³⁰

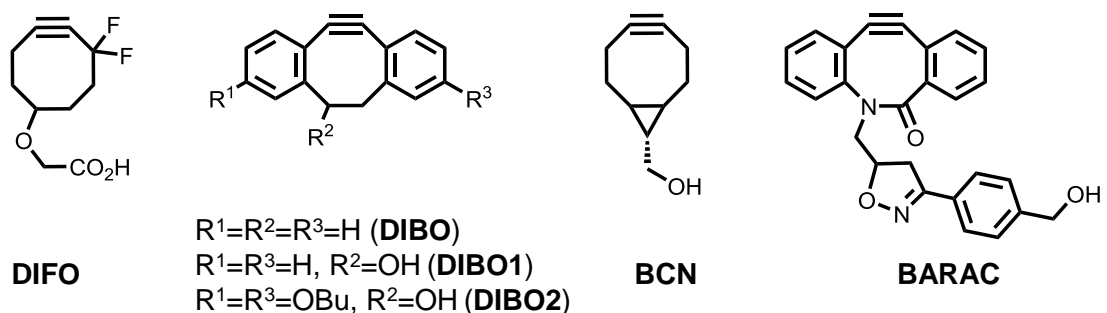
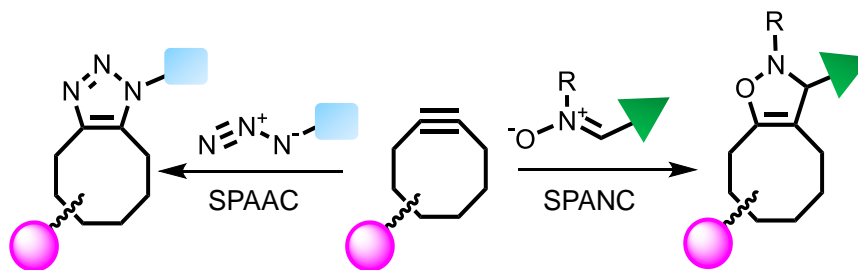


Figure 1.8. Examples of cyclooctyne derivatives investigated for strain-promoted cycloadditions.

The main incentive to increase the SPAAC reaction rate has been to lower the concentrations of the labelling reagents for bioorthogonal reactions, thereby lowering the risk of potential toxicity, interference with cellular processes and residual fluorescence or non-specific labelling. Until recently, most efforts have focused on increasing the reactivity of the cyclooctyne reagent. However, the scope of metal free click reactions was further expanded when Pezacki and co-workers reported the first strain-promoted alkyne-nitrone cycloaddition (SPANC) in 2010.¹³¹ Nitrones have been used in place of azides as partners in SPANC reaction as illustrated in Scheme 1.4 for applications such as protein modification. SPANC reactions represent versatile tools for chemical biology and define their utility by the observation of rapid reaction kinetics (k_2 up to $60 \text{ M}^{-1} \text{ s}^{-1}$), biological stability of reagents and products, compatibility with living systems, and systematic tunability through substitution of groups on both the carbon and nitrogen atoms of the nitron dipole.

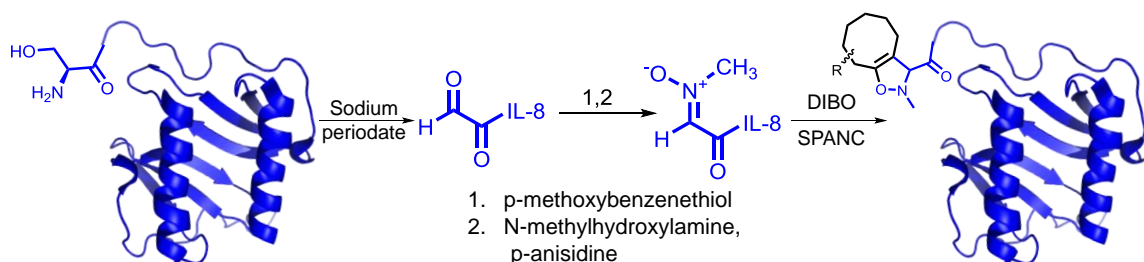


Scheme 1.4. Schematic representation of two strain-promoted cycloaddition reactions: SPAAC and SPANC.

Recently, it was reported that nitrones are rapid alternatives to azides in SPANC reactions with dibenzocyclooctyne, proceeding up to 25 times faster than similar reactions of azides.¹³¹ Pezacki *et al.* demonstrated that nitrones bearing electron-withdrawing groups at the α -C position react faster than the unsubstituted parent nitron, or those bearing electron-donating groups. They also recently expanded on the cyclic nitron scope and kinetics of doubly-strained SPANC and have successfully applied this modular labelling strategy in efficient labelling of cancer cell surface proteins with live-cell imaging applications.¹³²

The bioorthogonal SPANC reaction has applications that range from protein labeling^{128,133,134} and cell surface¹³² to material science.¹³⁵ Classic methods of achieving protein modification, which most commonly target the cysteine thiol or the lysine primary amine group, can lead to protein dimerization, poor solubility or loss of protein function depending on the location of the modified amino acid.¹³⁶ Several methods exist for site-selective metabolic incorporation of azide-functionalized amino acids into

proteins, however, they require both genetic engineering and manipulation of translational machinery.¹³⁷ By contrast, N-terminal serine is the sole requirement for nitron conversion and subsequent functionalization and labeling of peptides or proteins through SPANC.^{128,132-134} In 2010, Van Delft and co-workers reported the SPANC between DIBO and nitron to generate the N-alkylated isoxazoline. The reaction proceeded 32 times faster than the SPAAC reaction with DIBO. They demonstrated the utility of SPANC in protein modification using chemokine interleukin-8 (IL-8) with a naturally occurring N-terminal serine residue. When this serine was converted to Nitron, N-terminal peptide or protein labeling was made possible via SPANC by incubation with the tagged cyclooctyne. Mass spectrometry analysis revealed a single product with mass corresponding to the isoxazoline-IL-8 conjugate (Scheme 1.5).¹²⁸



Scheme 1.5. N-terminal serine functionalization of IL-8 by SPANC. Reproduced with permission of reference 128.

Colombo *et al.* showed that cyclooctyne functionalized iron oxide nanoparticles, which have both fluorescence and superparamagnetic properties, can be conjugated to properly folded anti-HER2 antibodies containing an N-terminal nitron via SPANC.¹³³ These targeted multifunctional nanoparticles were found to localize only to HER2 positive breast cancer cells, highlighting the utility of SPANC towards the development of new targeted nanoparticles.

In addition to azides and nitrones, other 1,3-dipoles have emerged such as diazo-compounds and nitrile oxides for use in strain-promoted cycloadditions with cyclooctynes.¹³⁸

1.3 Gold Nanoparticles (AuNPs)

1.3.1 AuNPs and their properties

Gold nanoparticles (AuNPs) are defined as a stable colloidal solution of gold atom clusters in a range 1-100 nm. The AuNPs are comprised of a metal core and an organic ligand shell (protecting group, *e. g.* thiolate ligand) that stabilizes the metal core and prevents aggregation of nanoparticles (Figure 1.9, A). The oxidation state of the gold atoms in the core is 0. However, similar to bulk gold, the AuNP gold core doesn't oxidize at ambient conditions, making the AuNPs one of the most stable metal nanoparticles. AuNPs have long been utilized for decorative and medical purposes, but not much was done to develop the chemistry of gold until the 19th century due to inertness and high cost

of gold. Faraday was the first to demonstrate detailed experiments with gold colloids and thin films.¹³⁹ He prepared his colloidal gold by reducing an aqueous solution of gold salt, AuCl₄, with phosphorus in carbon disulfide. About 150 years later, transmission electron microscopy (TEM) images taken of Faraday's gold solution revealed that he had actually synthesized gold nanoparticles with an average size of 6 ± 2 nm (Figure 1.9, B).¹⁴⁰

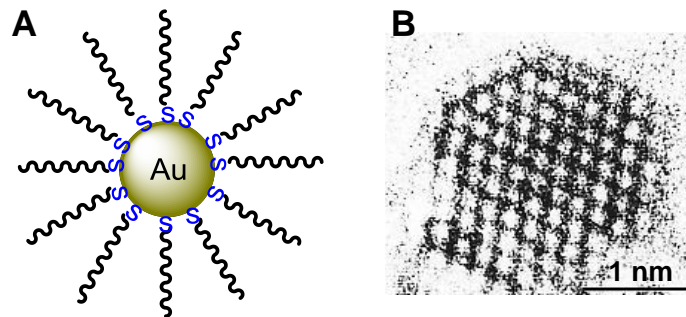


Figure 1.9. A) Cartoon representation of a thiolate-stabilized AuNP, B) High-resolution transmission electron microscopy (HRTEM) image of an individual thiolate-protected gold particle. Reprinted with permission of reference 140.

AuNPs have recently become a fundamental building block in nanotechnology due to their unique properties, such as their high surface area to volume ratio, size and shape dependent optical features, stability, and facile surface chemistry.¹⁴¹ One of the features that brought gold to the forefront of research is surface Plasmon resonance (SPR).^{142,143} The “Surface Plasmonic” theory explains that the six surface free electrons present in the conduction band of AuNPs oscillate back and forth, creating a Plasmon band with an

absorption peak at 530-540 nm, when hit by the electromagnetic field of the incoming light. Physical properties of AuNPs depend on the size and shape of the particles itself, particle-particle distance, the nature of a colloidal stabilizer as well as dielectric constant of the surrounding matter. By increasing the size of spherical AuNPs the Plasmon absorption red shift is increasing also, changing the color from red to purple.¹⁴⁴

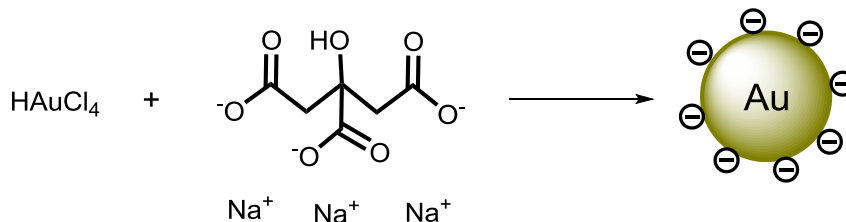
Surface of AuNPs can be derivatized with thiols, phosphines, and amines from both aqueous and organic solvents,¹⁴¹ allowing a range of chemistries to be utilized in particle modification. The AuNP surface enables one to create tailorable, multivalent interfaces, directing the particle to interact with its environment in a highly programmable manner in three dimensions. Additional functionality can be imparted to these particles when they are modified with ligands such as small molecules, polymers, or biomolecules through interfacial reactions. Modified AuNPs can be utilized in many applications, including detection,¹⁴⁵ therapeutics,¹⁴⁶ and imaging.¹⁴⁷

Another important feature of AuNPs is their biocompatibility. AuNPs have been used for imaging biological structures and as well as contrast agents for labelling biomolecules or selected structures in living cells and organisms.¹⁴⁸⁻¹⁵⁰ Furthermore, AuNPs can be modified by conjugation with various drug molecules to interact with target cells to carry out a specific function, such as drug delivery.^{151,152}

1.3.2 Synthesis of AuNPs

AuNP synthesis in the liquid phase usually begins with reduction of the gold salt leading to nucleation and formation of nanoparticles. To terminate the growth of the

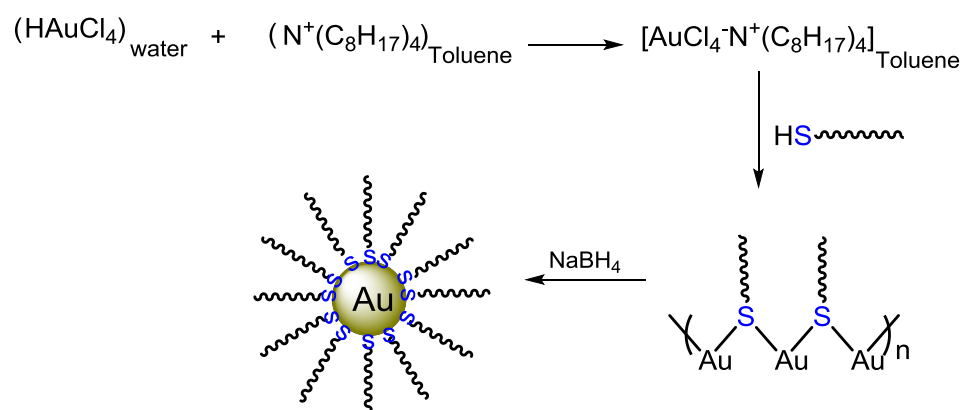
particles and prevent their aggregation, the particles need to be coated with a stabilizing layer. Many methods have been developed for the synthesis of AuNPs, but one of the most common methods is the Turkevich method.¹⁵³ The method pioneered by J. Turkevich *et al.* in 1951 and refined by Frens in 1970s,¹⁵⁴ is a rapid and reliable method, using chloroauric acid (HAuCl₄) as the precursor and trisodium citrate dihydrate as both the reducing agent and capping ligand (Scheme 1.6). After the two are mixed, the nucleation phase can be visually followed by the change in color to a dark blue after 30 seconds of boiling, and then the growth phase can be seen by the change in color to a bright red after 90 seconds. This method usually produces AuNPs of around 20 nm diameter.¹⁵³ The size distribution of AuNPs could be controlled between 16 to 147 nm by varying the temperature, the ratio of gold to citrate, and the order of addition of the reagents.¹⁵⁴ Despite being the most common method of producing AuNPs, citrate-stabilized nanoparticles are disadvantageous for several reasons. First, they cannot be isolated from solution, making it difficult to store or study them in the solid state. Second, their stability with changes in pH or ionic strength is minimal. Finally, and most importantly, their functionalization, either through ligand exchange or derivatization of carboxylic acids in the ligand shell, is extremely limited. To partially overcome these shortcomings, Dahl *et al.* has recently developed diafiltration methods that may allow for ligand exchange with thiols, thus extending the utility of nanoparticles prepared via the citrate route.¹⁵⁵



Scheme 1.6. Cartoon representation of AuNPs using Turkevich method.

Brust, Schiffrin and others have devised a direct synthesis method for the preparation of modified AuNPs.¹⁵⁶ In the Brust-Schiffrin two-phase synthesis (Scheme 1.7), aqueous AuCl_4 is first transferred into the organic phase (toluene) by the phase transfer agent (tetrabutylammonium bromide, TOAB). Upon addition of a thiol to the organic phase, the gold (III) salt is reduced to the gold (I)-thiol polymeric form, $[(\text{Au(I)SR})_n]$, accompanied by a decolorization of the organic phase. The disappearance of the gold (III) orange color after addition of thiol indicates the occurrence of the reaction between gold (III) and thiol in accordance with the formation of the polymeric structure. It is noteworthy that the gold(I)-thiol polymeric structures are known and the synthesis and characterization of them have been reported.^{157,158} Lastly, addition of a reducing agent (NaBH_4) converts the gold(I)-thiol polymer to the AuNPs where the oxidation state of gold is (0). Though in theory, 1/4 equivalents of the borohydride are needed to reduce the Au(I) species to Au(0), a large excess of sodium borohydride, usually > 10 equivalent, is required to generate small and narrow dispersed AuNPs. Experiments using less sodium borohydride carried out by Murray's group yield large sized clusters and more insoluble aggregated clusters.¹⁵⁹ The resulting AuNPs are in the

size range of ~1 – 4 nm, depending on the reaction conditions.¹⁵⁶ The size of the AuNPs can be tuned by varying the molar ratio of thiol to gold, the temperature, and the rate of reductant addition. For example, a large excess of thiol results in smaller nanoparticles,¹⁶⁰ cooler reaction temperatures produce more monodispersed nanoparticles,^{159,161} and faster addition of the reducing agent¹⁶¹ or quenching the reaction immediately after reduction¹⁶² result in the generation of smaller nanoparticles. The two-phase Brust-Schiffrin method have been extended to the use of various alkanethiols (different chain lengths),^{163,164} dialkyl disulfides,^{165,166} thiol-terminated dendrimers¹⁶⁷ and polyethylene glycol thiolate (PEG-SH)^{168,169} for the preparation of AuNPs.



Scheme 1.7. Cartoon representation of Brust-Schiffrin two-phase synthesis of AuNPs.

A number of modifications have been made to the Brust-Schiffrin approach. The two-phase method has been extended to one phase method trying to avoid the phase transfer reagent^{170,171} or use other kinds of protecting ligands, such as amines,¹⁷² or

phosphines.¹⁷³ The synthesis of monodispersed AuNPs was demonstrated by Peng and co-workers.¹⁷⁴ When aliphatic amines were utilized as protecting ligands, monodispersed amine-capped AuNPs (3.2 nm) were produced. Subsequently, amines were replaced by thiolate ligands to produce thiol protected AuNPs. The rationale suggested for such behavior is that thiols typically cause slow activity of the clusters present in the nucleation step, leading to the formation of polydispersed AuNPs due to the stronger binding of thiol compared to amine to gold. Also, Digestive ripening, i.e. heating a colloidal suspension near the boiling point in the presence of alkanethiols, significantly reduced the average particle size and polydispersity in a convenient and efficient way. This technique also led to the formation of 2D and 3D superlattices.¹⁷⁵

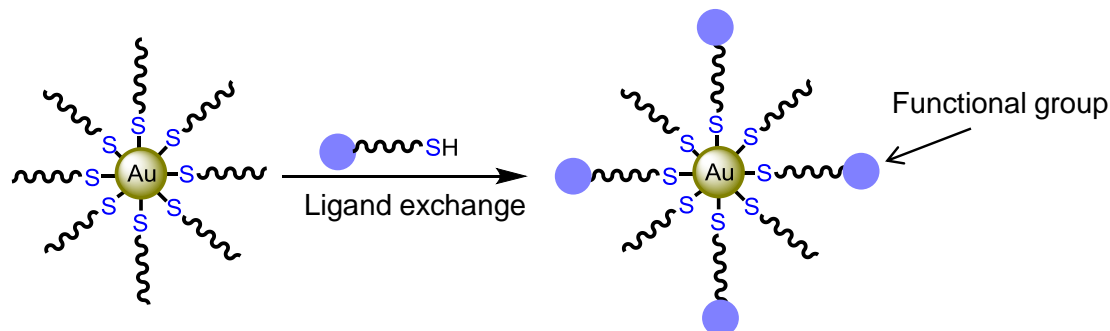
The Brust-Schiffrin method provides very robust AuNPs that are stable and can be repeatedly isolated and re-dissolved in commonly used organic solvents without irreversible aggregation or dissociation, which is crucial for performing post-synthesis modifications on AuNPs.¹⁴¹

1.3.3 Approaches towards Preparation of Functionalized AuNPs

The properties of AuNPs are determined by their core size as well as the surrounding ligands. Development of AuNPs that incorporate complex ligands or molecules, *e.g.* functional AuNPs, needed for interfacial interaction (chemically or physically) with other molecules or substrates is crucial for the expansion of their application in areas such as catalysis, biological and chemical sensors. There are three

main strategies for the preparation of functionalized AuNPs, which include direct synthesis, ligand exchange reactions, and post-synthesis interfacial reactions on AuNPs.

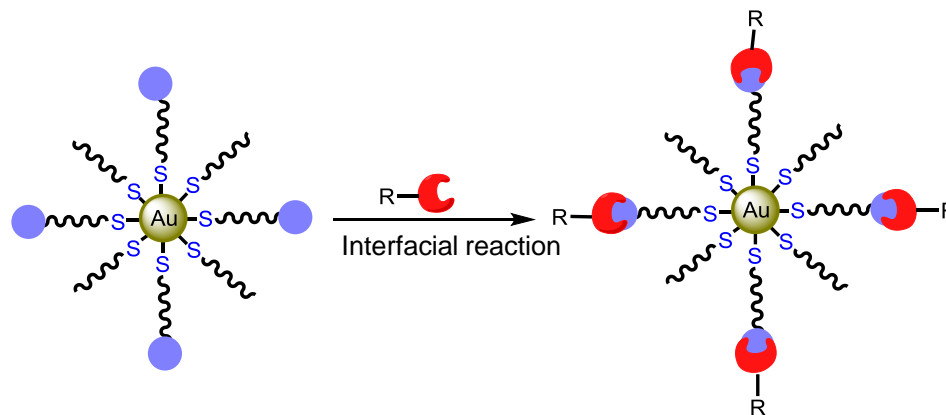
The functional diversity of AuNPs can be extended through the formation of mixed monolayer protected AuNPs that can be synthesized directly or through post functionalization of AuNPs. Because the preparation of AuNPs requires the use of sodium borohydride, substrates containing functional groups that are easily reduced are incompatible with this procedure. A versatile method for the creation of mixed monolayer protected AuNPs is the ligand exchange reaction developed by Murray (Scheme 1.8).¹⁷⁶ In the ligand exchange reaction the bonded thiolate ligands on the originally synthesized AuNPs are readily exchanged with another ligand, simply by exposing the AuNPs to a large excess of the new thiol. The resulting AuNPs usually contain a mixture of both alkanethiolate and functionalized thiolate ligands. Mechanistic studies suggest that the ligand exchange reaction follows a second order-associative (S_N2 -type) pathway in which the rate-determining step depends on the concentration of both the incoming ligand and AuNPs.^{177,178} However, the overall rate and extent of the exchange reaction are affected most by the core size,¹⁷⁸ the electronic charge of the AuNP,¹⁷⁹ and the nature of the incoming ligands, in particular the steric effects.



Scheme 1.8. Functionalization of AuNP by a ligand exchange reaction where resulting AuNP contains a mixture of initial thiol groups and functionalized (incoming) thiols.

Various functional AuNPs have been prepared via the direct synthesis or ligand exchange reactions. However, the synthesis of these thiols can often be tedious and time consuming, or even challenging at times. Therefore, there remains a demand for an alternative approach for AuNP construction. Such methods can include functionalization of AuNPs through an organic reaction of a terminal functional group exposed on the surface of template nanoparticles with various reactants. Using AuNP as a macromolecular-type reagent and carrying out organic reactions on the surface monolayer containing suitable functionality has been shown as a promising method to incorporate new functionality onto AuNPs (Scheme 1.9)^{176,180} Post synthesis interfacial chemical reactions enable the introduction of functional ligands onto the gold core, which are not compatible with thiols or could not be prepared using the direct synthesis or ligand exchange methods. Interfacial reactions can be used as a synthetic platform that allows for simple post-modification of AuNPs. This is a desirable strategy for introducing functionality to the AuNP surface while circumventing the need to synthesize the

nanoparticles and new ligands from the ground up. In addition, the vast majority of interfacial interactions on AuNPs can directly be involved in the application of the nanoparticle itself. For example, nanoparticles used for bio-sensors,¹⁸¹ drug delivery,¹⁸² and optical sensors¹⁸³ all require some form of an interfacial interactions.



Scheme 1.9. Cartoon representation of interfacial reaction on AuNPs to introduce new functionality (R).

1.3.4 Photochemical and Thermal Interfacial Reactions on the Surface of AuNPs

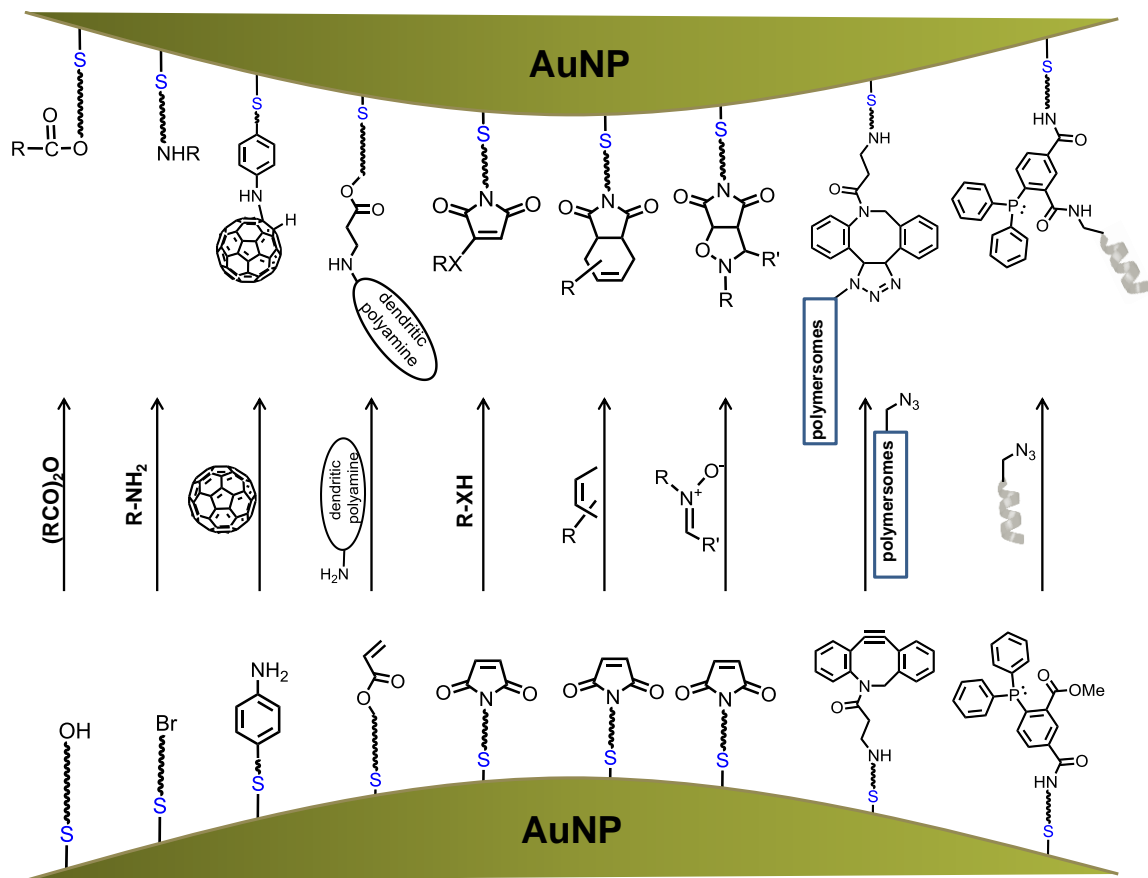
The chemical modification of AuNPs by interfacial reactions has been the subject of numerous studies and it was pursued immediately after the synthesis of the first thiol-protected AuNPs. Brust *et al.* demonstrated the reactivity of *p*-mercaptophenol-protected AuNPs toward esterification of the surface bound phenolic hydroxyl group.¹⁷¹ Since Brust's report, a variety of thermal and photochemical reactions have been explored to modify the surface of AuNPs. Murray's group studied the nucleophilic substitution of

bromide with various alkylamines on bromoalkanethiol modified AuNPs.¹⁸⁴ Shon and co-workers studied the nucleophilic addition of C₆₀ and 4-aminothiophenol/hexanethiolate-protected AuNPs.¹⁸⁵ This methodology has been further applied to the layer-by-layer assembly of the C₆₀-adduct AuNPs film on solid surfaces.¹⁸⁶ Michael addition, is one of the most powerful and useful bond-forming reactions. Simplicity and high yield of this type of reaction make it an ideal candidate for the AuNP modification. Chechik *et al.* investigated Michael addition reactions between acrylate-modified AuNPs and dendritic polyamine.¹⁸⁷ According to their reports these Michael addition reactions on the surface of AuNPs were slightly retarded compared to a similar solution phase Michael addition between a model acrylate and polyamine. Furthermore, the reaction was accompanied by a side trans-esterification reaction of acrylate-modified AuNPs with the solvent (i.e. methanol). Workentin *et al.* utilized Michael addition reactions of amines to modify AuNPs. According to their reports these interfacial Michael additions are rather sluggish at ambient temperature and pressure, often taking days to weeks to go to completion. The rates and efficacies of the these same reactions are drastically increased at hyperbaric pressure conditions (11000 atm) with no observed adverse effect to the AuNPs stability.¹⁸⁸

Cycloaddition reactions are very important tools for organic chemists to generate rings. Azide modified AuNPs have been utilized for the preparation of triazole modified AuNPs through cycloaddition reaction with a variety of alkynes. Williams and co-workers reported the modification of azide terminated AuNPs with a variety of activated alkynes without catalyst.¹⁸⁹ However, according to their results long reaction times (1 - 4

days) were required and the yield of the desired products was extremely low (less than 13% after a 60h reaction in dioxane, depending on the alkynes and could only be slightly improved by altering solvent). Brennan *et al.* attached an acetylene-functionalized lipase onto azide functionalized AuNPs. Their approach suffered from long reaction times (4 days). Meanwhile, a large excess of catalyst and extensive purification were required.¹⁹⁰

Workentin and co-workers studied the reactivity of the organic solvent-soluble maleimide-AuNPs towards the 1,3-dipolar cycloaddition and Diels-Alder reaction.^{191,192} These reactions at the AuNP interface were found to be effective, but with slow kinetics and dominated by steric effects. They addressed this issue by employing very high pressure reaction conditions. Using triethylene glycol monomethyl ether modified AuNPs as building blocks, Workentin *et al.* prepared a series of clickable AuNPs bearing azides, dibenzocyclooctyne (DBCO) or 2-(diphenylphosphino)benzoate moieties through ligand exchange reaction. The azide modified AuNPs were utilized for the preparation of CNT-AuNP hybrid nanomaterials, by reacting the azide functionality attached to the gold core with the DBCO modified CNTs.¹⁹³ The reactivity of the DBCO-AuNPs towards the interfacial SPAAC reaction was demonstrated by using azide-decorated polymersomes as bioorthogonal reaction partner.¹⁹⁴ To showcase the potential utility of the 2-(diphenylphosphino)benzoate functionalized AuNPs in bioorganic chemistry, an AuNP-bioconjugate was prepared by reacting the AuNPs with a novel azide-labeled CRGDK peptide through Staudinger ligation.¹⁹⁵ Some examples of the thermal interfacial reactions on the surface of AuNPs are presented in Scheme 1.10.



Scheme 1.10. Examples of thermal interfacial reactions on AuNPs; left to right: esterification, S_N2 substitution, amination reaction of C_{60} , Michael addition, maleimide Michael addition, Diels Alder, 1,3-dipolar cycloaddition, SPAAC reaction of DBCO, and Staudinger ligation.

Photochemical reactions of suitably functionalized AuNPs can be used to chemically modify nanoparticles. Utilizing photochemical methods simply eliminates the need for the destructive reaction conditions for AuNPs (high temperature and catalyst) and AuNPs can be chemically modified under mild photoreaction conditions at ambient (or lower) temperatures. Workentin *et al.* have done extensive research on photo-initiated chemical reactions to probe interfacial reactivity of organic substrates anchored to AuNPs

and to modify their surfaces. *Ortho*-methylbenzophenone modified AuNPs were irradiated in the presence of a series of dienophiles.¹⁹⁶ Upon irradiation, photogenerated dienols were formed (via γ -hydrogen abstraction) on the AuNPs, followed by a Diels Alder reaction between the attached dienol and the dienophile. They also reported on photochemical interfacial reactions of diazirine functionalized AuNPs that upon irradiation yield reactive carbenes at the AuNP interface. The subsequent insertion reactions of the photo-generated carbenes with trapping reagents such as alcohols, amines, and alkenes afforded AuNPs modified with new functionality.²⁸ They then exploited the same photochemical approach to prepare AuNP-hybrid nanomaterial using diazirine as a tether.¹¹⁻¹³ They later showed that photo-generation of a nitrene on the aryl azide modified AuNPs in the presence of a series of nanomaterials drives the formation of covalently assembled AuNP-based hybrid materials via nitrene insertion reactions. Using this method, hybrids including AuNP-CNT, AuNP-graphene, and AuNP-diamond were prepared.¹⁹⁷

1.3.5 Characterization of AuNPs

Once synthesized, it is important to characterize the AuNPs. Imaging of AuNPs is, perhaps, the most powerful characterization tool available. Visualization of AuNPs can be accomplished by either scanning electron microscopy (SEM)¹⁹⁸ or transmission electron microscopy (TEM). The importance of these imaging techniques comes from the ability to examine multiple characteristics simultaneously. Through examination of images obtained from microscopic techniques information can be obtained about the structure of the nanoparticles²⁰⁰ as well as the shape and size distribution of the AuNPs.

The solubility of AuNPs prepared via the Brust-Schiffrin method in a variety of solvents provides the opportunity to employ traditional analytical techniques to characterize the protecting ligands anchored to the nanoparticles. Nuclear magnetic resonance (NMR) spectroscopy is one of the strongest tools that offers significant information about the composition and structure of the ligands attached onto the AuNPs. Figure 1.10, A displays an example (from our own work) of a typical ^1H NMR spectrum of 2.3 nm functionalized AuNPs (diazirine modified AuNPs). As can be seen, the signals in the ^1H NMR spectrum of functionalized AuNPs are broad; the broadness of the peaks corresponding to ligands attached onto the AuNPs is due to the inhomogeneous AuNP surfaces and Au-S bonding sites, leading to more diverse chemical shifts. Furthermore, slow rotation of thiolates bound to the AuNP core causes a very fast spin-spin relaxation (T_2), which is another factor contributing to this broadening.²⁰¹ The ^1H NMR spectroscopy is also used to investigate the purity of AuNPs. The presence of the free non-bound ligands appears as sharp ^1H NMR signals, while bound ligands (on AuNPs) will appear at the same chemical shift as their non-bound counterparts, however the signals will become much broader as illustrated in Figure 1.10.

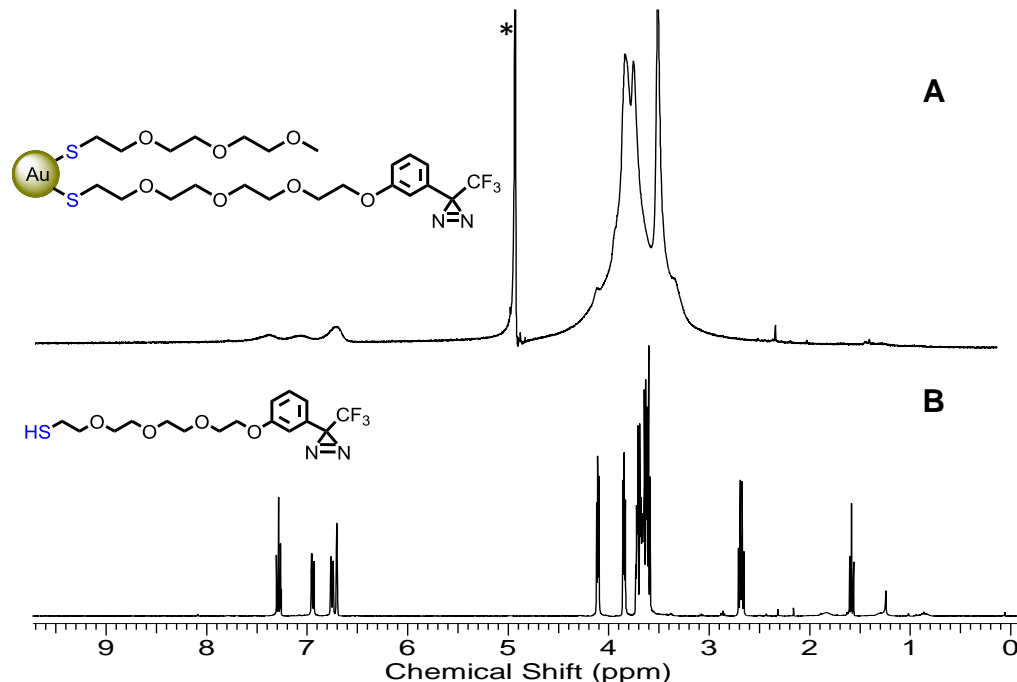


Figure 1.10. ^1H NMR spectra of A) diazirine functionalized AuNPs and B) diazirine-EG₃-SH. * is the residual solvent peak.

As discussed previously, the awareness of the existence of AuNPs came from the characteristic red to purple color. This leads to UV-visible spectroscopy being a very useful characterization tool for AuNPs. The presence of a strong absorption peak, the PR, in the UV-visible spectrum in the range of 500-600 nm is considered diagnostic of the presence of AuNPs larger than 5 nm. One can also use the size and shape of this PR peak to determine the approximate size of the AuNPs in a given medium.²⁰² The peak absorbance wavelength increases with particle diameter and for uneven shaped particles such as gold nanourchins, the absorbance spectrum shifts significantly into the far-red region of the spectrum when compared to a spherical particle of the same diameter.

However, the PR is not observed for the smaller AuNPs with a core diameter less than ~5 nm because of the large band gap.

After determination of the gold core size, number of ligands with respect to the number of gold atoms on the AuNPs, could be easily derived from thermogravimetric analysis (TGA).¹⁵⁹ TGA measures the changes in the weight of a sample as a function of temperature and/or time under a controlled atmosphere (*e. g.* nitrogen). As the temperature increases, the organic ligands are cleaved from the gold core surface and vaporized. The corresponding mass loss accompanying this stage indicates the percentage of organic ligands contained on the surface of the AuNPs.

X-ray Photoelectron Spectroscopy (XPS) is a quantitative technique that characterizes surfaces by atomic composition. The spectroscopic technique works by bombarding the surface with a beam of X-rays and measuring the kinetic energy of electrons that escape from the top 1 to 10 nm of the material being analyzed. XPS has been utilized to characterize AuNPs.²⁰³ A typical XPS spectrum of AuNPs shows peaks corresponding to Au (4f), (4d) and (4p), and S (2s). Sulfur to gold atomic ratio of functionalized gold nanoparticles can be calculated using the Au (4f) and S (2s) peak areas. Furthermore, XPS can provide detail about the various chemical environments analyzed for a particular element present on the surface of AuNPs by exhibiting characteristic peaks.

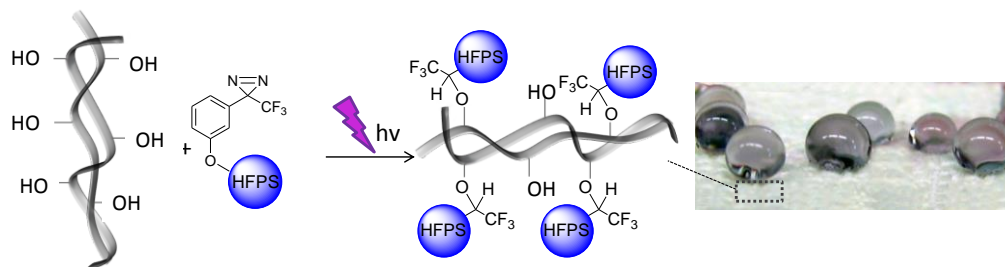
1.4 Thesis objectives

In recent years, surface and interface reactions have dramatically affected device fabrication and material design. Novel surface functionalization techniques with diverse chemical approaches make the desired physical, thermal, electrical, and mechanical properties attainable. Surface modification and functionalization techniques can be applied to a variety of different substrates and nanomaterials to tailor their target properties by designing appropriate chemical reactions. This serves as a crucial step for their subsequent application ranging from electronics to nanomedicine.

In the past, the Workentin group has demonstrated the utility of various thermal and photochemical reactions for modification of organic solvent soluble AuNPs, as well as their usefulness for preparation of hybrid materials. This thesis aims to extend these methodologies for surface modification of materials and to demonstrate their subsequent applications.

Chapters 2 and 3 will present our efforts towards utilizing diazirine photo-precursor as a tether to modify different surfaces. In chapter 2, we describe the synthesis of 3-aryl-3-(trifluoromethyl) diazirine functionalized highly fluorinated phosphonium salts (HFPS). We further demonstrated their utility as photoinduced carbene precursors for covalent attachment of the HFPS onto cotton/paper to impart hydrophobicity to these surfaces (Scheme 1.11). Additionally we show that the chemically grafted hydrophobic coating exhibit high durability towards wash cycles and sonication in organic solvents.

Also, because of the mode of activation to covalently tether the hydrophobic coating, photo-patterning is made possible when employing a photo-mask.

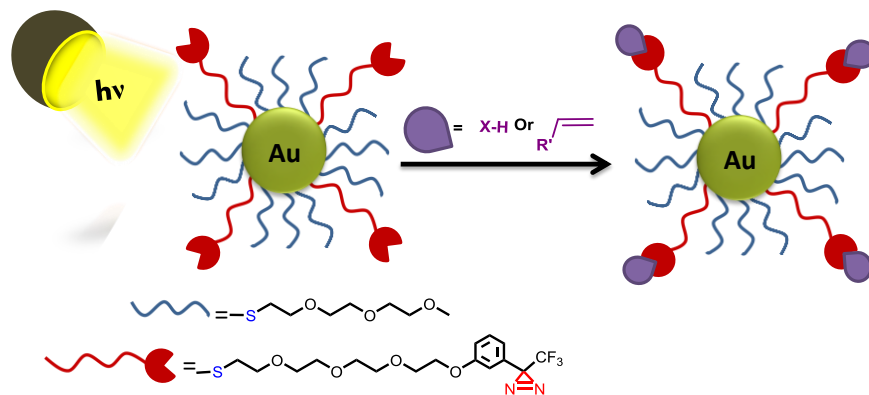


Scheme 1.11. Illustration of the photochemical approach used for surface modification of cotton and paper to prepare hydrophobic surfaces.

AuNPs continue to be an active area of research due to their tunable physical and electronic properties.¹⁴¹ Their application in biomedicine, biotechnology, electronics or catalysis^{204,205} is induced by the characteristics they possess. For the applied use of AuNPs, the nanoparticle's surface needs to be protected by a monolayer of organic ligands with an appropriate functionality. Stabilization of AuNPs by an organic monolayer of choice is not only important for their long term stability, but has also a major effect on their subsequent application. Therefore, developing techniques for manufacturing nanoparticles bearing specific moieties or functionalities can be a key component of all AuNP applications. In this dissertation we demonstrate how versatile photochemical and thermal reactive groups at the interface of AuNPs can be exploited as

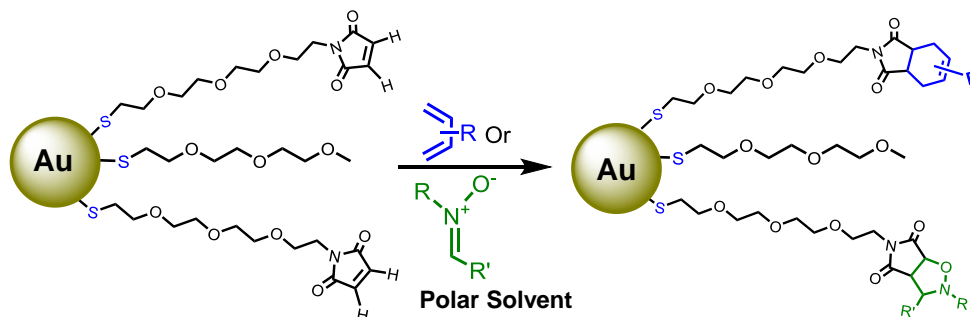
a means for their further modification, preparation of AuNP-conjugates or hybrid materials.

As mentioned previously, AuNPs are sensitive to high temperature or the use of many catalysts. Given that photochemical reactions usually take place under mild reaction conditions, without the need for high temperature or catalyst, they open a new avenue for AuNP modification. Workentin group has previously reported on photochemical interfacial reactions of organic solvent-soluble diazirine functionalized AuNPs that upon irradiation yield reactive carbenes at the AuNP monolayer. The subsequent insertion reactions of the photogenerated carbenes with trapping reagents such as alcohols, amines, and alkenes afforded AuNPs modified with new functionality.²⁸ Chapter 3 reports on the synthesis of novel water- and organic solvent-soluble diazirine functionalized AuNPs and their subsequent photochemical modification (Scheme 1.12). The unique feature of these AuNPs is their amphiphilic character, which expands their potential applications.



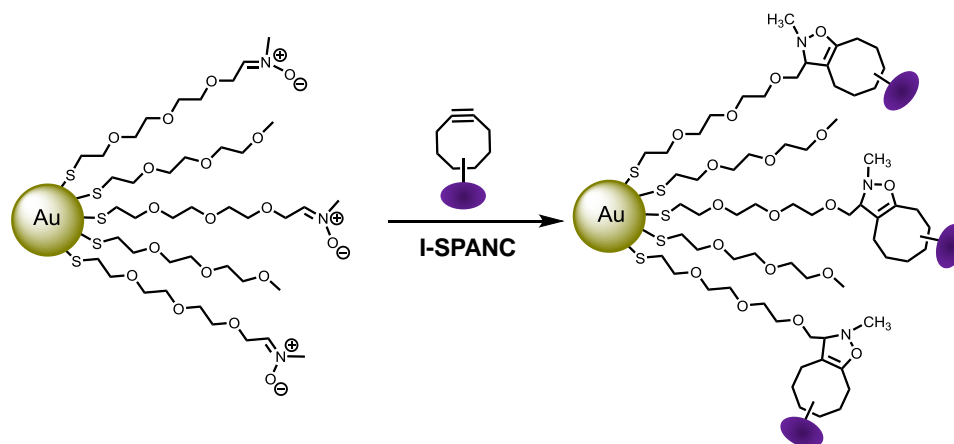
Scheme 1.12. Cartoon representation of photo-induced carbene generation and reactivity of diazirine functionalized AuNPs for interfacial modification.

Chapter 4 and 5 depict the use of “click-type” reactions for the modification of water soluble AuNPs. One of the more attractive functional groups that we successfully introduced onto the AuNP organic shell is the maleimide moiety. A special feature of maleimide reactivity is the double activation of the C=C bond which makes them excellent dipolarophile partners. They are widely known to readily react with a variety of dienes and 1,3- dipoles leading to various carbo- and heterocyclic products. In chapter 4, we demonstrate that by incorporating a maleimide moiety onto the surface of water-soluble AuNPs, it is possible to modify their surfaces cleanly and efficiently using Diels Alder and 1,3-dipolar cycloaddition reactions (Scheme 1.13). Their versatility of these nanoparticles is highlighted by their solubility in a host of organic solvents as well as water and by their ability to quickly undergo three different click reactions under mild conditions, while preserving their size-dependent properties. This ensures an effective, efficient, and safe way to create new nanomaterials and AuNP-bioconjugates.



Scheme 1.13. Schematic representation of water soluble maleimide functionalize AuNPs and their interfacial reactions: Diels Alder (blue), and 1,3-dipolar cycloaddition (green).

Strained cyclooctynes react with nitrones under ambient conditions without need for catalysis. The development and applications of SPANC reactions have brought about new tools for rapid and specific functionalization of biomolecules as well as materials. In chapter 5, we describe a method for the synthesis of AuNPs that incorporate an interfacial nitronium moiety that can be used as a reactive template and undergo an interfacial SPANC reaction (i-SPAAC) with strained alkyne reagents (Scheme 1.14). The fast kinetic, mild reaction conditions and very high yields of SPANC allow us to prepare ^{18}F -labeled AuNPs with potential applications in PET imaging. This methodology can be extended to materials science. To showcase the utility of SPANC for material surface modification, we prepared CNT-AuNP hybrids through the interfacial reaction of nitronium modified AuNPs and BCN functionalized CNTs.



Scheme 1.14. Schematic illustration of i-SPANC reaction using water-soluble AuNPs and a strained alkyne modified substrate.

1.5 References

- 1) Tindale, J. J.; Ragona, P. J. *Chem. Commun.* **2009**, 14, 1831.
- 2) Dorman, G.; Prestwich, G. D. *Biochemistry* **1994**, 33, 5661.
- 3) Delamarche, E.; Sundarababu, G.; Biebuyck, H.; Michel, B.; Gerber, C.; Sigrist, H.; Wolf, H.; Ringsdorf, H.; Xanthopoulos, N.; Mathieu, H. J. *Langmuir* **1996**, 12, 1997.
- 4) Jeyaprakash, J. D.; Samuel, S.; Ruhe, J. *Langmuir* **2004**, 20, 10080.
- 5) Pei, Z.; Yu, H.; Theurer, M.; Waldn, A.; Nilsson, P.; Yan, M.; Ramstrm, O. *ChemBioChem* **2007**, 8, 166.
- 6) Deng, L.; Norberg, O.; Uppalapati, S.; Yan, M.; Ramstrom, O. *Org. Biomol. Chem.* **2011**, 9, 3188.
- 7) Ito, Y. *Biotechnology Progress* **2006**, 22, 924.

- 8) Wang, X.; Ramström, O.; Yan, M. *Adv. Mater.* **2010**, 22, 1946.
- 9) Angeloni, S.; Ridet, J. L.; Kusy, N.; Gao, H.; Crevoisier, F.; Guinchard, S.; Kochhar, S.; Sigrist, H.; Sprenger, N. *Glycobiology* **2005**, 15, 31.
- 10) Chevolut, Y.; Bucher, O.; Léonard, D.; Mathieu, H. J.; Sigrist, H. *Bioconjugate Chem.* **1999**, 10, 169.
- 11) Ismaili, H.; Geng, D.; Sun, A. X.; Kantzas, T. T.; Workentin, M. S. *Langmuir* **2011**, 27, 13261.
- 12) Ismaili, H.; Lagugné-Labarhet, F.; Workentin, M. S. *Chem. Mater.* **2011**, 23, 1519.
- 13) Ismaili, H.; Workentin, M. S. *Chem. Commun.* **2011**, 47, 7788.
- 14) Blencowe, A.; Cosstick, K.; Hayes, W. *New J. Chem.* **2006**, 30, 53.
- 15) Liu, M. T. H.; Choe, Y.-K.; Kimura, M.; Kobayashi, K.; Nagase, S.; Wakahara, T.; Niino, Y.; Ishitsuka, M. O.; Maeda, Y.; Akasaka, T. *J. Org. Chem.* **2003**, 68, 7471.
- 16) Graham, W. H. *J. Am. Chem. Soc.* **1962**, 84, 1063.
- 17) Hafner, K.; Pelster, H. *Angew. Chem.* **1960**, 72, 781.
- 18) Schmitz, E.; Ohme, R. *Chem. Ber.* **1961**, 94, 2166.
- 19) Graham, W. H. *J. Am. Chem. Soc.* **1965**, 87, 4396.
- 20) Smith, R. A. G.; Knowles, J. R. *J. Am. Chem. Soc.* **1973**, 95, 5072.
- 21) Smith, R. A. G.; Knowles, J. R. *J. Chem. Soc., Perkin Trans. 2* **1975**, 7, 686.
- 22) Bayley, H.; Knowles, J. R. *Biochemistry* **1978**, 17, 2420.

- 23) Rosenberg, M. G.; Brinker, U. H. *J. Org. Chem.* **2003**, 68, 4819.
- 24) Frey, H. M.; Scaplehorn, A. W. *J. Chem. Soc. A: Inorg., Phys., Theor.* **1966**, 968.
- 25) Ford, F.; Yuzawa, T.; Platz, M. S.; Matzinger, S.; Fülcher, M. *J. Am. Chem. Soc.* **1998**, 120, 4430.
- 26) Admasu, A.; Gudmundsdottir, A.; Platz, M.; Watt, D.; Kwiatkowski, S.; J. Crocker, P. *J. Chem. Soc., Perkin Trans. 2* **1998**, 5, 1093.
- 27) Blencowe, A.; Hayes, W. *Soft Matter.* **2005**, 1, 178.
- 28) Ismaili, H.; Lee, S.; Workentin, M. S. *Langmuir* **2010**, 26, 14958.
- 29) Brunner, J.; Senn, H.; Richards, F. M. *J. Biol. Chem.* **1980**, 255, 3313.
- 30) Das, J. *Chem. Rev.* **2011**, 111, 4405.
- 31) Hashimoto, M.; Hatanaka, Y. *Eur. J. Org. Chem.* **2008**, 15, 2513.
- 32) Brooks, S. A.; Dontha, N.; Davis, C. B.; Stuart, J. K.; O'Neil, G.; Kuhr, W. G. *Anal. Chem.* **2000**, 72, 3253.
- 33) Lutz, J.-F. *Angew. Chem., Int. Ed.* **2007**, 46, 1018.
- 34) Devaraj, N. K.; Collman, J. P. *QSAR & Combinatorial Science* **2007**, 26, 1253.
- 35) Kolb, H. C.; Finn, M. G.; Sharpless, K. B. *Angew. Chem., Int. Ed.* **2001**, 40, 2004.
- 36) Tietze, L. F.; Ketschau, G. *Stereoselective Heterocyclic Synthesis I* **1997**, 189, 1.
- 37) Waldmann, H. *Synthesis-Stuttgart* **1994**, 6, 535.
- 38) Huisgen, R. *Angew. Chem., Int. Ed.* **1963**, 2, 565.

- 39) Kagabu, S.; Kaiser, C.; Keller, R.; Becker, P. G.; Müller, K.-H.; Knothe, L.; Rihs, G.; Prinzbach, H. *Chem. Ber.* **1988**, 121, 741.
- 40) Suami, T.; Ogawa, S.; Uchino, H.; Funaki, Y. *J. Org. Chem.* **1975**, 40, 456.
- 41) Vogel, E.; Kuebart, F.; Marco, J. A.; Andree, R.; Guenther, H.; Aydin, R. *J. Am. Chem. Soc.* **1983**, 105, 6982.
- 42) Kashemirov, B. A.; Bala, J. L. F.; Chen, X.; Ebetino, F. H.; Xia, Z.; Russell, R. G. G.; Coxon, F. P.; Roelofs, A. J.; Rogers, M. J.; McKenna, C. E. *Bioconjugate Chem.* **2008**, 19, 2308.
- 43) Chandrasekhar, M.; Sekar, G.; Singh, V. K. *Tetrahedron Lett.* **2000**, 41, 10079.
- 44) Im, S. G.; Bong, K. W.; Kim, B.-S.; Baxamusa, S. H.; Hammond, P. T.; Doyle, P. S.; Gleason, K. K. *J. Am. Chem. Soc.* **2008**, 130, 14424.
- 45) Adolfsson, H.; Converso, A.; Sharpless, K. B. *Tetrahedron Lett.* **1999**, 40, 3991.
- 46) Katsuki, T.; Martin, V. In *Org. React.*; John Wiley & Sons, Inc.: 2004.
- 47) Katsuki, T. *J. Mol. Catal. A Chem.* **1996**, 113, 87.
- 48) Kolb, H. C.; VanNieuwenhze, M. S.; Sharpless, K. B. *Chem. Rev.* **1994**, 94, 2483.
- 49) Evans, D. A.; Faul, M. M.; Bilodeau, M. T. *J. Org. Chem.* **1991**, 56, 6744.
- 50) Diels, O.; Alder, K. *Justus Liebigs Ann. Chem* **1928**, 460, 98.
- 51) Fringuelli, F.; Taticchi, A. *The Diels-Alder Reaction: Selected Practical Methods*; John Wiley & Sons: West Sussex, England, 2002.
- 52) Nicolaou, K. C.; Snyder, S. A.; Montagnon, T.; Vassilikogiannakis, G. *Angew. Chem., Int. Ed.* **2002**, 41, 1668.

- 53) Sauer, J.; Sustmann, R. *Angew. Chem., Int. Ed.* **1980**, 19, 779.
- 54) Telan, L. A.; Firestone, R. A. *Tetrahedron* **1999**, 55, 14269.
- 55) Sakai, S. *J. Phys. Chem. A* **2000**, 104, 922.
- 56) Burke, L. A. *Int. J. Quantum. Chem.* **1986**, 29, 511.
- 57) Fleming, I. *Molecular Orbitals and Organic Chemical Reactions: Reference Edition*; John Wiley & Sons: New York, USA, 2010.
- 58) Alder, K.; Stein, G. *Angew. Chem.* **1937**, 50, 510.
- 59) Fotiadu, F.; Michel, F.; Buono, G. *Tetrahedron Lett.* **1990**, 31, 4863.
- 60) Powers, T. S.; Jiang, W.; Su, J.; Wulff, W. D.; Waltermire, B. E.; Rheingold, A. *J. Am. Chem. Soc.* **1997**, 119, 6438.
- 61) García, J. I.; Mayoral, J. A.; Salvatella, L. *Acc. Chem. Res.* **2000**, 33, 658.
- 62) Yeo, W.-S.; Yousaf, M. N.; Mrksich, M. *J. Am. Chem. Soc.* **2003**, 125, 14994.
- 63) Yousaf, M. N.; Mrksich, M. *J. Am. Chem. Soc.* **1999**, 121, 4286.
- 64) Yousaf, M. N.; Houseman, B. T.; Mrksich, M. *Proc. Natl. Acad. Sci. U. S. A.* **2001**, 98, 5992.
- 65) Dillmore, W. S.; Yousaf, M. N.; Mrksich, M. *Langmuir* **2004**, 20, 7223.
- 66) Proupin-Perez, M.; Cosstick, R.; Liz-Marzan, L. M.; Salgueirino-Maceira, V.; Brust, M. *Nucleos. Nucleot. Nucl.* **2005**, 24, 1075.
- 67) McElhanon, J. R.; Wheeler, D. R. *Org. Lett.* **2001**, 3, 2681.
- 68) Szalai, M. L.; McGrath, D. V.; Wheeler, D. R.; Zifer, T.; McElhanon, J. R. *Macromolecules* **2007**, 40, 818.

- 69) Li, M.; De, P.; Gondi, S. R.; Sumerlin, B. S. *J. Polym. Sci. Polym. Chem.* **2008**, 46, 5093.
- 70) Kim, T.-D.; Luo, J.; Tian, Y.; Ka, J.-W.; Tucker, N. M.; Haller, M.; Kang, J.-W.; Jen, A. K. Y. *Macromolecules* **2006**, 39, 1676.
- 71) Shi, Z.; Luo, J.; Huang, S.; Cheng, Y.-J.; Kim, T.-D.; Polishak, B. M.; Zhou, X.-H.; Tian, Y.; Jang, S.-H.; Knorr, J. D. B.; Overney, R. M.; Younkin, T. R.; Jen, A. K. Y. *Macromolecules* **2009**, 42, 2438.
- 72) Dag, A.; Sahin, H.; Durmaz, H.; Hizal, G.; Tunca, U. *J. Polym. Sci. Polym. Chem.* **2011**, 49, 886.
- 73) Tonga, M.; Cengiz, N.; Kose, M. M.; Dede, T.; Sanyal, A. *J. Polym. Sci. Polym. Chem.* **2010**, 48, 410.
- 74) Gungor, E.; Hizal, G.; Tunca, U. *J. Polym. Sci. Polym. Chem.* **2009**, 47, 3409.
- 75) T. Beck, M.; Mándy, G.; Papp, S.; Dékány, I. *Colloid Polym. Sci.* **2004**, 283, 237.
- 76) Guhr, K. I.; Greaves, M. D.; Rotello, V. M. *J. Am. Chem. Soc.* **1994**, 116, 5997.
- 77) Nebhani, L.; Barner-Kowollik, C. *Macromol. Rapid Commun.* **2010**, 31, 1298.
- 78) Ménard-Moyon, C.; Dumas, F.; Doris, E.; Mioskowski, C. *J. Am. Chem. Soc.* **2006**, 128, 14764.
- 79) Hayden, H.; Gun'ko, Y. K.; Perova, T. S. *Chem. Phys. Lett.* **2007**, 435, 84.
- 80) Chang, C.-M.; Liu, Y.-L. *Carbon* **2009**, 47, 3041.
- 81) Delgado, J. L.; de la Cruz, P.; Langa, F.; Urbina, A.; Casado, J.; Lopez Navarrete, J. T. *Chem. Commun.* **2004**, 15, 1734.
- 82) Curtius, T. *Ber. Deut. Bot. Ges.* **1883**, 16, 2230.

- 83) Buchner, E. *Ber. Deut. Bot. Ges.* **1888**, 21, 2637.
- 84) Beckmann, E. *Ber. Deut. Bot. Ges.* **1890**, 23, 3331.
- 85) Werner, A.; Buss, H. *Ber. Deut. Bot. Ges.* **1894**, 27, 2193.
- 86) Pechmann, H. V. *Ber. Deut. Bot. Ges.* **1894**, 27, 1888.
- 87) Michael, A. *J. Prakt. Chem.* **1893**, 48, 94.
- 88) Huisgen, R. *Angew. Chem., Int. Ed.* **1963**, 2, 633.
- 89) Firestone, R. A. *J. Org. Chem.* **1968**, 33, 2285.
- 90) Huisgen, R. *J. Org. Chem.* **1968**, 33, 2291.
- 91) Huisgen, R. *J. Org. Chem.* **1976**, 41, 403.
- 92) Houk, K. N.; Firestone, R. A.; Munchausen, L. L.; Mueller, P. H.; Arison, B. H.; Garcia, L. A. *J. Am. Chem. Soc.* **1985**, 107, 7227.
- 93) Sustmann, R. *Pure Appl. Chem.* **1974**, 40, 569.
- 94) Sustmann, R. *Tetrahedron Lett.* **1971**, 12, 2717.
- 95) Bokach, N. A.; Kukushkin, V. Y. *Russ. Chem. B.* **2006**, 55, 1869.
- 96) Gothelf, K. V.; Hazell, R. G.; Jørgensen, K. A. *J. Org. Chem.* **1996**, 61, 346.
- 97) Padwa, A.; Pearson, W. H. *Synthetic Applications of 1,3-Dipolar Cycloaddition Chemistry Towards Heterocycles and Natural Products*; John Wiley and Sons: New York, USA, 2002.
- 98) Kim, Y.; Kim, J.; Park, S. B. *Org. Lett.* **2009**, 11, 17.

- 99) Jen, W. S.; Wiener, J. J. M.; MacMillan, D. W. C. *J. Am. Chem. Soc.* **2000**, 122, 9874.
- 100) Alemparte, C.; Blay, G.; Jørgensen, K. A. *Org. Lett.* **2005**, 7, 4569.
- 101) Carmona, D.; Lamata, M. P.; Viguri, F.; Rodríguez, R.; Oro, L. A.; Lahoz, F. J.; Balana, A. I.; Tejero, T.; Merino, P. *J. Am. Chem. Soc.* **2005**, 127, 13386.
- 102) Nájera, C.; Sansano, J. M. *Angew. Chem., Int. Ed.* **2005**, 44, 6272.
- 103) Yan, X.-X.; Peng, Q.; Zhang, Y.; Zhang, K.; Hong, W.; Hou, X.-L.; Wu, Y.-D. *Angew. Chem., Int. Ed.* **2006**, 45, 1979.
- 104) Vretik, L.; Ritter, H. *Macromolecules* **2003**, 36, 6340.
- 105) Singh, I.; Zarafshani, Z.; Heaney, F.; Lutz, J.-F. *Polymer Chem.* **2011**, 2, 372.
- 106) Lee, Y.-G.; Koyama, Y.; Yonekawa, M.; Takata, T. *Macromolecules* **2009**, 42, 7709.
- 107) Georgakilas, V.; Kordatos, K.; Prato, M.; Guldi, D. M.; Holzinger, M.; Hirsch, A. *J. Am. Chem. Soc.* **2002**, 124, 760.
- 108) Tagmatarchis, N.; Prato, M. *J. Mater. Chem.* **2004**, 14, 437.
- 109) Callegari, A.; Cosnier, S.; Marcaccio, M.; Paolucci, D.; Paolucci, F.; Georgakilas, V.; Tagmatarchis, N.; Vazquez, E.; Prato, M. *J. Mater. Chem.* **2004**, 14, 807.
- 110) Banerjee, S.; Wong, S. S. *J. Phys. Chem. B* **2002**, 106, 12144.
- 111) Mawhinney, D. B.; Naumenko, V.; Kuznetsova, A.; Yates, J. T.; Liu, J.; Smalley, R. E. *J. Am. Chem. Soc.* **2000**, 122, 2383.

- 112) Zhang, Y.; Luo, S.; Tang, Y.; Yu, L.; Hou, K.-Y.; Cheng, J.-P.; Zeng, X.; Wang, P. G. *Anal. Chem.* **2006**, 78, 2001.
- 113) Hartzel, L. W.; Benson, F. R. *J. Am. Chem. Soc.* **1954**, 76, 667.
- 114) Rostovtsev, V. V.; Green, L. G.; Fokin, V. V.; Sharpless, K. B. *Angew. Chem., Int. Ed.* **2002**, 41, 2596.
- 115) Tornøe, C. W.; Christensen, C.; Meldal, M. *J. Org. Chem.* **2002**, 67, 3057.
- 116) Himo, F.; Lovell, T.; Hilgraf, R.; Rostovtsev, V. V.; Noodleman, L.; Sharpless, K. B.; Fokin, V. V. *J. Am. Chem. Soc.* **2005**, 127, 210.
- 117) Rodionov, V. O.; Presolski, S. I.; Díaz Díaz, D.; Fokin, V. V.; Finn, M. G. *J. Am. Chem. Soc.* **2007**, 129, 12705.
- 118) Chan, T. R.; Hilgraf, R.; Sharpless, K. B.; Fokin, V. V. *Org. Lett.* **2004**, 6, 2853.
- 119) Agard, N. J.; Prescher, J. A.; Bertozzi, C. R. *J. Am. Chem. Soc.* **2004**, 126, 15046.
- 120) Wittig, G.; Krebs, A. *Chem. Ber.* **1961**, 94, 3260.
- 121) Ess, D. H.; Jones, G. O.; Houk, K. N. *Org. Lett.* **2008**, 10, 1633.
- 122) Turner, R. B.; Jarrett, A. D.; Goebel, P.; Mallon, B. J. *J. Am. Chem. Soc.* **1973**, 95, 790.
- 123) Bach, R. D. *J. Am. Chem. Soc.* **2009**, 131, 5233.
- 124) Agard, N. J.; Prescher, J. A.; Bertozzi, C. R. *J. Am. Chem. Soc.* **2005**, 127, 11196.
- 125) Kennedy, D. C.; Lyn, R. K.; Pezacki, J. P. *J. Am. Chem. Soc.* **2009**, 131, 2444.

- 126) Varga, B. R.; Kállay, M.; Hegyi, K.; Béni, S.; Kele, P. *Chem. Eur. J.* **2012**, 18, 822.
- 127) Jewett, J. C.; Sletten, E. M.; Bertozzi, C. R. *J. Am. Chem. Soc.* **2010**, 132, 3688.
- 128) Ning, X.; Temming, R. P.; Dommerholt, J.; Guo, J.; Ania, D. B.; Debets, M. F.; Wolfert, M. A.; Boons, G.-J.; van Delft, F. L. *Angew. Chem., Int. Ed.* **2010**, 49, 3065.
- 129) Dommerholt, J.; Schmidt, S.; Temming, R.; Hendriks, L. J. A.; Rutjes, F. P. J. T.; van Hest, J. C. M.; Lefeber, D. J.; Friedl, P.; van Delft, F. L. *Angew. Chem., Int. Ed.* **2010**, 49, 9422.
- 130) Chigrinova, M.; McKay, C. S.; Beaulieu, L.-P. B.; Udachin, K. A.; Beauchemin, A. M.; Pezacki, J. P. *Org. Biomol. Chem.* **2013**, 11, 3436.
- 131) McKay, C. S.; Moran, J.; Pezacki, J. P. *Chem. Commun.* **2010**, 46, 931.
- 132) McKay, C. S.; Blake, J. A.; Cheng, J.; Danielson, D. C.; Pezacki, J. P. *Chem. Commun.* **2011**, 47, 10040.
- 133) Colombo, M.; Sommaruga, S.; Mazzucchelli, S.; Polito, L.; Verderio, P.; Galeffi, P.; Corsi, F.; Tortora, P.; Prosperi, D. *Angew. Chem., Int. Ed.* **2012**, 51, 496.
- 134) Temming, R. P.; Eggermont, L.; van Eldijk, M. B.; van Hest, J. C. M.; van Delft, F. L. *Org. Biomol. Chem.* **2013**, 11, 2772.
- 135) Ledin, P. A.; Kolishetti, N.; Boons, G.-J. *Macromolecules* **2013**, 46, 7759.
- 136) Sletten, E. M.; Bertozzi, C. R. *Angew. Chem., Int. Ed.* **2009**, 48, 6974.
- 137) Liu, W.; Brock, A.; Chen, S.; Chen, S.; Schultz, P. G. *Nat. Methods* **2007**, 4, 239.

- 138) Sanders, B. C.; Friscourt, F.; Ledin, P. A.; Mbua, N. E.; Arumugam, S.; Guo, J.; Boltje, T. J.; Popik, V. V.; Boons, G.-J. *J. Am. Chem. Soc.* **2011**, 133, 949.
- 139) Faraday, M. *Philos. Trans. R. Soc. London* **1857**, 147, 145.
- 140) Edwards, P. P.; Thomas, J. M. *Angew. Chem., Int. Ed.* **2007**, 46, 5480.
- 141) Daniel, M.-C.; Astruc, D. *Chem. Rev.* **2004**, 104, 293.
- 142) Hu, M.; Chen, J.; Li, Z.-Y.; Au, L.; Hartland, G. V.; Li, X.; Marquez, M.; Xia, Y. *Chem. Soc. Rev.* **2006**, 35, 1084.
- 143) Ghosh, S. K.; Pal, T. *Chem. Rev.* **2007**, 107, 4797.
- 144) Bohren, C. F.; Huffman, D. R. *Absorption and Scattering of Light by Small Particles*; Wiley-Interscience: New York, USA, 1983.
- 145) Rosi, N. L.; Mirkin, C. A. *Chem. Rev.* **2005**, 105, 1547.
- 146) Giljohann, D. A.; Seferos, D. S.; Daniel, W. L.; Massich, M. D.; Patel, P. C.; Mirkin, C. A. *Angew. Chem., Int. Ed.* **2010**, 49, 3280.
- 147) Jain, P. K.; Huang, X.; El-Sayed, I. H.; El-Sayed, M. A. *Acc. Chem. Res.* **2008**, 41, 1578.
- 148) Huang, X.; El-Sayed, M. A. *J. Adv. Res.* **2010**, 1, 13.
- 149) Loo, C.; Lin, A.; Hirsch, L.; Lee, M.-H.; Barton, J.; Halas, N.; West, J.; Drezek, R. *Technology in Cancer Research & Treatment* **2004**, 3, 33.
- 150) Huang, X.; Jain, P. K.; El-Sayed, I. H.; El-Sayed, M. A. *Nanomedicine* **2007**, 2, 681.
- 151) Patra, C. R.; Bhattacharya, R.; Mukhopadhyay, D.; Mukherjee, P. *Adv. Drug Deliver. Rev.* **2010**, 62, 346.

- 152) Xie, J.; Lee, S.; Chen, X. *Adv. Drug Deliver. Rev.* **2010**, 62, 1064.
- 153) Turkevich, J.; Stevenson, P. C.; Hillier, J. *Discussions of the Faraday Society* **1951**, 11, 55.
- 154) Frens, G. *Kolloid-Zeitschrift und Zeitschrift für Polymere* **1972**, 250, 736.
- 155) Dahl, J. A.; Maddux, B. L. S.; Hutchison, J. E. *Chem. Rev.* **2007**, 107, 2228.
- 156) Brust, M.; Walker, M.; Bethell, D.; Schiffrin, D. J.; Whyman, R. *J. Chem. Soc., Chem. Commun.* **1994**, 7, 801.
- 157) Briñas, R. P.; Hu, M.; Qian, L.; Lyman, E. S.; Hainfeld, J. F. *J. Am. Chem. Soc.* **2008**, 130, 975.
- 158) Bachman, R. E.; Bodolosky-Bettis, S. A.; Glennon, S. C.; Sirchio, S. A. *J. Am. Chem. Soc.* **2000**, 122, 7146.
- 159) Hostetler, M. J.; Wingate, J. E.; Zhong, C.-J.; Harris, J. E.; Vachet, R. W.; Clark, M. R.; Londono, J. D.; Green, S. J.; Stokes, J. J.; Wignall, G. D.; Glish, G. L.; Porter, M. D.; Evans, N. D.; Murray, R. W. *Langmuir* **1998**, 14, 17.
- 160) Leff, D. V.; Ohara, P. C.; Heath, J. R.; Gelbart, W. M. *J. Phys. Chem.* **1995**, 99, 7036.
- 161) Whetten, R. L.; Khoury, J. T.; Alvarez, M. M.; Murthy, S.; Vezmar, I.; Wang, Z. L.; Stephens, P. W.; Cleveland, C. L.; Luedtke, W. D.; Landman, U. *Adv. Mater.* **1996**, 8, 428.
- 162) Schaaff, T. G.; Shafigullin, M. N.; Khoury, J. T.; Vezmar, I.; Whetten, R. L.; Cullen, W. G.; First, P. N.; Gutiérrez-Wing, C.; Ascensio, J.; Jose-Yacamán, M. J. *J. Phys. Chem. B* **1997**, 101, 7885.

- 163) Andres, R. P.; Bielefeld, J. D.; Henderson, J. I.; Janes, D. B.; Kolagunta, V. R.; Kubiak, C. P.; Mahoney, W. J.; Osifchin, R. G. *Science* **1996**, 273, 1690.
- 164) Terrill, R. H.; Postlethwaite, T. A.; Chen, C.-h.; Poon, C.-D.; Terzis, A.; Chen, A.; Hutchison, J. E.; Clark, M. R.; Wignall, G. *J. Am. Chem. Soc.* **1995**, 117, 12537.
- 165) Porter, L. A.; Ji, D.; Westcott, S. L.; Graupe, M.; Czernuszewicz, R. S.; Halas, N. J.; Lee, T. R. *Langmuir* **1998**, 14, 7378.
- 166) Shon, Y.-S.; Mazzitelli, C.; Murray, R. W. *Langmuir* **2001**, 17, 7735.
- 167) Chechik, V.; Crooks, R. M. *Langmuir* **1999**, 15, 6364.
- 168) Levin, C. S.; Bishnoi, S. W.; Grady, N. K.; Halas, N. J. *Anal. Chem.* **2006**, 78, 3277.
- 169) Wuelfing, W. P.; Gross, S. M.; Miles, D. T.; Murray, R. W. *J. Am. Chem. Soc.* **1998**, 120, 12696.
- 170) Rowe, M. P.; Plass, K. E.; Kim, K.; Kurdak, Ç.; Zellers, E. T.; Matzger, A. J. *Chem. Mater.* **2004**, 16, 3513.
- 171) Brust, M.; Fink, J.; Bethell, D.; Schiffrin, D. J.; Kiely, C. *J. Chem. Soc., Chem. Commun.* **1995**, 16, 1655.
- 172) Hiramatsu, H.; Osterloh, F. E. *Chem. Mater.* **2004**, 16, 2509.
- 173) Weare, W. W.; Reed, S. M.; Warner, M. G.; Hutchison, J. E. *J. Am. Chem. Soc.* **2000**, 122, 12890.
- 174) Jana, N. R.; Peng, X. *J. Am. Chem. Soc.* **2003**, 125, 14280.
- 175) Prasad, B. L. V.; Stoeva, S. I.; Sorensen, C. M.; Klabunde, K. J. *Chem. Mat.* **2003**, 15, 935.

- 176) Templeton, A. C.; Wuelfing, W. P.; Murray, R. W. *Acc. Chem. Res.* **2000**, 33, 27.
- 177) Hostetler, M. J.; Templeton, A. C.; Murray, R. W. *Langmuir* **1999**, 15, 3782.
- 178) Caragheorghopol, A.; Chechik, V. *PhysChemChemPhys* **2008**, 10, 5029.
- 179) Song, Y.; Murray, R. W. *J. Am. Chem. Soc.* **2002**, 124, 7096.
- 180) Chechik, V. *Annu. Rep. Prog. Chem. Sec. B: Org. Chem.* **2006**, 102, 357.
- 181) Guo, S.; Wang, E. *Nano Today* **2011**, 6, 240.
- 182) Gibson, J. D.; Khanal, B. P.; Zubarev, E. R. *J. Am. Chem. Soc.* **2007**, 129, 11653.
- 183) Ghosh, S. K.; Pal, T. *PhysChemChemPhys* **2009**, 11, 3831.
- 184) Templeton, A. C.; Hostetler, M. J.; Kraft, C. T.; Murray, R. W. *J. Am. Chem. Soc.* **1998**, 120, 1906.
- 185) Deng, F.; Yang, Y.; Hwang, S.; Shon, Y.-S.; Chen, S. *Anal. Chem.* **2004**, 76, 6102.
- 186) Shon, Y.-S.; Choo, H. *Chem. Commun.* **2002**, 21, 2560.
- 187) Koenig, S.; Chechik, V. *Langmuir* **2003**, 19, 9511.
- 188) Hartlen, K. D.; Ismaili, H.; Zhu, J.; Workentin, M. S. *Langmuir* **2012**, 28, 864.
- 189) Fleming, D. A.; Thode, C. J.; Williams, M. E. *Chem. Mater.* **2006**, 18, 2327.
- 190) Brennan, J. L.; Hatzakis, N. S.; Tshikhudo, T. R.; Razumas, V.; Patkar, S.; Vind, J.; Svendsen, A.; Nolte, R. J. M.; Rowan, A. E.; Brust, M. *Bioconjugate Chem.* **2006**, 17, 1373.

- 191) Zhu, J.; Lines, B. M.; Ganton, M. D.; Kerr, M. A.; Workentin, M. S. *J. Org. Chem.* **2008**, 73, 1099.
- 192) Zhu, J.; Ganton, M. D.; Kerr, M. A.; Workentin, M. S. *J. Am. Chem. Soc.* **2007**, 129, 4904.
- 193) Gobbo, P.; Novoa, S.; Biesinger, M. C.; Workentin, M. S. *Chem. Commun.* **2013**, 49, 3982.
- 194) Gobbo, P.; Mossman, Z.; Nazemi, A.; Niaux, A.; Biesinger, M. C.; Gillies, E. R.; Workentin, M. S. *J. Mater. Chem. B* **2014**, 2, 1764.
- 195) Gobbo, P.; Luo, W.; Cho, S. J.; Wang, X.; Biesinger, M. C.; Hudson, R. H. E.; Workentin, M. S. *Org. Biomol. Chem.* **2015**, 13, 4605.
- 196) Kell, A. J.; Montcalm, C. C.; Workentin, M. S. *Can. J. Chem.* **2003**, 81, 484.
- 197) Snell, K. E.; Ismaili, H.; Workentin, M. S. *ChemPhysChem* **2012**, 13, 3185.
- 198) Zhou, W.; Wang, Z. L. *Scanning Microscopy for Nanotechnology*; Springer: New York, USA, 2006.
- 199) Reimer, L.; Kohl, H. *Transmission Electron Microscopy*; Springer-Verlag: New York, 2008.
- 200) Schmid, G.; Corain, B. *Eur. J. Inorg. Chem.* **2003**, 17, 3081.
- 201) Song, Y.; Harper, A. S.; Murray, R. W. *Langmuir* **2005**, 21, 5492.
- 202) Kelly, K. L.; Coronado, E.; Zhao, L. L.; Schatz, G. C. *J. Phys. Chem. B* **2003**, 107, 668.
- 203) Castner, D. G.; Hinds, K.; Grainger, D. W. *Langmuir* **1996**, 12, 5083.

204) Stewart, M. E.; Anderton, C. R.; Thompson, L. B.; Maria, J.; Gray, S. K.; Rogers, J. A.; Nuzzo, R. G. *Chem. Rev.* **2008**, 108, 494.

205) Thanh, N. T. K.; Green, L. A. W. *Nano Today* **2010**, 5, 213.

Chapter 2

Photoinduced Carbene Generation from Diazirine Modified Task Specific Phosponium Salts to Prepare Robust Hydrophobic Coatings

- This chapter has been published as a full paper. The corresponding reference is: Sara Ghiassian, Hossein Ismaili, Brett D. W. Lubbock, Jonathan W. Dube, Paul J. Ragona, and Mark S. Workentin, *Langmuir*, **2012**, 28, 12326-12333.
- Hossein Ismaili and Brett D. W. Lubbock were involved in the initiation of the project. Jonathan W. Dube helped setting up the reactions with phosphines in the glove box. All the experimental work reported in chapter 2 was carried out by Sara Ghiassian under the supervision of Dr. Workentin. The manuscript was initially drafted by Sara Ghiassian and Dr. Workentin and Dr. Ragona provided assistance with editing and final preparation.
- All of the schemes, figures, and text in chapter 2 reprinted with permission from ©2012 American Chemical Society.

2.1 Introduction

There is a host of potential applications of hydrophobic coatings in such things as microfluidic ¹ or biomedical devices,² self-cleaning and impermeable textiles,^{3,4} as well as in the printing and packaging industries.⁵ Recent successful efforts to prepare superhydrophobic surfaces have involved the incorporation of nanoparticles (to provide uniform surface roughness) or using a mechanically roughened rigid surface prior to deposition of the hydrophobic layer.^{6,7} The chemical modification of surfaces with low-surface-energy functionalities, especially fluorine-containing hydrocarbons or perfluorosilanes, is an efficient and practical method to fabricate a hydrophobic surface. In addition to the more common use of small fluorinated molecules for preparing coatings, fluorinated silica nanoparticles have also been used to produce rough superhydrophobic surfaces.^{8,9,10} However, in many cases the deposited layer on the surface should have a thickness equal or higher than the particle diameter and having such a thick layer of coating can change the intrinsic properties of the substrate and damage its transparency.

Highly fluorinated phosphonium salts (HFPS) have demonstrated promise in a wide variety of fields over the last several years ¹¹ in areas such as surfactants,¹² solvents for phase transfer catalysis,¹³ but only more recently have we demonstrated it as an effective medium for imparting hydrophobic properties to various metal surfaces such as Au and Ag.^{14,15} The advantage the HFPS systems possess, compared to other strategies, is that the phosphonium salts can be readily modified using selective substitution chemistry on

the phosphorus center, which is much more difficult to obtain in related C- or Si-centered and even polymer systems. In this way, using a small number of simple quantitative transformations one can impart specific functionality onto the cation. A drawback of the HFPS we described earlier and indeed other systems mentioned above is that they lack a *universal tether* or they need to have functionality tailored for a specific surface. So, despite the many successes there remains a need for the development of materials that allow for facile, efficient and mild approaches to impart hydrophobic character more universally on any surface.

Using photolinkers is a versatile method for covalent attachment of molecules onto surfaces. Common highly efficient photolinkers used generally include diaryldiazo,¹⁶⁻¹⁹ azide,²⁰⁻²² and diazine²³⁻²⁶ molecules that generate highly reactive carbene or nitrene intermediates that then react with functionality native to or deliberately functionalized onto the desired surface. To the best of our knowledge only diaryldiazo and azide photoactivation have been used to tether hydrophobic substrates onto surfaces. For example, very recently Ling *et al.* reported the use of azide functionalized silica nanoparticles as a way to impart hydrophobicity to cotton fiber.²⁷ To date the diazine moiety has not been used in this sort of technology. However, it has been suggested that diazine as a photolinker can be more beneficial because aryl azides can generate a singlet nitrene that can undergo a ring expansion and to a much less reactive species and many diazo-compounds suffer from low thermal stability. The use of diazine however combines the high reactivity of a carbene with its inherent high stability. Compounds containing 3-aryl-3-(trifluoromethyl) diazine moieties are accessible synthetically useful

carbene precursors. Their most common application is in photoaffinity labeling, prolific in biological applications.²⁸⁻³⁰ The ease of synthesis, excellent thermal and chemical stability of the diazirine as well as its nearly quantitative photochemical generation of a reactive carbene, which reacts with a wide range of functionalities (*e.g.* C=C; X-H bonds),^{23,30,31} are the basis of its widespread use in these applications.³² However utilizing the diazirene functionality for the modification of substrates in polymer and materials science remain relatively unexplored. Hayes and coworkers in particular have utilized this chemistry creatively, mainly for the modification of polymers.^{23,30,33-35} We have recently established the utility of this diazirine moiety as the carbene precursor for the modification of other materials, including CNT, diamond, graphene and glass surfaces with gold nanoparticles.²⁴⁻²⁶ In these studies the photochemistry of 3-aryl-3-(trifluoromethyl)diazirine is utilized to generate the carbene to tether the attached gold nanoparticles (AuNPs) via insertion into the native C=C or C-H, or O-H functionality inherent on these substrates. The result is a suite of covalent hybrid materials containing the properties of both the host material and the AuNP. Lawrence et al. has used this protocol recently to append acyl ferrocene as a redox active functional group onto CNT.^{36,37}

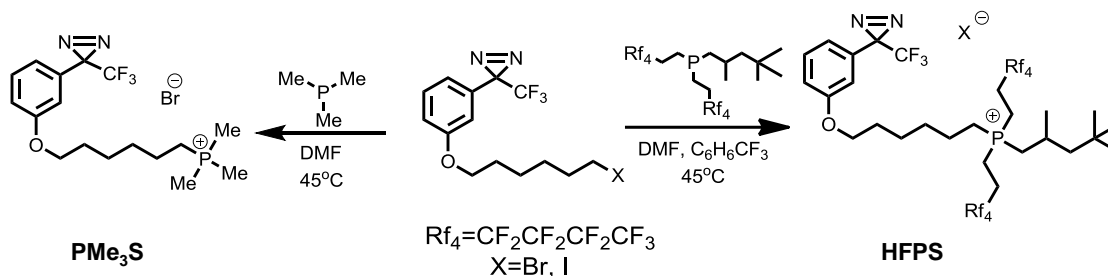
In the present report we extend the applications of the photochemistry of diazirines to new functional materials by incorporating the photoactive diazirine moiety onto the structure of a novel hydrophobic HFPS. The high hydrophobicity imparted by the HFPS especially given the relatively small fluorinated chain length makes this material commercially viable from an environmental perspective, compared to many that use

longer fluorinated hydrocarbons. We utilize the high reactivity of the photo-generated carbene to attach the HFPS to form robust hydrophobic coatings on model cotton and paper surfaces simply and efficiently. Because the carbene reacts with virtually any functional group, the approach provides a way to marry the high reactivity of the carbene with the newly discovered use of HFPS to introduce hydrophobicity efficiently and generally to any substrate/surface. The process is photochemically activated and allows for the coverage of macro-scale substrates and surface patterning, which has implications for the application of this technology at the micro- and nanoscale. Because the highly fluorinated phosphine used in the synthesis of our novel diazirine-HFPS is available in commercial quantities and can be made in the 100g-1Kg scale in our lab and the required diazirine can be prepared in multi-gram quantities through a series of simple organic transformations, the approach allows for the exploration of potential applications of the proof of concept results described herein.

2.2 Results and Discussion

The 3-aryl-3-(trifluoromethyl)diazirine functionalized perfluorinated phosphonium salts HFPS [X] (X = Br or I) were prepared by reacting the 3-(3-(6-haloheptyloxy)phenyl)3-(trifluoromethyl)-3H diazirine derivatives (halo = Br or I) with a highly fluorinated alkyl phosphine (RP[(CH₂)₂Rf₄]₂ (R = 2,4,4-trimethylpentyl, Rf₄ = (CF₂)₄CF₃) via a quaternization reaction, with bromide or iodide as the counter ion. The reaction involved mixing a solution of the diazirine in dimethylformamide with a solution

of $C_8H_{17}P(CH_2Rf_4)_2$ in trifluorotoluene under inert atmosphere (N_2), as illustrated in Scheme 2.1.



Scheme 2.1. Reaction pathway towards the synthesis HFPS and the model compound PMe_3S .

The reaction mixture was stirred at 45 °C, and monitored by $^{31}P \{^1H\}$ NMR spectroscopy over this period, by following the disappearance of the phosphine ($\delta_p = -30$ ppm) and the appearance of the signal from the phosphonium ion. Upon disappearance of the characteristic resonance of the precursor phosphine, the reaction was exposed to air to convert any trace unreacted phosphine to the oxide then worked up with water. The product was characterized using multinuclear NMR and IR spectroscopy, mass spectrometry and TGA. Although both the bromide and iodide salts of HFPS behaved similarly in further chemical tests and exhibited all the specifications that were sought for surface modification of various substrates, the I^- salt is the preferred target: the quaternization reaction is generally slow due to the attenuated nucleophilicity of the fluorinated phosphine and because the reaction is performed at temperatures not exceeding 45 °C to avoid thermal degradation of the diazirine. To achieve a faster and

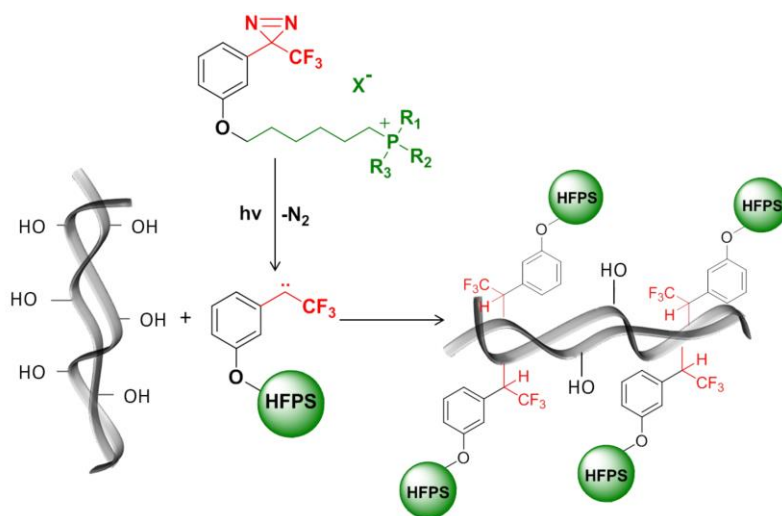
more efficient method for synthesizing the target, the 3-(3-(6-iodohexyloxy)phenyl)3-(trifluoromethyl)-3H diazirine derivative, formed by halide exchange from the corresponding bromo derivative is preferred and using it results in a pure product.³⁹ The HFPS were viscous liquids, exhibiting single signals in the ³¹P NMR spectrum ($\delta_p = 35$ ppm), and the expected signals in the ¹⁹F NMR spectrum ($\delta_F = -65$ ppm (CF₃ of diazirine), and -81, -114, -124 and -126 ppm (fluorinated alkyl chains). The glass transition temperature ($T_g = -27.2$ °C) and decomposition temperature ($T_d = 304.2$ °C) were also determined for HFPS [I]. The model compound PMe₃S was also prepared in a similar manner using trimethylphosphine; in this case the reaction proceeds much more readily (3 h) because of the more nucleophilic and less sterically encumbered phosphine. Compound PMe₃S was used as a model to demonstrate that any change observed in the surface properties of the substrates is in fact due to grafting the HFPS on the surfaces and not simply due to the diazirine CF₃ or phosphonium ion moieties.

As a proof of principle of using the diazirine moiety as the carbene precursor to insert into the native functionality of the surfaces to act as a molecular tether, the reactivity of the salt HFPS was studied upon exposure to UV light in the presence of methanol as a model O-H containing molecule. The *m*-methoxyphenyl(trifluoromethyl) carbene is known to be a ground state triplet, however, its reactivity generally corresponds to that of the singlet carbene (namely insertion reactions).⁴⁰ A solution of HFPS [I] in methanol was purged with argon to remove any oxygen, and then irradiated ($\lambda > 300$ nm) with a medium pressure Hg lamp. The course of the reaction was monitored with ¹⁹F NMR spectroscopy. The starting material peak at $\delta_F = -65$ ppm (CF₃ of

diazirine) disappeared and a new peak at $\delta_F = -77$ ppm known to be that due to the methanol insertion product appeared quantitatively, verifying the reactivity of carbene for insertion into O-H bonds.³⁸ The details of these model reactions are provided in the experimental section.

To demonstrate the utility of HFPS as a photo precursor to a reactive carbene that can be used to graft the hydrophobic properties of the HFPS, we chose cotton fabric and paper as proof of concept materials. Both of these substrates are known to be rich in O-H and C-H bonds on the surface, which can react with the photo generated carbene via insertion reactions. The 100% cotton fabric was purchased and cleaned by washing with detergent and deionized water three times and then dried in a 60 °C oven. The paper substrate (simple plain white printer paper, 92 Bright) was used as obtained with no pre-treatment. For photo coating, cotton or paper substrate was immersed into a solution of the prepared HFPS in THF for 10 mins and allowed to dry in the dark. This process was repeated up to three times to ensure a film of the HFPS was on the surface of each substrate. Next, the coated sample was placed in a sealed Pyrex vessel, which was purged with argon gas for 30 mins and then irradiated with UV light ($\lambda > 300$ nm) on both sides using a medium pressure Hg lamp. Upon irradiation the diazirine loses N_2 and generates a carbene reactive intermediate that inserts into X-H bonds.^{30,38} The general photochemical reaction that was utilized for grafting the salts HFPS and PMe_3S onto the surfaces of cotton and paper is illustrated in Scheme 2.2. After irradiation, to remove any unbound, physisorbed HFPS from the surface, the HFPS-photo-coated sample was washed repeatedly with THF and dichloromethane, respectively and then allowed to air

dry. In parallel, dark control samples consisting of cotton/paper samples that were similarly prepared with the HFPS, were left in the dark for 24 hrs (not exposed to UV irradiation) and then washed using the same protocol as used for the light treated samples.



Scheme 2.2. Illustration of photochemical reaction used for surface modification of cotton and paper using HFPS and PMe_3S .

To demonstrate the influence of the HFPS solution concentration on the resulting wetting behavior, we prepared HFPS-coated surfaces on cotton and paper using the same protocol explained above, with concentrations of 1, 2, 5, 7, 10 and 20 mg/mL of HFPS [I] in THF and irradiated them for 1 hour. Figure 2.1 shows the dependency of the water contact angle on the concentration of the solution used for coating. Even surfaces coated with very dilute solution (1 mg/mL) exhibit high contact angles after the irradiation and

washing protocol. Although there is an increase in the water repellency when using more concentrated solutions, we observed that with concentrations higher than 10 mg/mL we not only damage the transparency of the substrate but also decrease the contact angle. We believe that, when too concentrated a solution is used, the density of the diazirine molecules on the surface increases. When exposed to UV light, this high density can lead to dimerization of the reactive carbene species at the expense of reactions of the carbene reacting with the OH groups present on the surface. These dimers would simply be rinsed away in the washing protocol.

Using the optimized coating concentration (5 mg/mL solution of HFPS [I] in THF) we then performed experiments to monitor the effect of irradiation time on the resulting hydrophobicity of the light treated substrates while all the other factors were kept constant. Figure 2.1 shows the change in the water contact angles on cotton with time under our irradiation conditions. There are two important observations. The first is that even after very short irradiation times the samples show high degree of hydrophobicity (anti-wetting). The second is that while there is an increase in contact angle with the increase in UV exposure no significant change was observed over 60 mins of irradiation under our conditions. Using more lamps (increased intensity) will lead to shorter irradiation times, but for consistency, especially when treating the small analytical samples in this study we used 60 mins of irradiation under our conditions to prepare the hydrophobic substrates for further testing.

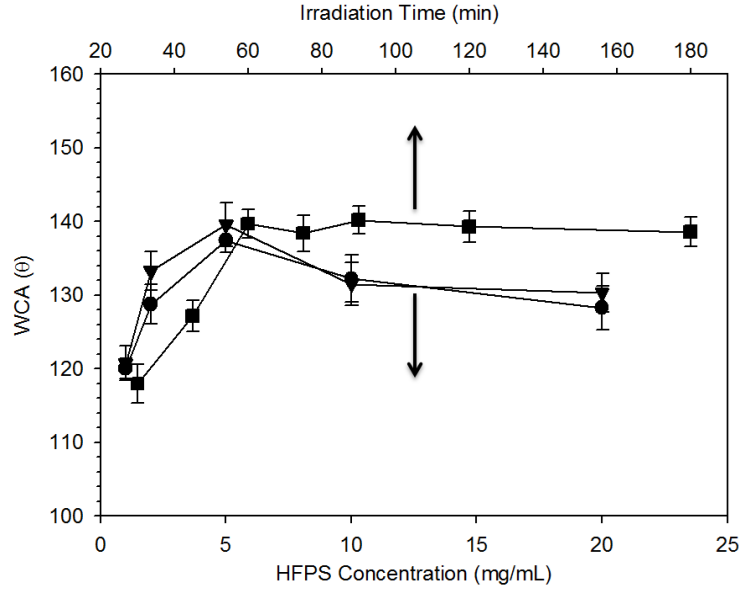


Figure 2.1. Variation in water contact angles as a function of irradiation time of 5 mg/ml samples (square, top scale) and as a function of the HFPS [I] concentration on both cotton (inverted triangle, bottom scale) and paper (circle, bottom scale).

We investigated the surface characteristics of treated samples and compared with those of the untreated samples visually and analytically using SEM, XPS and contact angle measurements. The surface morphology of treated and untreated cotton/paper was examined using SEM (see Figure S2.1). In this study we used the optimized concentrations of the HFPS, which leads to a very thin layer on the surface. SEM micrographs of the modified samples and their unmodified counterpart did not show any obvious change in diameter or structure of the fibers. There were likewise no other visible changes in color or bulk morphology to the irradiated samples under the conditions of the irradiation. The fact that no obvious change was observed after treating/irradiating substrates supports the thinness of the coatings. As a result we did not

damage the transparency or color of the cotton or paper. The surface of modified samples was also smooth and no destruction of cotton/cellulose fibers was indicated.

More dramatic was the change in the surface wetting properties of the samples, which were evaluated visually and by measuring water contact angles (Figure 2.2). The stability of the water droplets on treated cotton/paper was in complete contrast with the untreated ones. It is well known that both cotton and paper are rich in hydroxyl groups and are therefore very hydrophilic. After chemically grafting the surface with HFPS all the light treated samples were found to be highly hydrophobic as illustrated by the photographs in Figure 2.2, while the water droplet soaked into the untreated and dark surfaces immediately after deposition. In Figure 2.2 the water droplets were colored for more easily visualization. Also included in this figure are images showing the hydrophobic nature from contact angle measurements using water placed on the irradiated cotton and paper substrates (Figure 2.2, D and H). The water contact angles were measured 30 s after a 5 μ L water droplet was placed on the surface. It is worth noting that those fibers protruding out from the cotton surface made the contact angle measurement somewhat difficult. Due to the inherent roughness of the cotton fabric determining the baseline is less straightforward and this can lead to possible underestimation of the contact angle data. For each specimen, the contact angle reported is the average of at least 5 different readings on different spots on the surface. The irradiated cotton and paper surfaces treated with HFPS exhibited average water contact angles (θ) as high as 139.5° and 137.4°, respectively. The lack of hydrophobicity of the dark samples demonstrates that the photo treatment is necessary and suggests that it is the

formation of the carbene and subsequent covalent bonding to the substrate via carbene insertion reactions that leads to the robust hydrophobic coating. The magnitude of the observed contact angles are approaching those of surfaces that have a micro/nanoscale roughness, and are ultimately superhydrophobic ($\theta \geq 150^\circ$).⁸⁻¹⁰ The effect is dramatic especially when one considers that the surfaces that did not undergo irradiation prior to washing simply absorb the water due to the abundance of the hydroxyl groups in the structure.

On the light treated surfaces (Figure 2.2, C and G) the water droplet remained on the surface indefinitely while maintaining their shape and high contact angles; only disappearing through evaporation. These droplets could be simply removed by picking up the substrate and shaking them off or wicking using a Kimwipe or pipette (see Figure S2.2).

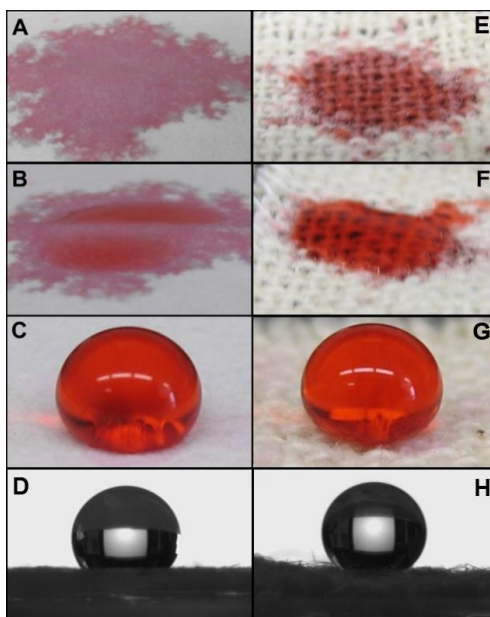


Figure 2.2. Pictures of colored water droplets (colored to aid visualization) placed on standard printer paper samples (left column) and cotton (right column): A and E untreated, B and F treated-dark sample (no irradiation), and C and G treated with HFPS and irradiated. D (paper) and H (cotton) are representative pictures of water contact angle measurements.

Interestingly, even though the surface was coated with a low surface energy compound and exhibited large water contact angles, while measuring contact angle hysteresis we observed “petal effect” on all the treated surfaces.^{41,42} For all the paper/cotton fabric surfaces contact angle hysteresis was relatively high ($>10^\circ$). The small water droplets stuck to the surface when the sample was tilted vertically (90°) or even turned upside down (180°) (See Figure S2.3). This indicates that there is a strong adhesion between the water droplet and the modified surfaces. Such surfaces are expected to have many potential applications, such as sticky tapes,⁴³ for liquid transportation in microfluidic devices,⁴⁴ or two-dimensional lab on paper devices.⁴⁵

Larger water droplets, like those from a Pasteur pipette bead or larger, roll off of the substrates.

To obtain further evidence of coating of the HFPS on the surface of cotton and paper, XPS analysis was performed on both treated light and dark samples and untreated samples. Analysis of the spectra (Figure 2.3) indicates that there is a relatively large peak related to fluorine (10.3 %) in the light treated cotton spectrum that is not observed in XPS of the native sample. This proves that they are in fact coated with a film of HFPS. Although the fluorine peak is also present in XPS of the dark sample, the relative intensity is significantly smaller (1.9%) by comparison to the C and O signals. With the paper sample the results are 7.4 and 1.4%, respectively. Contact angle measurements confirm that the much lower fluorine incorporation in the dark control sample (likely due to some physical absorption or thermal carbene activation) is not enough for the sample to exhibit hydrophobicity.

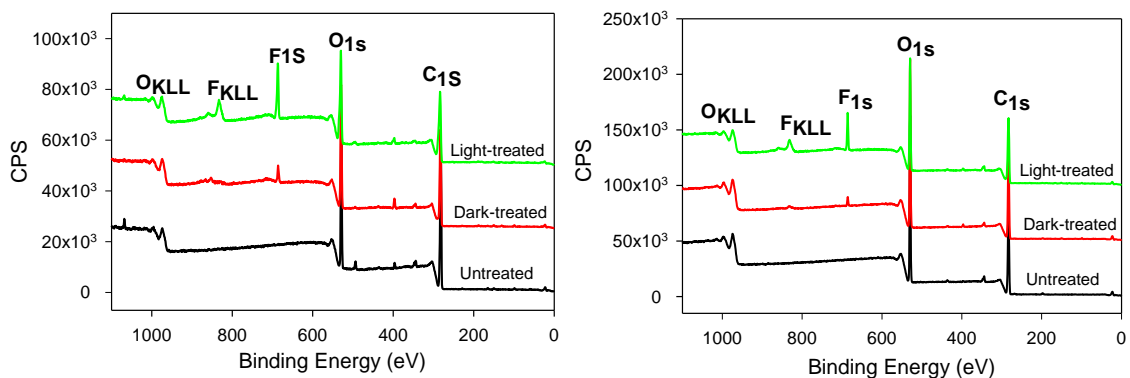


Figure 2.3. XPS spectra of: treated, treated with no light (dark treated) and untreated cotton (left) and paper (right) with HFPS.

Control over interfacial adhesion is particularly important when integrating the material into a device design. In our case, the photogenerated carbene can be used to impart well-defined surface functionality with water repellent properties. The chemical stability and overall robustness of this coating is dictated by the molecular interaction between the coating and the substrate. As a result, in order to remove the chemically grafted HFPS coating from the substrate, covalent bonds must be broken. To find out how strongly the hydrophobic layer is attached to the surface, we subjected the treated samples to two washing protocols. Hydrophobic substrates were immersed in sonication baths of 3 different solvents that wet the surface completely (EtOH, THF and DCM), for 5 min periods each time. Water contact angle measurements reveal that even after repeated sonication there is no significant change in the wetting properties of these surfaces. For a representative piece of treated cotton, water contact angles were measured to be $138.7^{\circ} \pm 2.4^{\circ}$ and $136.8^{\circ} \pm 3.7^{\circ}$ before and after the sonication process, respectively. We also subjected the coated cotton samples to simulated wash cycles where the samples were washed in water containing detergent for 15 mins and then rinsed in water for 15 mins. After each wash cycle the substrate was dried before measuring the contact angle. Illustrated in Figure 2.4, is measure of the water contact angle as a function of wash cycle; no significant change was observed in the water contact angles even after 10 of these wash cycles. These results support the claim of robustness of our coating that originates from covalent bond between the HFPS and the surface.

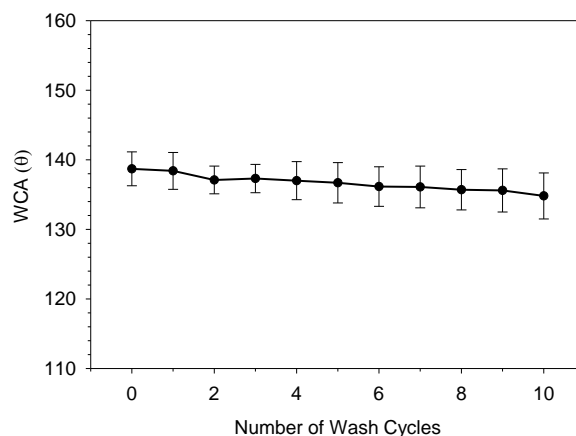


Figure 2.4. Change in the water contact angle (WCA) as a function of simulated wash cycles on treated cotton sample treated with HFPS [I], irradiated and washed.

Having demonstrated that the HFPS can modify the wetting behavior of the cellulose fiber material surfaces and produce hydrophobic surfaces, we also carried out additional sets of control experiments. Samples of cotton and paper were treated with the non-fluorinated salt PMe_3S , according to the previously explained procedure. Hydrophobicity tests performed on these treated surfaces after irradiation and washing cycles, showed no hydrophobic properties, with the water absorbing promptly after deposition. This suggests that it is the highly fluorinated phosphonium moiety that imparts the (majority of) hydrophobicity and that the CF_3 of the diazirine is not sufficient. Of course, the alkyl phosphonium salt (no fluorinated chains) would be expected to make the sample hydrophilic and mask any potential hydrophobicity imparted by the CF_3 of the diazirine or the appended alkyl chain. Cotton/paper samples treated with either 3-(3-methoxyphenyl)3-trifluoromethyl)-3Hdiazirine or 3-(3-(6-iodohexyloxy)phenyl)3-

(trifluoromethyl)-3H diazirine at the same concentrations used for HFPS and subjected to identical irradiation conditions were similarly found to be non-hydrophobic.

By taking advantage of the photosensitivity of the diazirine in HFPS, patterning can be achieved on the surfaces using a crude photo-mask. This is a simple and inexpensive method that enables us to develop any hydrophobic pattern on various surfaces even in the microscale that can be utilized in biochemical assay devices.⁴⁶⁻⁴⁸ As a proof of concept, to produce a simple patterned hydrophobic surface, a paper substrate coated with HFPS was covered with a shadow mask with only circular gap allowing the substrate to be exposed to the light in that area. After irradiation followed by rinsing the paper with THF, the surface wetting properties were tested. The circular area exposed to light (indicated by a dark circle drawn with pencil to aid in visualization) exhibited the high hydrophobicity while water soaked into the other masked areas (see Figure 2.5). With such a simple method for patterning one can create well-defined hydrophobic and hydrophilic channels. This method is compatible with small pieces of paper as well as large. By using the patterning method we will have control over the hydrophobicity of the paper surface. Therefore, these surfaces can serve as paper-based lab-on-a-chip devices (lab-on-paper) that allow the transport, mixing or sampling of the liquid droplets all on the paper surfaces.⁴⁵

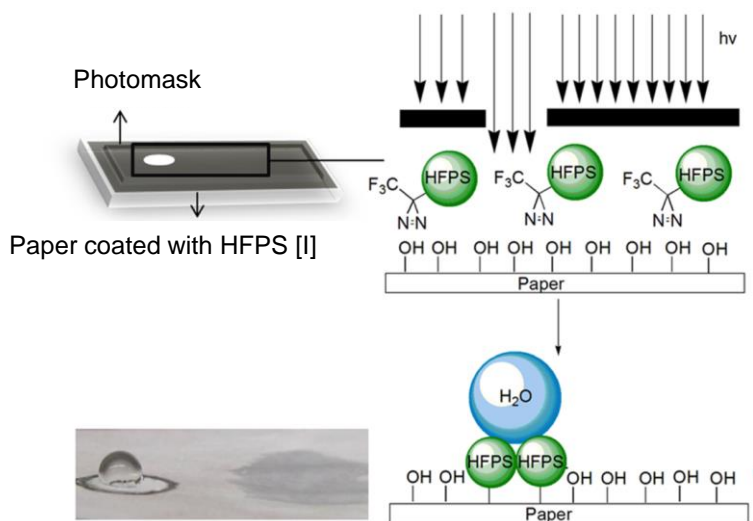


Figure 2.5. Cartoon of the macro-patterning and a photograph of the paper surface after patterning. Spot on the left, indicated by the penciled circle is where the mask let light through. The spot on the right is where the mask was dark.

2.3 Conclusion

We have demonstrated for the first time a powerful, new efficient and easy photochemical approach utilizing the photochemistry of diazine modified HFPS to imposing highly effective water barrier coatings on two model substrates, cotton and paper. Evidence presented here suggests that the photosensitive salt was covalently grafted onto the surface of cotton and paper surfaces via the generated carbene intermediate by insertion into one of the surface-active groups (likely O-H). This work represents a new class of materials for forming hydrophobic coatings that marry the recently demonstrated hydrophobic character of the HFPS to a diazine moiety as a photoactivated tethering agent. Like the more ubiquitous diazo- and azide substrates used

in materials chemistry, this work further demonstrates that the diazirine as an emerging new platform for material modification. The diazirine-HFPS was prepared in a convergent synthesis, bringing the two task specific moieties together in the final step. The materials are easy to prepare and can be made in large quantities. The phosphine precursor can be prepared in our laboratory in the 100 g-kg scale, but is made commercially in tanker car quantities. The synthesis of the diazirine, while requiring several steps to prepare, is routine and can be made in multigram quantities.⁴⁹ While the applications of robust hydrophobic coatings on cotton and other fabrics (water-proofing) and paper (document protection) are fairly obvious, because of the high reactivity of the carbene intermediate this protocol can be used to form robust hydrophobic coatings on a host of materials including glass, CNT, graphene, diamond, and other fabrics to name a few. These studies, along with a systematic examination of altering the ligands of the HFPS, demonstration of the photopatterning allowed by this method are currently being examined.

2.4 Experimental

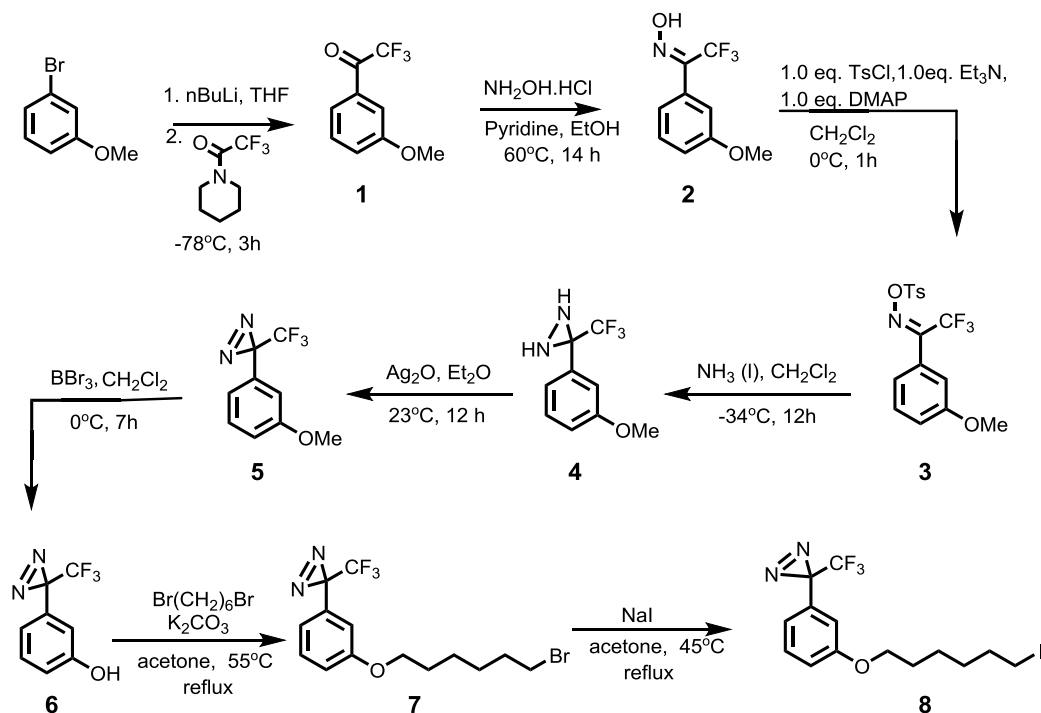
General Materials and Methods

The di (3,4,5,6-nonafluoro)hexyl-mono-2,4-trimethyl-pentylphosphine ($C_8H_{17}P(C_2H_4Rf_4)_2$) was donated from Cytec Industries and was used as received. 3-bromoanisole, n-butyllithium, hydroxylamine hydrochloride, (N,N-dimethylamino) pyridine, piperidine, p-toluenesulfonylchloride, silver(I) nitrate, boron tribromide,

potassium thioacetate, acetyl chloride, triethyl amine, trifluoroacetic anhydride, 1,6-dibromohexane, and potassium carbonate were purchased from Sigma-Aldrich and used as received without further purification. Cotton fabric (Muslin and Osanaburgh, 100% Cotton, Natural) was purchased from fabric store. The following solvents were obtained from Caledon Laboratories and used as received: dichloromethane, dimethylformamide, ethyl ether, hexanes, hydroxylamine hydrochloride, n-pentane and tetrahydrofuran. α,α,α -trifluorotoluene and trimethylphosphine were obtained from Alfa Aesar. Deuterated chloroform (CDCl_3) was obtained from Cambridge Isotope Laboratories and also used as received.

^1H , ^{13}C , ^{31}P $\{^1\text{H}\}$ and ^{19}F $\{^1\text{H}\}$ NMR spectra were recorded on either a Varian INOVA 400 MHz, Varian Mercury 400 MHz spectrometer. All samples for ^1H NMR spectroscopy were referenced to the residual protons in the solvent chloroform-d (7.26 ppm), relative to tetramethylsilane. Phosphorus-31 chemical shifts were reported relative to an external standard (85% H_3PO_4 ; 0.00 ppm) and ^{19}F $\{^1\text{H}\}$ NMR data were referenced to an external standard $\text{CF}_3(\text{C}_6\text{H}_5)$ (-63.9 ppm). Mass spectrometry measurements were recorded using a Micromass LCT (electrospray time-of-flight) mass spectrometer. Infrared spectra were recorded on a Bruker Vector 33 FTIR spectrometer and are reported in wavenumbers (cm^{-1}). The decomposition temperature for compound HFPS [I] and PMe_3S were determined using Thermal Gravimetric Analysis Q600 SDT TA Instrument. A 0.005-0.010 g sample was heated at a rate of $10^\circ\text{C}/\text{min}$ over a temperature range of 30°C – 600°C under a flow of N_2 (g) (100 mL/min). The XPS analysis were carried out with a Kratos Axis Ultra spectrometer using a monochromatic AlK(alpha) source (15 mA, 14

Kv). Scanning electron microscopy (SEM) images were recorded on a TM3000 Hitachi Scanning Electron Microscope.



Scheme 2.3. Reaction pathway towards the preparation of diazirine 8.

Synthesis of 3-(3-(6-bromohexyloxy) phenyl)-3-(trifluoromethyl)-3H diazirine (7)

All steps in preparation and synthesis were performed in accordance with the literature procedure³⁸ as illustrated in Scheme 2.3. In short, reaction of 3-bromoanisole with n-butyl lithium gave the aryl lithium which was converted to the ketone 1 using diethyltrifluoroacetamide. Hydroxylamine hydrochloride was then added to 1 to yield

oxime 2. Treatment of the synthesized oxime with p-toluenesulfonyl chloride gave p-tolylsulfonyl oxime 3. Compound 4 was formed upon addition of 3 to liquid ammonia and was later oxidized by silver oxide providing 5. Alterations to the referenced procedure include the substitution of 1, 12-dibromododecane with 1, 6-dibromohexane. A solution of 5 (930 mg, 4.30 mmol) in dry CH_2Cl_2 (10 mL) was cooled in ice bath. BBr_3 (1 M in CH_2Cl_2 , 8.75 mL, 8.75 mmol) was added over a 5 min period and the reaction mixture was stirred for 12 h at 0 °C. Water was added to the mixture and the organic compounds were extracted with diethyl ether (30 mL \times 3). The combined organic layers were washed using water (3 \times 20 mL) and the ethereal layer was dried over MgSO_4 , filtered and concentrated *in vacuo* to give the corresponding phenol 6 (800 mg, 3.96 mmol, 92% yield). Without further purification, 6 was used for the alkylation reaction. K_2CO_3 (614 mg, 4.45 mmol) was added to a solution of 6 (800 mg, 3.96 mmol) and excess 1,6-dibromohexane (5.12 g, 21.00 mmol) in acetone (20 mL). The reaction mixture was refluxed overnight and then filtered. After evaporation of solvent, the residue was partitioned between water (20 mL) and CH_2Cl_2 (30 mL). The organic layer was washed with water (3 \times 30 mL), dried over MgSO_4 , filtered and concentrated *in vacuo*. Purification of the crude product was performed by column chromatography (5:1; Hexanes: Dichloromethane). Yield 80%, 1.15 g, 3.168 mmol; ^1H NMR (400 MHz, CDCl_3) δ (ppm); 1.50-1.52 (broad, 4H), 1.78 (q, $J_{\text{H-H}} = 6.7$ Hz, 2H), 1.89 (q, $J_{\text{H-H}} = 7.1$ Hz, 2H), 3.42 (t, $J = 6.9$ Hz, 2H), 3.93 (t, $J_{\text{H-H}} = 6.5$ Hz, 2H), 6.76(s, 1H), 6.90 (d, $J_{\text{H-H}} = 7.8$ Hz, 1H), 6.93 (dd, $J_{\text{H-H}} = 2.5, 8.3$ Hz, 1H), 7.28 (t, $J_{\text{H-H}} = 7.9$ Hz, 1H); ^{13}C NMR (400 MHz, CDCl_3) δ (ppm); 25.2, 27.9, 28.9, 32.6, 33.7, 67.8, 112.8, 115.6, 118.6, 122.1 (q,

$^1J_{C-F} = 275.0$ Hz), 129.9, 130.5, 159.3. ^{19}F { 1H } NMR (400 MHz, $CDCl_3$) δ (ppm); -65.5.
HRMS m/z ; 364.0392.

Synthesis of HFPS [Br]

Under an inert atmosphere (N_2) a solution of diazirine **7** (200 mg, 0.55 mmol) in DMF (1 mL) and $CF_3(C_6H_5)$ (1 mL), was added to $(CH_3)_3CCH_2CH(CH_3)CH_2P((CH_2)_2(CF_2)_2CF_3)_2$ (380 mg, 0.60 mmol). The reaction mixture was stirred for 4 weeks at 45 °C. The reaction was continually monitored by ^{31}P { 1H } NMR. The precursor fluorinated phosphine ($\delta_P = -30.4$ ppm) was converted to a singlet in the region consistent with the target product phosphonium species ($\delta_P = 35.2$ ppm), an oxide was also present in the reaction mixture ($\delta_P = 44.0$ ppm) but was removed by purification. After ^{31}P { 1H } NMR showed complete conversion from reactants to product, water was added to the mixture and the organic compounds were extracted with dichloromethane. The organic layer was washed with water (3×10 mL), the mixture was centrifuged and aqueous layers discarded. The organic phase was dried over $MgSO_4$ and decanted. HFPS [Br] was then precipitated out of pentane to remove all the impurities present in the mixture; the precipitate was concentrated *in vacuo* overnight to yield HFPS [Br] as a viscous amber liquid. Yield: 61%, 0.336 g, 0.334 mmol. ^{31}P { 1H } NMR (400 MHz, $CDCl_3$) δ (ppm); 35.2; ^{19}F { 1H } NMR (400 MHz, $CDCl_3$) δ (ppm); -65.2 (s); -76.9 (s); -81.0 (m); -114.4 (m); -123.7 (s); -126.1 (m); 1H NMR (400 MHz $CDCl_3$); 0.93 (s, 9H), 1.2 (d, 3H), 1.38-1.40 (broad, 2H), 1.50-1.70 (broad, 3H), 1.74-1.85 (broad, 3H), 2.58-2.74 (m, 4H), 2.76-2.94 (m, 4H), 2.95-3.15 (m, 4H), 3.93 (t, 2H), 6.65 (s, 1H), 6.76

(d, 1H), 6.91 (dd, 1H), 7.29 (t, 1H); FT-IR (cm^{-1} , dropcast on NaCl); 521.5, 552.1, 635.4, 699.1, 745.4, 790.9, 848, 881.7, 937.5, 1014.7, 1061.8, 1133.7, 1230.1, 1356.2, 1445.4, 1581.9, 1605.2, 1655.3, 1720.1, 2871.2, 2954.2. HRMS m/z ; 923.2 [M^+], 1927 [M_2Br^+].

Synthesis of HFPS [I]

First diazirine 8 was prepared from the reaction of 7 with sodium iodide in acetone in 92% yield.⁵⁰ To prepare HFPS [I], under an inert atmosphere (N_2) a solution of 8 (225 mg, 0.55 mmol) in DMF (1 mL) and $\text{CF}_3(\text{C}_6\text{H}_5)$ (1 mL), was added to $(\text{CH}_3)_3\text{CCH}_2\text{CH}(\text{CH}_3)\text{CH}_2\text{P}((\text{CH}_2)_2(\text{CF}_2)_2\text{CF}_3)_2$ (380 mg, 0.60 mmol). The reaction mixture was stirred for 2 weeks at 45 °C. The reaction was continually monitored by ^{31}P { ^1H } NMR, the fluorinated phosphine ($\delta_{\text{P}} = -30.4$ ppm) was converted to a singlet in the region consistent with the target product phosphonium species ($\delta_{\text{P}} = 35.9$ ppm, an oxide was also present in the reaction mixture ($\delta_{\text{P}} = 44.1$ ppm) but was removed by purification. After ^{31}P { ^1H } NMR showed complete conversion from reactants to product, the reaction was exposed to air and precipitated out in n-pentane to remove any residual starting material and the oxide. Next, the solvent was removed under reduced pressure leaving HFPS [I] as a viscous orange oil. Yield: 76%, 0.438 g, 0.417 mmol. $T_{\text{g}} = -27.09$ °C, $T_{\text{d}} = 304.21$ °C; ^{31}P { ^1H } NMR (400 MHz, CDCl_3) δ (ppm); 35.9; ^{19}F { ^1H } NMR (400 MHz, CDCl_3) δ (ppm); -65.5; -81.30; -114.4; -123.8; -126.2; ^1H NMR (400 MHz CDCl_3); 0.93 (s, 9H), 1.22 (d, 3H), 1.41 (d, 2H), 1.54- 1.65 (broad, 6H), 1.78 (m, 3H), 2.63- 2.73 (m, 4H), 2.63-2.73 (m, 4H), 2.78-2.88 (m, 4H), 2.94-3.15 (m, 4H), 3.93 (t, 2H), 6.65 (s, 1H), 6.74 (d, 1H), 6.92 (dd, 1H), 7.28 (t, 1H); ^{13}C NMR (400 MHz CDCl_3); 12.7, 13.2, 20.8,

21.9, 23.9, 24.6, 25.4, 28.7, 29.9, 30.1, 30.3, 31.2, 52.8, 52.9, 67.6, 110, 112.9, 115.4, 118.6, 120.7, 122.6, 123.4, 130, 130.1, 130.4, 159.1; FT-IR (cm^{-1} , dropcast on NaCl); 516.2, 547.5, 651.1, 734.5, 794.9, 842.7, 867.4, 938.3, 1026.4, 1057.4, 1148.8, 1225.9, 1344.2, 1443.2, 1452.6, 1529.1, 1590.8, 1666.6, 1708.8, 2868.1, 2937.5. HRMS m/z ; 923.2 [M^+], 1973.3 [M_2I^+].

Synthesis of PMe_3S

Under an inert atmosphere (N_2), PMe_3 (19 mg, 0.25 mmol, 26 mL) was added to a solution of the diazirine 7 (109 mg, 0.238 mmol) in DMF (2 mL) and the reaction mixture was stirred for 3 h at 45 °C. The reaction was monitored by ^{31}P { ^1H } NMR, upon completion brine was added to the mixture and the organic compounds were extracted with CH_2Cl_2 (30 mL). The organic layer was washed with Brine (3×10 mL), the mixture was centrifuged and aqueous layers discarded. The organic phase was dried over MgSO_4 and decanted; the phosphonium salt was then precipitated out in n-pentane and concentrated *in vacuo* overnight to give PMe_3S as a viscous amber liquid. Yield: 91%, 96 mg, 0.218 mmol. $T_g = -35.31^\circ\text{C}$; $T_d = 88.29^\circ\text{C}$; ^{31}P { ^1H } NMR (CDCl_3) δ (ppm); 26.9; ^{19}F { ^1H } NMR (CDCl_3) δ (ppm); -65.1; ^1H NMR (CDCl_3) δ (ppm); 1.45-1.5 (m, 6H); 1.7 (m, 2H); 2.1 (m, 9H); 2.5 (m, 2H); 3.9 (m, 2H); 6.6 (s, 1H), 6.7 (d, $J=7.8$, 1H); 6.9 (m, 1H); 7.2 (m, 1H); ^{13}C NMR (CDCl_3) δ (ppm); 8.90 (d, $J_{\text{P-H}} = 54.3$ Hz); 21.62; 23.39 ($J_{\text{P-H}} = 55.10$ Hz); 25.48; 28.77 ; 30.18 (d, $J_{\text{P-C}} = 16.10$ Hz); 67.66; 112.80; 115.54; 118.61; 120.69; 130.04; 159.14. HRMS m/z ; 361.13 [M^+], 801.23 [M_2Br^+].

General procedure for the model photolysis reaction of diazirine functionalized HFPS and the Insertion of carbene

HFPS [I] (5 mg) was dissolved in methanol (1 mL) and the mixture was transferred to a Pyrex NMR tube (filters below 300 nm) and purged with argon for 15 mins. The sample was irradiated using a medium pressure mercury lamp (Hanovia S9 PC 451050 /805221), which was contained in quartz water jacket, approximately 10 cm from the NMR tube. After 30 mins, (time for disappearance of diazirine) the remaining methanol was evaporated and the product was characterized using ^{31}P { ^1H } and ^{19}F NMR spectroscopy. In the ^{19}F NMR spectra the signal at -65 ppm, which is representative of the CF_3 group of the diazirine, disappeared and a new signal appeared at -77.03 corresponding to the product after the carbene insertion was observed. ^{31}P { ^1H } NMR (400 MHz, CDCl_3) δ (ppm); 35.9; ^{19}F { ^1H } NMR (400 MHz, CDCl_3) δ (ppm); -77.0; -81.5; -114.8; -123.6; -126.0. HRMS m/z ; 927.4 [M^+], 1981.3 [M_2I^+].

Surface modification of cotton fabric and paper

The 1, 2, 5, 10, and 20 mg/mL solutions of HFPS in THF were prepared. Prior to photo-coating cotton substrate was pre-treated by washing with deionized water and detergent three times to remove any surfactants or chemical coatings, subsequently, washed with distilled water and then dried in a 60 °C oven. The paper samples were used as obtained with no pre-treatment. Both the cotton and paper substrates were treated by submersion into solution of HFPS [X] and were allowed to air-dry until the solvent evaporated. Next, the HFPS-coated substrates were placed in a sealed vessel that was

purged with argon. All of the substrates were irradiated with ultra-violet light on both sides, using a medium pressure mercury lamp (Hanovia S9 PC 451050 /805221), which was contained in quartz water jacket, approximately 10 cm from the samples (*ca.* 1800 mJ/cm²). After irradiation, all substrates were thoroughly rinsed with THF and DCM to remove any unbound HFPS and yield the light treated samples.

Patterning paper

Simple plain white printer paper, 92 Bright was soaked in a solution of HFPS [I] in THF for 15 min and allowed to air dry until no solution remained. A photo-mask made out of cardboard with a circular gap (1 cm in diameter) was placed on top of the HFPS-coated paper substrate and the back side was covered with a full mask to avoid any light exposure from the back side. Next, it was placed in a sealed vessel that was purged with argon and irradiated with ultra-violet light, using a medium pressure mercury lamp (Hanovia S9 PC 451050 /805221). After irradiation the treated paper was thoroughly rinsed with THF and DCM to afford the patterned surface.

Simulated wash cycles

Two washing methods were used for coated samples. In a typical experiment, a piece of 2 × 2 cm treated cotton fabric was washed in a 50 ml flask that contained 30 ml of aqueous detergent solution and a stir bar. The fabric was stirred at 500 rpm for 15 mins. It was then rinsed with distilled water and stirred for another 15 mins in a flask containing 30 mL distilled water to remove any adsorbed detergent. Fabric was then dried

for 10 mins in a 60 °C oven before it was used for contact angle measurement. In a separate experiment a piece of 2 × 2 cm treated cotton was immersed in three different solvents and sonicated for 5 min periods : EtOH, DCM, THF subsequently. Water contact angles were measured before and after sonication.

Contact angle measurement

Contact angles were measured with deionized water using Kruss DSA 100 goniometer with DSA (Drop Shape Analysis) software, at room temperature (21 °C). All the static water contact angles were determined by averaging values measured for 5 µL droplets at five different spots on each substrate. Laplace-Young fitting method was used to calculate all the static contact angles. Contact angle hysteresis was determined by placing a 5 µL droplet on the surface, rotating the stage 30 degrees and measuring the difference between the advancing and receding contact angles.

Other techniques

The decomposition temperature for compound HFPS [I] and PMe₃S were determined using Thermal Gravimetric Analysis Q600 SDT TA Instrument. A 0.005-0.010 g sample was heated at a rate of 10 °C /min over a temperature range of 30 °C–600 °C under a flow of N₂ (g) (100 mL/min). XPS was carried out using a Kratos Axis Ultra spectrometer using a monochromatic AlK(alpha) source (15 mA, 14 Kv). SEM images were recorded on a TM3000 Hitachi Scanning Electron Microscope.

2.5 References

- 1) Li, X.; Tian, J.; Garnier, G.; Shen, W. *Colloids Surf. B* **2010**, 76, 564.
- 2) Ma, M.; Hill, R. M. *Curr. Opin. Colloid. In.* **2006**, 11, 193.
- 3) Blossey, R. *Nat. Mater.* **2003**, 2, 301.
- 4) Bahners, T.; Textor, T.; Opwis, K.; Schollmeyer, E. *J. Adhes. Sci. Technol.* **2008**, 22, 285.
- 5) Samyn, P.; Schoukens, G.; Vonck, L.; Stanssens, D.; Abbee, H. V. D. *Langmuir* **2011**, 27, 8509.
- 6) Lathe, S. S.; Gurav, A. B.; Maruti, S. C.; Vhatkar, R. S. *JSEMAT* **2012**, 2, 76.
- 7) Li, X.-M.; Reinhoudt, D.; Crego-Calama, M. *Chem. Soc. Rev* **2007**, 36, 1350.
- 8) Wang, H.; Fang, J.; Cheng, T.; Ding, J.; Qu, L.; Dai, L.; Wang, X.; Lin, T. *Chem. Commun.* **2008**, 877.
- 9) Yu, M.; Gu, G. T.; Meng, W. D.; Qing, F. L. *Appl. Surf. Sci.* **2007**, 253, 3669.
- 10) Vilčnik, A.; Jerman, I.; Vuk, A. S.; Koželj, M.; Orel, B.; Tomšič, B.; Simončič, B.; Kovač, J. *Langmuir* **2009**, 25, 5869.
- 11) Plechkova, N. V.; Seddon, K. R. *Chem. Soc. Rev.* **2008**, 37, 123.
- 12) Merrigan, T. L.; Bates, E. D.; Dorman, S. C.; Davis Jr., J. H. *Chem. Commun.* **2000**, 2051.
- 13) Emnet, C.; Weber, K. M.; Vidal, J. A.; Consorti, C. S.; Stuart, A. M.; Gladysza, J. *A. Adv. Synth. Catal.* **2006**, 348, 1625.

- 14) Tindale, J. J.; Ragogna, P. J. *Chem. Commun.* **2009**, 14, 1831.
- 15) Tindale, J. J.; Moulard, K. L.; Ragogna, P. J. *J. Mol. Liquids* **2010**, 152, 14.
- 16) Griffiths, J.-P.; Moloney, M. G. PCT/GB2006/000139.
- 17) Moloney, M. G. *J. Phys. D: Appl. Phys.* **2008**, 41, 174006.
- 18) Leonard, D.; Moloney, M. G.; Thompson, C. *Tet. Lett.* **2009**, 50, 3499.
- 19) Griffiths, J. -P.; Maliha, B.; Moloney, M. G.; Thompson, A. L.; Hussain, I. *Langmuir* **2010**, 26, 14142.
- 20) Ito, Y. *Biotechnol.Prog.* **2006**, 22, 924.
- 21) Yan, M.; Ren, J. *J. Mater. Chem.* **2005**, 15, 523.
- 22) Liu, L. H.; Yan, M. *Nano Lett.* **2009**, 9, 3375.
- 23) Blencowe, A.; Cosstick, K.; Hayes, W. *New J. Chem.* **2006**, 30, 53.
- 24) Ismaili, H.; Lagugne-Labarthe, F.; Workentin, M. S. *Chem. Mater.* **2011**, 23, 1519.
- 25) Ismaili, H.; Workentin, M. S. *Chem. Commun.* **2011**, 47, 7788.
- 26) Ismaili, H.; Geng, D.; Kantzas, T. T.; Sun, X.; Workentin, M. S. *Langmuir*, **2011**, 27, 13261.
- 27) Zhao, Y.; Zhiguang, X.; Wang, X.; Lin, T. *Langmuir* **2012**, 28, 6328.
- 28) Brunner, J.; Senn, H.; Richards, F. M. *J. Biol. Chem.* **1980**, 255, 3313.
- 29) Hashimoto, M.; Hatanaka, Y. *Eur. J. Org. Chem.* **2008**, 2513.
- 30) Blencowe, A.; Hayes, W. *Soft Matter.* **2005**, 1, 178.

- 31) Admasu, A.; Gudmundsdóttir, A. D.; Platz, M. S.; Watt, D. S.; Kwiatkowski, S.; Crocker, P. J. *J. Chem. Soc., Perkin Trans. 2* **1998**, 1093.
- 32) Das, J. *Chem. Rev.* **2011**, 1111, 4405.
- 33) Blencowe, A.; Blencowe, C.; Cosstick, K.; Hayes, W. *React. Funct. Polym.* **2008**, 68, 868.
- 34) Blencowe, A.; Caiulo, N.; Cosstick, K.; Fagour, W.; Heath, P.; Hayes, W. *Macromolecules* **2007**, 40, 939.
- 35) Blencowe, A.; Fagour, W.; Blencowe, C.; Cosstick, K.; Hayes, W. *Org. Biomol. Chem.* **2008**, 6, 2327.
- 36) Lawrence, E. J.; Wildgoose, G. G.; Aldous, L.; Wu, Y. A.; Warner, J. H.; Compton, R. G.; McNaughter, P. D. *Chem. Mater.* **2011**, 23, 3740.
- 37) Wildgoose, G. G.; Lawrence, E. J.; Bear, J. C.; McNaughter, P. D. *Electrochem. Commun.* **2011**, 13, 1139.
- 38) Ismaili, H.; Lee, S.; Workentin, M. S. *Langmuir* **2010**, 26, 14958.
- 39) The reaction of the bromo derivative takes several weeks longer and subsequently results in some impurities due to the slow degradation of the diazirine under the conditions of the coupling reaction.
- 40) Song, M.-G.; Sheridan, R. S. *J. Am. Chem. Soc.* **2011**, 133, 19688.
- 41) Guo, Z. -G. *Appl. Phys. Lett.* **2007**, 90, 223111.
- 42) Feng, L.; Zhang, Y.; Xi, J.; Zhu, Y. Wang, N.; Xia, F.; Jiang, L. *Langmuir* **2008**, 24, 4114.
- 43) Geim, A.K.; Dubonos, S. V.; Grigorieva, I. V.; Novoselov, K. S.; Zhukov, A. A.; Shapoval, S. YU. *Nature Materials*, **2003**, 2, 461.

- 44) Martinez, A. W.; Phillips, S. T.; Whitesides, G. M. *Proc. Natl. Acad. Sci. USA* **2008**, 105, 19606.
- 45) Balu, B.; Berry, A. D.; Hess, D. W.; Breedveld, V. *Lab Chip*, **2009**, 9, 3066.
- 46) Martinez, A. W.; Phillips, S. T.; Butte, M. J.; Whitesides, G. M. *Angew. Chem. Int. Ed.* **2007**, 46, 1318.
- 47) Martinez, A. W.; Phillips, S. T.; Wiley, B. J.; Gupta, M.; Whitesides, G. M. *Lab Chip*, **2008**, 8, 2146.
- 48) Yager, P.; Edwards, T.; Fu, E.; Helton, K.; Nelson, K.; Tam, M. R.; Weigl, B. H. *Nature*, **2006**, 442, 412.
- 49) Bentz, E. L.; Gibson, H.; Hudson, C.; Moloney, M. G.; Seldon, D. A.; Wearmouth, E. S. *Synlett* **2006**, 0247.
- 50) Snider, B. B.; Hawryluk, N. A. *Org. Lett.* **2001**, 3, 569.

2.6 Supporting Information

This section contains the data to support the work carried out in chapter two of this thesis. This includes SEM images of treated and untreated samples, representative water contact angle measurement pictures and pictures of water droplets being picked up from a treated cotton sample leaving a dry surface behind.

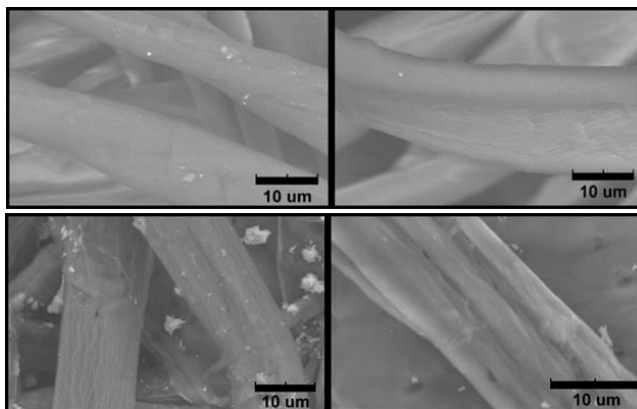


Figure S2.1. SEM micrographs of: cotton samples (top column) and paper samples (bottom column): untreated (right) and treated (left) with HFPS [Br].

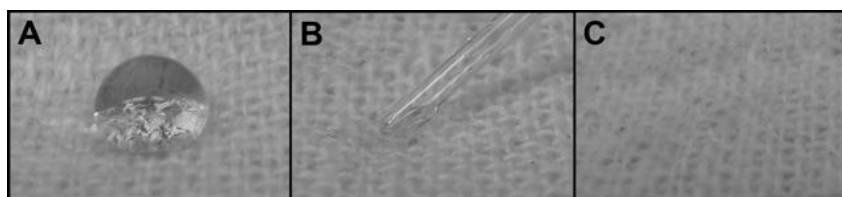


Figure S2.2. Pictures of water droplets A) placed on the treated and irradiated 100% cotton fabric and then B) drawn up with pipette to yield a C) dry surface modified substrate.

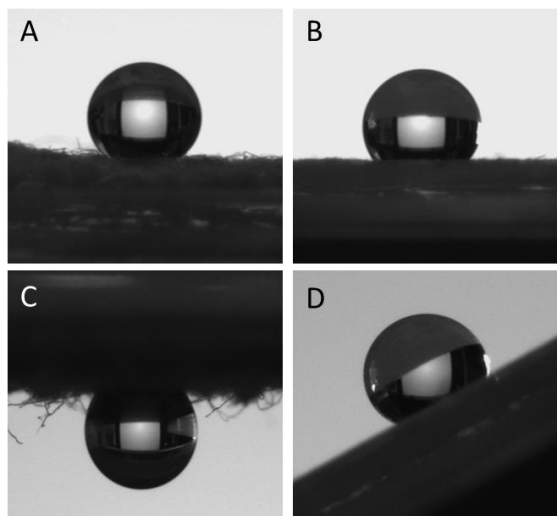


Figure S2.3. Representative pictures of water contact angle measurements using 5 μL droplets on A) cotton and B) paper C) cotton when it is turned upside down D) paper at 20° tilt angle, all coated with HFPS [I], irradiated and washed.

Chapter 3

Synthesis of Small Water-Soluble Diazirine-Functionalized Gold Nanoparticles and Their Photochemical Modification

- This chapter has been published as a full paper. The corresponding reference is: Sara Ghiassian, Mark C. Biesinger and Mark S. Workentin, *Can. J. Chem.* **2015**, 93, 98-105.
- Mark C. Biesinger performed the XPS analysis. Sara Ghiassian carried out all the work reported in this chapter under the supervision of Dr. Workentin. The manuscript was initially drafted by Sara Ghiassian and Dr. Workentin provided assistance with editing and final preparation.
- All of the schemes, figures, and text in Chapter 3 reprinted with permission from NRC Research Press.

3.1 Introduction

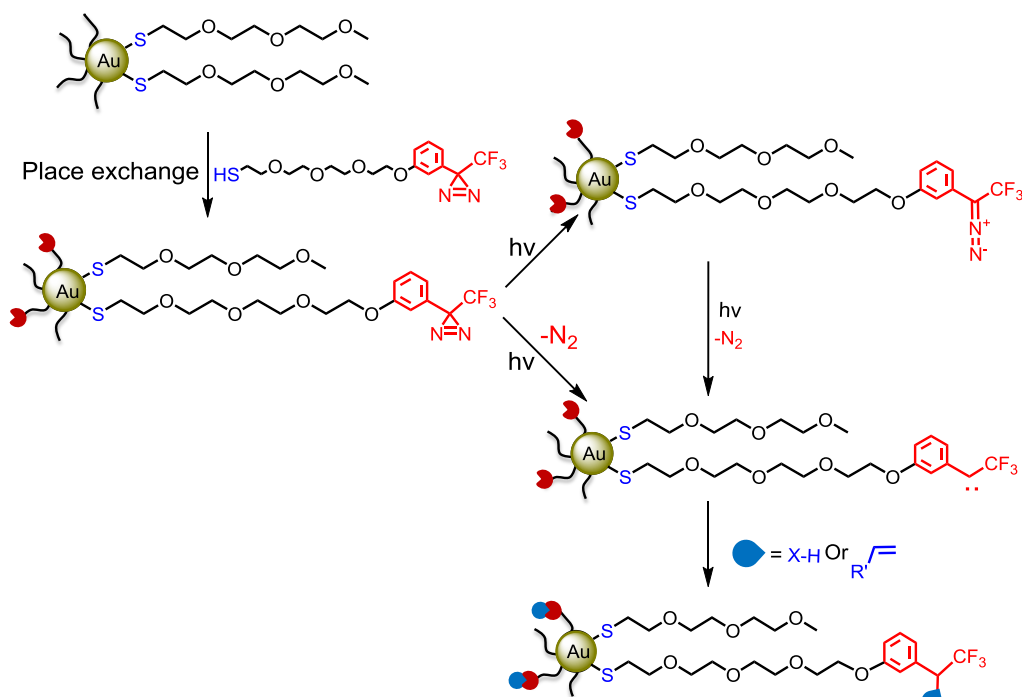
Gold nanoparticles (AuNPs) possess unique physical and chemical properties which make them outstanding candidates for numerous applications ranging from electronics, catalysis, biology and sensor science.¹⁻⁶ Many of these applications are correlated with the nature of the protecting ligand attached to the gold core. Therefore, developing techniques to prepare nanoparticles with specific moieties or functionalities directly or by means of chemical reactions at the interface of the protecting shells can be a key factor affecting the final AuNP application. Interfacial reactions on the surface of AuNP can be an outstanding alternative to conventional methods when there is a need to incorporate new functionalities onto the gold surface. A moiety at the gold interface that can be thermally or photochemically activated can be utilized as a reactive template for further modification of AuNPs. Such a procedure circumvents the tedious and time consuming chemical synthesis of ligands prior to the AuNP synthesis.

In several cases, compared to other chemical routes, photochemical reactions have the advantage of yielding a product via shorter routes, without the need to carry on several synthetic reactions. Because AuNPs are sensitive to elevated temperatures, they can be subject to loss of the protecting ligands or even decomposition, so another advantage is the possibility of performing photochemical reactions at ambient temperature. Phenyl (trifluoromethyl) diazirine, is a popular photo-active group used in photoaffinity labeling for the structural elucidation of biological substrates.⁷⁻⁹ Diazirine is chemically and thermally stable prior to photolysis but can be activated upon irradiation

with UV light. When diazirine molecules absorb light of 365 nm, where most biomolecules are transparent, they form a highly reactive carbene intermediate that can initiate addition reaction with double bonds, insertion into O-H, N-H, S-H or even C-H functional groups and form covalent bonds with target substrates that are within molecular vicinity at the time of photo-activation.^{7,10} Although mostly used for biological applications, diazirine has remained rather unexplored in other areas such as surface modification of other molecules. Diazirine has been used for the modification of polymeric substrates.^{10,11} or to incorporate a redox active functional group onto nanomaterials such as CNTs.^{12,13} Our group has demonstrated that diazirine functionality can also be a convenient photo-precursor for surface modification when it is attached to a highly fluorinated phosphonium salt. This approach enables preparation of robust hydrophobic surfaces on any material including cotton and paper through a simple photochemical treatment.¹⁴

Recently, we prepared a diazirine/alkanethiolate stabilized gold nanoparticle which is very stable for prolonged periods when kept in the dark, but is able to undergo interfacial reactions upon diazirine photo-activation.¹⁵ These particles proved to be excellent photo-precursors for the introduction of AuNPs to various materials including CNTs, graphene, diamond and glass.¹⁶⁻¹⁸ Despite all their advantages, the solubility of dodecane diazirine modified AuNPs is limited to a narrow range of organic solvents. The lack of solubility in water or other polar solvents in general limits their application for modification to materials which are soluble or dispersible in non-polar media.

Ethylene glycol thioalkylated AuNPs have shown great promise for the synthesis of robust water soluble AuNPs.^{19,20} Previously we have developed a straightforward procedure for the synthesis of small water soluble AuNPs through thiol exchange reactions, using triethylene glycol monomethyl ether functionalized AuNPs as the building blocks. Such AuNPs have the added benefit of solubility in a wide range of organic solvents as well as aqueous media.^{21,22} Furthermore, capping the gold core with shorter tri- or tetra-ethylene glycol chains versus polyethylene glycol thiolates employed previously, allows for producing mixed monolayer protected AuNPs and their complete and straightforward characterization at any stage. Through a combination of characterization techniques such as TGA, NMR, and XPS one is able to calculate the number of ligands surrounding the gold core. Such information can be further used to determine the ratio of the different ligands after a place exchange reaction has occurred and hence the number of new ligands introduced to the surface.



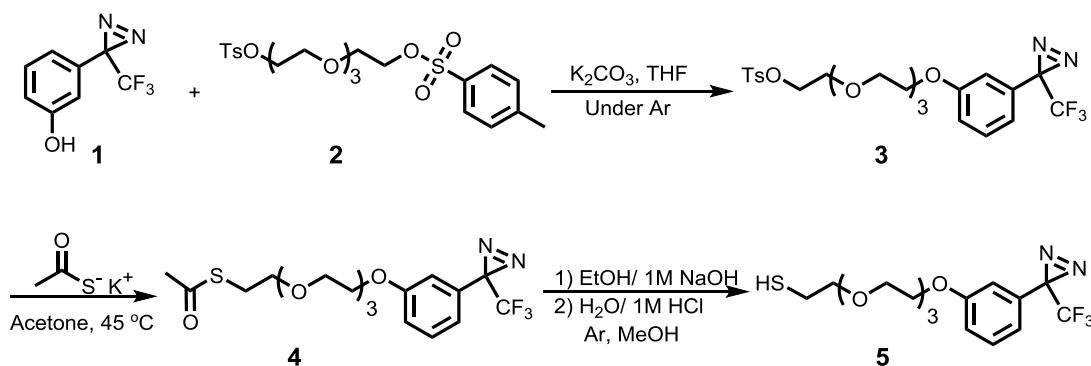
Scheme 3.1. Cartoon representation of thiol exchange reaction for the preparation of Diaz-EG₄-AuNPs and their photo-induced carbene generation and reactivity for interfacial modification.

In this work, we report the synthesis and characterization of a new type of robust, stable and water soluble AuNP containing a diazirine moiety at the interface to serve as a photoactivated template to incorporate additional functionality onto the AuNP. Diazirine/ triethylene glycol capped AuNPs are prepared through a thiol exchange reaction on small triethylene glycol monomethyl ether particles (Scheme 3.1). The novel feature of these AuNPs is that it combines the photo-reactivity of the diazirine/alkanethiolate functionalized AuNPs with excellent solubility in water and importantly other polar organic solvents. We believe that such particles can be useful in

photochemical immobilization of AuNPs on biomolecules as well as other materials under mild conditions and are not limited to use in a narrow range of solvents.

3.2 Results and Discussion

To prepare the 3-aryl-3-(trifluoromethyl) diazirine modified AuNPs (Diaz-EG₄-AuNPs), we utilized a place exchange reaction incorporating 3-aryl-3-(trifluoromethyl) diazirine tetraethylene glycol thiolate (Diaz-EG₄-SH) onto small triethylene glycol monomethyl ether modified AuNPs as illustrated in Scheme 3.1. The 3-(3-Hydroxyphenyl)-3-(trifluoromethyl)-3H-diazirine (**1**) was synthesized according to previous reports¹⁵ and was then used in the preparation of Diaz-EG₄-SH (**5**) according to Scheme 3.2.



Scheme 3.2. Pathway towards the synthesis of Diaz-EG₄-SH (**5**).

The Me-EG₃-AuNPs were prepared according to our previously reported literature procedure.²¹ It is important to note that methyl terminated triethylene glycol stabilized AuNPs were selected as the basic building block for the synthesis of water soluble AuNPs for several reasons: While oxygenated chains of the triethylene glycol ligand allow water solubility of the particles, unlike the more commonly used citrate capped gold clusters that are charged and prone to agglomeration on removal of the solvent, thiolate triethylene glycol stabilized particles remain stable after solvent evaporation and can be re-dissolved in the solvent. Additionally, incorporating triethylene glycol monomethyl ether ligands onto the gold core enables solubility in a range of organic solvents as well as water. Consequently, such nanoparticles can be used in wide range of organic (both polar and non-polar) or aqueous media for various applications. Also, unlike PEG stabilized AuNPs, these short chain triethylene glycol building blocks allow utilizing thiol exchange reactions to incorporate new functionalities on the gold core in one easy step. They can be then fully characterized through several complementary techniques such as NMR, TGA, TEM, and XPS.

After the synthesis of Me-EG₃-AuNPs, they were subsequently subjected to a place exchange reaction in the presence of Diaz-EG₄-SH (**5**) in a mixture of acetone and methanol. In a typical exchange reaction, Me-EG₃-AuNPs (100 mg) and Diaz-EG₄-SH (20 mg) were stirred in a mixture of MeOH: acetone (8: 2). After 10 minutes solvent was removed under reduced pressure to stop the exchange reaction and form a film. The film was then washed with cyclohexane to remove any unreacted thiol **5** or any disulfide that might have formed during the synthetic procedure. Initially, the success of the place

exchange reaction was confirmed by means of ^{19}F and ^1H NMR spectroscopy. The ^1H NMR spectrum of the Diaz-EG₄-AuNPs (recorded in D₂O) exhibits the expected broad peaks at δ_{H} : 3-4.2 ppm due to the methyl and methylene groups present in the triethylene glycol chains. In addition, after the place exchange reaction, three broad peaks appear in the aromatic region (δ_{H} : 6.5, 6.9 and 7.2 ppm). These new signals can be assigned to the aromatic protons of the 3-aryl-3-(trifluoromethyl) diazine moiety, when the ^1H NMR spectrum of the Diaz-EG₄-AuNPs is compared to the corresponding spectrum of the free diazine thiol **5** (Figure 3.1). In addition the signals at 1.6 and 2.7 ppm present in the free thiol spectrum, which are respectively due to the thiol proton (SH) and methylene group alpha to the sulfur (CH₂-SH), disappear after the place exchange reaction which further confirms binding of the sulfur to the gold. Also important is the lack of any sharp signals in the ^1H NMR spectrum of the final AuNPs. This confirms the effectiveness of the washing protocol in removing any unbound thiol **5** or disulfide.

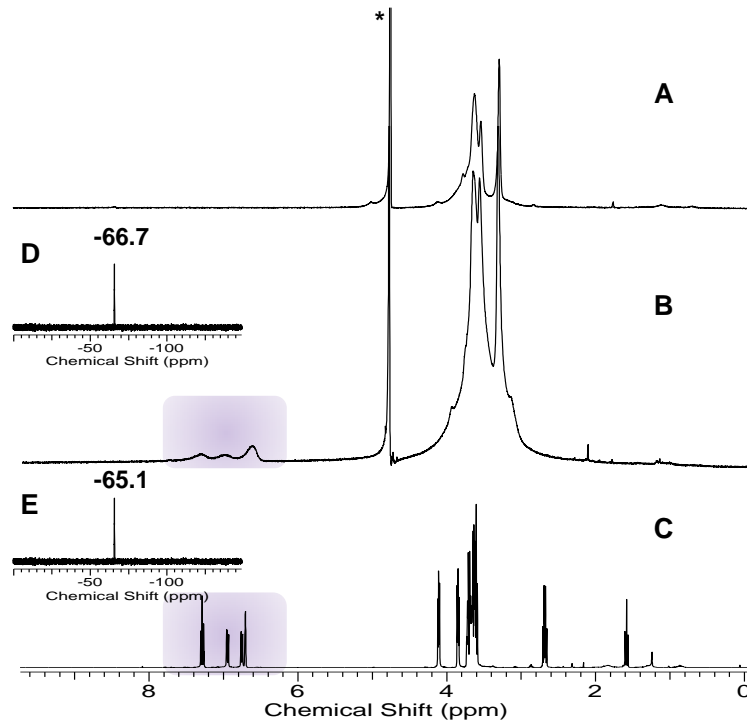


Figure 3.1. A: ^1H NMR spectrum of the Me-EG₃-AuNPs; B and D: ^1H and ^{19}F NMR spectra of the Diaz-EG₄-AuNP (recorded in D₂O). C and E: ^1H and ^{19}F NMR spectra of the Diaz-EG₄-SH (recorded in CDCl₃). * indicates residual H₂O.

Through the integration of either of the three signals in the aromatic region relative to the integration of the peak at 3.3 ppm that corresponds to the three protons of the methyl group of the Me-EG₃-S- ligands, it was possible to determine that the 15% of the protecting ligands are comprised of the Diaz-EG₄-S-, while the 85% consist of Me-EG₃-S-. It is noteworthy that while these AuNPs are soluble in organic media, our goal is to balance the extent of diazirine ligand incorporation while maintaining water solubility. The composition 85: 15 allows the amphiphilic property of the AuNP to be retained and therefore permit the subsequent photochemical modification in either organic or aqueous

media. Longer exchange reaction time leads to a higher incorporation of Diaz-EG₄-SH ligands onto the gold core (>20%), but results in a significant decrease in the water solubility of the final particles. Also, the choice of solvent for the place exchange reaction has a major effect on the solubility of the final AuNPs. Because the thiol exchange reaction (to the extent that it does not harm the water solubility) happens in a matter of minutes, we used acetone-methanol mixture, which allows faster and more efficient removal of the free thiols after the place exchange.

Due to the presence of the CF₃ group, further characterization of the particles can be achieved using ¹⁹F NMR spectroscopy. The fluorine atoms of the CF₃ group give rise to a signal at -66.7 ppm when NMR spectrum is measured in D₂O or -65.2 ppm when measured in CDCl₃ which confirms the incorporation of the diazirine functionality onto the gold core. (Figure 3.1 C). Additionally, the fluorine signal can be later employed to follow the photo-modification reactions of Diaz-EG₄-AuNPs. It is important to note that the NMR spectra of the Diaz-EG₄-AuNPs were collected in D₂O in order to demonstrate their excellent water solubility. However, the corresponding Diaz-EG₄-SH is characterized in CDCl₃ mainly because of their lower solubility in water. The slight difference in the chemical shifts of the fluorine signals (-65.1 vs. -66.7 ppm) in the free thiol and Diaz-EG₄-AuNPs is only due to the solvent effects.

From TGA data we can obtain information about the quantity of the organic ligands attached to the gold core. Both Me-EG₃-AuNPs and Diaz-EG₄-AuNPs were examined using TGA. Comparison of the two TGA profiles confirms the presence of the diazirine

moiety. The total mass loss for Me-EG₃-AuNP is 35.7% when heated from 25-750 °C. However, in case of Diaz-EG₄-AuNP the total mass loss is 42.3% and the first mass loss observed at ~ 100 °C is 6.6% of the total mass loss (calculated from the ratio of the peak areas in the first derivative of the TGA curve, Figure 3.2, left graph). Assuming all this mass loss at ~ 100 °C is due to the nitrogen extrusion from the diazirine ring, the ratio of the diazirine ligands to the triethylene glycol ligands will be 15:85 which is consistent with the ¹H NMR analysis. Using the TGA and TEM data, and assuming that the gold core has a spherical shape, we can determine a simplified formula of Au₄₀₀(S-EG₄-Diaz)₄₀(S-EG₃-Me)₂₃₀ for the Diaz-EG₄-AuNPs.

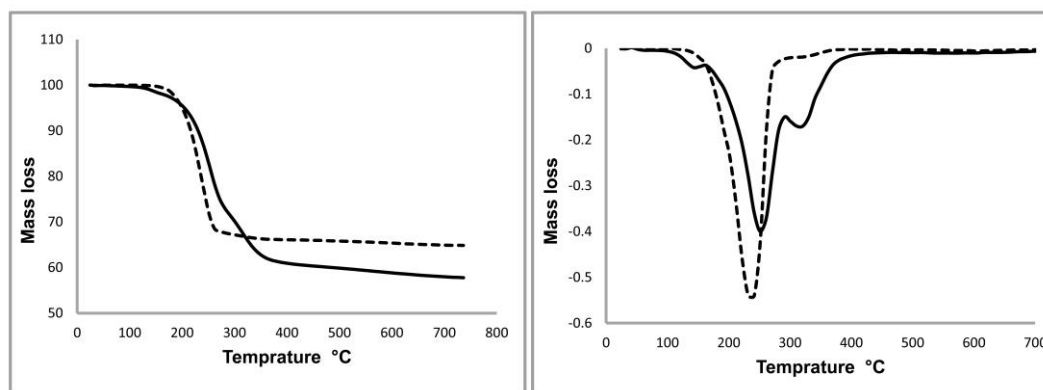


Figure 3.2. TGA graphs of Me-EG₃-AuNP (dashed line) and Diaz-EG₄-AuNP (solid line): Mass loss curves (left) and the first derivative of the mass loss curves (right).

XPS analysis further confirmed the successful preparation of Diaz-EG₄-AuNPs and the ratio between the two different ligands on the gold core (Figure 3.3). The Au 4f_{7/2}

core line appears at 84.3 eV that is shifted to a binding energy higher than that of the bulk gold (83.95 eV) due to particles size effects.²³ The S 2p core line shows the presence of two major components, the S 2p_{3/2} at 162.8 eV and S 2p_{1/2} at 164.0 eV, in a 2:1 spin orbit splitting ratio for the Au-S bonds.²⁴ Finally, the high-resolution scan of C 1s peak, F 1s peak and N 1s confirmed the presence of diazirine functional group on the gold core. The C 1s core line shows the appearance of a component at 292.8 eV typical of the CF₃ group. The F 1s core line also shows the emergence of a peak at 688.4 eV. From the molecular structure of the two ligands that surround the gold core and from the relative percentages of the C 1s component at 292.8 eV and that at 286.3 eV related to the C-O of the ethylene glycol units of both the ligands, the composition of the organic layer protecting the gold core can be estimated with good precision. Through this independent method we could confirm that 15 ± 2 % of the ligands are Diaz-EG₄-S- that was also estimated from the integration of the ¹H NMR spectrum. See supporting information for details of calculation.

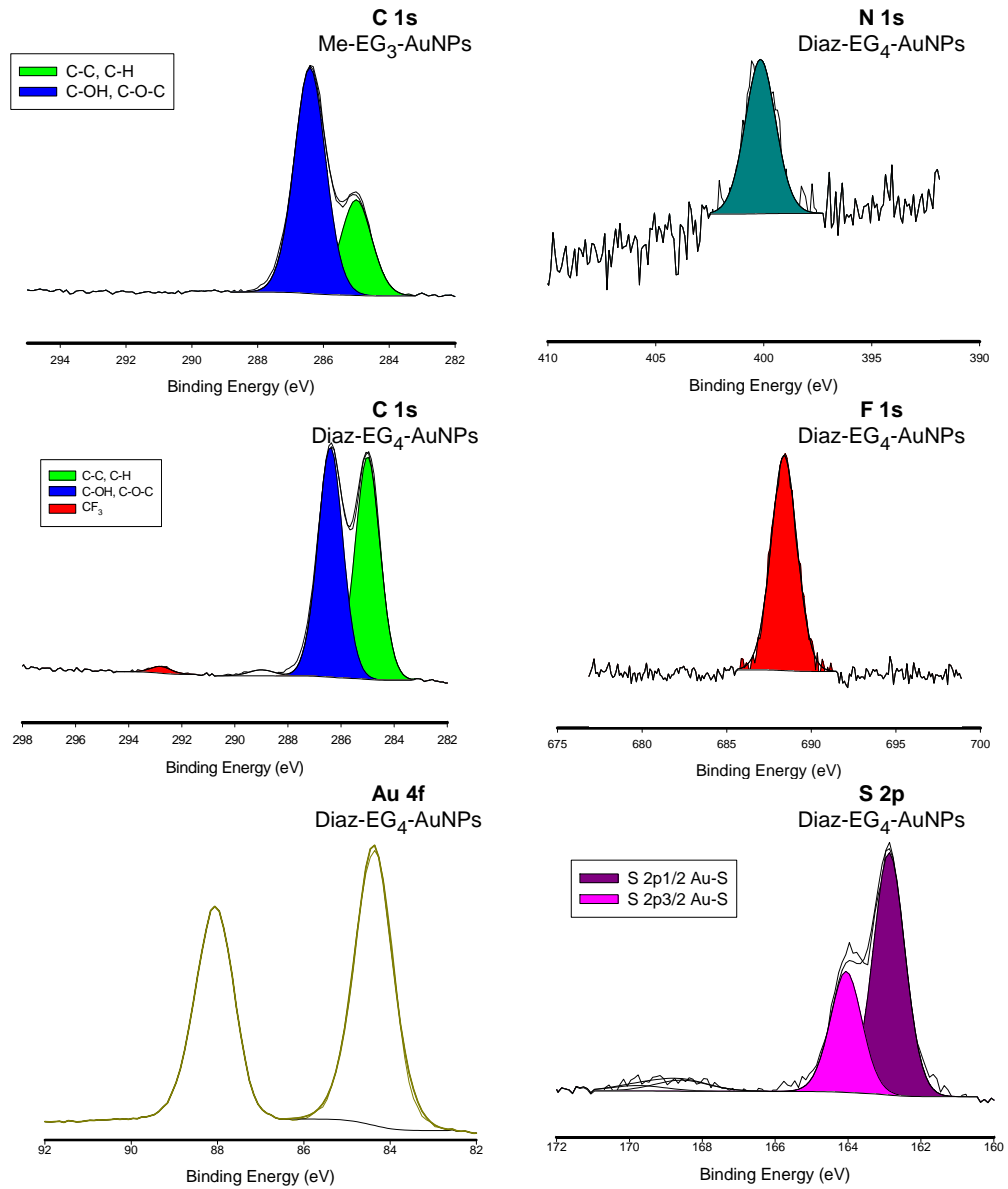


Figure 3.3. High resolution XPS spectra of Me-EG₃-AuNP and Diaz-EG₄-AuNP.

Photochemical modification of Diaz-EG₄-AuNPs through carbene insertion reactions

The UV-Vis spectrum of the Diaz-EG₄-SH exhibits an absorption band around 350 nm due to the presence of the diazirine ring (see supporting information, Figure S3.11). Upon irradiation of Diaz-EG₄-AuNPs with a medium pressure Hg lamp ($\lambda > 300$ nm), the diazirine loses N₂ and generates a highly reactive carbene which can then undergo insertion (into X-H bonds) or addition (to alkenes) reactions. At least a certain percentage of the irradiated diazirine forms the diazo compound (as can be observed in Figure 3.4). However, further irradiation of the diazo isomer will lead to the generation of the carbene as well. The course of photochemical reactions can be monitored using ¹⁹F NMR spectroscopy through the disappearance of the signal at -65 ppm (corresponding to the CF₃ of the diazirine) and the appearance of new signals in the ¹⁹F NMR spectrum.

To demonstrate that we can further modify the nanoparticles using the diazirine functionality as a template, we studied the photolysis of Diaz-EG₄-AuNPs in the presence of different carbene trapping agents. As a simple proof of concept, we chose methanol as our first carbene scavenger. A solution of Diaz-EG₄-AuNPs and methanol in benzene was purged with argon for 15 minutes and sealed to avoid any oxygen. The mixture was then irradiated at $\lambda > 300$ nm and the progress of reaction was monitored using ¹⁹F NMR spectroscopy. Through the photochemical reaction of methanol with the diazirine modified AuNPs (Figure 3.4) ¹⁹F NMR spectrum exhibits three distinct signals: i) the signal at -66.7 ppm which is due to the parent diazirine and decreases in intensity over

time, ii) the signal at -58 ppm can be attributed to the diazo intermediate formed upon photolysis (see Scheme 3.1).^{11,15} This peak initially grows and then disappears upon continued irradiation, iii) the signal at -77.9 ppm that emerges due to the insertion of the carbene into O-H bond and increases in intensity as the reaction moves towards completion.^{11,15} No C-H insertion product was observed, as the ¹⁹F NMR spectrum showed only a single signal after reaction completion.

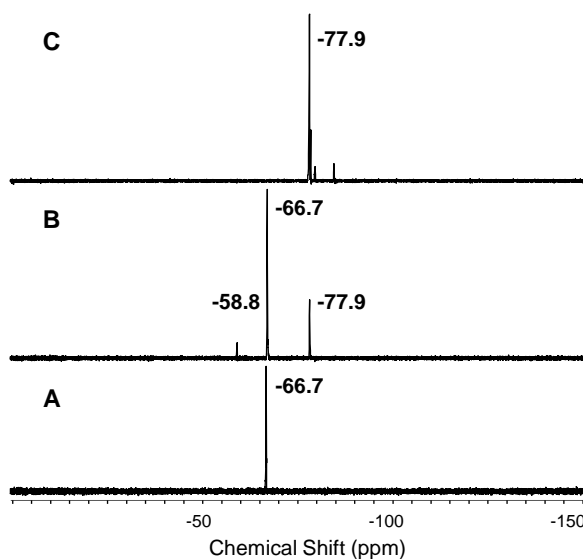


Figure 3.4. ¹⁹F NMR spectrum of Diaz-EG₄-AuNPs in methanol during photolysis at different times A) t = 0 B) t = 90 mins C) t = 12 h.

To prove that we can obtain a clean insertion reaction product if O-H bonds are available, we repeated the same photochemical protocol for acetic acid as another model reaction. Ethyl vinyl ether was also used as a model to examine the reactivity of the

photo-generated carbene towards alkenes. All the products were characterized using ^1H and ^{19}F NMR spectroscopy which showed a complete conversion of Diaz-EG₄-AuNPs to the corresponding insertion products. ^{19}F NMR spectra showed complete conversion to the desired products as the signal at -66.7 disappeared and new signals appeared depending on the substrate used (Figure 3.5). In the case of insertion into methanol the product has a F appearing at -77.9 ppm, insertion into the alkene of ethyl vinyl ether gives two signals at -63.5 and -69.4 due to the two diastereomers formed on insertion to form the cyclopropane, and insertion into the O-H of acetic acid exhibits a signal at -77.5 ppm.^{11,15} The formation of the products was also confirmed by the appearance of new peaks in ^1H NMR spectra (See supporting information). While photochemical modification proceeds efficiently, due to the increase in the organic character of the target molecules, solubility of the AuNPs changed after the photochemical reactions. Water solubility of the particles decreased, while they remain perfectly soluble in other polar solvents such as methanol or acetonitrile. To address this solubility issue and to obtain clear signals in the NMR spectra with a high signal to noise ratio we conducted all the NMR measurements in deuterated methanol.

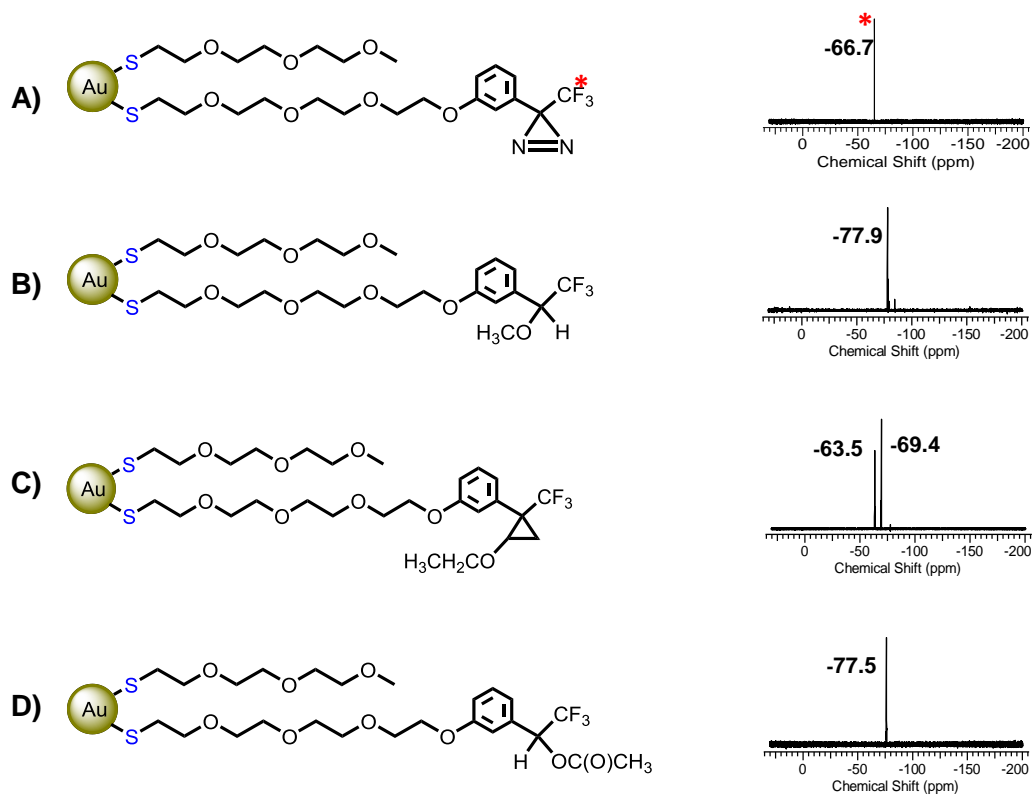


Figure 3.5. Cartoon representation of Diaz-EG₄-AuNP (A) and its carbene insertion products (left) and their ^{19}F NMR spectra (right): B) Methanol; C) Ethyl vinyl ether and D) Acetic acid.

It has been previously reported that the photo-generated carbene from Aryl-3-(trifluoromethyl)-diazirine is highly reactive towards O-H bonds.^{14,15} Carbohydrates are one of the most common biomolecules in living cells with available O-H bonds for insertion of the carbene. Carbohydrate functionalized gold nanoparticles have gained great attention as drug delivery vehicles and cellular probes. Such materials have been used as biolabels for the study of carbohydrate-carbohydrate or carbohydrate-protein interactions.^{23,24} To explore the ability of the reactive carbene to serve as a template to modify the AuNPs in aqueous solutions we used non-derivatized mannose as a proof of

principle. Mannose is a carbohydrate with numerous accessible hydroxyl groups for the reaction with carbene. In a typical experiment, a solution of Diaz-EG₄-AuNPs and excess mannose in milliQ water was purged with argon for 15 minutes and then irradiated in a pyrex vessel ($\lambda > 300$ nm). The progress of photolysis was followed using ¹⁹F NMR. When a concentrated solution of AuNPs (10 mg of AuNPs in 1 mL of milliQ water) was used for photolysis, ¹⁹F NMR spectrum showed formation of the azine as the major product ($\delta_F = -67$ ppm) resulting from reaction of a carbene with a diazo intermediate and the minor product of insertion into O-H bonds of mannose ($\delta_F = -77$ ppm). When a more dilute solution (10 mg of AuNPs in 10 ml of milliQ water) was prepared to prevent any dimerization a signal at -77 ppm appeared as the major component, which can be attributed to the desired product of the insertion into the hydroxyl groups of the mannose. However, water insertion also occurred to some extent that can be verified by the signal at $\delta_F = -79$ ppm (Figure 3.6).¹¹ Although these results demonstrate that we can construct mannose capped AuNPs through photochemical reaction of diazirine, the efficiency of such reactions are lower due to the lower reactivity of the mannose OH and the unspecific reactivity of the carbene towards each other or solvent molecules in their vicinity.

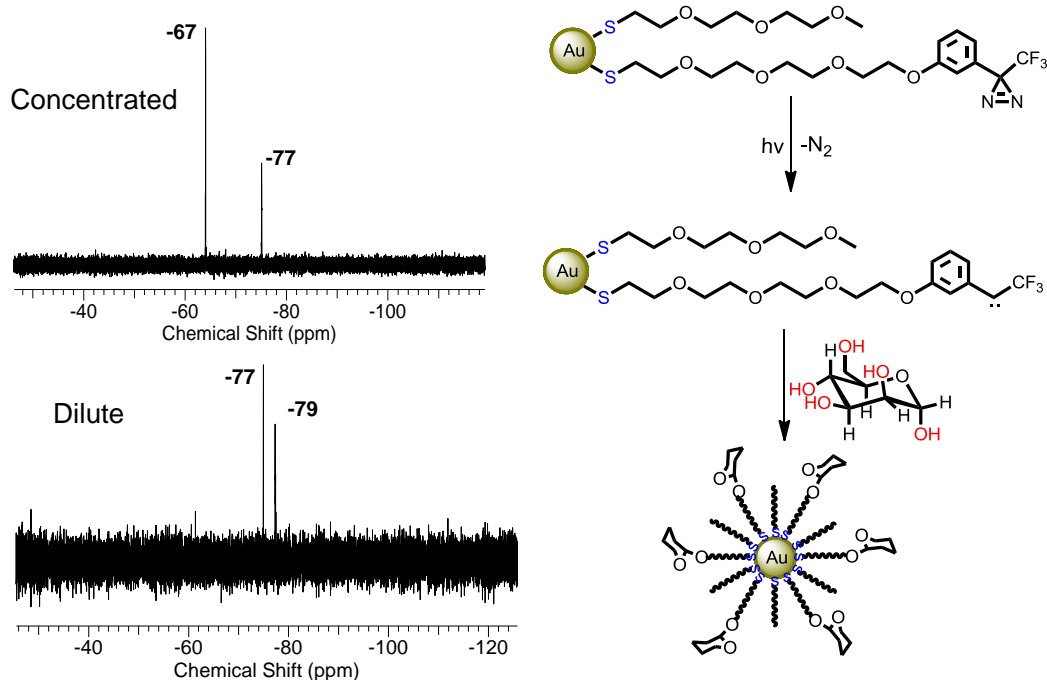


Figure 3.6. Cartoon representation of photolysis of Diaz-EG₄-AuNP in the presence of mannose and the formation of the desired insertion product (right) and ¹⁹F NMR spectra of the reaction products in different concentrations (left).

To study the effect of UV irradiation on the size of the particles we used TEM. The average size of the Diaz-TEG-AuNPs was measured to be 2.3 ± 0.5 nm before photo-modification. As Figure 3.7 shows, there is no distinct change in the size or shape of the gold core after photolysis and the average size is 2.3 ± 0.7 nm after surface modification. This confirms that UV irradiation has no effect on the size of the particles.

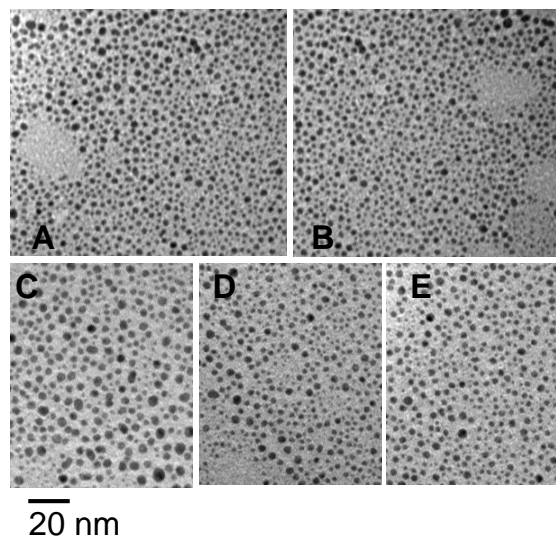


Figure 3.7. TEM images of A) Me-EG₃-AuNP B) Diaz-EG₄-AuNP and the insertion products of Diaz-EG₄-AuNP with C) Methanol D) Acetic Acid E) Ethyl vinyl ether.

3.3 Conclusion

In this work, we have described the synthesis and characterization of small water and organic soluble diazirine functionalized AuNPs. The Diaz-EG₄-AuNPs were characterized through ¹H and ¹⁹F NMR spectroscopy, TGA, TEM, and XPS and the amount of diazirine functionality on the corona was estimated with good precision through two independent methods (15% of the total ligands). In particular we demonstrated that XPS is a powerful tool for quantifying the newly introduced moieties after a place exchange reaction with rather high precision. The unique feature of Diaz-EG₄-AuNPs is their amphiphilic character, which expands their potential applications. Due to the presence of the diazirine moiety, these AuNPs generate a highly reactive

carbene upon photolysis. We have demonstrated here that the diazirine functionality can act as an effective template that can be used for further modification of AuNPs through insertion reactions with O-H and C=C bonds, while maintaining their solubility in polar solvents.

3.4 Experimental

General compounds and instrumentation

The compounds hydrogen tetrachloroaurate (III), sodium borohydride, triethylene glycol monoethyl ether, tetraethylene glycol, 4-dimethylamino pyridine (DMAP), potassium thioacetate, p-toluenesulfonyl chloride, 3-bromoanisole, n-butyllithium, hydroxylamine hydrochloride, silver nitrate (I), boron tribromide, ethylvinyl ether were purchased from Sigma Aldrich and used as received. Deuterated water (D_2O), deuterated chloroform ($CDCl_3$) and deuterated methanol (CD_3COD) (Cambridge Isotope Laboratories) were all used as received. All common solvents, triethyl amine, dry methanol, hydrochloric acid and sodium hydroxide were purchased from Caledon Laboratories Ltd. Glacial acetic acid (99.7%) was purchased from BDH.

1H , ^{13}C and ^{19}F $\{^1H\}$ NMR spectra were recorded on either a Varian Inova 400 MHz or a Varian Mercury 400 MHz spectrometer. Thermo Gravimetric Analysis (TGA) measurements were recorded by loading the sample in 70 μL ceramic crucible and heating from 25-750 $^{\circ}C$ with a rate of 10 $^{\circ}C$ min^{-1} . The experiments were performed

under a nitrogen flow of 70 ml min^{-1} in a Mettler Toledo TGA/SDTA 851 instrument. Transmission electron microscopy (TEM) images were recorded from a TEM Philips CM10. The TEM grids (Formvar carbon film on 400 mesh copper grids) were purchased from Electron Microscopy Sciences and prepared by drop casting solution of nanoparticles directly onto the grid surface. UV-Vis spectra were collected employing a Varian Cary 300 Bio spectrometer. Mass spectrometry measurements were carried out using a Micro mass LCT (electrospray time-of-flight) mass spectrometer. The XPS analyses were carried out with a Kratos Axis Ultra spectrometer using a monochromatic Al K(alpha) source (15mA, 14kV). The instrument work function was calibrated to give a binding energy (BE) of 83.96 eV for the Au $4f_{7/2}$ line for metallic gold and the spectrometer dispersion was adjusted to give a BE of 932.62 eV for the Cu $2p_{3/2}$ line of metallic copper. Specimens were mounted on a double sided adhesive tape and the Kratos charge neutralizer system was used on all specimens. Survey scan analyses were carried out with an analysis area of 300 x 700 microns and pass energy of 160 eV. High resolution analyses were carried out with an analysis area of 300 x 700 microns and pass energy of 20 eV. Spectra have been charge corrected when needed to the main line of the carbon 1s spectrum set to 285.0 eV for aliphatic carbon. Spectra were analyzed using CasaXPS software (version 2.3.14).

Synthetic details

Compound 1

All steps in the preparation of 1 were performed in accordance with the literature procedure.¹⁵ Briefly, reaction of 3-bromoanisole with n-butyl lithium gave the aryl lithium which was subsequently converted to the corresponding ketone, 2,2,2-trifluoro-1-(3-methoxyphenyl)ethanone, using diethyl trifluoroacetamide. Addition of hydroxylamine hydrochloride to this product yielded an oxime. The oxime was converted to p-tolylsulfonyl oxime and then oxidized to give the 3-(3-methoxyphenyl)-3-(trifluoromethyl)-3H-diazirine. Later it was treated with boron tribromide at 0 °C to give the corresponding phenol, 3-(3-hydroxyphenyl)-3-(trifluoromethyl)-3H-diazirine 1. ¹H NMR (CDCl₃, 400 MHz): δ (ppm): 6.69 (s, 1H), 6.77 (d, 1H), 6.94 (dd, 1H), 7.31 (t, 1H), ppm. ¹⁹F {¹H} (400 MHz, CDCl₃): -65.6 ppm.

Compound 2

Compound 2 was synthesized according to the literature procedure²¹ by the addition of triethyl amine and dimethylaminopyridine (DMAP) to a solution of tetraethylene glycol. ¹H NMR (CDCl₃, 400 MHz) δ (ppm): 2.45 (singlet, 6H), 3.57 (multiplet, 8H), 3.68 (triplet, 4H, J=8Hz), 4.16 (triplet, 4H, J=8Hz), 7.34 (multiplet, 4H), 7.80 (multiplet, 4H).

Compound 3

To 4.1 g (8 mmol) of 2 was added 0.45 g (2.2 mmol) of 1 and they were dissolved in 100 ml of dry acetone. After the solution was purged with argon for 15 minutes, 370 mg (2.7 mmol) of potassium carbonate was added quickly. The final mixture was purged for 10 more minutes with argon. The reaction solution was stirred under inert atmosphere for 72 hours at room temperature. After reaction completion, acetone was evaporated. Next, the residue was partitioned between water (10 ml) and dichloromethane (20 ml). The organic layer was washed with water (3x10), dried over MgSO₄, filtered and concentrated. The crude product was used in the next step without further purification. ¹H NMR (400 MHz, CDCl₃) δ (ppm); 2.4 (s, 3H), 3.6-3.7 (m, 10H), 3.8 (t, 2H), 4.0-4.1 (m, 4H), 6.7 (s, 1H), 6.7 (d, 1H), 6.9 (dd, 1H), 7.2 (t, 1H), 7.3 (d, 2H), 7.8 (d, 2H); ¹⁹F {¹H} NMR (400 MHz, CDCl₃) δ (ppm); -65.2.

Compound 4

To 780 mg (1.46 mmol) of compound 3 was added 217 mg (1.9 mmol) of potassium thioacetate and then they were dissolved in 25 ml of acetone and refluxed at 50 °C overnight. After reaction completion, the mixture was filtered and the solvent was evaporated. The residue was partitioned between water (10 mL) and dichloromethane (20 ml). The organic layer was washed three times with brine and dried over MgSO₄. After filtration, the solvent was evaporated to afford 4. Purification of the crude product by column chromatography (1:1 ethylacetate: hexanes) gave 4 in quantitative yield as yellow oil. ¹H NMR (400 MHz, CDCl₃) δ (ppm); 2.3 (s, 3H), 3.1 (t, 2H), 3.6-3.7 (m,

10H), 3.9 (t, 2H), 4.1 (t, 2H), 6.7 (s, 1H), 6.8 (d, 1H), 6.9 (dd, 1H), 7.3 (t, 1H); ^{13}C NMR (400 MHz CDCl_3); 28.8, 30.5, 41.7, 67.5, 69.5, 69.7, 70.3, 70.5, 70.6, 70.8, 113.0, 115.7, 118.8, 129.9, 130.4, 158.9, 195.4; ^{19}F { ^1H } NMR (400 MHz, CDCl_3) δ (ppm); -65.2; m/z ($\text{C}_{18}\text{H}_{23}\text{F}_3\text{N}_2\text{O}_5\text{S}$) calculated: 436.128, found: 436.127.

Synthesis of Compound 5

Dry methanol (2 mL) was used to dissolve 60 mg (0.2 mmol) of compound 4 and the solution was purged with argon for 15 minutes. In a separate flask, 120 μl of 1 M NaOH solution in EtOH was purged with argon for 15 minutes. Using a cannula, the base solution was transferred to the methanol solution and the reaction mixture was stirred under inert atmosphere for 45 minutes. In the meantime, 250 μl of 1 M HCl in miliQ water was purged with argon in a third flask for 15 minutes. After the 45 minute period, the acid solution was transferred to the reaction mixture using a cannula. The solution was then stirred for 10 minutes under argon. Next, the reaction was stopped and the thiol was extracted with dichloromethane. After 3 consecutive extractions, all the combined organic phases were dried over MgSO_4 . After filtration, the solvent was removed under reduced pressure to afford compound 5 as yellow oil in quantitative yield. ^1H NMR (400 MHz, CDCl_3) δ (ppm); 1.6 (t, 1H), 2.7 (q, 2H), 3.6-3.7 (m, 10H), 3.9 (t, 2H), 4.1 (t, 2H), 6.7 (s, 1H), 6.8 (d, 1H), 6.9 (dd, 1H), 7.3 (t, 1H); ^{13}C NMR (400 MHz CDCl_3); 28.2, 29.0, 67.4, 69.3, 69.4, 69.9, 70.1, 70.3, 112.7, 115.7, 118.4, 129.9, 130.1, 159.3, 195.6; ^{19}F { ^1H } NMR (400 MHz, CDCl_3) δ (ppm); -65.2. HRMS m/z for ($\text{C}_{16}\text{H}_{21}\text{F}_3\text{N}_2\text{O}_4\text{S}$) calculated: 394.117, found: 394.116.

Preparation of Diazirine modified AuNPs (Diaz-EG₄-AuNPs)

Diazirine modified AuNPs were synthesized through a place exchange reaction. First, triethylene glycol monomethyl ether AuNPs (Me-EG₃-AuNPs) were synthesized in accordance with our previously reported procedure.^[21] Next, to introduce the diazirine tetraethylene glycol thiol ligands onto the nanoparticle shell, 5 mg of freshly prepared thiol **5** was dissolved in 1 ml of MeOH : acetone (8 : 2). This solution was then added to a solution of Me-EG₃-AuNPs (25 mg in 10 ml of MeOH: acetone (8: 2). After vigorously stirring the reaction mixture for 10 minutes, the solvent was evaporated to form a film of nanoparticles. This film was washed with cyclohexane (x3) to remove the excess diazirine thiol **5**. ¹H NMR (400 MHz, D₂O) δ (ppm); 3.1-3.4 (broad), 3.5-4.2 (broad), 6.5-6.6 (broad), 6.8-7.0 (broad), 7.1-7.3 (broad); ¹⁹F {¹H} NMR (400 MHz, D₂O) δ (ppm); -65.7.

Photochemical modification of Diaz-EG₄-AuNPs

Diaz-EG₄-AuNP (10 mg) was dissolved in 10 mL benzene and 10 eq of the target substrate (methanol, ethylvinyl ether or acetic acid) was added. The mixture was transferred to a Pyrex flask (filters light below 300 nm) and purged with argon for 15 minutes. The sample was then irradiated using a medium pressure mercury lamp (Hanovia S9 PC 451050 /805221), which was contained in quartz water jacket, approximately 10 cm from the flask. After reaction completion, (time for disappearance of diazirine, followed by ¹⁹F NMR spectroscopy) all the solvent was evaporated to form a film of nanoparticles. The film was then washed with cyclohexane (x3) to remove any

unreacted substrate from the modified AuNPs. Over the course of reaction, in the ^{19}F NMR spectra the signal at -65 ppm, which is representative of the CF_3 group of the diazirine, gradually disappeared and a new signal appeared corresponding to the product formed via the carbene insertion.

3.5 References

- 1) Jain, P. K. *Angew. Chem. Int. Ed.* **2014**, 53, 1197.
- 2) Hutchings, G. J.; Brust, M.; Schmidbaur, H. *Chem. Soc. Rev.* **2008**, 37, 1759.
- 3) Corma, A.; Hermenegildo, G. *Chem. Soc. Rev.* **2008**, 37, 2096.
- 4) Tiwari, P.M.; Vig, K.; Dennis, V.A.; Singh, S.R. *Nanomaterials* **2011**, 1, 31.
- 5) Daniel, M. C.; Astruc, D. *Chem. Rev.* **2004**, 104, 293.
- 6) Saha, K.; Agasti, S. S.; Kim, C.; Li, X.; Rotello, V. M. *Chem. Rev.* **2012**, 112, 2739.
- 7) Hashimoto, M.; Hatanaka, Y. *Eur. J. Org. Chem.* **2008**, 2008, 2513.
- 8) Blencowe, A.; Hayes, W. *Soft Matter.* **2005**, 1, 178.
- 9) Dubinsky, L.; Kromb, B. P.; Meijler, M. M. *Bioorg. Med. Chem.* **2012**, 20, 554.
- 10) Blencowe, A.; Cosstick, K.; Hayes, W. *New J. Chem.* **2006**, 30, 53.
- 11) Blencowe, A.; Caiulo, N.; Cosstick, K.; Fagour, W.; Heath, P.; Hayes, W. *Macromolecules*, **2007**, 40, 939.

- 12) Lawrence, E. J.; Wildgoose, G. G.; Aldous, L.; Wu, Y. A.; Warner, J. H.; Compton, R. G.; McNaughter, P. D. *Chem. Mater.* **2011**, 23, 3740.
- 13) Wildgoose, G. G.; Lawrence, E. J.; Bear, J. C.; McNaughter, P. D. *Electrochem. Commun.* **2011**, 13, 1139.
- 14) Ghiassian, S.; Ismaili, H.; Lubbock, B. D.; Dube, J. W.; Ragona, P. J.; Workentin, M. S. *Langmuir* **2012**, 28, 12326.
- 15) Ismaili, H.; Lee, S.; Workentin, M. S. *Langmuir* **2010**, 26, 14958.
- 16) Ismaili, H.; Lagugne-Labarthe, F.; Workentin, M. S. *Chem. Mater.* **2011**, 23, 1519.
- 17) Ismaili, H.; Workentin, M. S. *Chem. Commun.* **2011**, 47, 7788.
- 18) Ismaili, H.; Geng, D.; Kantzas, T. T.; Sun, X.; Workentin, M. S. *Langmuir*, **2011**, 27, 13261.
- 19) Wuelfing, W. P.; Gross, S. M.; Miles, D. T.; Murray, R. W. *J. Am. Chem. Soc.* **1998**, 120, 12696.
- 20) Kannars, A. G.; Kamounah, F. S.; Schaumburg, K.; Kiely, C. J.; Brust, M. *Chem. Commun.* **2002**, 2294.
- 21) Gobbo, P.; Workentin, M. S. *Langmuir*, **2012**, 28, 12357.
- 22) Gobbo, P.; Novoa, S.; Biesinger, M.; Workentin, M. S. *Chem. Commun.* **2013**, 49, 3982.
- 23) Bourg, M. C.; Badia, A.; Lennox, R. B. *J Phys Chem B*, **2000**, 104, 6562.
- 24) Castner, D. G.; Hinds, K.; Grainger, D. W. *Langmuir*, **1996**, 12, 5083.

- 25) Rojo, J.; Diaz, V.; De la Fuente, J. M.; Segura, I.; Barrientos, A. G.; Riese, H. H.; Bernad, A.; Penades, S. *ChemBioChem* **2004**, 5, 291.
- 26) Reichardt, N. C.; Lomasab, M. M.; Penades, S. *Chem. Soc. Rev.* **2013**, 42, 4358.

3.6 Supporting Information

This section contains the data to support the work carried out in chapter three of this thesis. It includes NMR spectra and UV-Vis spectra of Me-EG₃-AuNP, Diaz-EG₄-AuNP and all the photochemically prepared products, deconvolution of the TGA graph of Diaz-EG₄-AuNP and calculations made based on the high resolution XPS spectra to calculate the ratio of the two ligands on the gold core.

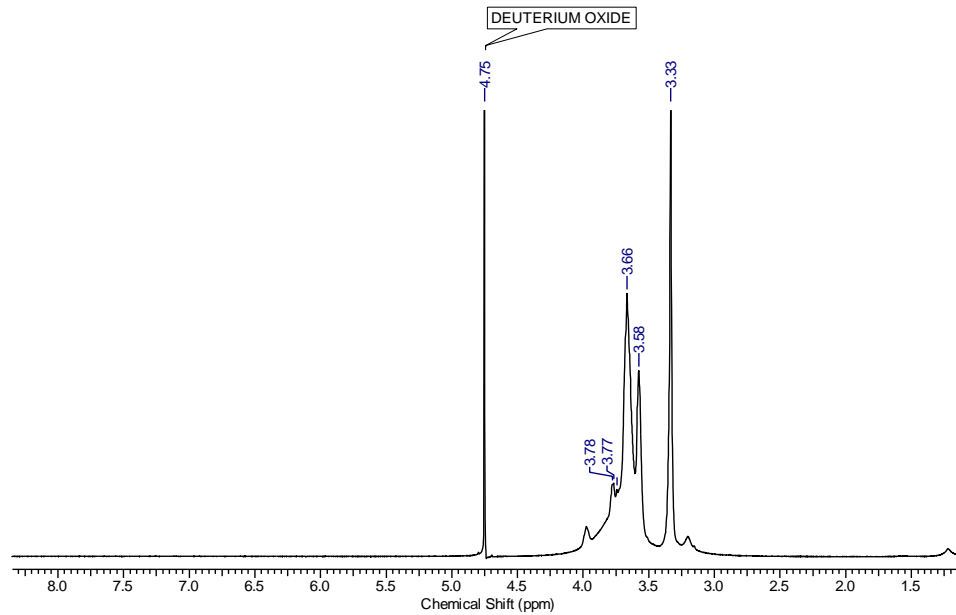


Figure S3.1. ^1H NMR spectrum of Me-EG₃-AuNP in D₂O.

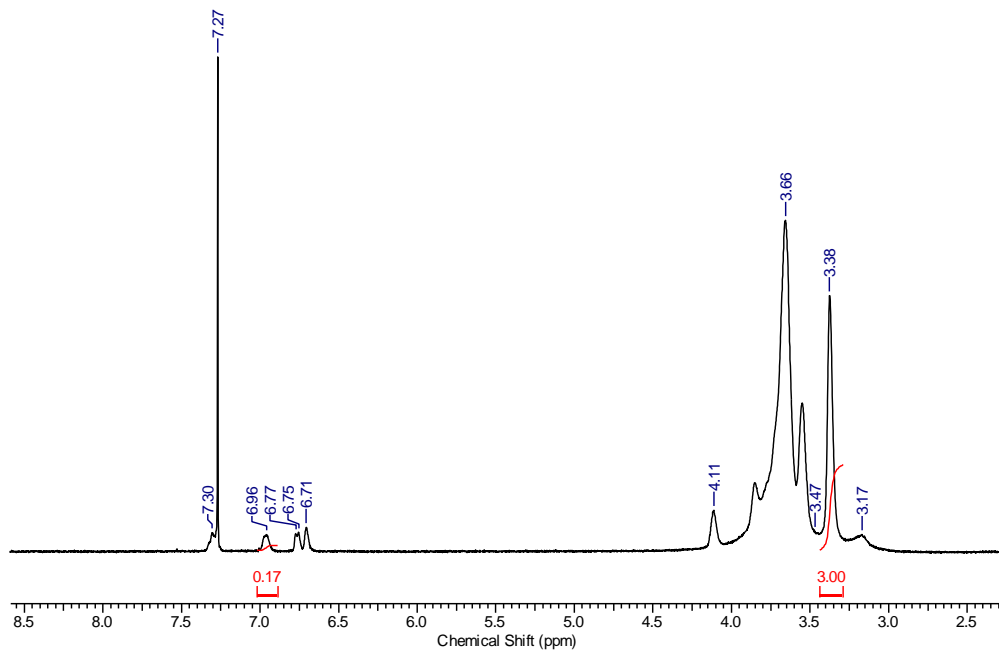


Figure S3.2. ^1H NMR spectrum of Diaz-EG₄-AuNP in CDCl₃.

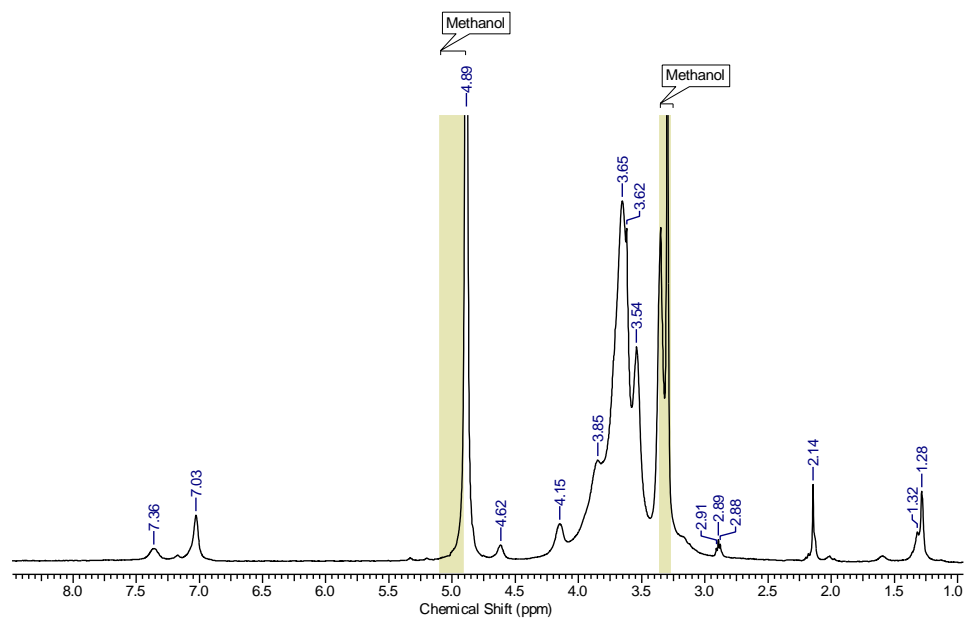


Figure S3.3. ^1H NMR of the insertion product of Diaz-EG₄-AuNP into methanol, recorded in CD₃OD.

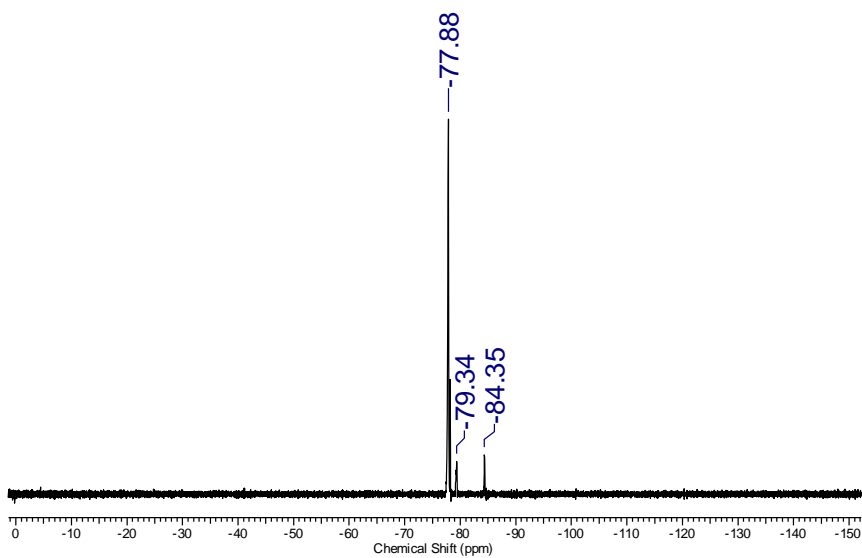


Figure S3.4. ^{19}F NMR spectrum of the insertion product of Diaz-EG₄-AuNP into methanol, recorded in CD₃OD.

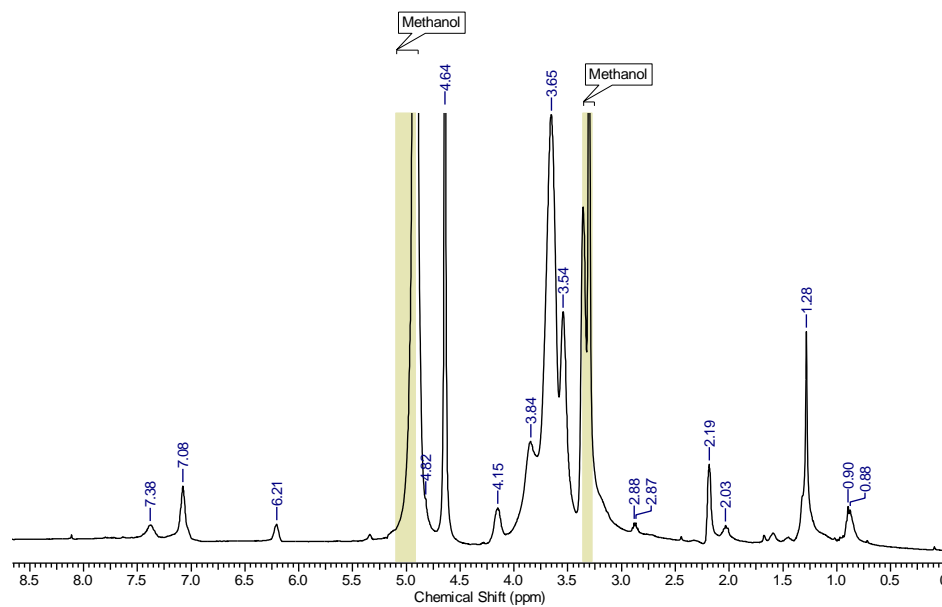


Figure S3.5. ^1H NMR spectrum of the insertion product of Diaz-EG₄-AuNP into acetic acid, recorded in CD₃OD.

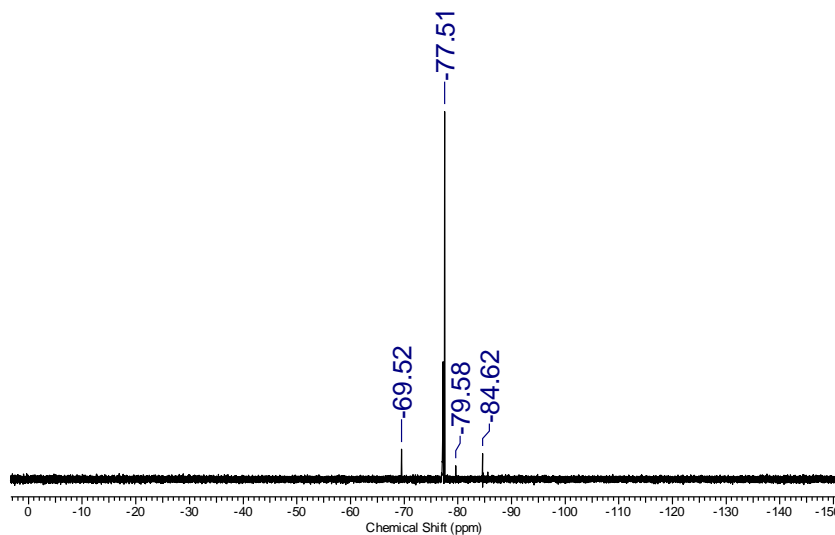


Figure S3.6. ^{19}F NMR spectrum of the insertion product of Diaz-EG₄-AuNP into acetic acid, recorded in CD₃OD.

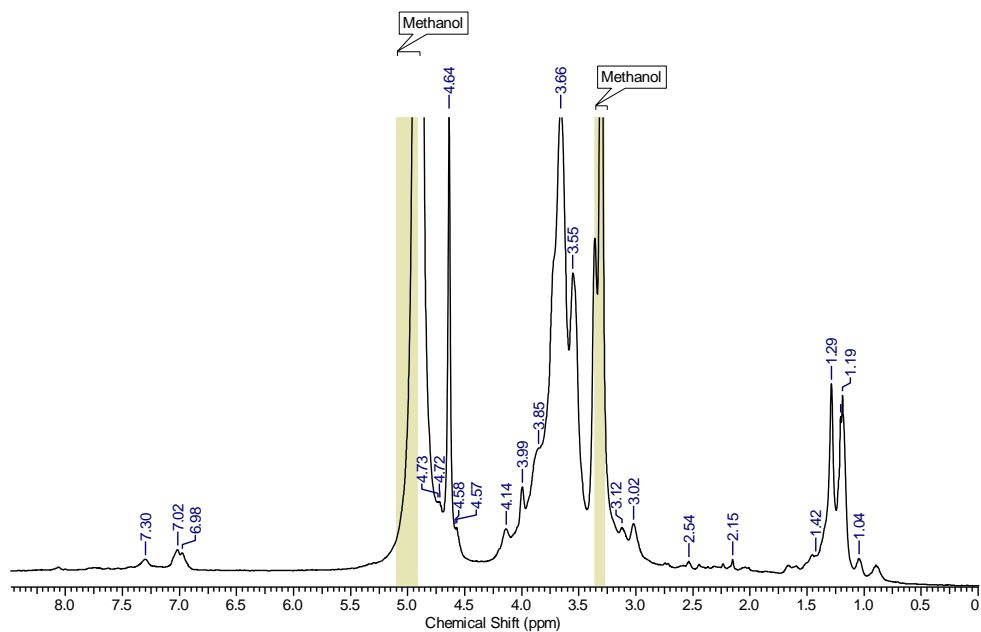


Figure S3.7. ^1H NMR spectrum of the insertion product of Diaz-EG₄-AuNP into ethyl vinyl ether, recorded in CD₃OD

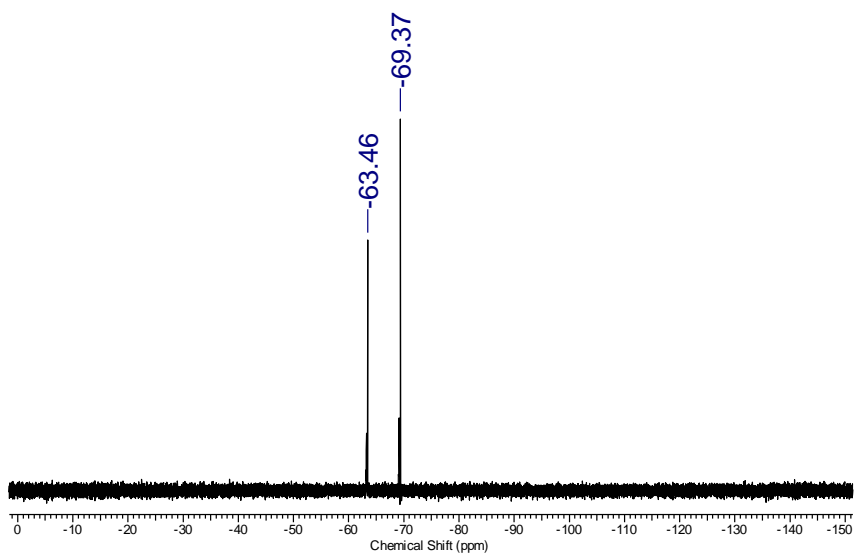


Figure S3.8. ^1H NMR spectrum of the insertion product of Diaz-EG₄-AuNP into ethyl vinyl ether, recorded in CD₃OD

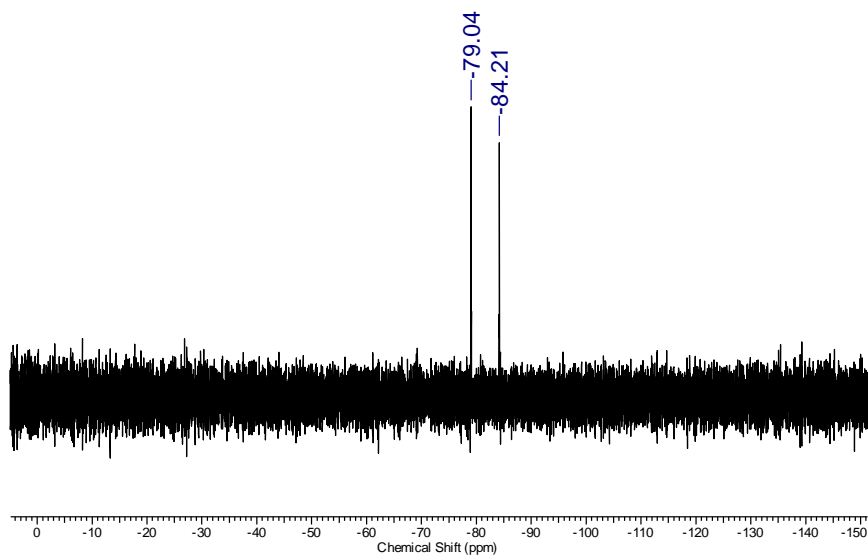


Figure S3.9. ^{19}F NMR of the insertion product of Diaz-EG₄-AuNP into H₂O, recorded in CD₃OD

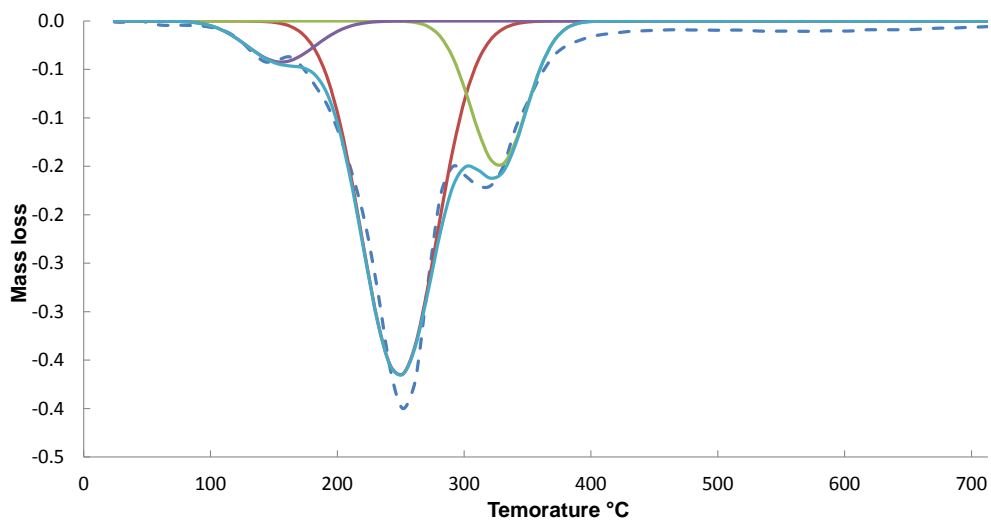


Figure S3.10. First derivative of the TGA graph of Diaz-EG₄-AuNPs (blue dashed line), fit 1 (purple), fit 2 (red), fit 3 (green), sum of fits (blue solid line).

By fitting 3 functions into the TGA diagram and using ratio of fit 1 to the sum of fits, we calculated the mass loss in the first step (loss due to the nitrogen extrusion) to be 6.6% of the overall mass loss.

Determining composition of the AuNPs corona from XPS data

The percentage of carbon corresponding to the C*F₃ is 1.2%, while the one corresponding to the C*-O (common to both ligands) is 49.5%. Because of the ligand structures, the percentage of diazirine functionalities is proportional to the number of CF₃-terminated ligands (Diaz-EG₄-S), while the percentage of C-O is related to the percentage of the two ligands.

$$1.2 = [-C^*F_3] = [\text{Diaz-EG}_4\text{-S}] \text{ (\% of Diazirine-terminated ligands)}$$

$$49.5 = [C^*\text{-O}] = 6[\text{Me-EG}_3\text{-S}] + 8[\text{Diaz-EG}_4\text{-S}]$$

(6 = number of C*-O per each Me-EG₃-S ligand and 8 = number of C*-O per each Diaz-EG₄-S ligand)

$$[\text{Me-EG}_3\text{-S}] = (49.5 - 9.6) / 6 = 6.65 \text{ (\% of Me-EG}_3\text{-S ligands)}$$

The relative % of the two ligands and the composition of the corona can now be easily calculated:

$$(1.2 * 100) / (6.65 + 1.2) = 15.3 \text{ (\% of Diaz-EG}_4\text{-S on the corona)}$$

$$100 - 15.3 = 84.7 \text{ (\% of Me-EG}_3\text{-S on the corona)}$$

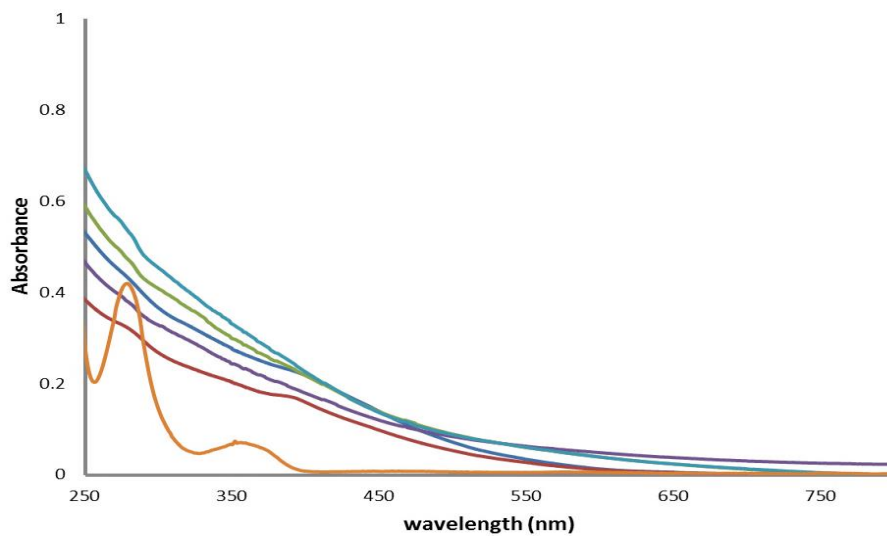


Figure S3.11. UV-vis spectra of Diaz-EG₄-SH (orange), Me-EG₃-AuNP (dark blue), Diaz-EG₄-AuNP (red), and insertion products of Diaz-EG₄-AuNP with methanol (green), ethyl vinyl ether (purple), acetic acid (light blue).

Chapter 4

Water Soluble Maleimide Modified Gold Nanoparticles (AuNPs) as a Platform for Cycloaddition Reactions

- This chapter has been accepted for publication as a full paper. The corresponding reference is: Sara Ghiassian, Pierangelo Gobbo and Mark S. Workentin, *Eur. J. Org. Chem.* **2015**, DOI: 10.1002/ejoc.201500685.
- All the experimental work reported in chapter 2 was carried out by Sara Ghiassian under the supervision of Dr. Workentin. The manuscript was initially drafted by Sara Ghiassian and Dr. Workentin provided assistance with editing and final preparation.
- All of the schemes, figures, and text in Chapter 4 reprinted with permission from John Wiley and Sons.

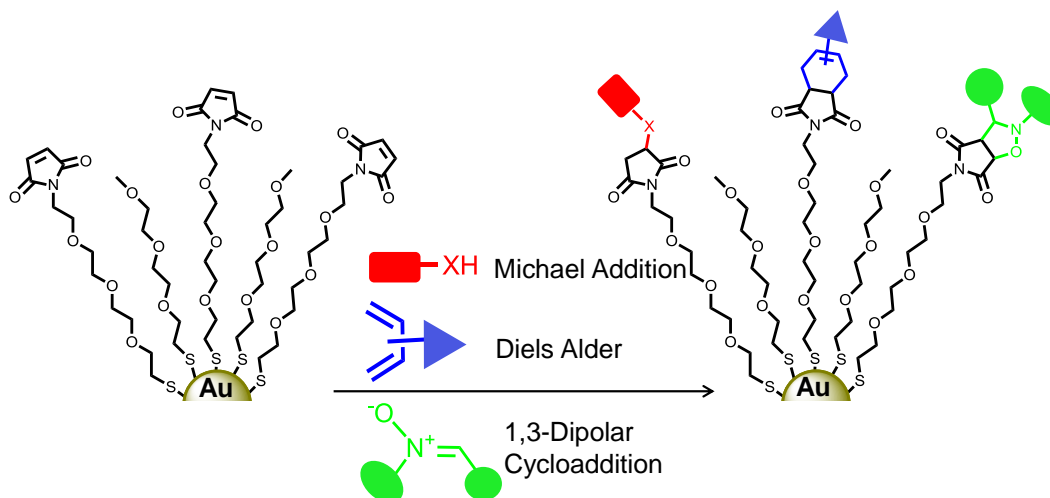
4.1 Introduction

Maleimides are important building blocks in organic synthesis and materials science, frequently employed in Michael addition, 1,3-dipolar cycloaddition or Diels-Alder reactions. Maleimide thiol/amine Michael addition has been utilized in the synthesis of cross linked polymers¹ such as hydrogels,² thermoset resins,³ and coatings.⁴ Furthermore, owing to the high yield and excellent selectivity of maleimide with thiols under physiological conditions, such chemistry is frequently employed for the surface immobilization of biomolecules.⁵⁻⁷ There have been reports of methods for immobilizing biologically active ligands onto self-assembled monolayers of alkanethiolates on gold (SAMs). Mrksich *et al.* reported that SAMs presenting a maleimide functional group can be conveniently used for the preparation of biochips upon reaction with thiol-modified biologically active ligands.⁸ A maleimide group at the interface of a AuNP would allow for the exploitation of this type of reactivity in the use of the nanoparticle in applications such as drug or substrate delivery or as an optical marker for diagnostics in biological systems.⁹⁻¹⁰

The 1,3-dipolar cycloaddition is a highly useful reaction in generating a variety of structurally different heterocycles that can be desirable in pharmaceuticals.^{11,12} Of particular importance for synthetic purposes are the 1,3-dipolar cycloaddition reactions of nitrones which can lead to a variety of products by further manipulations of the initially formed isoxazolidine.¹³ Furthermore, there are reports of 1,3-dipolar cycloadditions for polymer modification,^{14,15} generation of nano-structured semiconductors,¹⁶ surface modification of ordered mesoporous carbons,¹⁷ synthesis of fluorescent single-walled

carbon nano-tubes, which is used for the diagnosis and controlled drug delivery in medical field ¹⁸ and synthesis of modified DNA and RNA as molecular diagnostic tools.¹⁹⁻²¹

Another cycloaddition reaction that can be achieved using a maleimide platform is the Diels Alder reaction, which is without a doubt one of the most versatile carbon-carbon bond forming reactions. Such chemistry is very important in natural product synthesis, as this often involves polycyclic compounds with many chiral centers, and a Diels Alder reaction is often the only feasible route to these types of structures.^{22,23} Furthermore, synthesis of macromolecules with advanced architectures can be achieved through the Diels Alder strategy.²⁴



Scheme 4.1. Cartoon representation of Mal-EG₄-AuNPs and their versatile interfacial reactions: Michael addition (red), Diels Alder (blue), and 1,3-dipolar cycloaddition (green).

These are just a few of many applications that having a maleimide functional group present, can offer. In 2006, we reported the functionalization of AuNPs with thiols bearing maleimide moieties.²⁵ The reactivity of these organic solvent-soluble Maleimide/dodecane thiol-AuNPs was subsequently examined towards the Michael addition reaction,²⁶ the 1,3-dipolar cycloaddition,²⁷ and the Diels-Alder cycloaddition.²⁸ Although this contribution was an important step forward for their use as a template for building new architectures, it was limited to the use of a narrow range of organic solvents for further modification of AuNPs, while requiring long reaction times. To improve the reaction kinetics high pressure reaction conditions (11000 atm) were employed. Taking advantage of the negative activation volumes for such reactions resulted in notably shrinking the reaction times from days/weeks to minutes.²⁶⁻²⁸ However, the fact that one would require a specific type of apparatus to reach such high pressures, limits the use of this method. Also, when it comes to the use of very delicate biological click partners, this method might not be as feasible.

Extending this methodology to water and polar solvent soluble AuNPs is advantageous as this will broaden the use of such AuNPs for applications where one is not limited to use of non-polar organic solvents only. However, use of maleimide in aqueous solutions is not without its challenges because the maleimide is prone to hydrolysis.²⁹

Herein, we present a functionalization strategy via cycloaddition reactions to overcome these shortcomings using water soluble maleimide functionalized AuNPs.

Recently our group reported an efficient method to prepare small water-soluble maleimide functionalized AuNPs utilizing a retro-Diels-Alder strategy based on the reversible cycloaddition reaction between furan and maleimide that avoids the hydrolysis of the maleimide as a complication.²⁹ The inherently broad substrate and solvent tolerance of this reaction makes it an ideal tool for the functionalization of nanomaterials and biomolecules.^{30,31} In regards to maleimide functionalities, while Michael addition has been extensively studied, Diels Alder and 1,3-dipolar cycloaddition reactions have remained rather unexplored. In the present publication, we report the modification of small water soluble maleimide functionalized AuNPs surfaces by use of the Diels Alder and 1,3-dipolar cycloaddition reactions. The approach offers an excellent system to modify the surface of AuNPs with many different reactive partners, starting from a single nanoparticle derivative that serves as a template for these types of reactions. Here we demonstrate the versatility of this approach using a small library of nitrones and dienes. We can take advantage of organic solvent solubility of these nanoparticles to avoid hydrolysis by carrying out all the interfacial reactions in polar organic media. The yields of all transformations are very high, and the reaction time is shorter than that of organic soluble Maleimide/dodacane thiol-AuNPs previously reported.^{27,28} All the AuNPs and cycloadducts remain soluble in water and a host of organic solvents. As illustrated in Scheme 4.1, the Michael partner, diene or nitron can be incorporated into diverse range of substrates, expanding the scope of the utility of these maleimide modified AuNPs. These groups, illustrated as geometric shapes in Scheme 4.1, can be small molecules, biomolecules, redox active species, or other nanomaterials to name a few. Hence one can

take advantage of this versatile organic synthetic procedure utilizing maleimide gold nanoparticle template, to build a variety of novel architectures.

4.2 Results and Discussion

Our approach to prepare maleimide functionalized AuNPs is shown in Figure 4.1. This methodology involves synthesis of methyl terminated triethylene glycol monolayer protected AuNPs (Me-EG₃-AuNPs). The methyl-terminated EG₃ ligands were selected as the base ligand on the nanoparticles because they impart both water and organic solvent solubility.²⁹ This is important because it enables us to prepare the Maleimide modified AuNPs (Mal-EG₄-AuNPs) under conditions that avoid water and the consequential undesired hydrolysis reaction of the maleimide moiety. This is very important when working with maleimide, as water can attack either of the two carbons of the imido group. Hence, maleimide functional groups gradually begin to hydrolyze into the non-reactive maleamic/maleic acid form.^{29,32}

The required Me-EG₃-SH (compound 1) and furan-protected tetraethylene glycol maleimide thiol (FP-Maleimide-EG₄-SH, compound 2) ligands were synthesized starting from the readily available triethylene glycol monomethyl ether (Me-EG₃-OH) and tetraethylene glycol (HO-EG₄-OH), respectively following the previously reported procedures.²⁹ It is noteworthy that the maleimide ligand was synthesized with one more ethylene glycol unit than the base ligand to lower the steric hindrance on the maleimide functionality and make it more prone to reactivity. The Me-EG₃-AuNPs base

nanoparticles were synthesized using a modified one-phase synthesis method according to previous reports.²⁹ To keep the nanoparticles in the 2-3 nm regime, a ratio of 1:3 (gold: thiol) was employed. The Me-EG₃-AuNPs were then subjected to place exchange reaction in the presence of the FP-Maleimide-EG₄-SH. This reaction was carried out in a mixture of methanol and acetone as solvent. Protection of the maleimide group is necessary in this step due to its reactivity towards the thiol groups present in the reaction mixture. Finally, to prepare the desired template Mal-EG₄-AuNPs, deprotection of the maleimide at the AuNP interface was carried out through the retro Diels-Alder reaction at 110 °C in toluene/Acetonitrile (95: 5) (Figure 4.1). Purification of the final gold nanoparticles was straightforward: the solvent was evaporated to form a film of nanoparticles; this film was subsequently washed repeatedly using cyclohexane to remove the furan and any residual unbound thiol or disulfide that might be present.

The Mal-EG₄-AuNPs were characterized using transition electron microscopy (TEM), UV-vis and NMR spectroscopy. The presence of the maleimide functionality on the AuNPs was initially confirmed by ¹H NMR spectroscopy. The ¹H NMR spectrum recorded in D₂O for the FP-Maleimide-EG₄-AuNP (Figure 4.1, B) exhibits the expected signals for the furan-maleimide adduct: (a) olefinic protons at 6.60 ppm, (b) the protons adjacent to the bridged oxygen at 5.25 ppm and (c) the two protons closer to the carbonyl groups at 3.07 ppm. After the deprotection reaction and removal of the furan the signals corresponding to the Diels-Alder adduct at 6.60, 5.25 and 3.07 ppm disappear along with the concurrent appearance of a signal at 6.77 ppm that represents the alkene protons of the maleimide (d) (Figure 4.1, C). The ¹H NMR spectrum showed no indication of the

double hydrolysis products that would have appeared as a signal at 6.23 ppm due to the formation of maleic acid, or the mono hydrolysis product that would have shown two doublets at 6.24 and 5.84 ppm due to the formation of maleamic acid.²⁹ Through the integration of maleimide signal at 6.77 ppm relative to the integration of the peak at 3.38 ppm that corresponds to the three protons of the methyl group of the Me-EG₃-S- ligands (e), it is possible to determine that approximately 30% of the protecting ligands are comprised of maleimide terminated ligands, while 70% are methyl terminated ones. This information allows for a more quantitative approach when following their interfacial reactivity in the subsequent steps.

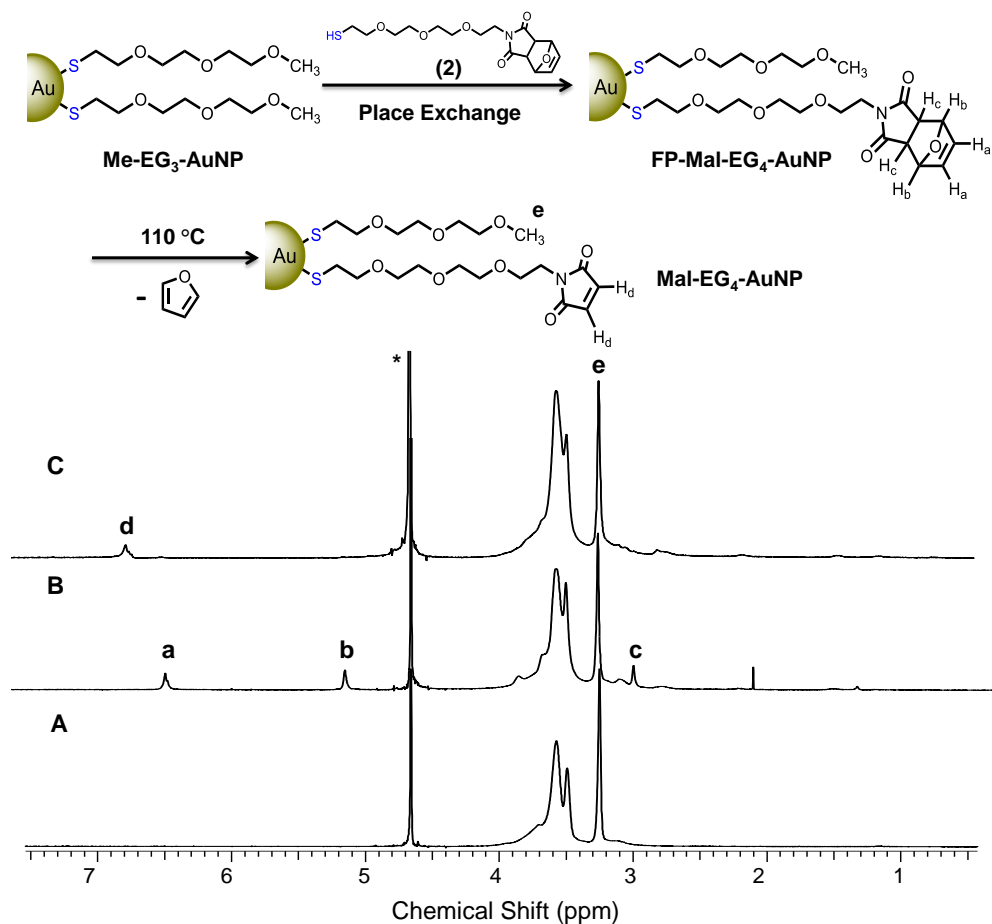


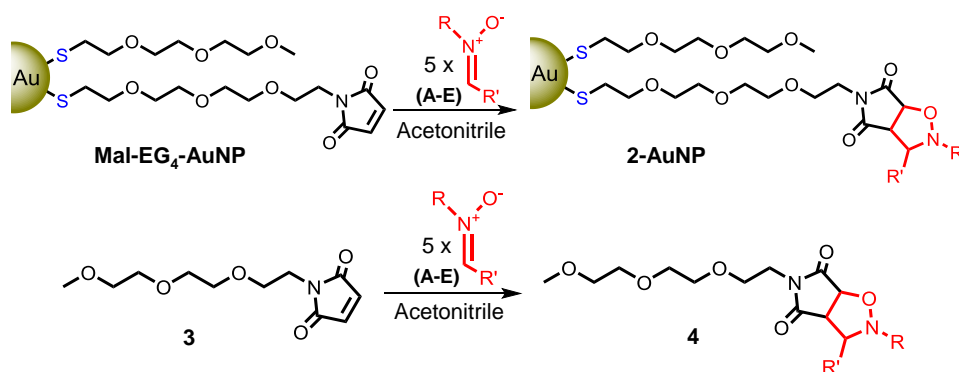
Figure 4.1. Schematic representation of the synthetic approach towards preparation of Mal-EG₄-AuNPs and the ¹H NMR spectra of: A) Me-EG₃-AuNPs, B) FP-Mal-EG₄-AuNPs, and C) Mal-EG₄-AuNPs. * indicates residual H₂O.

TEM images reveal that the FP-Mal-EG₄-AuNPs are 2.2 ± 0.3 in size. According to these images there is no significant change in the size or shape of the gold core after the deprotection process as the average size of Mal-EG₄-AuNPs is 2.5 ± 0.7 nm. This confirms that the nanoparticles retained their structural integrity after being subjected to thermal deprotection. (See Figure 4.6, A and B).

Subsequently the reactivity of Mal-EG₄-AuNPs towards the 1,3-dipolar cycloaddition and Diels-Alder reactions was investigated using a series of nitrones and dienes. In addition, because of the synthetic complexity of the cycloadducts formed using the Mal-EG₄-AuNP template, a model compound (methoxytriethylene glycol maleimide, compound 3) was prepared that resembles the maleimide thiol incorporated on the surface of nanoparticles (Figure 4.2). In case of model reactions, we can easily follow the course of reaction using ¹H NMR spectroscopy observing the disappearance of the maleimide olefin protons signal at 6.77 ppm and avoid NMR line broadening and loss of multiplicity caused by AuNPs which would hinder the characterization. All reactions were carried out under ambient pressure and biological temperature (1 atm, 37 °C).

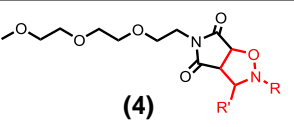
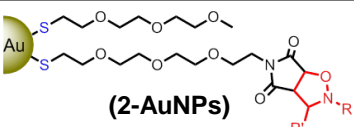
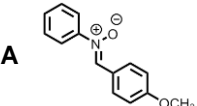
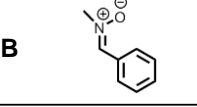
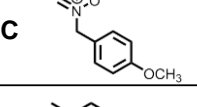
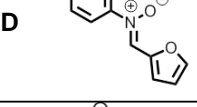
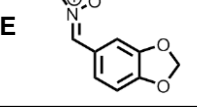
The solvent can play a pivotal role in determining the reaction pathway, stereoselectivity and rate of reaction. Noteworthy is that, there have been reports of substantial to moderate rate enhancements for several Diels Alder and dipolar cycloaddition reactions respectively when carried out in water.³³⁻³⁶ However, knowing that maleimide can gradually hydrolyze in water,²⁹ we chose not to work in aqueous media to avoid more complicated NMR spectra due to the formation of hydrolysis products as well as the desired cycloadducts. To choose the best solvent for our experiments, we carried out two specific Diels Alder and 1,3-dipolar cycloaddition reactions (1,3-dipolar cycloaddition between Mal-EG₄-AuNPs and Nitron D and Diels Alder reaction of Mal-EG₄-AuNPs and diene H) using a variety of organic solvents while keeping all the other parameters constant. When following the reaction progress using ¹H NMR spectroscopy, more polar solvents such as methanol and acetonitrile

proved to enhance the kinetics of both cycloaddition reactions to some extent compared to less polar solvents such as CH_2Cl_2 and CHCl_3 . Based on this information along with lower solubility of our cycloaddition partners (nitrones and dienes) in highly polar protic solvents (such as water and methanol) we chose acetonitrile as the solvent media for all the subsequent cycloaddition reactions.



Scheme 4.2. The 1,3-dipolar cycloaddition reaction of Mal-EG₄-AuNP and model compound 3 with nitrones A-E to form the corresponding isoxazolidine modified 2-AuNPs and model isoxazolidine products 4.

Table 4.1. Time for completion of 1,3-dipolar cycloaddition reactions of Mal-EG₄-AuNPs and model compound **3** with nitrones A-E under ambient pressure and at 37 °C.

Nitron	 (3)	 (2-AuNPs)
A 	6 hours	20 hours
B 	2 days	3 days
C 	2 hours	5 hours
D 	30 hours	2 days
E 	4 days	6 days

Nitrones are one of the most common species for 1,3-dipolar cycloaddition reactions owing to their ability to generate isoxazolidines with a high regio- and stereo-specificity. In the 1,3-dipolar cycloaddition reaction of nitrones with alkenes, up to three new contiguous chiral centers can be formed in the adduct. Furthermore, contrary to the majority of other 1,3-dipoles, most nitrones are stable compounds that do not require in situ formation.^{37,38} To investigate the interfacial 1,3-dipolar cycloaddition of Mal-EG₄-AuNPs, a series of structurally diverse nitrones were synthesized (See Scheme 4.2 and Table 4.1) and their reactivity towards 1,3-dipolar cycloaddition with maleimide was

evaluated by varying the stereoelectronic and steric character of substituents at both the carbon and nitrogen positions of the nitron group. Since characterization of the cycloadducts is crucial to demonstrate the feasibility of our approach, incorporating features that can facilitate this step is advantageous. Having aryl groups present on the nitrones has the benefit of introducing aromatic protons into the final isoxazolidine structure, where the starting Mal-EG₄-AuNPs/model compound lack any signals. Hence these signals can be exploited in confirming the reaction progress. Furthermore, the inductive effect exerted by N-aryl substituted nitrones was found to favor the reactivity by enhancing the dipolar nature of the nitron (Nitron A or D compared to B). The presence of electron-donating substituents affects the dipole character of the nitrones and decrease the reactivity (Nitron B compared to E). Steric hindrance was found to play a crucial role. Nitrones with less steric hindrance (such as Nitron C) work very efficiently in 1,3-dipolar cycloadditions. Because of the bulky character of the nanoparticles that imposes additional diffusional parameters and limits on the molecular orientation required for the reaction, sterically hindered nitrones were found to enhance the difference in the reaction kinetic between interfacial reaction and model reaction in solution (Nitron A and D). Finally, it is noteworthy that in case of furan-substituted nitron D which contains both a diene and a nitron groups available for cycloaddition, no Diels Alder adduct of furan with maleimide was detected and it exclusively reacted through the 1,3-dipolar cycloaddition to form the corresponding isoxazolidine.

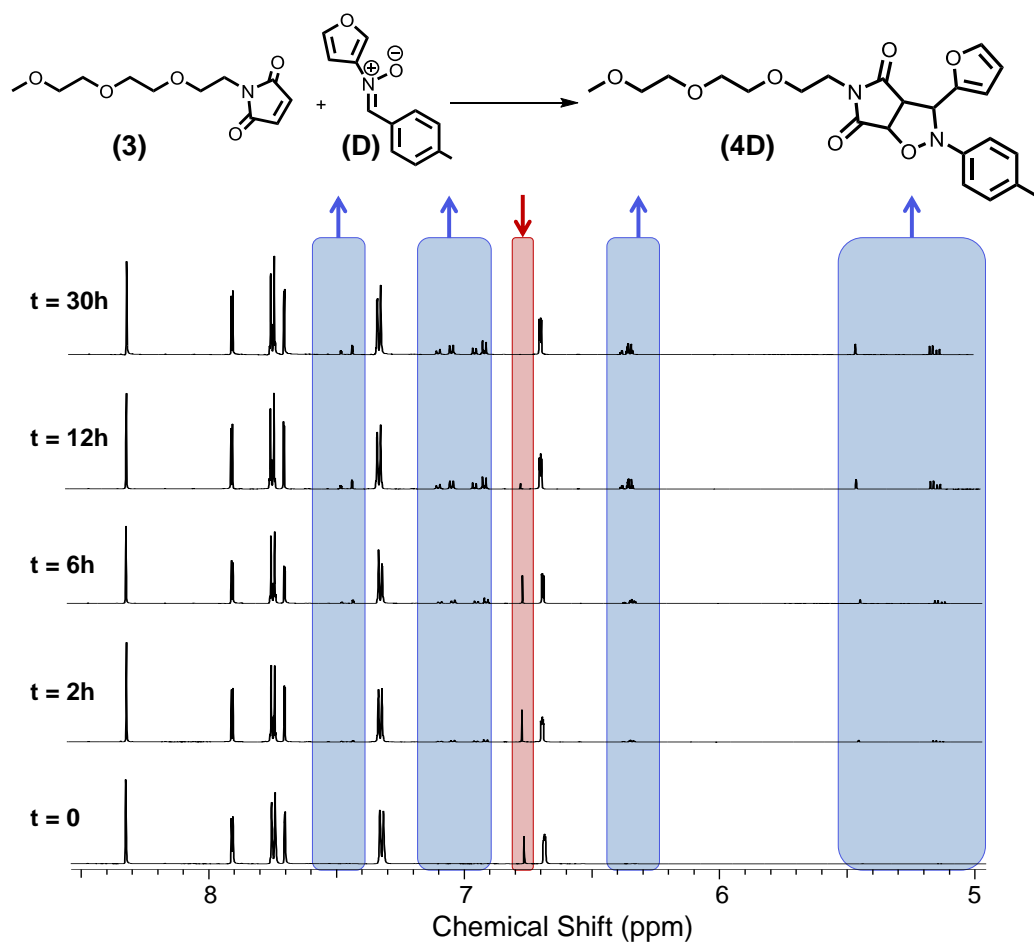


Figure 4.2. ¹H NMR spectra in 5-9 ppm region for the reaction of compound 3 and nitrene D at different time intervals.

All of the interfacially prepared cycloadducts (2(A-E)-AuNPs) were compared to the corresponding model cycloadducts (4A-4E) using compound 3 as a model maleimide molecule. Compound 3 was a useful model to study maleimide's cycloadditions, because it simplifies the analysis of the products by eliminating complications due to NMR line broadening and loss of multiplicity caused by the nanoparticles. In a typical reaction one

equivalent of the Mal-EG₄-AuNPs/model maleimide compound 3 was dissolved in d₃-Acetonitrile and five equivalents of the nitron were added to it. Five times excess nitron was used to ensure reaction completion, meanwhile not overwhelming the NMR spectrum to allow using the maleimide functionality signal to follow the reaction progress. Noteworthy is that, one can improve the reaction kinetics by introducing more excess amounts of the nitron (>5x) to the system if using NMR to follow the reaction is not a concern. For each reaction, the time taken to completely convert the maleimide to the corresponding isoxazolidine was determined by recording ¹H NMR spectra at different time intervals. Reaction progress was monitored following the loss of the maleimide olefinic signal at 6.77 ppm and the appearance of the new signals related to the cycloaddition product. Figure 4.2 illustrates the reaction progress of model compound 3 and nitron D. As reaction proceeds the maleimide signal diminishes while new signals appear and start to grow corresponding to the isoxazolidine's protons. The results are summarized in Table 4.1. Both interfacial and the model reactions gave the cycloaddition product cleanly. As expected all nitrones react much more readily with the model maleimide molecule (ranging from hours to days) than towards the Mal-EG₄-AuNPs. In case of AuNPs, the mobility of functional thiols is limited, causing a pseudo-solid phase environment. Therefore the interfacial reactions taking place between interfacial functional groups on the nanoparticle and reactants can be substantially different from those taking place in a solution.

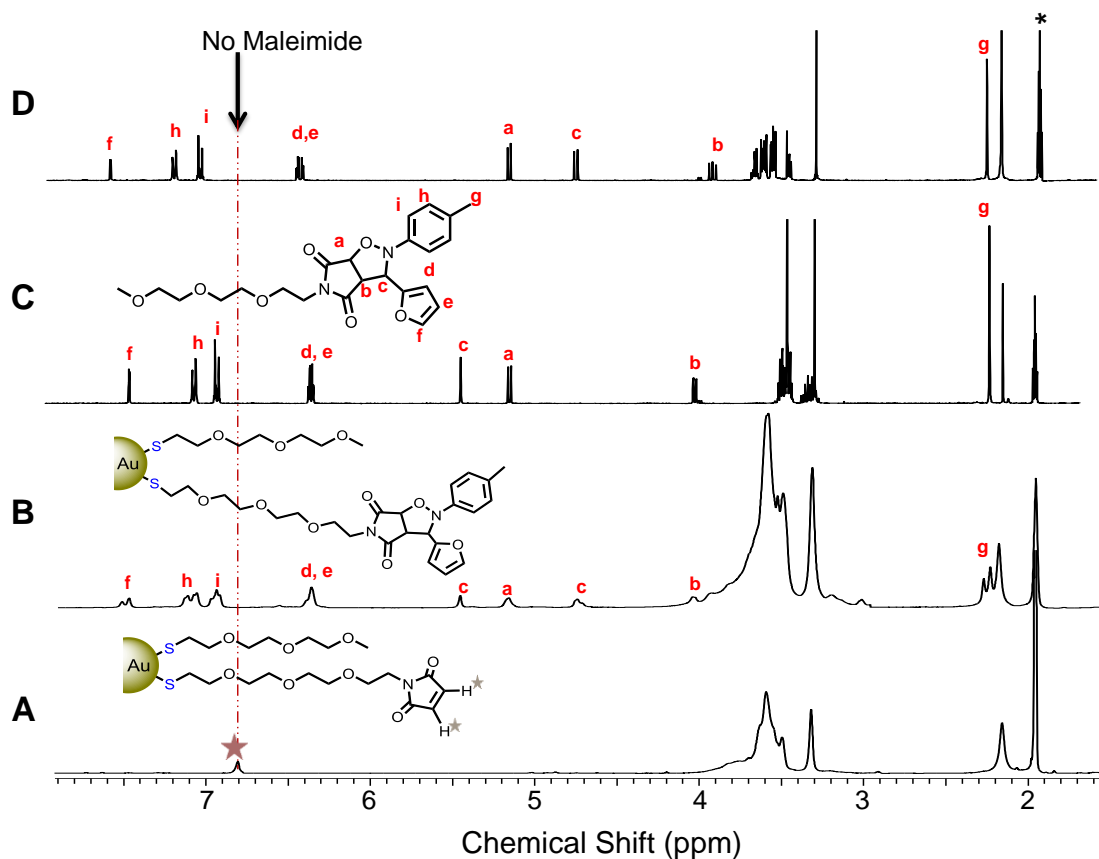
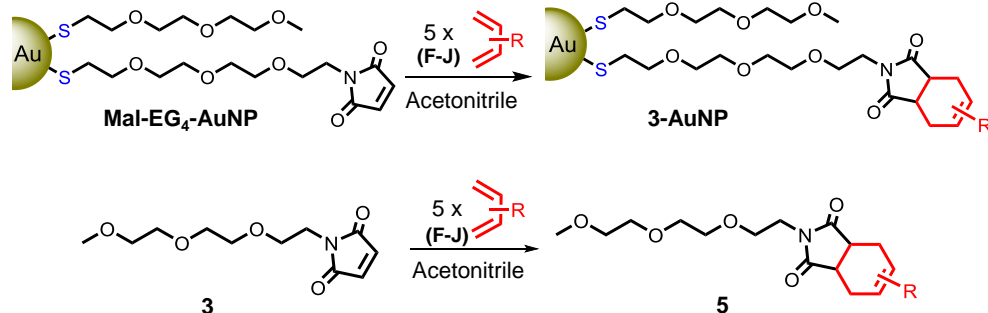


Figure 4.3. Representative ^1H NMR spectra of: A) Mal-EG₄-AuNPs and products from 1,3-dipolar cycloaddition reaction of Mal-EG₄-AuNPs with nitrone D to yield B) 2D-AuNP as a mixture of diastereomers and compound 3 with nitrone D to yield C) 4D-exo and D) 4D-endo respectively. * is residual acetonitrile.

Full characterization, including NMR spectra for both model and interfacial reaction products for all the nitrones is provided in the supporting information. There are two diastereomers, the endo and the exo isomers, expected to form in these cycloadditions. In case of the model 1,3-dipolar cycloaddition reactions, these diastereomers were separated using preparative TLC and fully characterized by ^1H and

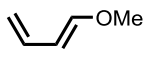
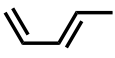
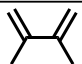

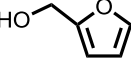
^{13}C NMR spectroscopy and high resolution mass spectrometry. However, in case of interfacially produced isoxazolidines we are unable to separate the endo and exo products because they are formed as a mixture on a single AuNP. Figure 4.3 demonstrates a representative example comparing the products formed from the model reactions (3 to 4) to that on the AuNPs (Mal-EG₄-AuNP to 2-AuNP) for nitrene D. After reaction completion and removal of the excess nitrene, ^1H NMR spectrum of the 2D-AuNPs (Figure 4.3-B) matches entirely with those of the model 4D (Figure 4.3-C and -D). This confirms the modification of AuNPs with nitrene D and formation of the expected product.

The reactivity of the Mal-EG₄-AuNPs towards the Diels-Alder reaction was also examined using a variety of dienes. As mentioned above, to facilitate the assignment of the protons of the ^1H NMR spectra, the reactions were also carried out using the solution-phase reaction of model compound 3 with the same dienes under the same reaction conditions as those used for AuNP modification to yield compounds 5F-5J. The results were then compared to those of the interfacially prepared cycloadducts, to confirm the formation of expected structures. To investigate the interfacial Diels Alder reaction of Mal-EG₄-AuNPs, a series of dienes with different steric and electronic characters were employed (See Scheme 4.3 and Table 4.2). As expected, electron rich and less sterically hindered dienes reacted much more readily with both the model compound and Mal-EG₄-AuNPs.



Scheme 4.3. Diels Alder reaction of Mal-EG₄-AuNP and model compound 3 with dienes F-J to form the corresponding modified 3-AuNPs and model Diels Alder cycloadducts 5.

Table 4.2. Time for completion of Diels Alder reactions of Mal-EG₄-AuNPs and model compound 3 with dienes F-J under ambient pressure and at 37 °C.

Diene	(5)	(3-AuNPs)
F 	4 hours	20 hours
G 	24 hours	3 days
H 	10 hours	30 hours
I 	3 days	7 days
J 	30 hours	5 days

Similar to 1,3-dipolar cycloadditions, in a typical reaction one equivalent of the Mal-EG₄-AuNPs/model compound 3 was dissolved in *d*₃-acetonitrile and five equivalents of the diene were added to it. The progress of the reactions was monitored by ¹H NMR

spectroscopy, following the appearance of signals from the cycloadducts and the disappearance of the maleimide olefinic proton signal. Figure 4 shows the ^1H NMR spectra for the Diels Alder reaction of compound 3 with diene H at different time intervals. Absence of the signal at 6.8 ppm corresponding to the maleimide moiety was taken as completion of the reaction. The results for the Diels Alder reactions of all the dienes are reported in Table 4.2. This information indicates that the reactions at the AuNP interface were always slower than in solution, reaching completion in the time scale of days instead of hours. This most likely is due to the bulky character of the AuNPs that imposes unique constraints on the orientation required for the reaction to occur causing a pseudo-solid phase environment.

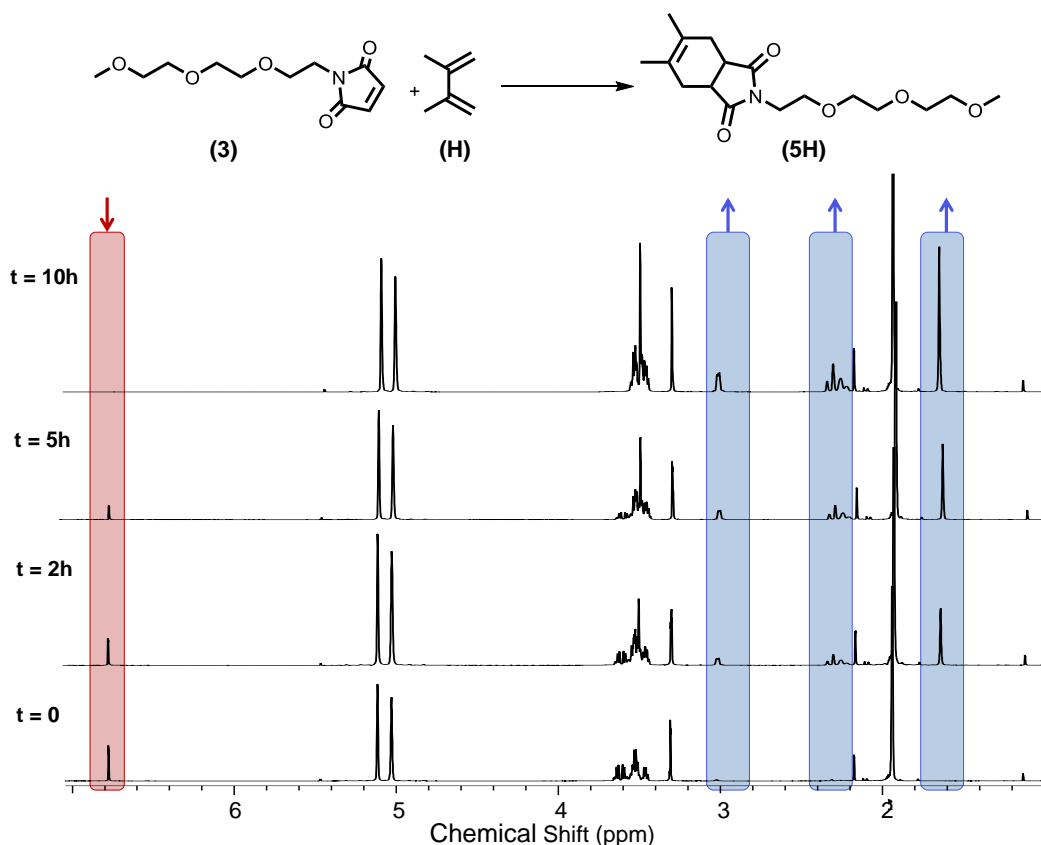


Figure 4.4. ^1H NMR spectra for the reaction of compound 3 and diene H at different time intervals.

All the Diels Alder reactions produced the expected endo isomer exclusively with the exception of diene J which yields a mixture of endo and exo isomers as demonstrated by NMR spectroscopy (see supporting information Figure S4.11). Compounds 5F–5J could be characterized more completely via ^1H and ^{13}C NMR spectroscopy and high resolution mass spectrometry. ^1H NMR spectra of all the 3-AuNP cycloadducts obtained are provided in the supporting information along with the spectral details of the corresponding reaction with the model compound 3. Because the ^1H NMR spectra of 5F–

5J are not broad like those of 3-AuNPs, they are more easily assignable, and hence they provide the confidence in the assignments of the spectra for 3-AuNPs. For example, Figure 4.5-B and Figure 4.5-C exhibits the ^1H NMR spectra of 3H-AuNPs and the model compound 5H, respectively. The appearance of signals at 1.62, 2.29 and 3.02 ppm and loss of maleimide signal at 6.77 ppm in the ^1H NMR spectra of both 3H-AuNP and 5H indicate the essentially quantitative conversion of the maleimide-terminated ligand to the corresponding cycloadducts.

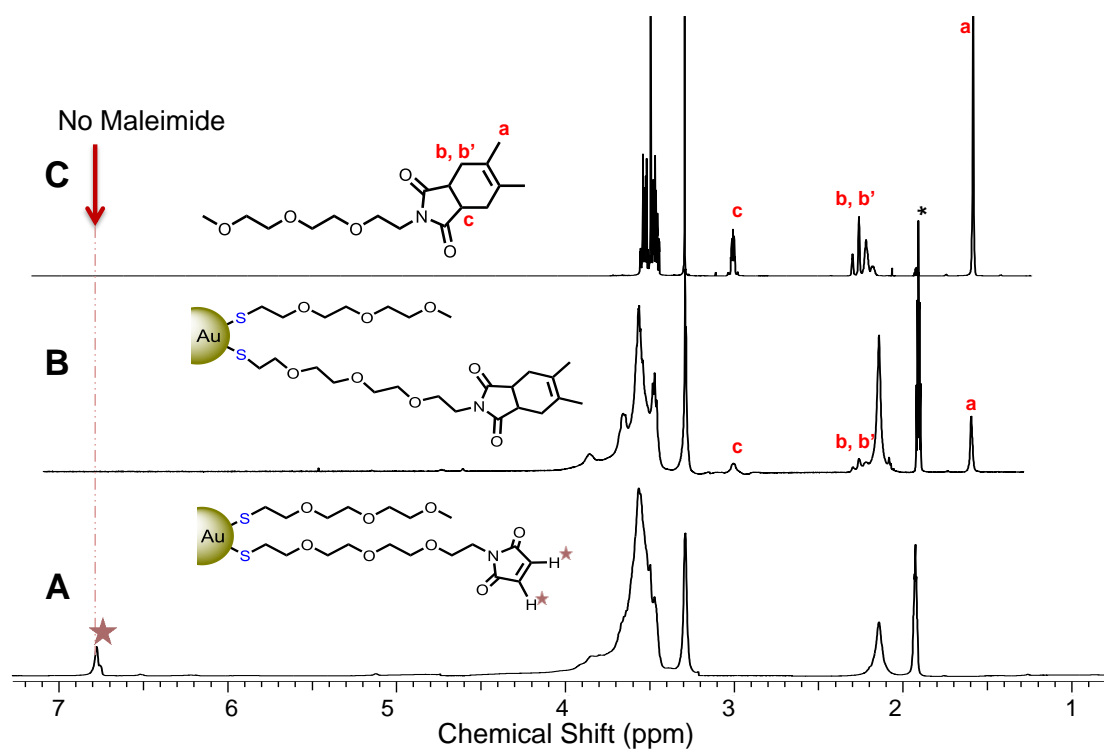


Figure 4.5. Representative ^1H NMR spectra of products from Diels Alder reaction of: A) Mal-EG₄-AuNP with 2,3-dimethyl 1,3-butadiene to yield B) 3H-AuNP and 3 with 2,3-dimethyl 1,3-butadiene to yield C) 5H. * is residual acetonitrile.

To confirm that reaction condition does not affect the size and shape of the nanoparticles we used TEM. The average size of the Mal-EG₄-AuNPs was measured to be 2.5 ± 0.7 nm initially and 2.4 ± 0.9 nm after surface modification for the representative cycloadduct-AuNPs (Figure 4.6). UV-Vis spectroscopy of all the AuNP-cycloadducts was also carried out in water. None of the surface modified AuNPs exhibit the plasmon band expected for larger AuNPs. This information along with the TEM images supports the fact that there is no distinct change in the size or shape of the gold core after the cycloaddition reactions.

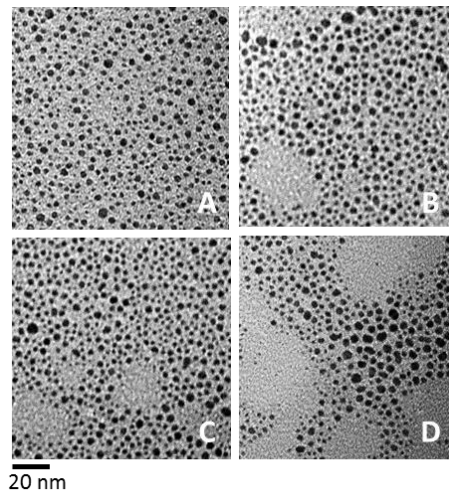


Figure 4.6. TEM images of A) FP-Ma-EG₄-AuNPs B) Mal-EG₄-AuNPs C) 2D-AuNPs D) 3H-AuNPs.

4.3 Conclusion

In summary, we have developed a synthetic protocol for the facile addition of various functionalities to AuNPs bearing interfacial maleimide functionalities through cycloaddition reactions in high yields at ambient pressure and biological temperature (1 atm, 37 °C). The versatility of the method was demonstrated for the library of nitrones and dienes studied. This methodology has a variety of advantages over some other AuNP functionalization methods, including (i) more flexibility for the synthesis of desired AuNP conjugates, (ii) reduced reaction times compared to the previously reported organic solvent soluble AuNPs, and (iii) easy purification methods. Our results demonstrate the additional potential of the Mal-EG₄-AuNPs as a platform for cycloaddition reactions with any substrate bearing a diene or nitron moiety. Due to the AuNPs' solubility in both water and a host of organic solvents, the application of these nanoparticles is not limited to a narrow range of solvents. Mal-EG₄-AuNPs interfacial reactions can be performed in aqueous media if the diene/nitron is water soluble as well. However, Hydrolysis of the maleimide can be easily avoided by carrying out all the interfacial reactions in organic solvents while maintaining the water solubility of the final cycloadduct-AuNPs. The strategy we have introduced here ensures an effective and efficient method for the development of novel nanomaterials and AuNP-conjugates, with potential applications in material chemistry, biology or nanomedicine.

4.4 Experimental

General Materials and Methods

The following reagents, unless otherwise stated, were used as received. Triethylene glycol monomethylether, tetraethylene glycol, 4-dimethylaminopyridine (DMAP), potassium thioacetate, deuterated acetonitrile (CD_3CN), deuterated chloroform (CDCl_3), tetrachloroauric acid trihydrate, sodium borohydride, *p*-toluenesulfonyl chloride, 1,3-pentadiene, 1-methoxy-1,3-butadiene, 2,3-dimethyl-1,3-butadiene, furfuryl alcohol, furan, and maleimide were purchased from Aldrich. All common solvents, triethylamine, magnesium sulfate, dry methanol, hydrochloric acid, sodium hydroxide, and potassium carbonate were purchased from Caledon. Deuterated water (D_2O) was purchased from Cambridge Isotope Laboratories. Ethanol was purchased from Commercial Alcohols. Glacial acetic acid (99.7%) was purchased from BDH. Maleic acid was purchased from Eastman Organic Chemicals. Dialysis membranes (MWCO 6000-8000) were purchased from Spectra/Por.

The ^1H and ^{13}C NMR spectra were recorded on either a Varian Inova 400 MHz or a Varian Mercury 400 MHz spectrometer. Transmission electron microscopy (TEM) images were recorded from a TEM Philips CM10. The TEM grids (Formvar carbon film on 400 mesh copper grids) were purchased from Electron Microscopy Sciences and prepared by drop casting solution of nanoparticles directly onto the grid surface. Mass spectrometry measurements were carried out using a Micro mass LCT (electrospray time-

of-flight) mass spectrometer. UV-Vis spectra were collected employing a Varian Cary 300 Bio spectrometer.

Synthetic details

Compound 1 (OMe-EG₃-SH)

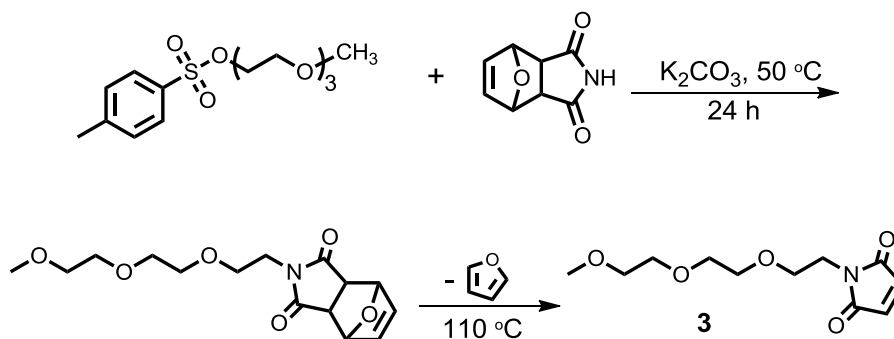
All steps in the preparation of 1 were performed in accordance with the literature procedure.²⁹ Briefly, Me-EG₃-OH was tosylated to convert the hydroxyl group into tosyl. The tosylated Me-EG₃-OH was then converted to its corresponding thioacetate via an S_N2 reaction using potassium thioacetate. The thiol was obtained through basic hydrolysis of the thioacetate functionality. Compound 1 has been fully characterized earlier. To confirm the integrity of compound 1 we used ¹H and ¹³C NMR spectroscopy that matches to that of previous reports.²⁹ ¹H NMR (400 MHz, CDCl₃) δ (ppm); 1.60 (t, 1H), 2.70 (q, 2H), 3.41 (s, 3H), 3.55 (m, 2H), 3.63 (m, 8H). ¹³C NMR (400 MHz, CDCl₃) δ (ppm); 24.2, 59.0, 70.2, 70.5, 71.9, 72.9, 110.1.

Compound 2 (FP-Mal-EG₄-SH)

All steps in the preparation of 2 were performed in accordance with the literature procedure. HO-EG₄-OH was ditosylated, then one of the tosyl groups was reacted with furan-protected maleimide and then the other tosyl extremity was converted to the thioacetate and subsequently hydrolyzed under basic conditions to generate the desired thiol, FP-Maleimide-EG₄-SH, as a light yellow oil. Compound 2 has been fully characterized before. To confirm the integrity of compound 2 we used ¹H NMR and ¹³C

NMR spectroscopy that matches to that of previous reports.²⁹ ¹H NMR (400 MHz, CDCl₃) δ (ppm); 1.60 (t, 1H), 2.70 (q, 2H), 2.87 (s, 2H), 3.65 (m, 14H), 5.27 (s, 2H), 6.52 (s, 2H). ¹³C NMR (400 MHz, CDCl₃) δ (ppm); 24.3, 47.5, 67.1, 70.1, 70.2, 70.5, 70.6, 72.6, 80.9, 136.5.

Compound 3



Scheme 4.4. Pathway towards the synthesis of maleimide model compound 3.

Compound 3 was prepared according to Scheme 4.4. In a two neck round bottom flask 1.45 g (4.55 mmol) of triethylglycol monomethyl ether tosylate was dissolved in 100 ml of dry acetonitrile. Then 0.96 g (6.75 mmol) of furan protected maleimide was added to the mixture and it was stirred until everything dissolved. Next, 0.94 g (6.80 mmol) of K_2CO_3 was added and the reaction mixture was heated at $50\text{ }^\circ\text{C}$ for 24 h. After reaction reached completion, the solvent was evaporated and the remaining oil was dissolved in dichloromethane and washed with water (x3). The organic layer was then dried over $MgSO_4$. The crude product was purified using column chromatography

(eluent: ethyl acetate) to give the furan protected triethylene glycol monomethyl ether as a yellow oil. Next, the obtained product was dissolved in toluene and heated at 110 °C for 12 h to undergo the retro-Diels Alder reaction. After evaporating the solvent, the crude product was purified using column chromatography (3:1 ethyl acetate/hexanes) to give the final product as light yellow oil. ¹H NMR (400 MHz, CDCl₃) δ (ppm); 3.36 (s, 3H), 3.62 (m, 12H), 6.70 (s, 2H). ¹³C NMR (400 MHz CDCl₃); 37.1, 58.9, 67.7, 70.0, 70.5, 71.8, 134.1, 170.5; HRMS: calc. *m/z* for C₁₁H₁₇NO₅ 243.1101, found: 243.1107.

Synthesis of Furan Protected AuNPs (FP-Mal-EG₄-AuNPs)

Furan protected Maleimide modified AuNPs were synthesized through a place exchange reaction. First, triethylene glycol monomethyl ether AuNPs (Me-EG₃-AuNPs) were synthesized in accordance with our previously reported procedure.²⁹ Next, to introduce the protected maleimide tetraethylene glycol thiol ligands onto the nanoparticle shell, 30 mg of freshly prepared thiol 2 was dissolved in 5 ml of MeOH : acetone (4: 1). This solution was then added to a solution of Me-EG₃-AuNPs (100 mg in 10 ml of MeOH: acetone (4: 1). After vigorously stirring the reaction mixture for 15 minutes, the solvent was evaporated to form a film of nanoparticles. This film was washed with cyclohexane (x3) to remove the excess thiol 2. The particles were then further purified by dialysis in water overnight.

Synthesis of maleimide functionalized AuNPs (Mal-EG₄-AuNPs)

The deprotection of the maleimide was carried out using the retro Diels-Alder reaction similar to that one reported previously for organic soluble maleimide AuNP. The FP-Mal-EG₄-AuNPs were dissolved in toluene: Acetonitrile (95:5) in a round bottom flask equipped with a condenser. The system was then heated at 110 °C overnight. The solvent was evaporated under vacuum and the resulting nanoparticle film inside the flask was washed with cyclohexane (x5).

Synthesis of Nitrones A-E

All the nitrones were prepared following the reference procedure. To a stirred solution of 5.0 g (1 eq.) of the prerequisite aldehyde in 300 ml 95% EtOH was added 2 eq. of the nitro compound followed by 3.0 eq. of powdered zinc. Finally, 6.0 eq. of acetic acid was added dropwise at 0°C and the mixture was allowed to stir at room temperature for 24 h. Following this time, the solvent was rotary-evaporated to half the original volume and the precipitated zinc was filtered off. The resulting liquid was purified by flash liquid chromatography elution (20 -50 % gradient of ethyl acetate to hexanes) to yield pure nitrone after rotary evaporation of the column fractions. All the nitrones have been characterized and reported previously.³⁹

General procedures for cycloaddition reactions of maleimide

1,3-Dipolar cycloaddition reactions:

Preparation of 2-AuNPs

Approximately 10 mg of Mal-EG₄-AuNPs was dissolved in 1 mL of deuterated acetonitrile and mixed with the appropriate nitron (5 eq.) (A-E). The mixture was then transferred to a NMR tube and placed in a 37 °C bath. After ¹H NMR spectroscopy showed reaction completion, the reaction was stopped by evaporating the solvent and forming a film of AuNPs. The products 2(A-E)-AuNPs were then purified by washing the film of nanoparticles with cyclohexane and then isopropanol to remove any unreacted nitron. ¹H NMR spectroscopy was used to characterize the resulting 2-AuNPs. These spectra were then compared to those of the products of the model reaction to ensure purity. All the NMR spectra are provided in the supporting information.

Preparation of 4A-4E

Approximately 20 mg of compound 3 and 5 eq. of nitrones A-E were dissolved in 2 mL of deuterated acetonitrile. The mixture was then transferred to a NMR tube and placed in a 37 °C bath. After ¹H NMR spectroscopy showed reaction completion, the reaction was stopped and the product was purified by preparative TLC plate (20 -50 % gradient of hexanes to ethyl acetate). The resulting products were then characterized by ¹H and ¹³C NMR spectroscopy and high resolution mass spectrometry. All the NMR spectra are provided in the supporting information.

Diels Alder reactions

Preparation of 3-AuNPs

Approximately 10 mg of Mal-EG₄-AuNPs was dissolved in 1 mL of deuterated acetonitrile and mixed the appropriate diene (5 eq.) (F-J). The mixture was then transferred to a NMR tube and placed in a 37 °C bath. After ¹H NMR spectroscopy showed reaction completion, the reaction was stopped by evaporating the solvent and forming a film of AuNPs. The products 3(F-J)-AuNPs were then purified by washing the film with cyclohexane and then isopropanol to remove any unreacted diene. ¹H NMR spectroscopy was used to characterize the resulting 3-AuNPs. These spectra were then compared to those of the products of the model reaction to ensure purity. All the NMR spectra are provided in the supporting information.

Preparation of 5F-5J

Approximately 20 mg of compound 3 and 5 eq. of dienes F-J were dissolved in 2 mL of deuterated acetonitrile. The mixture was then transferred to a NMR tube and placed in a 37 °C bath. After ¹H NMR spectroscopy showed reaction completion, the reaction was stopped and the product was purified by preparative TLC plate (20 -50 % gradient of hexanes to ethyl acetate). The resulting products were then characterized by NMR spectroscopy. All the NMR spectra are provided in the supporting information.

4.5 References

- 1) Mather, K. M.; Viswanathan, K.; Miller, K. M.; Long, T. E. *Prog. Polym. Sci.* **2006**, 31, 487.
- 2) Rizzi, S. C.; Hubbell, J. A. *Biomacromolecules*, **2005**, 6, 1226.
- 3) Pavlinec, J.; Moszner, N. *J. Polym. Sci. Part A. Polym. Chem.* **1997**, 10, 165.
- 4) Tamami, B.; Betrabet, C.; Wilkes, G. L. *Polym. Bull.* **1993**, 30, 293.
- 5) Zimmermann, J. L.; Nicolaus, T.; Neuert, G.; Blank, K. *Nat. Protoc.* **2010**, 5, 975.
- 6) Roberts, M. J.; Bentley, M. D.; Harris, J. M. *Adv. Drug Delivery Rev.* **2002**, 54, 459.
- 7) Petty, R. T.; Li, H. W.; Maduram, J. H.; Ismagilov, R.; Mrksich, M. *J. Am. Chem. Soc.* **2007**, 129, 8966.
- 8) Houseman, B. T.; Gawalt, E. S.; Mrksich, M. *Langmuir* **2003**, 19, 1522.
- 9) Jain, S.; Hirst, D. G.; O'Sullivan, J. M. *Br. J. Radiol.* **2012**, 85, 101.
- 10) Manju, S.; Sreenivasan, K. *J. Colloid Interface Sci.* **2012**, 368, 144.
- 11) Conti, P.; Dallanoce, C.; De Amici, M.; De Micheli, C.; Klotz, K. N. *Bioorg. Med. Chem.* **1998**, 6, 401.
- 12) Groutas, W. C.; Venkataraman, R.; Chong, L. S.; Yoder, J. E.; Epp, J. B.; Stanga, M. A.; Kim, E. H. *Bioorg. Med. Chem.* **1995**, 3, 125.
- 13) Padwa, A.; Pearson, W. H. *Synthetic application of 1,3-dipolar cycloaddition chemistry toward heterocycles and natural products*, Wiley, New York, **2003**.
- 14) Singh, I.; Zarafshani, Z.; Lutz, J. F.; Heaney, F. *Macromolecules* **2009**, 42, 5411.

- 15) Lee, Y.; Koyama, Y.; Yonekawa, M.; Takata, T. *Macromolecules* **2009**, 42, 7709.
- 16) Bakbak, S.; Leech, P. J.; Carson, B. E.; Saxena, S.; King, W. P.; Bunz, U. H. F. *Macromolecules* **2006**, 39,6793.
- 17) Wang, X.; Jiang, D. E.; Dai, S. *Chem. Mater.* **2008**, 20, 4800.
- 18) Bayazit, M. K.; Coleman, K. S. *J. Am. Chem. Soc.* **2009**, 131, 10670.
- 19) Gutmiedl, K.; Wirges, C. T.; Ehmke, V.; Carell, T. *Org. Lett.* **2009**, 11, 2405.
- 20) Amblard, F.; Cho, J. H.; Schinazi, R. F. *Chem. Rev.* **2009**, 109, 4207.
- 21) Li, Z. M.; Seo, T. S.; Ju, J. Y. *Tetrahedron Lett.* **2004**, 45, 3143.
- 22) Gandini, A.; Coelho, D.; Silvestre, A. J. D. *Eur. Polym. J.* **2008**, 44, 4029.
- 23) Tang, S. Y.; Shi, J.; Guo, Q. X. *Org. Biomol. Chem.* **2012**, 10, 2673.
- 24) Tasdelen, M. A. *Polym. Chem.* **2011**, 2, 2133.
- 25) Zhu, J.; Kell, A. J.; Workentin, M. S. *Org. Lett.* **2006**, 8, 4993.
- 26) Hartlen, K. D.; Ismaili, H.; Zhu, J.; Workentin, M. S. *Langmuir* **2012**, 28, 864.
- 27) Zhu, J.; Lines, B. M.; Ganton, M. D.; Kerr, M. A.; Workentin, M. S. *J. Org. Chem.* **2008**, 73, 1099.
- 28) Zhu, J.; Ganton, M. D.; Kerr, M. A.; Workentin, M. S. *J. Am. Chem. Soc.* **2007**, 129, 4904.
- 29) Gobbo, P.; Workentin, M. S. *Langmuir* **2012**, 28, 12357.
- 30) Gobbo, P.; Biesinger, M. C.; Workentin, M. S. *Chem. Commun.* **2013**, 49, 2831.
- 31) De, P.; Li, M.; Gondi, S. R.; Sumerlin, B. S. *J. Am. Chem. Soc.* **2008**, 130, 11288.

- 32) Kalia, J.; Raines, R. T. *Bioorg Med. Chem. Lett.* **2007**, 17, 6286.
- 33) Meijer, A.; Otto, S.; Engberts, J. B. F. N. *J. Org. Chem.* **1998**, 63, 8989.
- 34) Breslow, R. *Acc. Chem. Res.* **1991**, 24, 159.
- 35) Gholami, M. R.; Habibi Yangjeh, A. *Int. J. Chem. Kinet.* **2000**, 32, 431.
- 36) Pandey, P. S.; Pandey, I. K. *Tetrahedron Lett.* **1997**, 38, 7237.
- 37) Gothelf, K. V.; Jorgensen, K. A. *Chem. Rev.* **1998**, 98, 863.
- 38) Torssell, K. B. G. *Nitrile Oxides, Nitrones and Nitronates in Organic Synthesis*, VCH, Weinheim, **1988**.
- 39) Ganton, M. D.; Kerr, M. A. *J. Org. Chem.* **2004**, 69, 8554.

4.6 Supporting Information

This section contains the data to support the work carried out in chapter four of this thesis. It includes NMR spectra of 2-AuNPs, 3-AuNPs and all the corresponding 1,3-dipolar cycloaddition and Diels-Alder cycloadducts from model reaction of compound 3 with dienes and nitrones as well as UV-Vis spectra of all the cycloadduct-AuNPs.

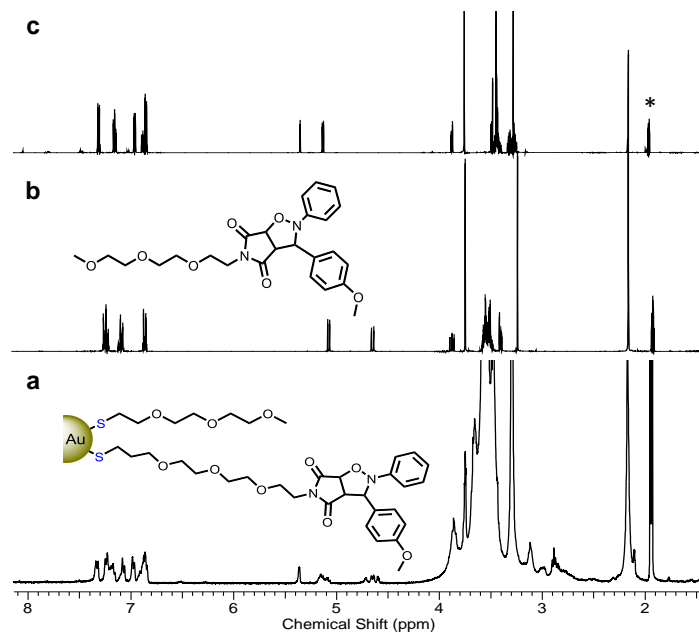


Figure S4.1. ^1H NMR spectra of: a) 2A-AuNPs, b) 4A-endo, c) 4A-exo recorded in CD_3CN . * indicates residual CH_3CN .

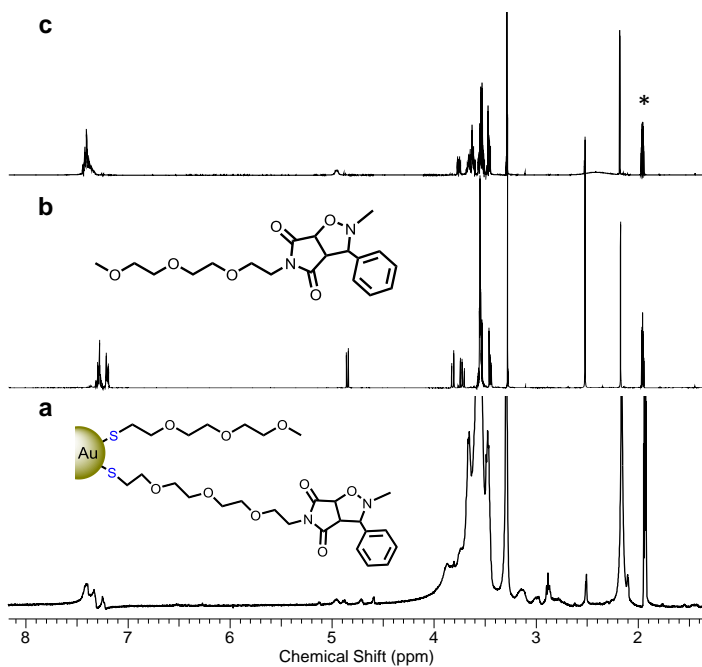


Figure S4.2. ^1H NMR spectra of: a) 2B-AuNPs, b) 4B-endo, c) 4B-exo recorded in CD_3CN . * indicates residual CH_3CN .

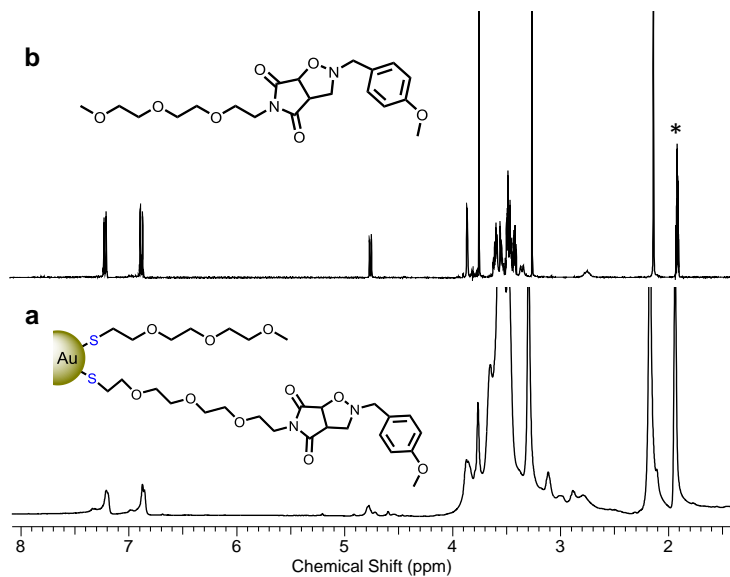


Figure S4.3. ^1H NMR spectra of: a) 2C-AuNPs and b) 4C recorded in CD_3CN . * indicates residual CH_3CN .

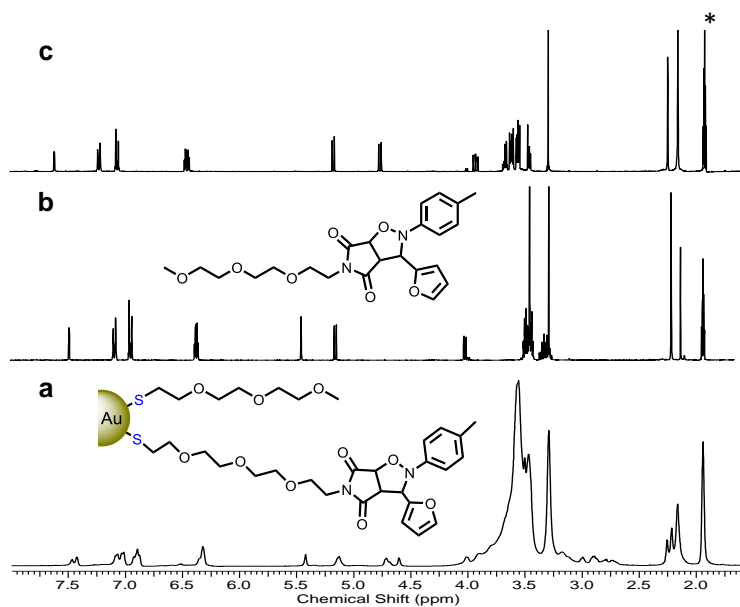


Figure S4.4. ^1H NMR spectra of: a) 2A-AuNPs, b) 4A-exo, c) 4A-endo recorded in CD_3CN . * indicates residual CH_3CN .

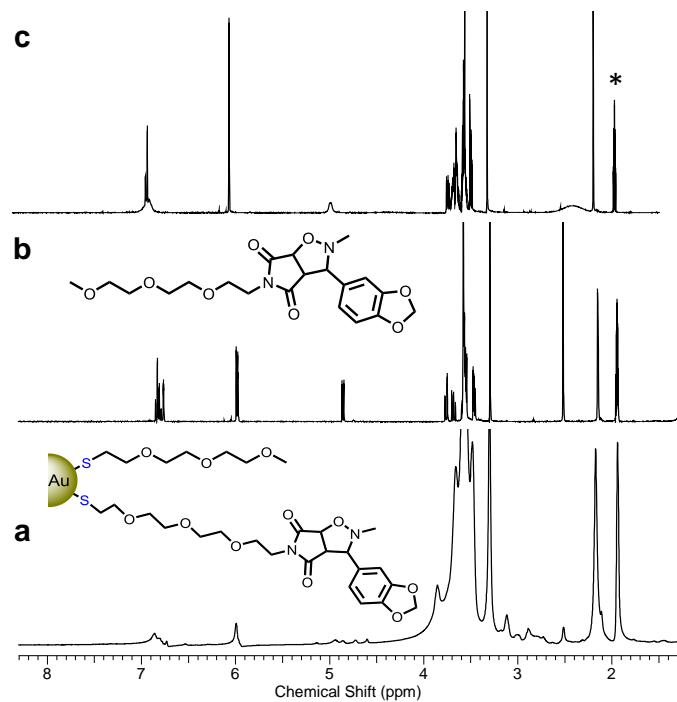


Figure S4.5. ^1H NMR spectra of: a) 2E-AuNPs, b) 4E-endo, c) 4E-exo recorded in CD_3CN . * indicates residual CH_3CN .

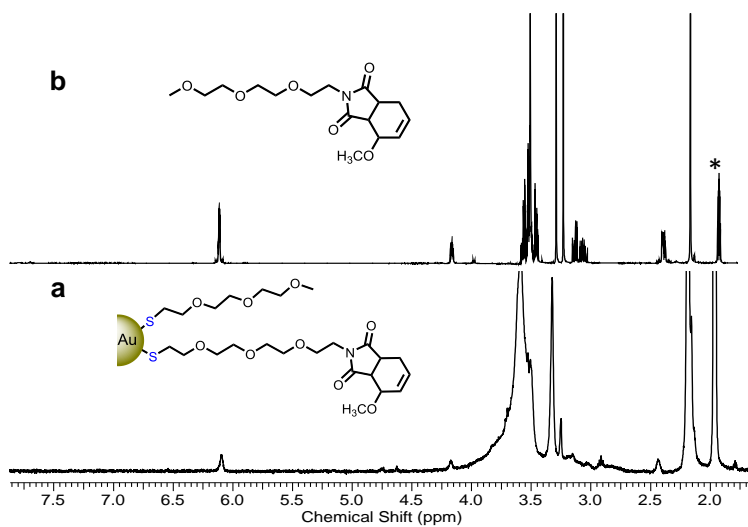


Figure S4.6. ^1H NMR spectra of: a) 3F-AuNPs and b) 5F recorded in CD_3CN . * indicates residual CH_3CN .

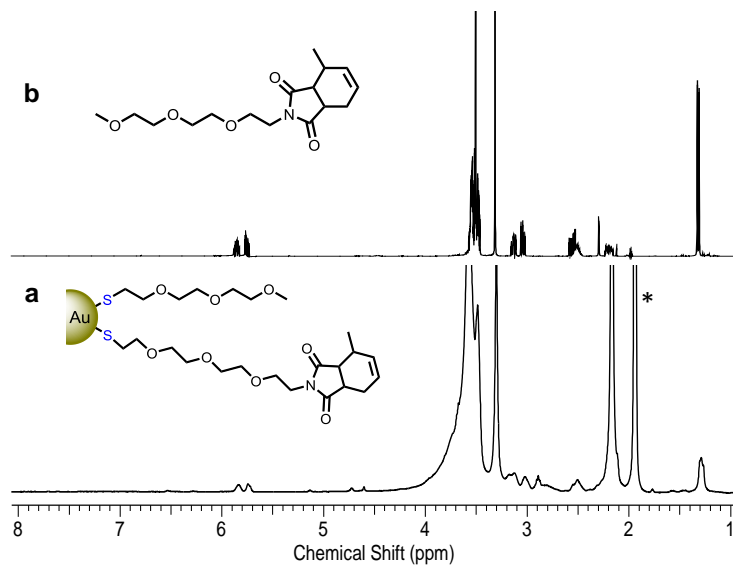


Figure S4.7. ^1H NMR spectra of: a) 3G-AuNPs and b) 5G recorded in CD_3CN . * indicates residual CH_3CN .

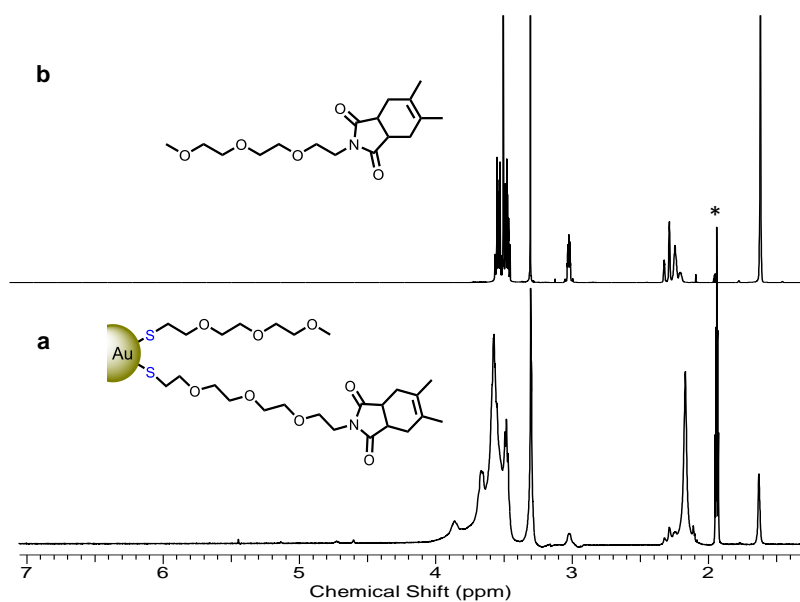


Figure S4.8. ^1H NMR spectra of: a) 3H-AuNPs and b) 5H recorded in CD_3CN . * indicates residual CH_3CN .

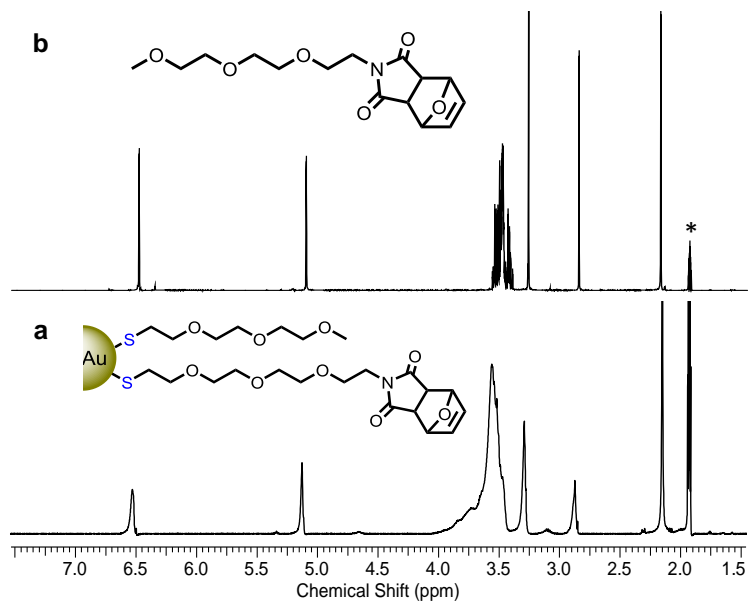


Figure S4.9. ^1H NMR spectra of: a) 3I-AuNPs and b) 5I recorded in CD_3CN . * indicates residual CH_3CN .

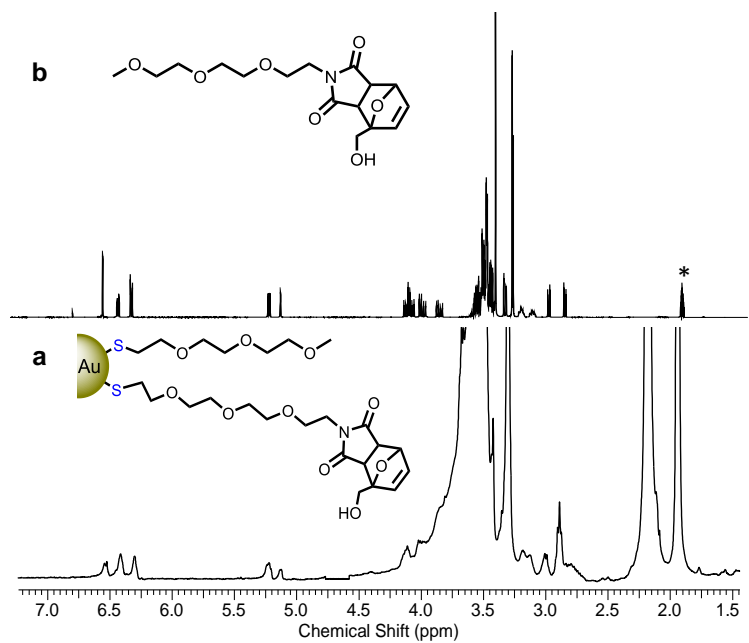


Figure S4.10. ^1H NMR spectra of: a) 3J-AuNPs and b) 5J (inseparable mixture of endo/exo) recorded in CD_3CN . * indicates residual CH_3CN .

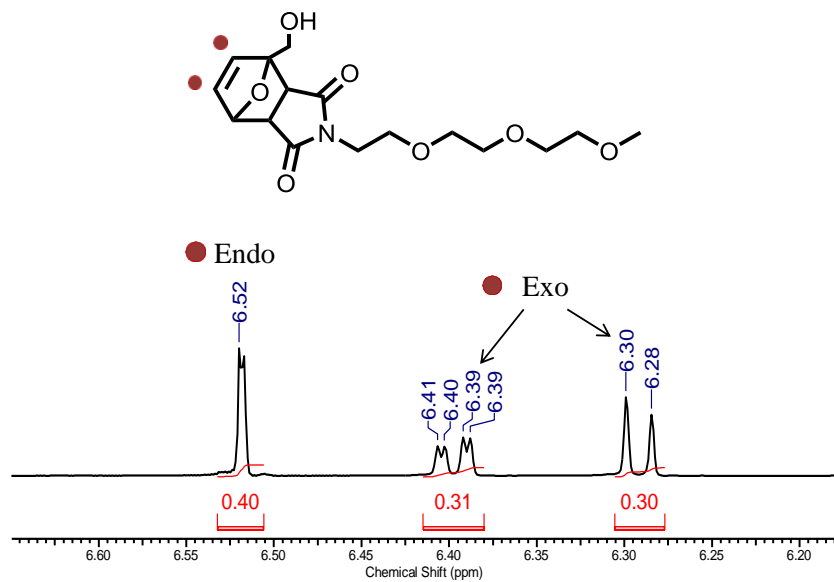


Figure S4.11. ¹H NMR spectrum of 5J with a close look at the *endo:exo* ratio which is 2:3.

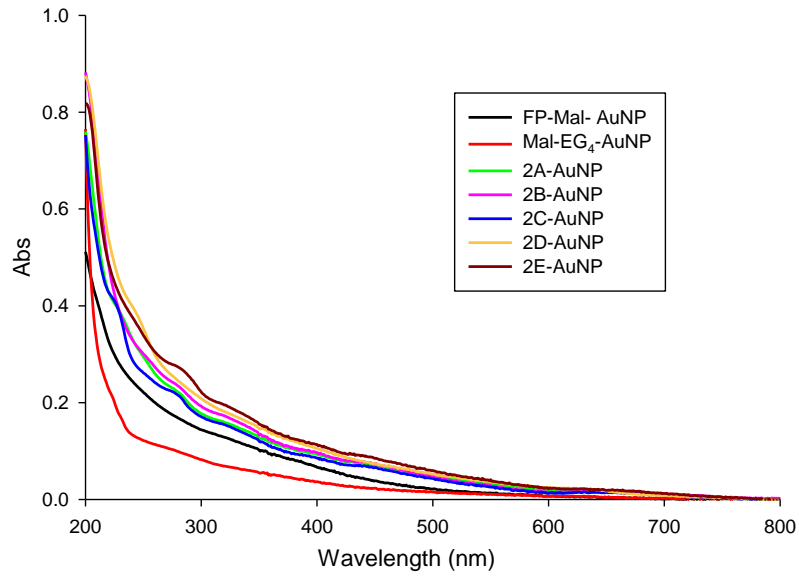


Figure S4.12. UV-vis spectra of FP-Mal-AuNP, Mal-EG₄-AuNP and 2(A-E)-AuNPs.

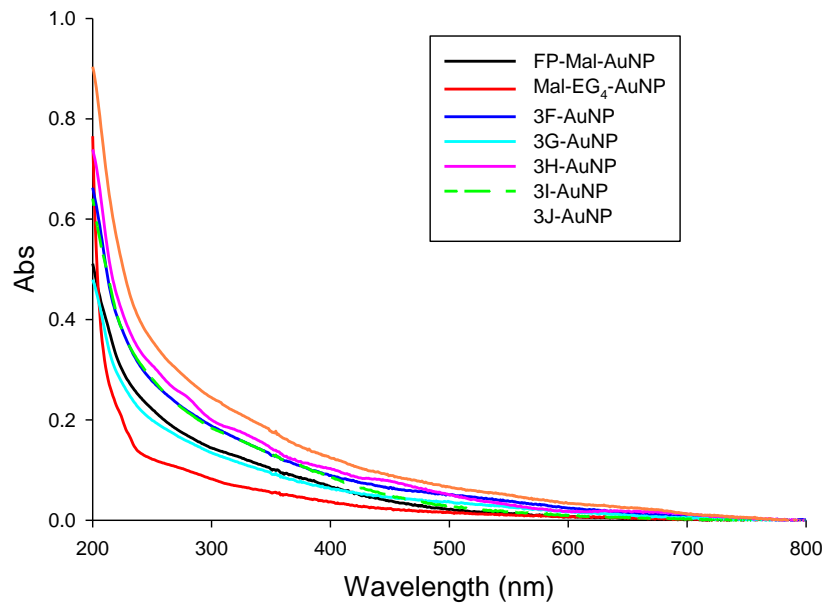


Figure S4.13. UV-vis spectra of FP-Mal-AuNP, Mal-EG₄-AuNP and 3(F-J)-AuNPs.

Chapter 5

Nitrone Modified Gold Nanoparticles: Synthesis, Characterization and Their Potential for the Development of ^{18}F -Labeled PET Probes and Hybrid Nanomaterials

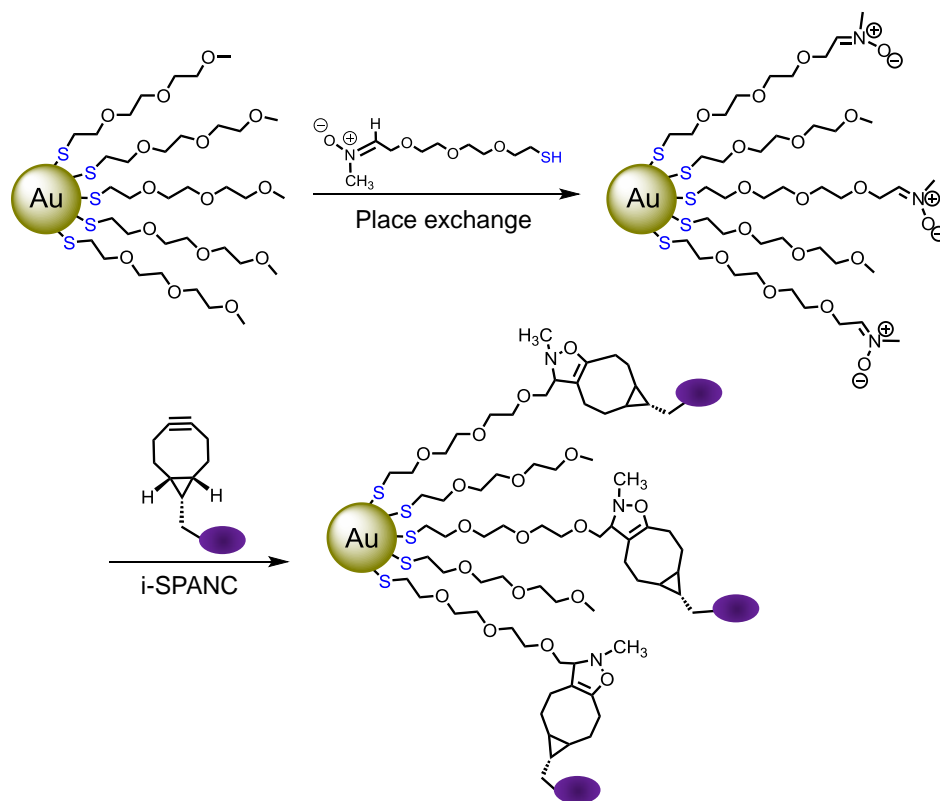
- This chapter includes data that has been obtained in collaboration with Luyt and Gillies research groups.
- Dr. Lihai Yu, a postdoctoral fellow from Professor Luyt's research group, has performed all the radiolabeling experiments. Pierangelo Gobbo prepared compound 5 and 12. Sara Ghiassian carried out all the other work reported in this chapter.
- Depending on the outcome of the PET animal studies, this chapter will be written as two separate papers. One paper covers the synthesis and characterization of Nitrone-AuNPs and all the radiolabeling and PET studies. The second paper will include the use of Nitrone-AuNPs for the preparation of hybrid materials including AuNP-CNTs shown here, as well as other data obtained in collaboration with Dr. Ali Nazemi (a previous PhD student from Gillies group) that is not included in this chapter.

5.1 Introduction

Gold nanoparticles (AuNPs) have received considerable attention in the biomedical field due to their biocompatibility, facile conjugation to biomolecules, and the unique optical properties.¹⁻³ Additionally, being that gold is resistant to oxidation under physiological or ambient conditions, it can be safely utilized in biological environments. In the imaging field, AuNPs have shown great promise for their utility in Raman spectral imaging,^{4,5} computed tomography^{6,7} and photoacoustic tomography.^{8,9} Several studies have also reported the use of AuNPs labeled with gamma emitters or positron emitters for multimodality imaging, such as PET/CT imaging.¹⁰⁻¹³

When creating AuNP-conjugates that are capable of functions *in vivo*, including targeting, image contrast, biosensing, or drug delivery, excellent selectivity and high sensitivity are of utmost importance. Hence, bioorthogonal conjugation reactions are suitable candidates for such purposes due to their fast kinetics, high yields and mild reaction conditions.¹⁴ One of the most promising bioorthogonal labeling reactions is the strain-promoted alkyne-azide cycloaddition (SPAAC), a variant of the copper (I)-catalyzed Huisgen azide-alkyne cycloaddition (CuAAC),¹⁵ that does not require the use of the cytotoxic metal catalyst. In order to extend the use of click chemistry to *in vivo* studies there was a need to overcome the detrimental effects of copper catalyst by introducing alternative methods to lower the activation energy of the alkyne-azide cycloaddition. Bertozzi *et al.* developed a new methodology for bioconjugation by using a more activated ring strained alkyne for the alkyne-azide cycloadditions.¹⁶ Until

recently, most efforts have focused on increasing the reactivity the cyclooctyne reagent in the azide-alkyne reactions in order to avoid the need for use of any catalyst.¹⁷⁻²³ Their typical reacting partner, azide, is generally easy to prepare and considered bioorthogonal because it is small, metabolically stable, and does not naturally exist in cells and thus has no competing biological side reactions,²⁴ and it is widely used in both CuAAC and SPAAC reactions. However, utilizing more reactive alternatives to azides can greatly enhance the reaction rate. Recently, a variant to SPAAC has been proposed, which replaces the azido functionality with a nitron group.^{25,26} Termed strain-promoted alkyne-nitron cycloaddition (SPANC), this reaction represents a new versatile tool for chemical biology due to rapid kinetics, biocompatibility, high reaction yields as well as tunability of the nitron moiety by using diverse substituents on both carbon and nitrogen atoms of the dipole.^{27,28} The bioorthogonal SPANC reaction has applications that range from protein modification,^{29,30} and cell surface labeling,²⁷ to material science.³¹ To date, there have been several reports on the specific N-terminal nitron functionalization and labeling of peptides or proteins containing serine as the first residue.^{27,29,30} Recently Colombo *et al.* reported on the use of SPANC for conjugation of a scFv variant of the anti-Her2 antibody to iron oxide magnetic nanoparticles. In this report authors demonstrate that SPANC can be utilized for conjugation of cycloalkyne modified nanoparticles and anti-HER2 antibodies containing an N-terminal nitron. These targeted multifunctional nanoparticles were found to localize only to HER2 positive breast cancer cells.³²



Scheme 5.1. Cartoon representation towards preparation of Nitron-AuNPs and their corresponding i-SPANC reaction.

The high selectivity, fast reaction rate, and aqueous compatibility of SPANC make this strategy an ideal approach for preparation AuNP-conjugates or hybrid materials through interfacial reactions. In this context, we report a facile and straightforward method for the synthesis of AuNPs with nitron moiety present on the gold corona (See Scheme 5.1). Nitron functionalities incorporated onto the gold core can be employed as a reactive template that undergoes interfacial SPANC (i-SPANC) reaction with any substrate bearing a strained alkyne. Nitron incorporation was achieved through a place

exchange reaction using triethylene glycol monomethyl ether functionalized AuNPs as the building blocks. This approach benefits from having control over the amount of interfacial nitron functionality and subsequently the solubility of the AuNPs. Interfacial ligands can be quantified and introduced in a controlled manner by changing the parameters in the ligand exchange reaction to match the specific application these AuNPs are intended for. Furthermore, interfacial reactions can be followed in a quantitative manner to determine the extent of conjugation. It is also important to note that, incorporating triethylene glycol monomethyl ether ligands onto the gold core enables solubility in a range of organic solvents as well as water. Consequently, such nanoparticles can be used in wide range of organic or aqueous media for various applications. To showcase this versatility we examined the utility of Nitron-AuNPs for biological applications as well as in material chemistry.

Initially we focused on preparing AuNP-conjugates with potential use for *in vivo* studies. When AuNP-conjugates are aimed for *in vivo* applications, to optimize the success and minimize long term side effects information about the biodistribution of AuNPs is crucial. Positron emission tomography (PET) is a highly sensitive, noninvasive isotopic imaging tool that allows the determination of quantitative biodistribution by imaging the uptake of the AuNPs by various organs. One of the main limitations on the development of new radiotracers for use in PET are the time constraints created by working with radionuclides having the short half-lives inherent to the main radionuclides (such as ^{18}F) used in PET radiotracer development. The combination of selectivity, modularity, orthogonality, and fast kinetics offered by strain-promoted cycloaddition

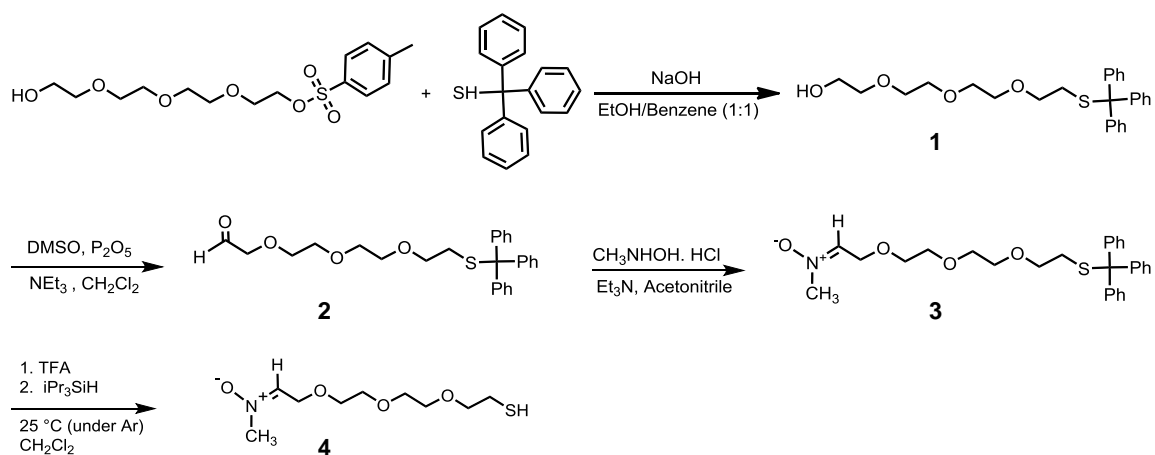
reactions make them an almost ideal synthetic methodology for the creation of radiopharmaceuticals. A recent development in the field of PET radiochemistry is the use of copper catalyzed 1,3-dipolar cycloaddition reactions to prepare ^{18}F -labeled compounds.³³⁻³⁵ Here, we explore the utility of the efficient biorthogonal i-SPANC chemistry to prepare ^{18}F -labeled AuNPs for potential application in PET.

In the second part of this study, we demonstrate the utility of the i-SPANC reaction to prepare hybrid nanomaterials using single-walled carbon nanotubes (SWCNTs). Interest in developing diverse AuNP-composite materials continues to grow. This is primarily motivated by the desire to simultaneously exploit the unique properties of both AuNPs and their composite partners in new hybrid materials. CNT have been extensively studied because of their outstanding mechanical, optical, electrical, and thermal properties.^{36,37} CNT combined with AuNPs resulting in AuNP–CNT hybrid materials combines the the high conductivity of the CNTs with the size-dependent opto-thermal properties of the AuNP with potential application in catalysts,^{38,39} sensing,⁴⁰ and nanomedicine.⁴¹ Such applications require the development of efficient strategies for the preparation of hybrid materials that lead to robust structures without significantly compromising the integrity of the underlying CNT framework. In this context, we present a bioorthogonal conjugation method to efficiently couple nitrene functionalized AuNPs to strained alkyne containing CNT, using the i-SPANC reaction, showing for the first time that it can successfully take place at the interface of two different nanomaterials to form a hybrid.

5.2 Results and Discussion

Scheme 5.1 displays the synthetic procedure used to prepare water soluble nitrone modified AuNPs (Nitrone-AuNPs). We utilized a place exchange reaction incorporating nitrone terminated thiol (Nitrone-EG₄-SH, compound 4) onto the surface of small triethylene glycol monomethyl ether functionalized AuNPs (Me-EG₃-AuNPs). The methyl-terminated EG₃ ligands were selected as the base ligand on the nanoparticles because they impart both water and organic solvent solubility. Also noteworthy is that for the interfacial reactions occurring on the surface of AuNPs, the reactivity of the nitrone group can be impeded by the spectator ligands (i.e. triethylene glycol monomethyl ether) if the nitrone ligand has a shorter chain length than the spectator ligands. For this reason, the nitrone ligand was synthesized with one more ethylene glycol unit than the base ligand to lower the steric hindrance and make it more prone to reactivity. The synthetic route to thiol 4 is illustrated in Scheme 5.2. Briefly, tetraethylene glycol monosulfonate was treated with triphenylmethanethiol to prepare the protected thiol. Then, alcohol 1 was oxidized to the aldehyde using dimethyl sulfoxide and phosphorus pentoxide. Aldehyde 2 was reacted with N-methyl hydroxylamine hydrochloride in the presence of base to afford nitrone 3. Finally, the desired thiol 4 was prepared by deprotection of 3 using 5% trifluoroacetic acid in dichloromethane. Details on the synthetic procedure can be found in the experimental section. Subsequently Me-EG₃-AuNPs were exposed to place exchange reaction conditions to introduce nitrone functionality onto the AuNP. The place exchange was carried out by stirring a solution of Me-EG₃-AuNPs in dichloromethane in presence of thiol 4 (1:6 AuNP to thiol ratio). After removing the solvent, the film of

AuNPs was washed with hexanes/isopropanol (10:1) several times. The Nitron-AuNPs were further purified by dialysis in milli-Q water to remove any unreacted thiol 4 or any disulfide that formed during the synthetic procedure. Characterization of the Nitron-AuNPs was achieved using ^1H NMR and UV-vis spectroscopy, TEM, TGA and XPS.



Scheme 5.2. Synthetic procedure towards the preparation of thiol 4.

Initially, the success of the place exchange reaction was confirmed using ^1H NMR spectroscopy (Figure 5.1). The ^1H NMR spectrum of the Nitron-AuNPs (recorded in D₂O) exhibits the expected broad peaks at δ_{H} : 3.3-3.8 ppm due to the methyl (protons c) and methylene groups of the triethylene glycol chains. Additionally, new signals appear after the exchange reaction at δ_{H} : 7.4 and 4.4 ppm corresponding to the proton α to the

nitrogen (proton a) and protons of the methylene group next to the nitron functionality (protons b) respectively, confirming the presence of nitron moiety on the gold core.

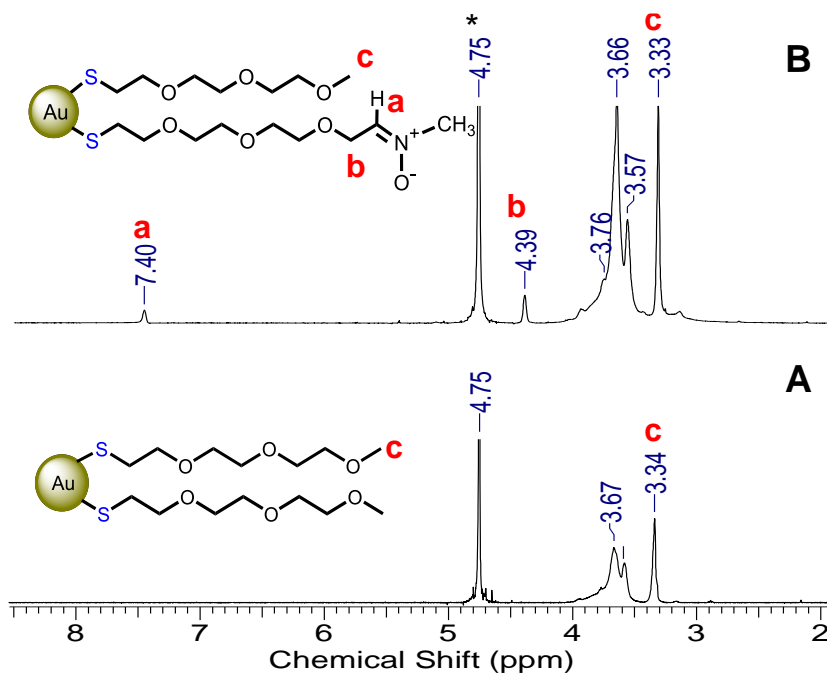


Figure 5.1. ^1H NMR spectra of A) Me-EG₃-AuNPs and B) Nitron-AuNPs in D_2O . * indicates residual H_2O .

The lack of any sharp signals in the ^1H NMR spectrum of the Nitron-AuNPs indicates that there is no free thiol present and confirms the efficiency of our purification protocol. Through the integration of the signal at δ_{H} : 7.4 ppm, correlating to H_a , and the integration of the signal at 3.3 ppm, that corresponds to the three protons of the methyl group of Me-EG₃-S- ligands (H_c), it was determined that the $18 \pm 2\%$ of the protecting

ligands are comprised of nitron terminated thiols, while $82 \pm 2\%$ consist of Me-EG₃-S-ones.

From TGA data, information about the quantity of the organic ligands present on the surface of AuNPs can be obtained. The total mass loss for Nitron-AuNPs when they are heated from 25-750 °C is 33%. This indicates that for each 1 mg of the Nitron-AuNPs, 0.33 mg is comprised of Me-EG₃-S- and Nitron-EG₄-S- ligands. Knowing that the mass loss corresponds to the mass of two types of ligands attached to the gold core and using the first derivative of the mass loss curve, it was calculated that 20% of the total ligands are Nitron-EG₄-S- and the 80% consist of the Me-EG₃-S- ligands. This is consistent with the NMR analysis (TGA graphs are displayed in the supporting information section Figure S5.7).

XPS analysis further confirmed the successful preparation of Nitron-AuNPs and the ratio between the two different ligands present on the gold core (See Figure 5.2). The Au 4f region exhibits a pair of peaks at 84.3 eV and 87.6 eV assigned to the Au 4f_{7/2} and Au 4f_{5/2} peaks, respectively, originating from the AuNP cores.⁴² The S 2p core line shows the presence of two major components, the S 2p_{3/2} at 162.8 eV and S 2p_{1/2} at 164.0 eV, in a 2:1 spin orbit splitting ratio related to the Au-S bonds.⁴³ Additionally, the XPS survey spectrum of Nitron-AuNPs clearly shows the appearance of the peak related to the nitrogen at 399.9 eV (N 1s) with 0.6 At% nitrogen incorporation, confirming the incorporation of the nitron group. From the ratio of sulfur (one sulfur per ligand, 3%) and nitrogen (exclusive to nitron terminated ligands, 0.6%) it was calculated that 20% of

the total ligands on the gold core consist of Nitron-EG₄-SH. This information matches that of NMR spectroscopy and TGA.

It is noteworthy that our goal is to balance nitron ligand incorporation while maintaining both water and organic solvent solubility. The 18 ± 2: 82 ± 2 composition allows the amphiphilic property of the AuNPs to be retained and therefore permit the subsequent interfacial reactions in either organic or aqueous media expanding the application of the AuNPs. While the amount of reactive nitron ligands incorporated onto the gold core can be increased by using higher ligand to gold ratios, longer exchange reaction time (>30 min) or exchange reactions in more polar solvents such as acetone and methanol, increasing the Nitron-EG₄-SH ligands to more than 30% of the total ligands results in AuNPs that are exclusively water soluble.

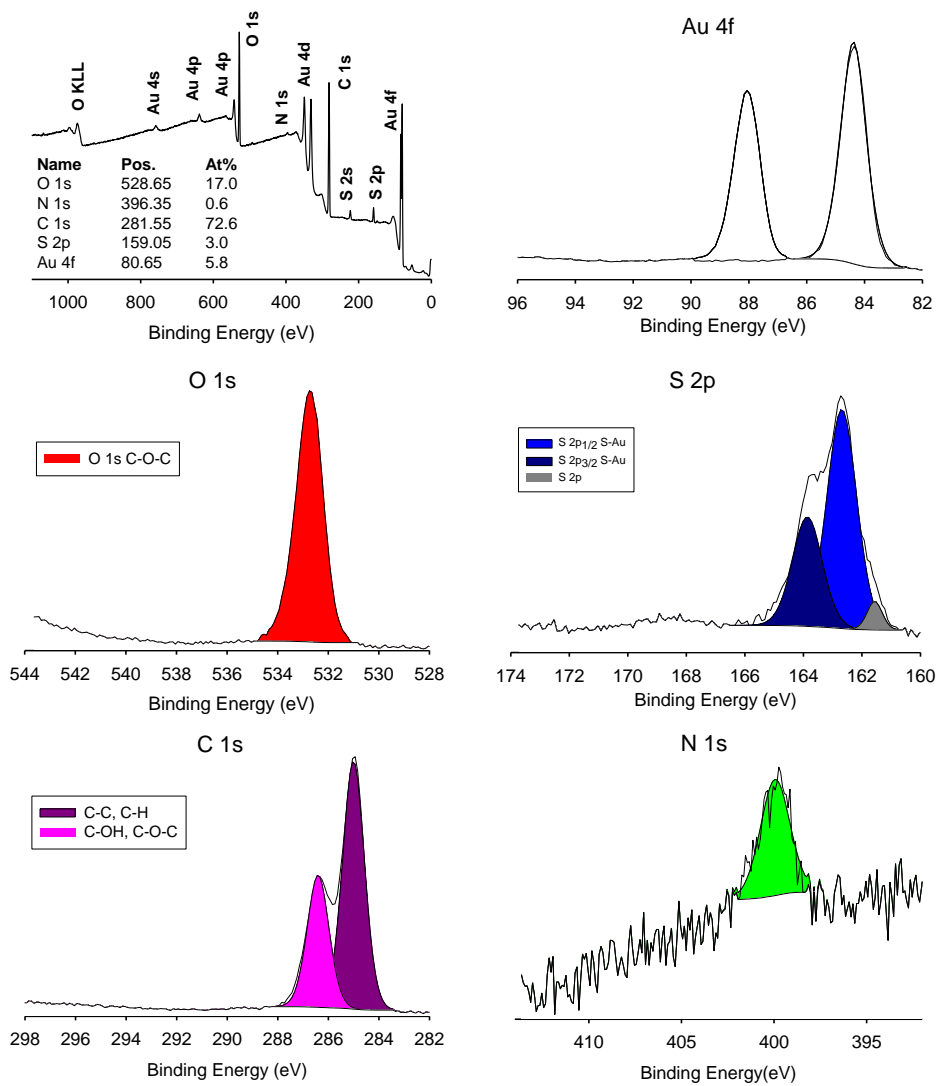
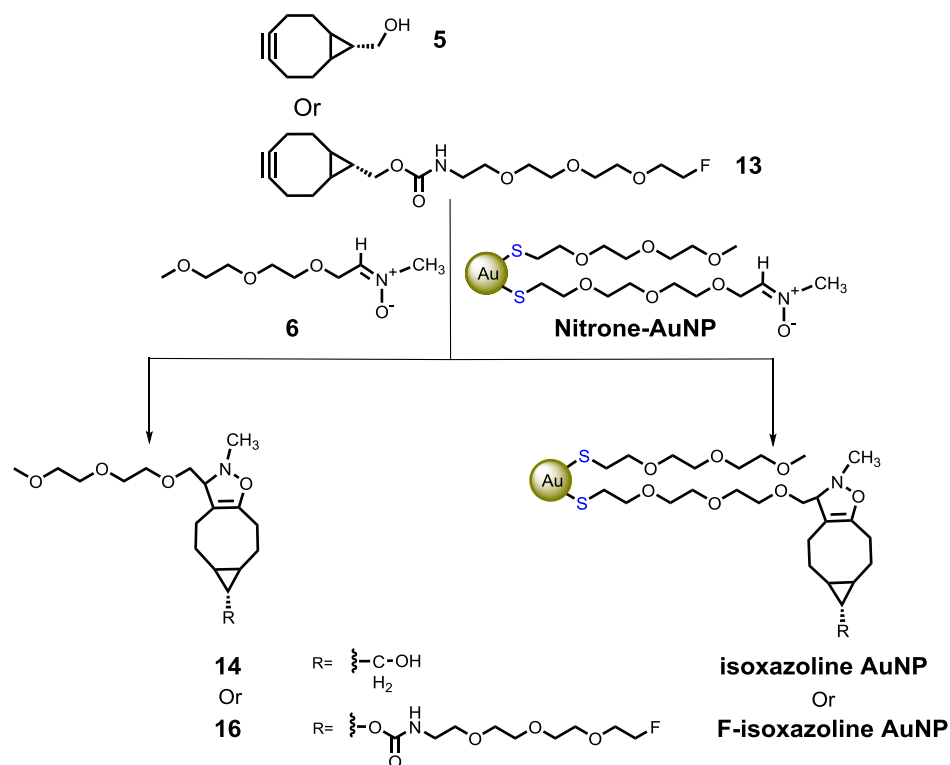


Figure 5.2. Survey scan and high resolution XPS of Nitron-AuNPs.

In this study the synthetic procedure was designed with the aim of preparing AuNPs in the 2-3 nm regime. This is important because recent studies indicate that the size diversity of AuNPs plays an important role in their biodistribution, which is of high

importance in biomedical applications.^{44,45} There are several reports on the use of AuNPs as contrast agents for *in vivo* imaging by different techniques.^{4-13,46,47} The majority of these studies use spherical nanoparticles or nanorods with 10-100 nm size that exhibit widespread organ biodistribution.^{10-13,45} Neither study reports detectable crossing of the blood-brain barrier (BBB) for AuNP >10 nm. Few studies have reported the possibility that particles with a diameter of approximately 10 nm or smaller can penetrate the BBB.⁴⁸⁻⁵¹ The potential to mediate the transfer of a molecule across the BBB makes AuNPs an important development platform for brain research.⁵² To confirm that we have in fact prepared small (2-3 nm) AuNPs, TEM was used. TEM images of Nitron-AuNPs show that they are 2.6 ± 0.5 nm in size (Figure S5.8).

Combining the ¹H NMR spectroscopy, TEM (2.6 nm) and TGA data and assuming a spherical shape for the gold core one can calculate a simplified formula for AuNPs.⁵³ Nitron-AuNPs have the formula of Au₅₀₀(Me-EG₃-S)₁₉₇(Nitron-EG₄-S)₄₉. TEM images, TGA graphs and calculations for determining the chemical formula can be found in the supporting information.



Scheme 5.3. Reaction scheme for the SPANC reaction of Nitron-AuNPs and model nitron **6** with two BCN derivatives (**5** and **13**) to prepare the corresponding isoxazolines.

In order to assess the utility of Nitron-AuNPs in bioorthogonal i-SPANC reactions, the efficiency of conversion to products was initially examined in presence of the endo-Bicyclo[6.1.0]non-4-yn-9-ylmethanol²⁶ (endo-BCN, compound **5**) as a representative ring strained alkyne. When characterizing the cycloadducts formed on the AuNPs, the broadness of the signals in the ¹H NMR spectra often makes the peak assignments difficult. To this end we prepared compound **6** as the model nitron to allow a confident assignment of the product signals. In a typical experiment one equivalent of Nitron-AuNPs/model compound **6** was stirred with two equivalents of the endo-BCN **5**.

Two equivalents of BCN were used to ensure reaction completion. Indeed, clean conversion into the expected isoxazoline conjugates upon SPANC labeling with endo-BCN 5 for both model and Nitron-AuNPs was achieved. Reaction progress was followed using ^1H NMR spectroscopy monitoring the disappearance of nitron signals at 4.4 and 7.4 ppm and appearance of new signals corresponding to the isoxazoline formed. Absence of the signal at 7.4 and 4.4 ppm related to the nitron moiety was taken as the completion of the reaction. In both cases (SPANC of model compound 6 and i-SPANC of Nitron-AuNPs) reaction was completed in short time scales only after 10-15 minutes. After reaction completion, the model isoxazoline 14 was fully characterized using ^1H and ^{13}C NMR spectroscopy as well as mass spectrometry. Comparing the ^1H NMR data obtained from model isoxazoline 14 (Figure 5.3-C) to that of the isoxazoline AuNPs (Figure 5.3-B) validates the success of reactions and the utility of our novel AuNPs for i-SPANC. Figure 5.3-A and B illustrate the ^1H NMR spectra of Nitron-AuNPs before and after the i-SPANC reaction, respectively. After the SPANC reaction, the signature nitron signals at 4.4 and 7.4 ppm disappear, concurrent the appearance of signals in 0.5-3 ppm region related to the cycloalkyne moiety and a signal at 2.5 ppm due to protons c, confirming the formation of the isoxazoline AuNPs.

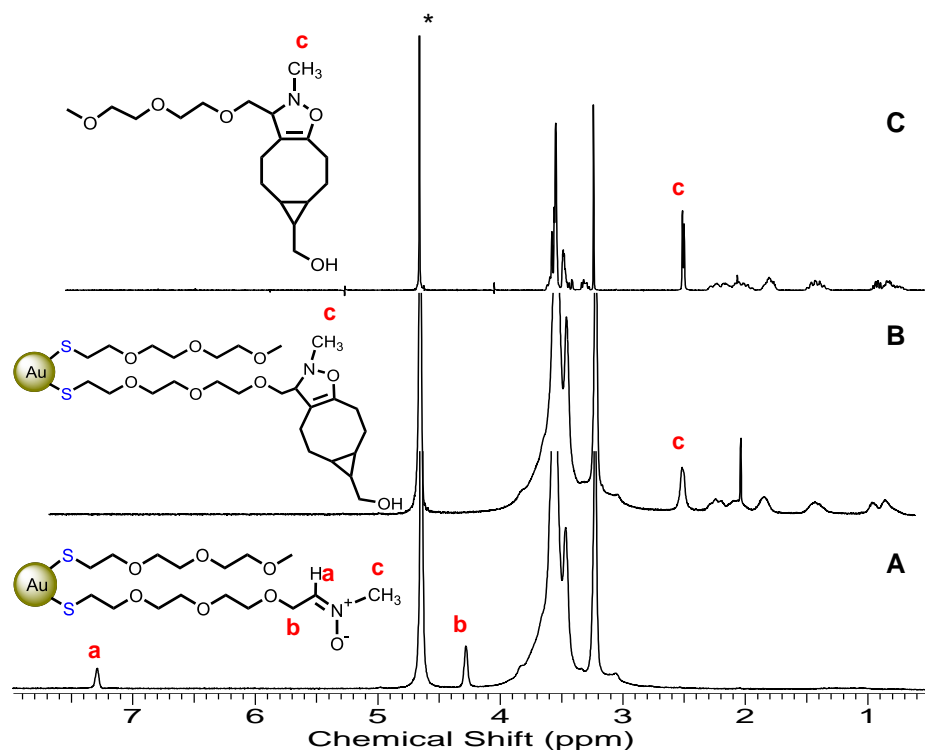
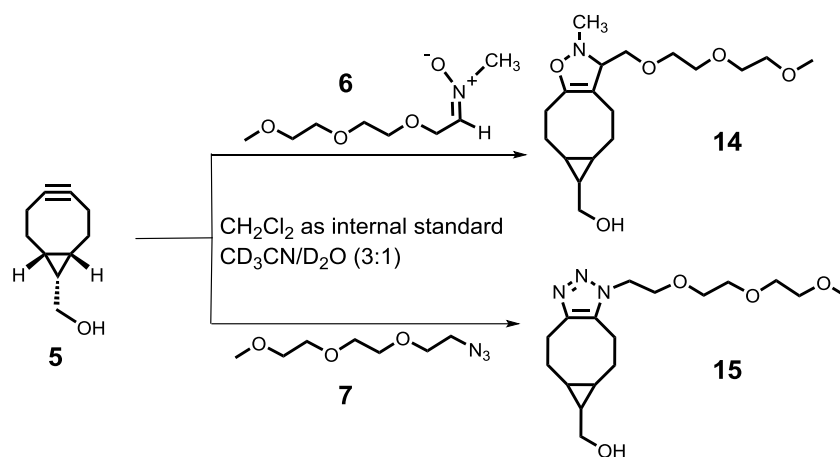


Figure 5.3. ^1H NMR spectra of A) Nitron-AuNPs B) isoxazoline AuNP and C) model isoxazoline 14. * is residual H_2O .

Both the SPAAC and SPANC reactions are bimolecular reactions and follow a second order kinetic equation. Hence larger rate constants allow these bioorthogonal reactions to proceed more efficiently with lower amounts of reagents used. This is of high significance for many biological applications where fast reactions are required while using a limiting amount of reagents. It has been previously reported that kinetics of SPANC is usually faster than similar SPAAC reaction due to the larger dipole moment of nitron moiety compared to azide.^{26,28} Encouraged by these reports, we studied the kinetics of both SPAAC and SPANC reactions using comparable parameters (See

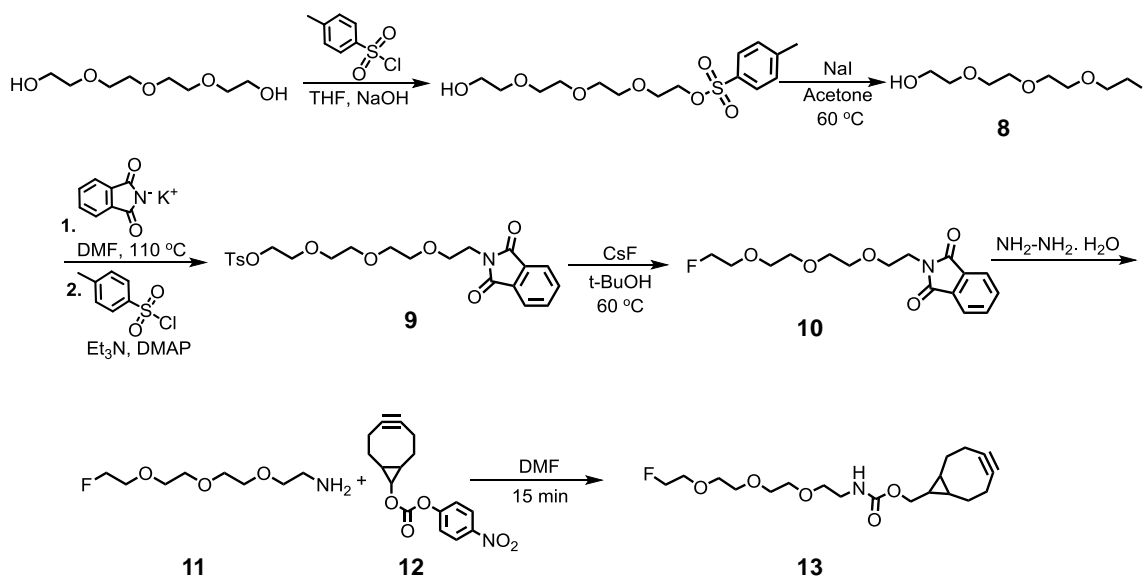
Scheme 5.4). In order to establish a kinetic profile for the strained promoted reactions of nitrene 6 and azide 7 with endo-BCN 5, the associated bimolecular rate constant was measured using ^1H NMR spectroscopy. ^1H NMR monitoring of cycloaddition of nitrene 6 or azide 7 model compounds with endo-BCN 5 was performed by rapid mixing ($t = 0$) of stock solutions of 6/7 with 5 (1:1 ratio) in an NMR tube and immediate insertion into a 400 MHz NMR spectrometer. NMR spectra were measured at preset time-intervals and each experiment was performed in triplicate. Kinetics of SPAAC and SPANC with endo-BCN were determined by measuring the decrease in the integral of the signature signals of nitrene or azide functional group, with respect to the integral of CH_2Cl_2 used as internal standard. Calculation of second-order reaction kinetics demonstrated that the SPANC ($k_2 = 0.14 \text{ M}^{-1} \text{ s}^{-1}$) has approximately 8.7-fold rate enhancement compared to the SPAAC reaction ($k_2 = 0.016 \text{ M}^{-1} \text{ s}^{-1}$). The rate plots for these kinetic studies are provided in the supporting information. Based on previous studies by our group it is expected that the interfacial reactions on the surface of AuNPs follow the same relative trend as observed for the model reactions.



Scheme 5.4. Strain-promoted cycloaddition reactions of BCN endo 5 with nitrone 6 and azide 7 to prepare isoxazoline 14 and triazole 15 respectively.

Having established the utility of Nitro-AuNPs for bioorthogonal SPANC reaction with faster kinetics compared to corresponding SPAAC reactions, we investigated their usefulness for the synthesis of ¹⁸F-radiolabeled AuNPs for potential application in PET imaging. There have been reports of CuACC,⁵⁴⁻⁵⁶ and SPAAC³³⁻³⁵ reaction used for preparation of ¹⁸F-radiolabeled peptides and nanoparticles. In principle, the SPANC reaction also seems particularly well suited for preparation of radiolabeled structures as it proceeds quickly and efficiently under mild reaction conditions. Prior to any radiolabeling or *in vivo* examination, proof of concept studies were performed using bicyclo [6.1.0]non-4-yn-9-ylmethyl(2-(2-(2-(2-fluoroethoxy)ethoxy)ethoxy)ethyl) carbamate (compound 13) as a model fluorine containing prosthetic group as shown in Scheme 5.3. Compound 13 was prepared over six steps as illustrated in Scheme 5.5. The synthetic strategy was designed so that incorporation of the fluorine into the structure of

BCN in the last step would be viable in a matter of minutes. This is indeed the key to the synthesis of the fluorine containing BCN molecule when preparing the ^{18}F -radiolabeled analogue of compound 13.



Scheme 5.5. Synthetic procedure towards the preparation of compound 13.

Using a 1:1 ratio of the AuNPs to strained alkyne 13, the SPANC reaction proceeded cleanly and rapidly and was completed within a reasonable reaction time (45 min), affording ^{19}F -labeled AuNPs in quantitative yield. After ^1H NMR spectroscopy showed reaction completion, the F-labeled AuNPs were purified by dialysis in milli-Q water and then characterized using ^1H and ^{19}F $\{^1\text{H}\}$ NMR and UV-vis spectroscopy, TEM and XPS. A similar reaction was carried out using model nitrene 6 and compound

13. The resulting isoxazoline was fully characterized using ^1H , ^{13}C and ^{19}F $\{^1\text{H}\}$ NMR spectroscopy as well as mass spectrometry and served as a reference in characterization of fluorine labeled AuNPs (F-isoxazoline-AuNPs) without the interference of broad signals caused by the presence of nanoparticles.

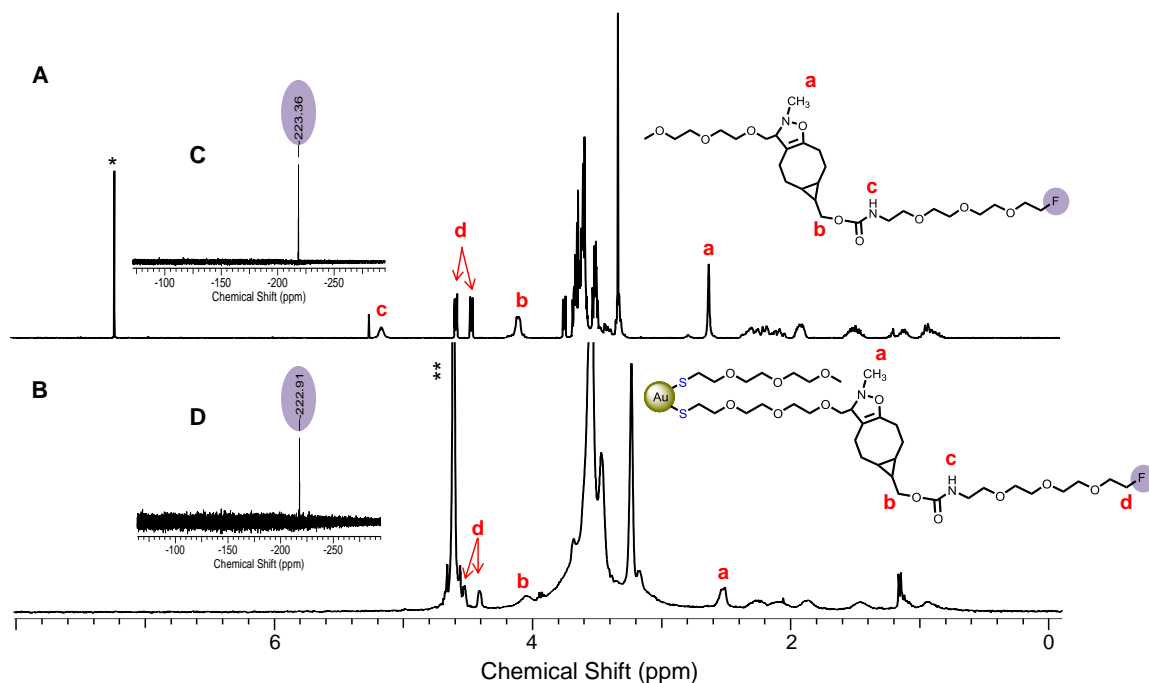


Figure 5.4. ^1H NMR spectra of A) model isoxazoline 16, and B) F-isoxazoline AuNPs. ^{19}F NMR spectra of C) model isoxazoline 16, and D) F-isoxazoline AuNPs * is residual CHCl_3 and ** indicates residual H_2O .

Figure 5.4 illustrates the ^1H and ^{19}F $\{^1\text{H}\}$ NMR spectra of isoxazoline 16 and the corresponding F-isoxazoline-AuNP. In case of F-isoxazoline-AuNPs the NMR has been

carried out in D₂O to demonstrate their water solubility even after the interfacial reaction. But for the model isoxazoline 16, the NMR has been carried out in CDCl₃ due to its higher solubility in organic media. Aside from the slight shifts in both spectra due to solvent effects, it can be observed that both ¹H and ¹⁹F NMR spectra of the model and AuNPs match after the SPANC reaction with compound 13. XPS was also employed to further confirm the formation of F-isoxazoline-AuNPs. The XPS survey of F-isoxazoline AuNPs (Figure 5.5) shows the appearance of the peak related to fluorine at 686.7 eV introduced with the interfacial coupling reaction. Also, the high resolution scan of the carbon 1s and oxygen 1s peaks for the F-isoxazoline AuNPs (Figure 5.5) compared to that of the Nitrone-AuNPs starting material (Figure 5.2) confirms the successful synthesis of the desired fluorine labeled AuNPs. The high resolution scan of the carbon peak exhibits the appearance of a shoulder at 288.0 eV and 289.2 eV related to O-C*=O, *C-F groups respectively. This is also confirmed by the appearance of a shoulder at 533.6 eV in the high resolution scan of the oxygen peak related to the O*-(C=O) group. It should be emphasized that a new peak for C-N bound should have appeared, however no such peak in C 1s spectra was observed. This is most probably due to its presence at the same binding energy region as that for C-OH/O-C-C groups. Nonetheless, the presence of such group is clearly shown in Figure 5.5, bottom left, representing the high resolution nitrogen 1s scan with a binding energy of ~400 eV. TEM shows that the AuNPs retain their shape and size after the interfacial reaction (Figure S5.8).

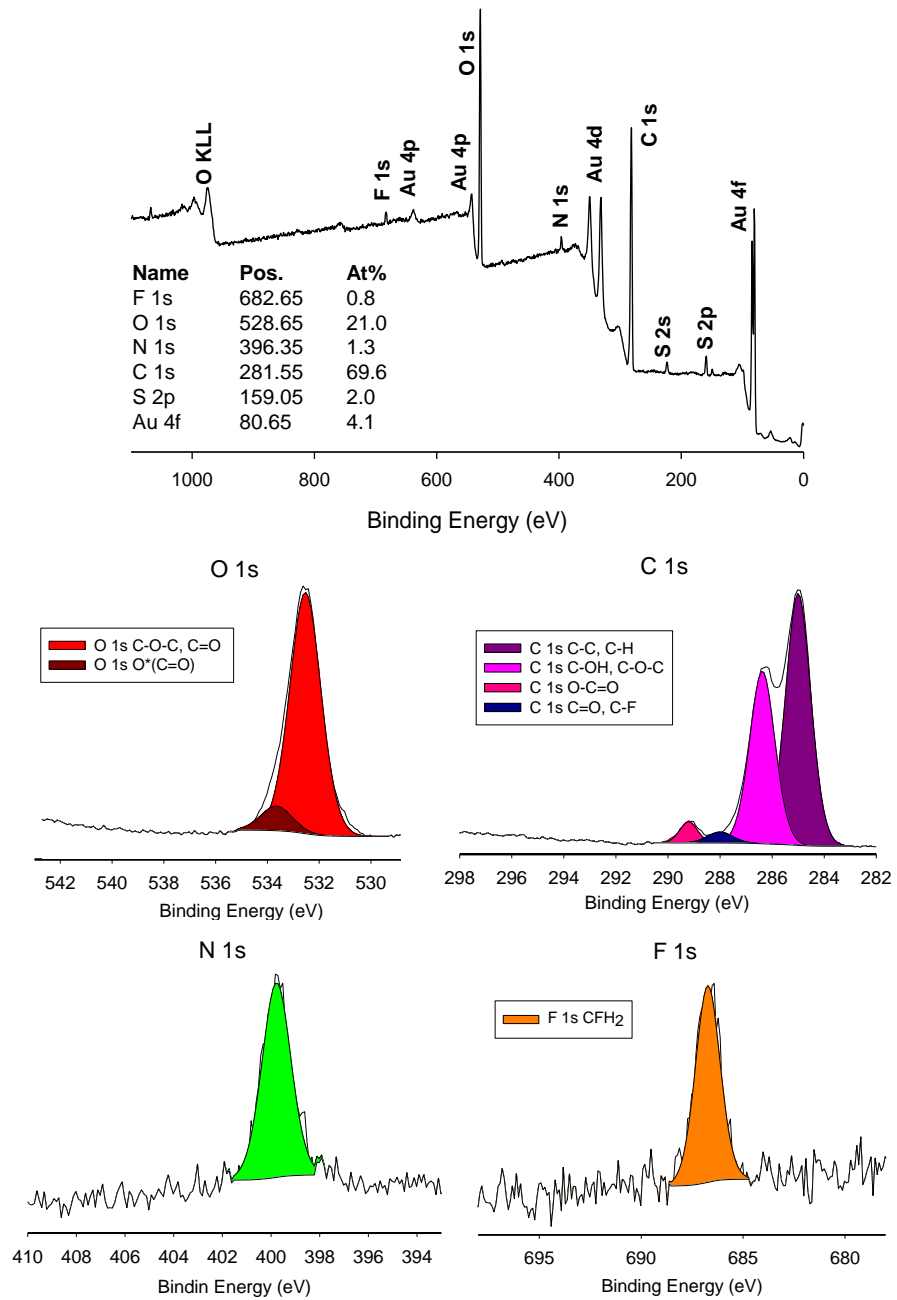


Figure 5.5. Survey scan and high resolution XPS spectra of F-isoxazoline AuNPs.

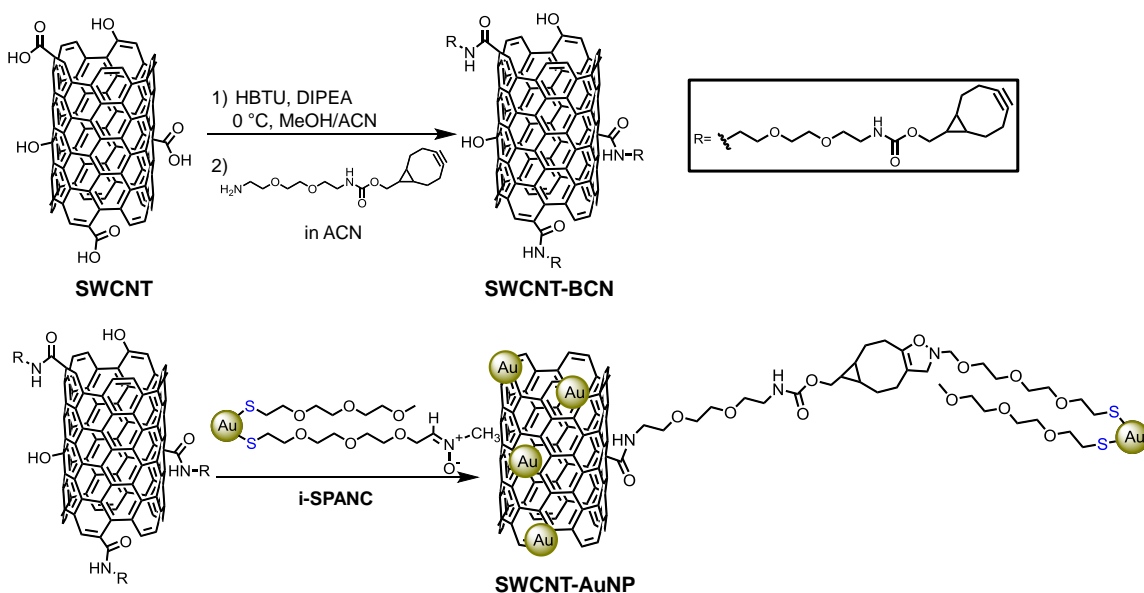
The strategy used for the model i-SPANC reaction of Nitrone-AuNPs and BCN 13 shows that the reaction occurs on the time scales of minutes. This proves that this approach can be useful for incorporation of the radioactive ^{18}F (with the half-life of 109.77 minutes) onto AuNPs surface quickly and efficiently by preparing the ^{18}F radioactive analogue of compound 13. The *in vivo* biodistribution of these nanoparticles can then be studied utilizing PET imaging.

All the radiolabeling experiments were carried out by Dr. Lihai Yu, a postdoctoral fellow in Professor Leonard G. Luyt's research lab.

For the biodistribution studies, the radioactive prosthetic probe ^{18}F -13 was prepared following the same synthetic strategy as compound 13 with some changes in order to satisfy the radiolabeling criteria as displayed in Scheme 5.9. Next, the ^{18}F -labeled AuNP conjugate was obtained through the i-SPANC reaction of Nitrone-AuNPs with compound [^{18}F] 13. AuNP radiolabelling with ^{18}F was confirmed by size exclusion column. The total radiochemical yield (RCY) after decay correction and four steps of synthesis was 6-10%. These results are very encouraging; however, further studies are required in order to optimize the RCY of AuNPs before we can proceed to the biodistribution studies in live animals using PET imaging.

In the second part of this study we extended the concept of the i-SPANC reaction to carbon based material chemistry, showing for the first time that it can successfully take place at the interface between different nanomaterials. To demonstrate this innovative

application of the SPANC reaction, as a proof of concept we prepared an AuNP-CNT hybrid material. In order to do so through the i-SPANC reaction, strained alkyne modified SWCNT was first prepared. Subsequently the strained alkyne moieties incorporated onto the side walls of the CNT underwent i-SPANC with the Nitron-AuNPs to create the final hybrid material.



Scheme 5.6. Synthetic approach towards the preparation of SWCNT-AuNP through i-SPANC reaction at the Nitron-AuNP interface.

Scheme 5.6 displays the synthetic strategy leading to the formation of the SWCNT-AuNP hybrid. The first step involves the introduction of BCN functionalities onto the CNT sidewalls through a coupling reaction between the commercially available BCN-

amine and the carboxylic groups already present on the native SWCNT (for details of synthesis see the experimental section). Noteworthy is that it is not necessary to pre-treat or oxidize the CNT before the coupling reaction as the amount of carboxylic groups already present on the CNT sidewalls allows for an efficient functionalization. The BCN-modified CNT was found to form stable dispersions in both water and polar organic solvents including acetonitrile, acetone and ethanol. The SWCNT-BCN was characterized using XPS and FTIR spectroscopy. The XPS survey scan of SWCNT-BCN (Figure 5.6, middle) compared to that of the starting material (Figure 5.6, left) clearly shows the appearance of the peak related to the amide nitrogen at 400.0 eV. The high resolution scan of the carbon 1s and oxygen 1s peaks for the SWCNT-BCN compared to that of the SWCNT starting material confirms the successful synthesis of BCN-modified CNT. The high resolution scan of the carbon peak shows the appearance of a shoulder at 285.0 eV related to the sp^3 -hybridized carbons and an increase in the intensity of the signal at 286.5 eV related to the C-O-C bonds as a result of the coupling reaction. This is also confirmed by the marked decrease of the $-(C=O^*)$ peak at 531.28 eV (light blue), with respect to the steady component at 532.61 eV of the -C-OH, C-O-C (dark blue) in the high resolution scan of the oxygen peak. This is due to the presence of oxygenated chains in the structure of the BCN-amine coupled to the CNT. Figure S5.18 shows the infrared spectra of raw and BCN functionalized SWCNTs. The band observed at 3460 cm^{-1} corresponds to the stretching vibrations of OH group, indicating the existence of carboxyl groups on the external surface of the SWCNTs. In addition, the band can be attributed to hydroxyl groups present in water physically adsorbed. The signal at 1092

cm^{-1} is assigned to the C-O stretching vibrations. The functionalization of SWCNT with BCN can be confirmed by the formation of secondary amide on the SWCNTs at 1580 cm^{-1} . In addition, the band at 1633 cm^{-1} is attributed to stretching of amide carbonyl (C=O). Also, a band at 2956 cm^{-1} appears which can be assigned to the asymmetric C-H stretching of the sp^3 -hybridized carbons of the BCN-amine.

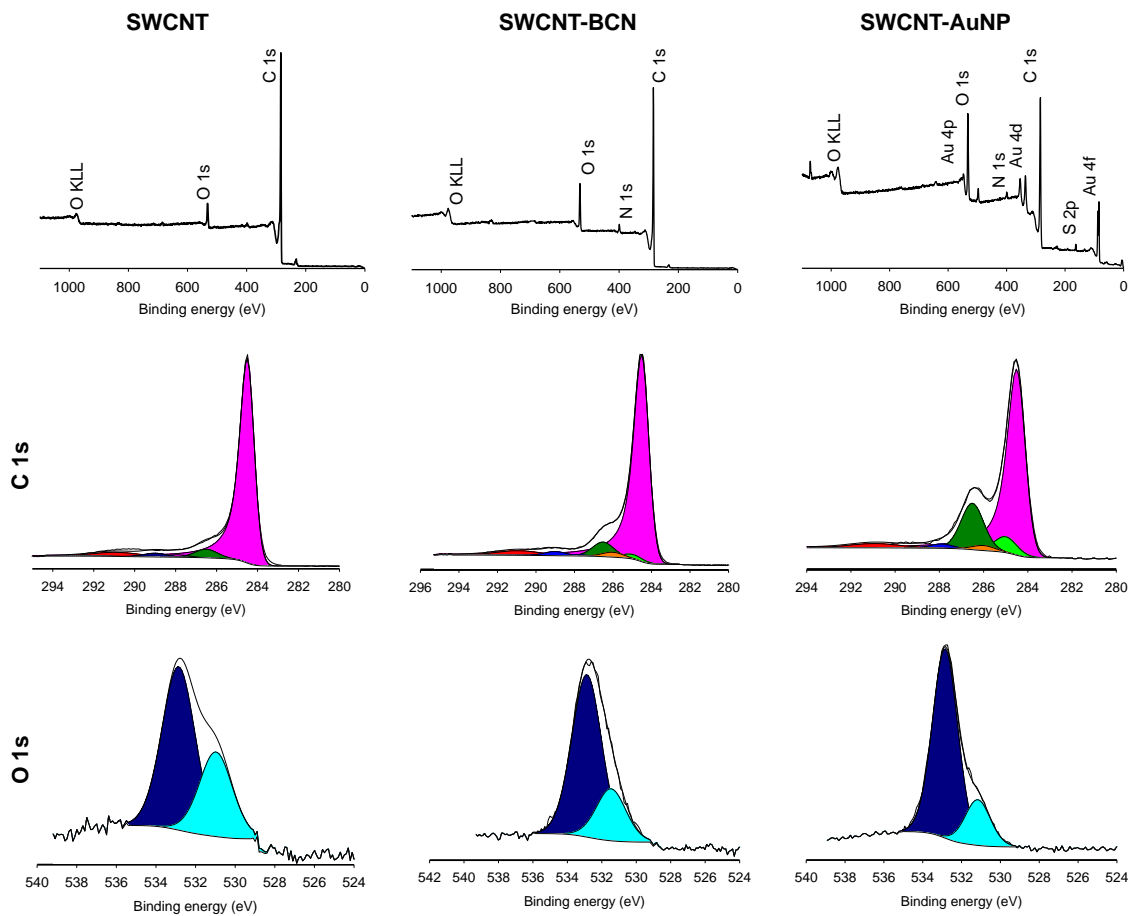


Figure 5.6. Survey scan and high resolution XPS spectra of SWCNT (left), SWCNT-BCN (middle), and SWCNT-AuNP hybrid (right).

The title SWCNT-AuNP hybrid nanomaterial was then easily prepared through the bioorthogonal i-SPANC reaction between the two partners: SWCNT-BCN and the Nitron-AuNP. The interfacial cycloaddition reaction was carried out simply by mixing the two in aqueous media. In a typical synthesis, to a 1 ml of the SWCNT-BCN mother solution was added 5 mg of Nitron-AuNP and the reaction volume was diluted to 5 ml with PBS pH 7 buffer. The system was stirred for 1 hour at room temperature and then the SWCNT-AuNPs were centrifuged in a Pyrex centrifuge test tube. The supernatant was removed, and the decorated CNT were dispersed in water, sonicated for 10 minutes and centrifuged. Subsequently, water was substituted first with acetone and then with dichloromethane, and the washing procedure (sonication and centrifugation) was repeated four more times. This protocol was to ensure removal of any non-covalently bound AuNPs. The successful synthesis and purification of the covalent SWCNT-AuNP hybrid was confirmed by XPS and TEM.

The XPS survey scan of SWCNT-AuNP (Figure 5.6, right) shows the appearance of the peaks from Au and from S. The Au 4f_{7/2} core line of AuNP is at 84.5 eV, this binding energy is shifted upwards from that of bulk Au (83.95 eV) due to particle size effects (Figure S5.16). The high-resolution carbon 1s spectrum shows a marked increase of the component at 286.30 eV related to the C–O–C of the AuNP glycol units, while the high-resolution oxygen 1s spectrum shows an increase of the corresponding component at 532.63 eV.

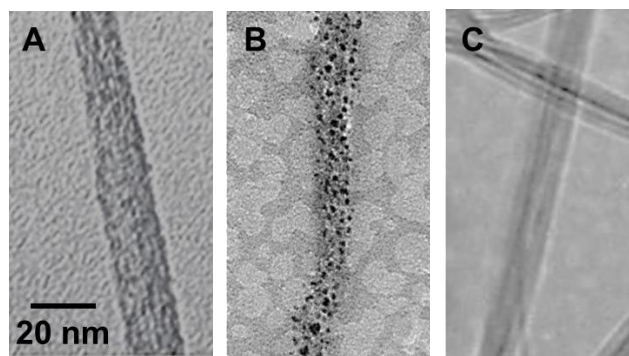


Figure 5.7. TEM images of A) SWCNT-BCN, B) SWCNT-AuNP hybrid, C) control experiment (SWCNT-BCN + Me-EG₃-AuNP).

TEM images of the hybrid nanomaterial (Figure 5.7, B) confirm that AuNPs are linked to the surface of CNT while maintaining their original shape and size. Also, there are no unbound particles present, confirming the efficiency of our washing procedure. Indeed, the use of sonication favors the detachment of the AuNP that are physisorbed on the CNT leaving behind those covalently bonded.

To provide support for the covalent assembly of the AuNPs onto CNTs and to exclude the possibility of unspecific physisorption of the AuNPs to the SWCNT-BCN, a control experiment was carried out under identical conditions and following the same experimental procedure but using the model Me-EG₃-AuNPs instead of the Nitron-AuNPs. The Me-EG₃-AuNPs, lacking the Nitron functionality, are not expected to undergo i-SPANC with the SWCNT-BCN. TEM images taken of the solid material (Figure 5.7, C) after the same centrifugation and washing cycle protocol (see experimental), showed just bare CNT with no AuNP attached onto the nanotubes. This

confirms the successful synthesis of AuNP-decorated SWCNT through the new i-SPANC reaction between SWCNT-BCN and Nitron-AuNP.

Finally, sonication was employed to test the stability and resilience of the final hybrid material. The SWCNT-AuNP was dispersed in PBS pH 7.0 and sonicated for one hour. The TEM images obtained from these samples were compared with those of the freshly prepared SWCNT-AuNP and they did not show any noticeable difference either in the density of chemisorbed AuNP or in the AuNP size distribution (Figure S5.19, D). This supports the efficiency of our synthetic approach and the robustness of the resulting AuNP-CNT hybrid. As demonstrated initially in this section the reaction of the Nitron-AuNP with BCN containing model compounds leads to efficient and total loading (complete reaction) on the AuNP. Hence, we believe that every accessible BCN group on the SWCNT reacts with Nitron-AuNP.

5.3 Conclusion

In summary, we reported the first synthesis of small (2-3nm) water- and organic solvent-soluble AuNPs with nitron functionalities incorporated onto the gold surface. These Nitron-AuNPs were fully characterized using a variety of techniques including ^1H NMR and UV-vis spectroscopy, TGA, TEM and XPS. The amount of nitron moieties present on the surface was calculated with good precision using independent methods that allows for a more quantitative approach for their further modification. Using bicyclononyne derivatives as the representative strained alkyne we demonstrated that

these Nitron-AuNPs undergo fast and efficient i-SPANC reaction with quantitative yield. To showcase the usefulness of i-SPANC reaction for *in vivo* applications we prepared ^{18}F -labeled AuNPs by designing a prosthetic group with strained alkyne available for the reaction with the nitron groups present on the nanoparticles' surface. Our ongoing studies will evaluate the utility of SPANC for the preparation of ^{18}F -radiolabeled AuNPs with higher yields. This will allow us to study their *in vivo* biodistribution and their usefulness for PET imaging applications. A major future application of the above approach is to use nanoparticle platforms for targeted molecular imaging. Nanoparticles allow multivalent attachment of various ligands, small molecules, biomolecules or even drugs. This together with optimized kinetics of SPANC reaction of the Nitron-AuNPs would allow a modular approach to rapidly building and testing such materials. Furthermore, in an attempt to extend the utility of i-SPANC reactions to material surface modification, we prepared CNT-AuNP hybrid materials. Efficiency of the i-SPANC reaction leads to a robust and stable hybrid material thanks to the covalent bond linking the two nano-partners. The strategy introduced here can be exploited for creating a wide variety of hybrid materials using other carbonaceous materials (*e.g.* graphene or micro-diamonds) for device applications.

5.4 Experimental

General Materials and Methods

The following reagents, unless otherwise stated, were used as received. Triethylene glycol monomethylether, tetraethylene glycol, 4-dimethylaminopyridine (DMAP), potassium thioacetate, deuterated acetonitrile (CD_3CN), deuterated chloroform (CDCl_3), tetrachloroauric acid trihydrate, sodium borohydride, *p*-toluenesulfonyl chloride, *N*-methylhydroxylamine hydrochloride, sodium azide, triphenylmethanethiol, triisopropylsilane (TIPS), *N,N*-Diisopropylethylamine (DIPEA), phthalimide potassium, sodium iodide, hydrazine monohydrate, cesium fluoride, single wall carbon nanotubes (carbon >90 %, $\geq 70\%$ carbon as SWCNT), and *O*-(Benzotriazol-1-yl)-*N,N,N',N'*-tetramethyluronium hexafluorophosphate (HBTU), and *N*-[(1*R*,8*S*,9*S*)-Bicyclo[6.1.0]non-4-yn-9-ylmethyloxycarbonyl]-1,8-diamino-3,6-dioxaoctane (BCN-amine) were purchased from Sigma-Aldrich. All common solvents, triethyleneamine, sodium sulfate anhydrous, dry methanol, tert-butanol, hydrochloric acid, trifluoroacetic acid, sodium hydroxide, sodium bicarbonate and potassium carbonate were purchased from Caledon. Deuterated water (D_2O) was purchased from Cambridge Isotope Laboratories. Ethanol was purchased from Commercial Alcohols. Glacial acetic acid (99.7%) was purchased from BDH. Dialysis membranes (MWCO 6000-8000) were purchased from Spectra/Por.

^1H , and ^{13}C and ^{19}F $\{^1\text{H}\}$ NMR spectra were recorded on either a Varian Inova 400 MHz, Varian Inova 600 MHz or a Varian Mercury 400 MHz spectrometer and were

calibrated against the residual protonated solvents. Transmission electron microscopy (TEM) images were recorded from a TEM Philips CM10. The TEM grids (Formvar carbon film on 400 mesh copper grids) were purchased from Electron Microscopy Sciences and prepared by drop casting solution of nanoparticles directly onto the grid surface. Mass spectrometry measurements were carried out using a Micro mass LCT (electrospray time-of-flight) mass spectrometer. Thermogravimetric Analysis (TGA) measurements were recorded by loading the sample in 70 μL ceramic crucible and heating from 25-750 $^{\circ}\text{C}$ with a rate of 10 $^{\circ}\text{C min}^{-1}$. The experiments were performed under a nitrogen flow of 70 ml min^{-1} in a Mettler Toledo TGA/SDTA 851 instrument. The XPS analyses were carried out with a Kratos Axis Ultra spectrometer using a monochromatic Al K(alpha) source (15mA, 14kV). The instrument work function was calibrated to give a binding energy (BE) of 83.96 eV for the Au 4f_{7/2} line for metallic gold and the spectrometer dispersion was adjusted to give a BE of 932.62 eV for the Cu 2p_{3/2} line of metallic copper. Specimens were mounted on a double sided adhesive tape and the Kratos charge neutralizer system was used on all specimens. Survey scan analyses were carried out with an analysis area of 300 x 700 microns and pass energy of 160 eV. High resolution analyses were carried out with an analysis area of 300 x 700 microns and pass energy of 20 eV. Spectra have been charge corrected when needed to the main line of the carbon 1s spectrum set to 285.0 eV for aliphatic carbon. Spectra were analyzed using CasaXPS software (version 2.3.14). UV-Vis spectra were collected employing a Varian Cary 300 Bio spectrometer in acetonitrile. The FTIR spectra were carried out using KBr pellets on a Bruker Vector33 spectrometer.

Synthetic details

Compound 1

Triphenylmethanethiol (0.99 g, 3.58 mmol) was dissolved in a solution of ethanol/benzene (1:1, 10 mL) and NaOH (0.18 g, 4.00 mmol) in 4 mL of H₂O was added. Then tetraethylene glycol monosulfonate (1.05 g, 3.00 mmol) was also dissolved in a solution of ethanol/benzene (1:1, 8 mL) and added to the triphenylmethanethiol mixture. The new reaction mixture was stirred overnight at room temperature. Once the reaction was completed (checked by TLC) all the mixture was poured into a saturated solution of NaHCO₃ and washed three times. The organic layer was separated and added into saturated solution of NaCl and also washed for three times. Afterward the organic layer was separated, dried over Na₂SO₄, and concentrated *in vacuo*. The crude product was purified by column chromatography over silica gel using ethyl acetate eluent to give 1 in 96% yield. ¹H NMR (400 MHz, CDCl₃) δ (ppm); 2.44 (t, *J* = 6.8 Hz, 2H), 3.31 (t, *J* = 6.8 Hz, 2H), 3.46 (dd, *J* = 5.7, 3.7 Hz, 2H), 3.57-3.72 (m, 10H), 7.19-7.30 (m, 9H), 7.42 (m, 6H); ¹³C NMR (400 MHz CDCl₃); 31.6, 61.7, 66.6, 69.6, 70.1, 70.3, 70.4, 70.6, 72.5, 126.6, 127.8, 129.6, 144.8. HRMS (ESI) [M]⁺ calcd for C₂₇H₃₂O₄S 452.2023; found 452.2021.

Compound 2

A flame-dried, two-necked, 250 mL round-bottomed flask was purged with Ar and then was charged with alcohol 1 (2.1 g, 4.6 mmol mmol) in dry CH₂Cl₂ (0.2 M in

starting alcohol). The flask was immersed in an ice-water bath. Dimethyl sulfoxide (360.1 mg, 9.2 mmol) and phosphorus pentoxide (1.3 g, 9.2) were added sequentially. The reaction mixture was allowed to stir and warm to room temperature until disappearance of starting material by TLC (4 h). The flask was immersed again in the ice-water bath; then triethylamine (1.63 g, 16.1 mmol) was added dropwise over 10 minutes. Stirring was continued for 45 minutes. The reaction was quenched with 10% aqueous HCl and extracted with CH₂Cl₂. The organic extracts were washed with saturated aqueous NaCl, dried over anhydrous Na₂SO₄ filtered, and concentrated *in vacuo*. The crude product was purified by column chromatography over silica gel using hexane/ethyl acetate (1:3 v/v) as the eluent providing aldehyde 2 as a light yellow oil in 77% yield. ¹H NMR (400 MHz, CDCl₃) δ (ppm); 2.42 (t, *J* = 6.7 Hz, 2H), 3.29 (t, *J* = 7.0 Hz, 2H), 3.44 (m, 2H), 3.55-3.70 (m, 6H), 4.11 (m, 2H), 7.18-7.26 (m, 9H), 7.40 (m, 6H), 9.67 (s, 1H); ¹³C NMR (400 MHz CDCl₃); 31.3, 66.3, 69.6, 69.8, 70.2, 70.4, 70.9, 126.3, 127.5, 129.3, 144.9, 200.5. HRMS (ESI) [M]⁺ calcd for C₂₇H₃₀N₂O₄S 450.1866; found 450.1864.

Compound 3

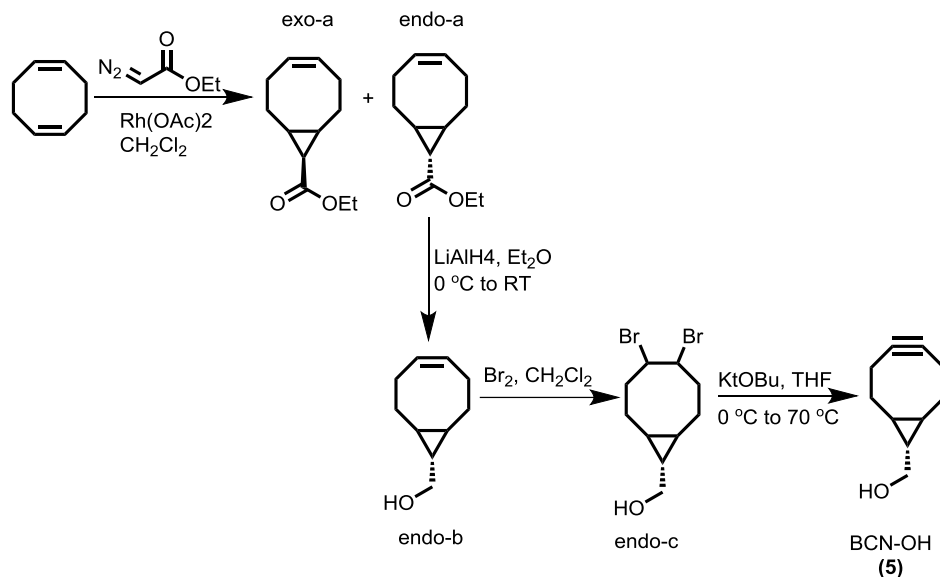
Aldehyde 2 (1.1 g, 2.3 mmol), N-methylhydroxylamine hydrochloride (450 g, 4.7 mmol), and triethylamine (875 mg, 9.4 mmol) were mixed in dry acetonitrile (50 mL). After reaction completion (3h, checked by TLC) the solvent was evaporated and substituted with CH₂Cl₂. The organic was then washed with saturated aqueous NaCl three times, dried over anhydrous Na₂SO₄, filtered, and concentrated *in vacuo*. The crude product was purified by column chromatography over silica gel using

dichloromethane/ethyl acetate/methanol (10:3:1 v/v) as the eluent to give nitrone 3 as a yellow oil in 89% yield. ^1H NMR (400 MHz, CDCl_3) δ (ppm); 2.44 (t, $J = 7.0$ Hz, 2H), 3.32 (t, $J = 7.0$ Hz, 2H), 3.48 (m, 2H), 3.58 (m, 2H), 3.62-3.67 (m, 6H), 4.44 (m, 2H), 6.89 (t, $J = 4.5$ Hz, 1H) 7.20-7.30 (m, 9H), 7.41 (m, 6H); ^{13}C NMR (400 MHz CDCl_3); 31.6, 52.0, 66.5, 66.6, 69.6, 70.1, 70.2, 70.5, 70.9, 126.6, 127.8, 129.5, 138.5, 144.7; HRMS (CI) $[\text{M}+\text{H}]^+$ calcd for $\text{C}_{28}\text{H}_{33}\text{NO}_4\text{S}$ 480.2209; found 480.2210.

Compound 4

To a solution of nitrone 3 (400 mg, 0.8 mmol) and TFA (1.9 g, 16.7 mmol) in DCM (20 mL) was added TIPS (0.21 mL, 1 mmol) as a carbocation scavenger. The reaction mixture was stirred under Ar for 1 h. The solution was washed with 0.2 M NaHCO_3 and brine, dried over Na_2SO_4 and concentrated. The crude was purified by column chromatography over silica gel using dichloromethane/ethyl acetate/methanol (10:3:1 v/v) as the eluent to give thiol 4 as a pale yellow oil. We were unsuccessful in purifying compound 4 completely as a small percentage hydrolyzes back to the aldehyde over the course of purification. ^1H NMR (400 MHz, CDCl_3) δ (ppm); 1.54 (t, $J = 8.2$ Hz, 1H), 2.56 (m, 2H), 3.54-3.63 (m, 14H), 4.40 (m, 2H), 6.86 (t, $J = 4.5$ Hz, 1H); ^{13}C NMR (400 MHz CDCl_3); 24.2, 52.1, 66.6, 70.2, 70.3, 70.5, 70.9, 72.8, 138.4. HRMS (CI) $[\text{M}+\text{H}]^+$ calcd for $\text{C}_9\text{H}_{20}\text{NO}_4\text{S}$ calculated: 238.1113, found: 238.1119.

Compound 5



Scheme 5.7. Synthetic procedure towards the preparation of compound 5.

All the steps in preparation of compound 5 were carried out according to previous reports as illustrated in Scheme 5.7.²² In a typical synthesis, $\text{Rh}_2(\text{OAc})_4$ (0.776 g, 1.76 mmol) was dissolved in dry CH_2Cl_2 (20 mL) under argon atmosphere. Cyclooctadiene (40 mL, 0.33 mmol) was then added to the solution. In a separate flask, ethyl diazoacetate (4.3 mL, 41 mmol) was also dissolved in dry CH_2Cl_2 (20 mL) and then slowly added to the cyclooctadiene solution. Evolution of nitrogen gas was observed right away. The dark green solution was stirred at room temperature for two days. After the solvent was evaporated, the excess cyclooctadiene was recovered by column chromatography on silica gel using hexanes as the eluent. After elution of cyclooctadiene, the *endo/exo-a*

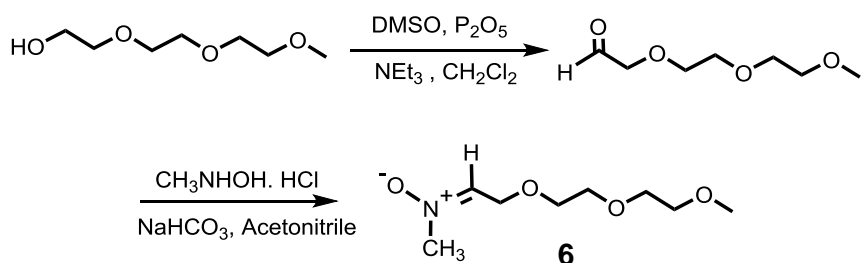
isomers were separated using hexanes/Et₂O 9:0.5 as the eluent. The two isomers were obtained as a colorless oil (6.979 g, 88% overall yield, 36% *endo* and 64% *exo*). R_f *exo* = 0.6, R_f *endo* = 0.4 in hexanes/Et₂O 9:0.5.

Only the *endo* isomer was used for the following steps. A suspension of LiAlH₄ (1.371 g, 36.11 mmol) in dry Et₂O (80 mL) was cooled to 0 °C. Compound *endo-a*, from the previous step, (7.8 g, 40.4 mmol) was also dissolved in dry Et₂O (90 mL) and cooled to 0 °C before dropwise addition to the reaction flask. The gray solution was stirred for 15 min at room temperature, then it was cooled again to 0 °C and distilled water was added dropwise under normal atmosphere until formation of a white precipitate was observed. The mixture was dried over Na₂SO₄, and the solids were filtered off and washed with Et₂O. The solvent was evaporated to obtain intermediate *endo* alcohol. No further purification was performed.

Compound *endo-b* from the previous step was dissolved in CH₂Cl₂ (250 mL) and cooled to 0 °C. A solution of Br₂ (2.6 mL, 51 mmol) in CH₂Cl₂ was added dropwise at 0 °C to the alkene solution until a light yellow color persisted. The reaction mixture was quenched with a 10% Na₂S₂O₃ solution (70 mL). After vigorous stirring for a few minutes, the solution turned colorless and was then extracted with CH₂Cl₂ (4 x 15 mL). The organic layer was dried with Na₂SO₄, filtered and concentrated *in vacuo* to give *endo-c* as a thick yellow oil in 90% yield over the two last steps. No further purification was performed.

The *endo-c* from the previous step was dissolved in dry THF (80 mL) and cooled to 0 °C. A 1M solution of KO*t*Bu in THF (120 mL) was added dropwise into the reaction flask. After addition the solution turned orange. At this point the ice-bath was removed, the temperature was raised to 70 °C, and the reaction mixture was refluxed for 2 h. After cooling to room temperature the reaction mixture was quenched with saturated NH₄Cl (200 mL) and the product was extracted with CH₂Cl₂. The collected organic fractions were dried with MgSO₄, filtered and concentrated *in vacuo*. The crude product was purified by column chromatography (3:1 Et₂O/hexanes) to give *endo*-BCN 5 as a white solid in 62% yield. ¹H NMR (CDCl₃, 400 MHz); δ (ppm) 0.90-0.99 (m, 2H), 1.30- 1.39 (m, 2H), 1.56-1.66 (m, 2H), 2.20-2.35 (m, 6H), 3.74 (d, *J* = 8.0 Hz, 2H). ¹³C NMR (CDCl₃, 400 MHz): 20.0, 21.4, 21.5, 29.0, 60.0, 98.9. HRMS (CI) [M+H]⁺ calcd for C₁₀H₁₅O 151.1123; found 151.1118.

Compound 6



Scheme 5.8. Synthetic procedure towards the preparation of compound 6.

Compound 6 was prepared according to Scheme 5.8. A flame-dried, two-necked, 250 mL round-bottomed flask was purged with Ar and then was charged with triethylene glycol monomethyl ether (2.0 g, 12.2 mmol) in dry CH_2Cl_2 (0.2 M in starting alcohol). The flask was immersed in an ice-water bath. Dimethyl sulfoxide (955 mg, 24.4 mmol) and phosphorus pentoxide (3.56 g, 24.4) were added sequentially. The reaction mixture was allowed to stir and warm to room temperature until disappearance of starting material by TLC (~3 h). The flask was immersed in the ice-water bath again; then triethylamine (4.32 g, 42.7 mmol) was added dropwise over 10 minutes. Stirring was continued for 45 minutes. The reaction was quenched with 10% aqueous HCl and extracted with CH_2Cl_2 . The organic extracts were washed with saturated aqueous NaCl, dried over anhydrous Na_2SO_4 filtered, and concentrated *in vacuo*. Next, without further purification the crude aldehyde (720 mg, 4.4 mmol), N-methylhydroxylamine hydrochloride (742 mg, 8.8 mmol), and triethylamine (1.8 g, 9.4 mmol) were mixed in 50mL of dry acetonitrile. After reaction completion (3h, checked by TLC) the solvent was evaporated and substituted with CH_2Cl_2 . The organic was then washed with saturated aqueous NaCl three times, dried over anhydrous Na_2SO_4 , filtered, and concentrated *in vacuo*. The crude product was purified by column chromatography over silica gel using dichloromethane/ethyl acetate/methanol (10:3:1 v/v) as the eluent to provide model nitrone 6 as a yellow oil in 64% overall yield. ^1H NMR (400 MHz, CDCl_3) δ (ppm); 3.93 (s, 3H), 3.57 (m, 2H), 3.65-3.70 (m, 10H), 4.46 (m, 2H), 6.95 (t, 1H, $J = 4.5$ Hz); ^{13}C NMR (400 MHz CDCl_3); 52.0, 58.9, 65.6, 70.2, 70.4, 70.8, 71.8, 138.6. HRMS (CI) $[\text{M}+\text{H}]^+$ calcd for $\text{C}_8\text{H}_{17}\text{NO}_4$ 192.1236; found 191.1236.

Compound 7

The model azide 7 was obtained by dissolving triethylene glycol monomethyl ether tosylate (1.9500 g, 6.1 mmol) in acetonitrile (20 mL) in a 50 ml three necks round bottom flask. To this solution NaN₃ (1.1969 g, 18.4 mmol) were added and the reaction mixture was refluxed for 72h. The solvent was evaporated under vacuum and the resulting orange oil was dissolved in CH₂Cl₂ and washed with distilled water. The organic phase was dried using anhydrous Na₂SO₄. After filtration, the solvent was removed under reduced pressure to give compound 7 as a yellow oil with 58% yield. ¹H NMR (CDCl₃, 400 MHz) 3.29 (s, 3H), 3.37 (t, *J* = 4 Hz, 2H), 3.46 (t, *J* = 4 Hz, 2H), 3.58 (m, 8H). HRMS (CI) [M+H]⁺ calcd for C₇H₁₅N₃O₃ 190.1193; found 190.1192.

Compound 8

Tetraethylene glycol monosulfonate (2.0 g, 5.7 mmol) and sodium iodide (0.9 g, 6.0 mmol) were dissolved in acetone (50 mL). The reaction mixture was stirred and heated at 60 °C in a pre-heated oil bath overnight and monitored by TLC (acetone/DCM 1:1) using UV light and potassium permanganate stain. The crude product purified by flash column chromatography (acetone/DCM 1:1) to give a light yellow oil as the desired intermediate in 81%. ¹H NMR (400 MHz, CDCl₃) δ (ppm); 3.27 (t, *J* = 8 Hz, 2H), 3.62 (t, *J* = 4 Hz, 2H), 3.63–3.68 (m, 8H), 3.73–3.78 (m, 4H); ¹³C NMR (400 MHz, CDCl₃); 2.8, 61.8, 70.2, 70.3, 70.5, 70.7, 72.0, 72.5; HRMS (CI) [M+H]⁺ calcd for C₈H₁₇IO₄ 305.0244; found 305.0243.

Compound 9

Compound 8 (1.24 g, 4.1 mmol) and potassium phthalimide (0.76 g, 4.1 mmol) were added into the reaction flask and dissolved in dry DMF (5 mL) under argon atmosphere. While stirring, the reaction flask was immersed in a pre-heated oil bath at 110°C and stirred overnight. The reaction progress was monitored by TLC (hexane/EtOAc/MeOH 7:7:1) using UV light. The reaction mixture was allowed to cool, filtered and concentrated *in vacuo*. Without further purification crude product (1.3 g, 4.1 mmol), triethylamine (1.0 g, 10.1 mmol) and DMAP (0.1 g, 0.9 mmol) were dissolved in CH₂Cl₂ (30 mL). The reaction mixture was cooled to 0°C then tosyl chloride (0.75 g, 4.4 mmol) was slowly added while stirring vigorously. The reaction was allowed to cool to room temperature overnight and the progress was monitored by TLC (7:7:1 hexane/EtOAc/MeOH). The crude product was purified by flash column chromatography (7:7:1 hexane/EtOAc/MeOH) to give the final product as a clear and colorless oil in 37 % yield). ¹H NMR (400 MHz, CDCl₃) δ (ppm); 2.45 (s, 3H), 3.50–3.53 (m, 4H), 3.55–3.58 (m, 2H), 3.61–3.66 (m, 4H), 3.73 (t, *J* = 4 Hz, 2H), 3.90 (t, *J* = 4 Hz, 2H), 4.14 (t, *J* = 4 Hz, 2H), 7.34 (dd, *J* = 8, 184 Hz, 2H), 7.72 (ddd, *J* = 4, 6, 52 Hz, 2H), 7.80 (dd, *J* = 8, 184 Hz, 2H), 7.85 (ddd, *J* = 4, 6, 52 Hz, 2H); ¹³C NMR (400 MHz, CDCl₃) 21.6, 37.3, 67.9, 68.7, 69.2, 70.1, 70.6, 70.7, 123.3, 128.0, 129.8, 132.1, 133.0, 144.7, 168.2. HRMS (ESI) [M]⁺ calcd for C₂₃H₂₇NO₈S 477.1457; found 477.1468.

Compound 10

Compound 9 (480 mg, 1 mmol) and CsF (760 mg, 5 mmol) were dissolved in *tert*-butanol (10 mL) and stirred at 60 °C for 5 h. after removal of the solvent, the crude was purified using column chromatography (19:1 DCM: MeOH) to provide compound 9 as a white solid in 86% yield. ¹H NMR (400 MHz, CDCl₃) δ (ppm); 3.62-3.76 (m, 12H), 3.91 (t, *J* = 5.8, 2H), 4.55 (dt, *J* = 4.0, 32.0, 2H), 7.72 (m, 2H), 7.86 (m, 2H); ¹³C NMR (400 MHz, CDCl₃) 37.3, 67.9, 70.1, 70.3, 70.6, 70.7, 82.3, 84.0, 123.2, 132.1, 133.9, 144.7, 168.2. HRMS (CI) [M+H]⁺ calcd for C₁₆H₂₀FNO₅ 325.1326; found 325.1335.

Compound 11

Compound 10 (470 mg, 1.45 mmol) was dissolved in 95% ethanol (15 mL). Hydrazine monohydrate (500 mg, 0.49 mL) was added to it and the reaction mixture was refluxed for 5 h. After TLC showed the reaction was complete, the reaction mixture was cooled to room temperature and the precipitated phthalyl hydrazide was filtered. The filtrate was then treated with 2M HCl and the solid residue was separated by filtration. The filtrate was concentrated and extracted with dichloromethane (x5). The combined organic solution was dried over Na₂SO₄ and concentrated. The crude was used in preparation of compound 12 without any further purification. ¹H NMR (400 MHz, CDCl₃) δ (ppm); 2.71 (t, *J* = 5.5, 2H), 3.40 (t, *J* = 5.5, 2H), 3.52-3.59 (m, 8H), 4.45 (m, 1H), 4.57 (m, 1H); HRMS (ESI) [M]⁺ calcd for C₈H₁₈FNO₃ 195.12714; found 195.1275.

Compound 12

Compound 12 was prepared according to the previous reports²² and was used in preparation of compound 13. To a solution of *endo*-BCN 5 (500 mg, 3.33 mmol) in CH₂Cl₂ (25 mL) was added pyridine (229 μL, 8.31 mmol) and *p*-NO₂PhOC(O)Cl (838 mg, 416 μmol). After stirring for 15 min at room temperature the mixture was quenched with saturated NH₄Cl-solution (75 mL) and extracted with CH₂Cl₂ (3 x 15 mL). The organic layer was dried over anhydrous Na₂SO₄ and concentrated *in vacuo*. The residue was purified by column chromatography on silica gel (Et₂O: Hexanes, 1:1) to afford 12 as a white solid in 76% yield. ¹H NMR (CDCl₃, 400 MHz) δ (ppm); 1.02-1.12 (m, 2H), 1.47-1.56 (m, 1H), 1.57-1.67 (m, 1H), 2.22-2.40 (m, 6H), 4.41 (d, *J* = 8.4 Hz, 2H), 7.40 (d, *J* = 9.6 Hz, 2H), 8.28 (d, *J* = 9.2 Hz, 2H); ¹³C NMR (CDCl₃, 400 MHz) 17.2, 20.5, 21.3, 29.0, 68.0, 98.7, 121.7, 125.3, 145.3, 152.5, 155.6.

Compound 13

Compound 12 (81 mg, 0.26 mmol) was dissolved in dry DMF (0.5 mL) and was cooled on ice while purging with argon. In a separate flask, compound 11 (200 mg, 1.02 mmol) was dissolved in dry DMF (1 mL) and NEt₃ (0.2 mL, 1.02 mmol) was added. After purging this mixture with argon for 15 minutes, it was transferred to the first flask using a canula and the reaction mixture was stirred at 0 °C for 20 minutes. After the TLC showed reaction was completed, the mixture was concentrated and then extracted (x5) using EtOAc. The combined organic solution was washed with brine and dried over Na₂SO₄ and concentrated. The crude was purified using column chromatography using

EtOAc providing compound 13 as very light yellow oil in 57% yield. ^1H NMR (400 MHz, CDCl_3) δ (ppm): 0.95 (m, 2H), 1.36 (m, 1H), 1.60 (m, 2H), 2.21-2.32 (m, 6H), 3.36 (m, 2H), 3.57 (t, $J = 4.9$ Hz, 2H), 3.62-3.73 (m, 8H), 3.74 (t, $J = 4$ Hz, 1H), 3.79 (t, $J = 4$ Hz, 1H), 4.14 (d, $J = 8.2$, 2H), 4.58 (dt, $J = 32, 2.4$, 2H), 5.28 (br.s, 1H); ^{13}C NMR (400 MHz, CDCl_3) 18.1, 20.4, 21.7, 29.3, 41.1, 42.1, 63.0, 70.4, 70.6, 70.8, 70.9, 70.9, 71.1, 82.6, 84.3, 99.1, 157.1. HRMS (ESI) $[\text{M}]^+$ calcd for $\text{C}_{19}\text{H}_{30}\text{FNO}_5$ 371.2109; found 371.2108.

Synthesis of Nitrone-AuNPs

The Me-EG₃-AuNPs were synthesized according to our previously established procedure.⁵³ $\text{HAuCl}_4 \cdot 3\text{H}_2\text{O}$ (1.4564 g, 3.7 mmol, 1.0 eq.) was dissolved in a mixture of dry methanol (503 mL) and glacial acetic acid (83 mL). To this yellow solution was added Me-EG₃-SH (2.0 g, 11 mmol, 3.0 eq.). The slightly darkened solution was stirred vigorously for 2 h and the solution color slightly faded. A solution of NaBH_4 (1.3997 g, 37 mmol, 10.0 eq.) in milli-Q water (96 mL) was added dropwise to the reaction mixture under vigorous stirring. The mixture turned dark brown immediately. After overnight stirring at ambient temperature, the solution was concentrated and diluted with brine. The Me-EG₃-AuNPs were extracted with toluene while adding sodium chloride to the aqueous phase after each extraction to maintain the saturation. The aqueous phase was eventually colorless. The combined organic phases were then concentrated *in vacuo*. Evaporation of the solvent left a thin film of nanoparticles which was then rinsed with

hexanes to remove the excess free thiol. The crude Me-EG₃-AuNPs were dissolved in nanopure H₂O and further purified by overnight dialysis.

Next, to a solution of Me-EG₃-AuNPs (180 mg) in CH₂Cl₂ (25 mL) was added a solution of thiol 4 (30 mg, 0.13 mmol) in CH₂Cl₂ (5 mL) while stirring vigorously. After 30 minutes of stirring, the solvent was evaporated to form a film of nanoparticles. This film was washed (x5) with hexanes/isopropanol (10:1) to remove most of the unbound thiols present. Next, AuNPs were dissolved in milli-Q water and further purified by overnight dialysis. All the characterization details can be found in the supporting information.

Proof of concept SPANC reactions using model nitrone 6 and Nitrone-AuNPs

Synthesis of isoxazoline 14

In a typical experiment, nitrone 6 (19.1 mg, 100 μmol) was mixed with endo-BCN 5 (30.0 mg, 200 μmol) at room temperature in a mixture of CH₃CN/H₂O (3: 1) (2 mL). After reaction went to completion, the solvent was removed to afford the endo-cycloadduct 14 as an inseparable mixture of isomers in quantitative yield. ¹H NMR (400 MHz, CDCl₃) δ (ppm); 0.87-1.04 (m, 2H), 1.13–1.19 (m, 1H), 1.49-1.63 (m, 2H), 1.95-2.05 (m, 2H), 2.11-2.28 (m, 2H), 2.29-2.43 (m, 2H), 2.68 (s, 3H), 3.39 (s, 3H), 3.44-3.74 (m, 14H); ¹³C NMR (400 MHz, CDCl₃); 18.5, 18.8, 18.9, 19.8, 20.1, 20.6, 20.7, 21.8, 22.1, 25.4, 25.6, 26.0, 26.1, 46.6, 59.0, 60.0, 70.5, 70.6, 70.7, 71.9, 72.8, 101.9, 102.2, 146.6, 146.9. HRMS (CI) [M+H]⁺ calcd for C₁₈H₃₁NO₅ 342.2228; found 342.2230.

Synthesis of isoxazoline AuNPs

To test the i-SPANC at the Nitron-AuNP interface, Nitron-AuNPs were reacted with endo-BCN 5. In a typical experiment of Nitron-AuNPs (10 mg, 8.4 μmol of nitron) were mixed with compound 5 (2.5 mg, 16.8 μmol) in a mixture of $\text{CH}_3\text{CN}/\text{H}_2\text{O}$ (3: 1) (1 mL). Reaction was followed using ^1H NMR spectroscopy following the disappearance of nitron's signature signals at 4.4 and 7.4 ppm. After reaction completion, the solvent was evaporated to form a film of nanoparticles. This film was then washed repeatedly (x5-7) to remove any excess BCN 5.

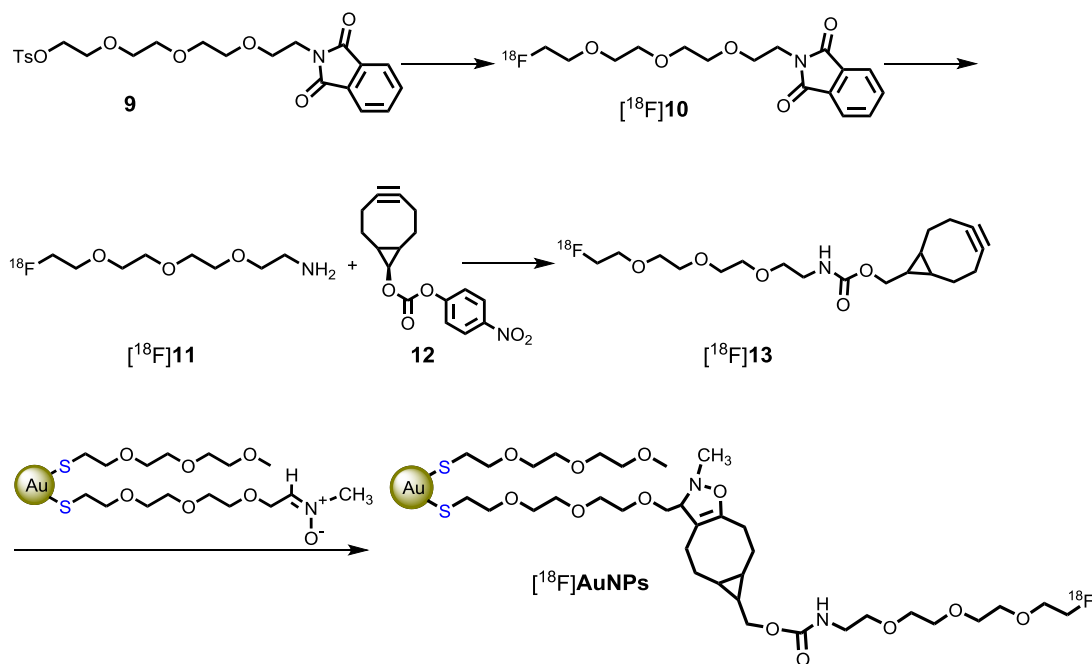
Synthesis of isoxazoline 16

In a typical experiment, nitron 6 (19.1 mg, 100 μmol) was mixed with endo-BCN 13 (37.1 mg, 100 μmol) at room temperature in a mixture of $\text{CH}_3\text{CN}/\text{H}_2\text{O}$ (3:1) (2 mL). After reaction went to completion, the solvent was removed. The crude product was purified using column chromatography (eluent: EtOAc) to afford the endo-cycloadduct 16 as an inseparable mixture of isomers in 91% yield. ^1H NMR (400 MHz, CDCl_3) δ (ppm); 0.86-1.05 (m, 2H), 1.13–1.22 (m, 1H), 1.48-1.63 (m, 2H), 1.91-2.02 (m, 2H), 2.07-2.40 (m, 2H), 2.68 (s, 3H), 3.33-3.42 (m, 5H), 3.50-3.74 (m, 21H), 3.80 (t, $J = 4$, 1H), 4.15 (m, 2H), 4.58 (dt, $J = 48$, 4, 2H), 5.21 (br.s 1H); ^{13}C NMR (400 MHz, CDCl_3); 18.5, 18.8, 18.9, 19.8, 20.1, 20.6, 20.7, 21.8, 22.1, 25.4, 25.6, 26.0, 26.1, 46.6, 59.0, 60.0, 70.5, 70.6, 70.7, 71.9, 72.8, 101.9, 102.2, 146.6, 146.9; ^{19}F $\{^1\text{H}\}$ NMR (400 MHz, CDCl_3) -223.36. HRMS (CI) $[\text{M}+\text{H}]^+$ calcd for $\text{C}_{27}\text{H}_{47}\text{FN}_2\text{O}_9$ 563.3345; found 563.3341.

Synthesis of F-isoxazoline AuNPs

In a typical experiment Nitron-AuNPs (10 mg, 8.4 μmol of nitron) were mixed with compound 13 (3.1 mg, 8.4 μmol) in a mixture of $\text{CH}_3\text{CN}/\text{H}_2\text{O}$ (3:1) (1 mL). Reaction was followed using ^1H NMR spectroscopy following the disappearance of nitron's signature signals at 4.4 and 7.4 ppm. After reaction completion, the solvent was evaporated to form a film of nanoparticles. This film was then washed repeatedly (x5-7) to remove any excess BCN 13. The resulting AuNPs were then further purified by dialysis in milli-Q water.

Synthesis of ^{18}F -AuNPs



Scheme 5.9. Reaction pathway towards the synthesis of [^{18}F] 13 prosthetic group and their i-SPANC reaction to prepare [^{18}F] AuNPs.

[¹⁸F] AuNPs were prepared following reaction Scheme 5.9. First, an aqueous [¹⁸F] fluoride solution was produced from cyclotron and trapped on the carbonated QMA cartridge. 1 mL of CH₃CN/H₂O (90/10; v/v) solution containing potassium carbonate (1 mg) and kryptofix 2.2.2 (6-8 mg) was used to elute [¹⁸F] fluoride into glass vial. The solvent was removed on at 75 °C in vacuum. [¹⁸F] fluoride was dried twice by adding 1 mL of anhydrous acetonitrile and evaporated in vacuum. 500 μL of anhydrous acetonitrile containing 10-20 mg of compound 9 reaction mixture was added to reaction vials and heated at 90 °C for 5 min. Next the reaction mixture was cooled down to room temperature, diluted with 3 mL of H₂O and purified on HPLC (eluent: flow rate 4 ml/min, acetonitrile/H₂O, 36% containing 0.1% TFA) to get [¹⁸F] 10. The solvent was evaporated on V-10 evaporator at 50 °C. Next, 500 μL of hydrazine monohydrate was added into the vial containing [¹⁸F] 10. The reaction mixture was heated at 60 °C for 5 mins, diluted with 1 mL of water and trapped on the C18 cartridge. Subsequently, 500 μL of acetonitrile was used to elute resulting [¹⁸F] 11 through C18 cartridge into the vial containing 3 mg of compound 12 in 200 μL of acetonitrile and then 50 μL of TEA was added. The reaction mixture was heated at 60°C for 20 min and diluted with 700 μL of water. Next, [¹⁸F] 13 was purified on semi-preparative C18 column (eluent: flow rate 4 ml/min, acetonitrile/H₂O, 50% containing 0.1% TFA) and dried on V-10 evaporator at 50 °C.

The [¹⁸F] AuNPs were prepared from the i-SPANC reaction between [¹⁸F] 13 and Nitron-AuNPs. An aqueous solution of [¹⁸F] 13 was added to 500 μg of AuNP in 200 μL of PBS buffer (0.1 M) and reacted at room temperature for 20 min. the reaction mixture

was purified on PD-10 desalting column to get [^{18}F] AuNP. The total yield is ~6% after decay correction.

Synthesis of SWCNT-BCN

In a typical synthesis, SWCNT (20 mg) were dispersed in dry MeOH (10 mL) in a round bottom flask. The system was cooled down to 0°C, and the solution was purged with argon for 10 minutes. In a separate flask, O-Benzotriazole-N,N,N',N'-tetramethyluronium-hexafluoro-phosphate (HBTU) (30 mg, 64 μmol) and N,N-Diisopropylethylamine (DIPEA) (23 μL , 128 μmol) were dissolved in a mixture of $\text{CH}_3\text{CN}/\text{MeOH}$ (1:2) (5 mL) and purged with argon for 10 min. After the two solutions were purged, the HBTU/DIPEA mixture was transferred using a glass syringe into the ice-cold solution of CNT suspension and the reaction mixture was left for 15 min at 0°C. In a third round bottom flask, a solution of N-[(1R,8S,9s)-Bicyclo[6.1.0]non-4-yn-9-ylmethoxycarbonyl]-1,8-diamino-3,6-dioxaoctane (BCN-amine) (41 mg, 128 μmol) in acetonitrile (2 mL) was purged with argon. After 15 min the solution of BCN-amine was injected into the ice-cold solution of CNT, HBTU and DIPEA mixture. The ice bath was removed and the reaction mixture was left overnight under vigorous stirring. The solution was then centrifuged (10 min, 6000 rpm) and the supernatant was removed. The resulting SWCNT-BCN was re-dispersed in acetonitrile, sonicated for 10 min, centrifuged again, and the solvent was decanted. This washing protocol was repeated once more, then acetonitrile was substituted with water and the SWCNT-BCN were washed and centrifuged twice. This ensured that there was no unreacted BCN-amine. Finally, the

solvent was evaporated and the SWCNT-DBCO was dispersed in a phosphate buffer solution (PBS) pH 7.0 to obtain a concentration of 2 mg/mL. This mother solution was later used for the SPANC reaction with the Nitron-AuNPs.

i-SPANC reaction between Nitron-AuNP and SWCNT-BCN

In a typical synthesis, to the mother solution of SWCNT-BCN (1 mL) Nitron-AuNPs (5 mg) were added, and the reaction mixture was then diluted to 5 ml with PBS pH 7.0. The system was stirred for 1 hour at room temperature and then the SWCNT-AuNPs were centrifuged in a Pyrex centrifuge test tube. The supernatant was removed, and the decorated CNT were dispersed in water, sonicated for 10 minutes and centrifuged. Subsequently, water was substituted first with acetone, then with dichloromethane, and the washing procedure (sonication and centrifugation) was repeated four more times. This protocol was to ensure removal of any non-covalently bound AuNP.

5.5 References

- 1) Yeh, Y.C.; Crerana, B.; Rotello, V. M. *Nanoscale* **2012**, 4, 1871.
- 2) Dykmana, L.; Khlebtsov, N. *Chem. Soc. Rev.* **2012**, 41, 2256.
- 3) Sperling, R. A.; Gil, P. R.; Zhang, F.; Zanellaa, M.; Parak, W. J. *Chem. Soc. Rev.* **2008**, 37, 1896.

- 4) Zavaleta, C. L.; Garai, E.; Liu, J. T.; Sensarn, S.; Mandella, M. J.; Van de Sompel, D.; Friedland, S.; Van Dam, J.; Contag, C. H.; Gambhir, S. S. *Proc. Natl. Acad. Sci. USA* **2013**, 110, E2288.
- 5) Qian, X.; Peng, X.-H.; Ansari, D. O.; Goen, Q. Y.; Chen, G. Z.; Shin, D. M.; Yang, L.; Young, A. N.; Wang, M. D.; Nie, S. *Nat. Biotechnol.* **2008**, 26, 83.
- 6) Kim, D.; Park, S.; Lee, J. H.; Jeong, Y. Y.; Jon, S. *J. Am. Chem. Soc.* **2007**, 129, 7661.
- 7) Da Xi, D.; Dong, S.; Meng, X.; Lu, Q.; Meng, L.; Ye, J. *RSC Adv.* **2012**, 2, 12515.
- 8) Li, W.; Chen, X. *Nanomedicine* **2015**, 10, 299.
- 9) Mallidi, S.; Larson, T.; Tam, J.; Joshi, P. P.; Karpiouk, A.; Sokolov, K.; Emelianov, S. *Nano Lett.* **2009**, 8, 2825.
- 10) Xie, H.; Diagaradjane P.; Deorukhkar, A. A.; Goins, B.; Bao, A.; Phillips, W. T.; Wang, Z.; Schwartz, J.; Krishnan, S. *Int. J. Nanomed.* **2011**, 6, 259.
- 11) Agarwal, A.; Shao, X.; Rajian, J. R.; Zhang, H.; Chamberland, D. L.; Kotov, N. A.; Wang, X. *J. Biomed. Opt.* **2011**, 16, 051307.
- 12) Shao, X.; Agarwal, A.; Rajaian, J. R.; Kotov, N. A.; Wang, X. *Nanotechnology* **2011**, 13, 135102.
- 13) Guerrero, S.; Herance, J. R.; Rojas, S.; Mena, J. F.; Gispert, J. D.; Acosta, G. A.; Albericio, F.; Kogan, M. J. *Bioconjugate Chem.* **2012**, 23, 399.
- 14) Sletten, E. M.; Bertozzi, C. R. *Angew. Chem. Int. Ed.* **2009**, 48, 6974.
- 15) Huisgen, R. *Angew. Chem. Int. Ed.* **1963**, 2, 565.
- 16) Agard, N. J.; Prescher, J. A.; Bertozzi, C. R. *J. Am. Chem. Soc.* **2004**, 126, 15046.

- 17) Agard, N. J.; Baskin, J. M.; Prescher, J. A.; Lo, A.; Bertozzi, C. R. *ACS Chem. Biol.* **2006**, 1, 644.
- 18) Baskin, J. M.; Prescher, J. A.; Laughlin, S. T.; Agard, N. J.; Chang, P. V.; Miller, I. A.; Lo, A.; Codelli, J. A.; Bertozzi, C. R. *Proc. Natl. Acad. Sci. USA* **2007**, 104, 16793.
- 19) Codelli, J. A.; Baskin, J. M.; Agard, N. J.; Bertozzi, C. R. *J. Am. Chem. Soc.* **2008**, 130, 11486.
- 20) Sletten, E. M.; Bertozzi, C. R. *Org. Lett.* **2008**, 10, 3097.
- 21) Ning, X.; Guo, J.; Wolfert, M. A.; Boons, G.-J. *Angew. Chem. Int. Ed.* **2008**, 47, 2253.
- 22) Dommerholt, J.; Schmidt, S.; Temming, R.; Hendriks, L. J.; Rutjes, F. P.; van Hest, J. C.; Lefeber, D. J.; Friedl, P.; van Delft, F. L. *Angew. Chem. Int. Ed.* **2010**, 49, 9422.
- 23) Jewett, J. C.; Sletten, E. M.; Bertozzi, C. R. *J. Am. Chem. Soc.* **2010**, 132, 3688.
- 24) Rostovtsev, V. V.; Green, L. G.; Fokin, V. V.; Sharpless, K. B. *Angew. Chem. Int. Ed.* **2002**, 41, 2596.
- 25) McKay, C. S.; Moran, J.; Pezacki, J. P. *Chem. Commun.* **2010**, 46, 931.
- 26) Dommerholt, J.; Schmidt, S.; Temming, R.; Hendriks, L. J.; Rutjes, F. P.; van Hest, J. C.; Lefeber, D. J.; Friedl, P.; van Delft, F. L. *Angew. Chem. Int. Ed.* **2010**, 49, 9422.
- 27) McKay, C. S.; Blake, J. A.; Cheng, J.; Danielson, D. C.; Pezacki, J. P. *Chem. Commun.* **2011**, 47, 10040.
- 28) Moran, J.; McKay, C. S.; Pezacki, J. P. *Can. J. Chem.* **2011**, 89, 148.

- 29) Ning, X.; Temming, R. P.; Dommerholt, J.; Guo, J.; Ania, D. B.; Debets, M. F.; Wolfert, M. A.; Boons, G.-J.; van Delft, F. L. *Angew. Chem. Int. Ed.* **2010**, *49*, 3065.
- 30) Temming, R. P.; Eggermont, L.; van Eldijk, M. B.; van Hest, J. C. M.; van Delft, F. L. *Org. Biomol. Chem.* **2013**, *11*, 2772.
- 31) Ledin, P.A.; Kolishetti, N.; Boons, G. J. **2013**, *46*, 7759.
- 32) Colombo, M.; Sommaruga, S.; Mazzucchelli, S.; Polito, L.; Verderio, P.; Galeffi, P.; Corsi, F.; Tortora, P.; Prospero, D. *Angew. Chem. Int. Ed.* **2012**, *51*, 496.
- 33) Lee, S. B.; Kim, H. L.; Jeong, H. J. Lim, S. T.; Sohn, M. H.; Kim, D. W. *Angew. Chem. Int. Ed.* **2013**, *52*, 10549.
- 34) Campbell-Verduyn, L. S.; Mirfeizi, L.; Schoonen, A. K.; Dierckx, R. A.; Elsinga, P. H.; Feringa, B. L. *Angew. Chem. Int. Ed.* **2011**, *50*, 11117.
- 35) Bouvet, V.; Wuest, M.; Wuest, F. *Org. Biomol. Chem.* **2011**, *9*, 7393.
- 36) Eder, D. *Chem. Rev.* **2010**, *110*, 1348.
- 37) Wu, H. C.; Chang, X.; Liu, L.; Zhao, F.; Zhao, Y. *J. Mater. Chem.* **2010**, *20*, 1036.
- 38) Schatz, A.; Reiser, O.; Stark, W. J. *Chem. Eur. J.* **2010**, *16*, 8950.
- 39) Chen, M.; Goodman, D. W. *Chem. Soc. Rev.* **2008**, *37*, 1860.
- 40) Wang, Z.; Ma, L. *Coord. Chem. Rev.* **2009**, *253*, 1607.
- 41) Chauhan, N.; Singh, A.; Narang, J.; Dahiya, S.; Pundir, S. C. *Analyst* **2012**, *137*, 5113.

- 42) Moulder, J. F.; Stickle, W. F.; Sobol, P. E.; Bomben, K. D. *Handbook of X-ray Photoelectron Spectroscopy*. Physical Electronics Inc. MN: Eden Prairie, **1995**.
- 43) Castner, D. G.; Hinds, K.; Grainger, D. W. *Langmuir* **1996**, 12, 5083.
- 44) Chithrani, B. D.; Ghazani, A. A.; Chan, W. C. W. *Nano Lett.* **2006**, 6, 662.
- 45) De Jong, W. H.; Hagens, W. I.; Krystek, P.; Burger, M. C.; Sips, A. J. A. M.; Geertsma, R. E. *Biomaterials*, **2008**, 29, 1912.
- 46) Jain, P. K.; Lee, K. S.; El-Sayed, I. H.; El-Sayed, M. A. *J. Phys. Chem. B* **2006**, 110, 7238.
- 47) Huang, X.; El-Sayed, I. H.; Qian, W.; El-Sayed, M. A. *J. Am. Chem. Soc.* **2006**, 128, 2115.
- 48) Hillyer, J. F.; Albrecht, R. M. *Microsc. Microanal.* **1999**, 4, 481.
- 49) Hillyer, J. F.; Albrecht, R. M. *J. Pharm. Sci.* **2001**, 90, 1927.
- 50) Frigell, J.; García, I.; Gomez-Vallejo, V.; Llop, J.; Penades, S. *J. Am. Chem. Soc.* **2014**, 136, 449.
- 51) Zhu, J.; Chin, J.; Wängler, C.; Wängler, B.; Lennox, R. B.; Schirmacher, R. *Bioconjugate Chem.*, **2014**, 25, 1143.
- 52) Weintraub, K. *Nature* **2013**, 495, S14.
- 53) Gobbo, P.; Workentin, M. S. *Langmuir*, **2012**, 28, 12357.
- 54) Hausner, S. H.; Marik, J.; Gagnon, M. K. J.; Sutcliffe, J. L. *J. Med. Chem.* **2008**, 51, 5901.

- 55) Doss, M.; Kolb, H. C.; Zhang, J. J.; Bélanger, M. J.; Stubbs, J. B.; Stabin, M. G.; Hostetler, E. D.; Alpaugh, R. K.; von Mehren, M.; Walsh, J. C.; Haka, M.; Mocharla, V. P.; Yu, J. Q. *J. Nucl. Med.* **2012**, 53, 787.
- 56) Nguyen, Q. D.; Smith, G.; Glaser, M.; Perumal, M.; Arstad, E.; Aboagye, E. O. *Proc. Natl. Acad. Sci. USA* **2009**, 106, 16375.

5.6 Supporting Information

This section contains the data to support the work carried out in chapter five of this thesis. It includes NMR spectra of Nitrore-AuNPs and the interfacially modified AuNPs, NMRs and rate plots for the kinetic studies, TGA graphs and TEM images and the calculations made thereafter to determine the AuNPs raw formula. High resolution XPS spectra of SWCNT-AuNP hybrid material, its IR spectrum, and TEM images of the hybrid CNT-AuNP and the control experiments are also included in this section.

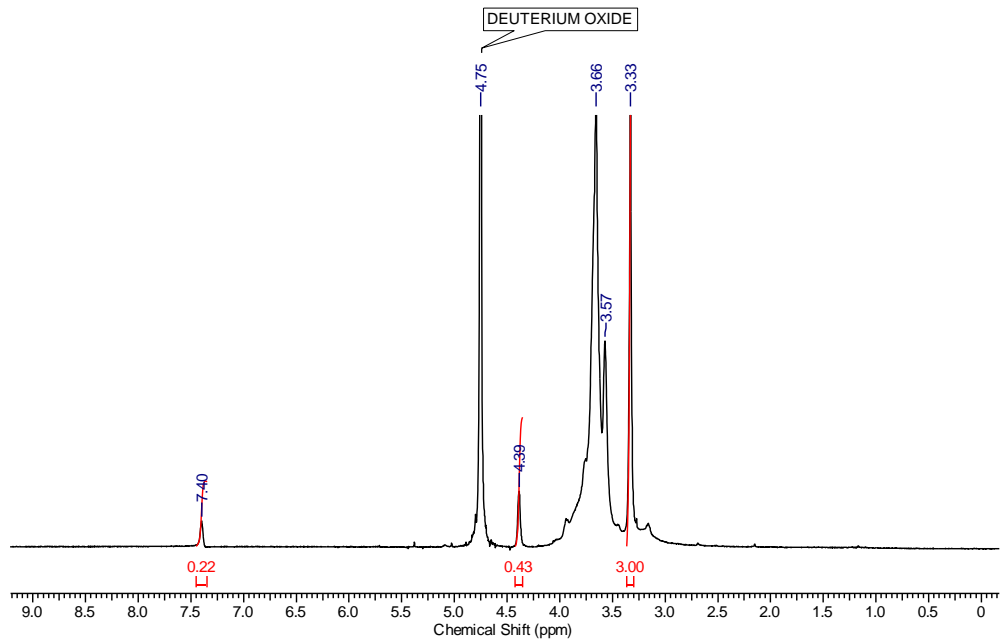


Figure S5.1. ^1H NMR spectrum of Nitron-AuNPs in D_2O .

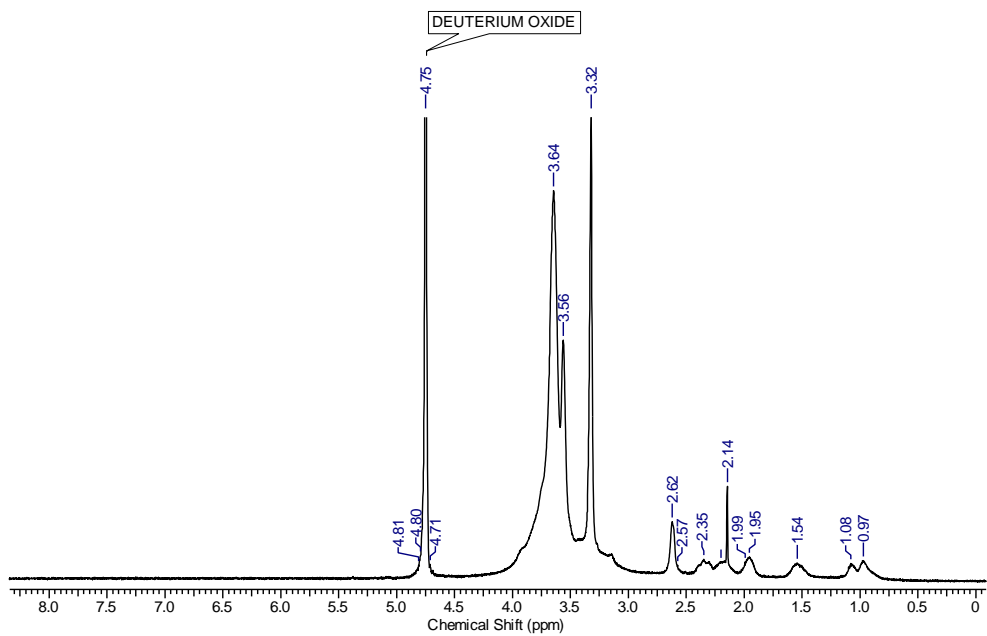


Figure S5.2. ^1H NMR spectrum of compound isoxazoline AuNPs in D_2O .

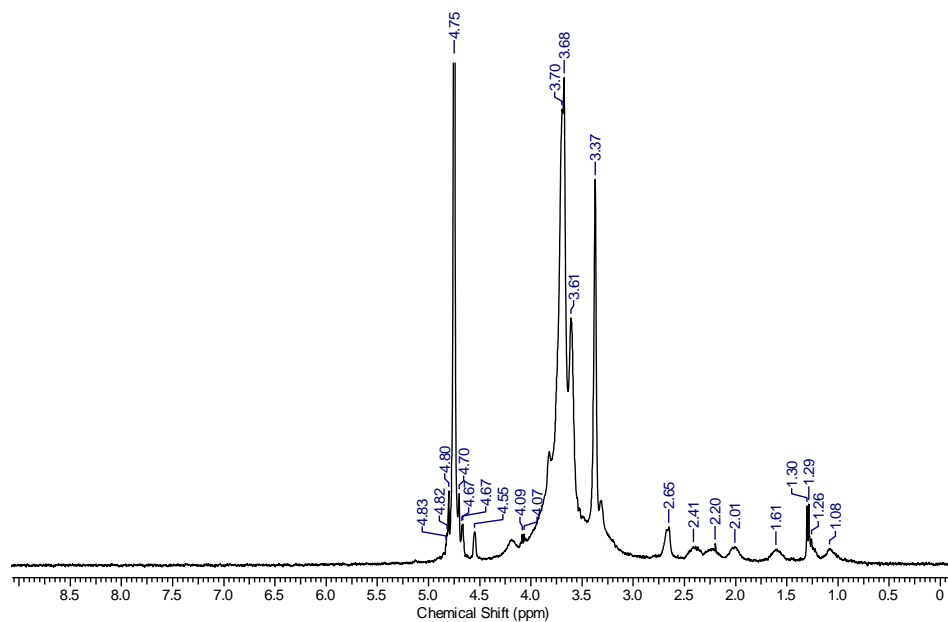


Figure S5.3. ^1H NMR spectrum of compound F-isoxazoline AuNPs in D_2O .

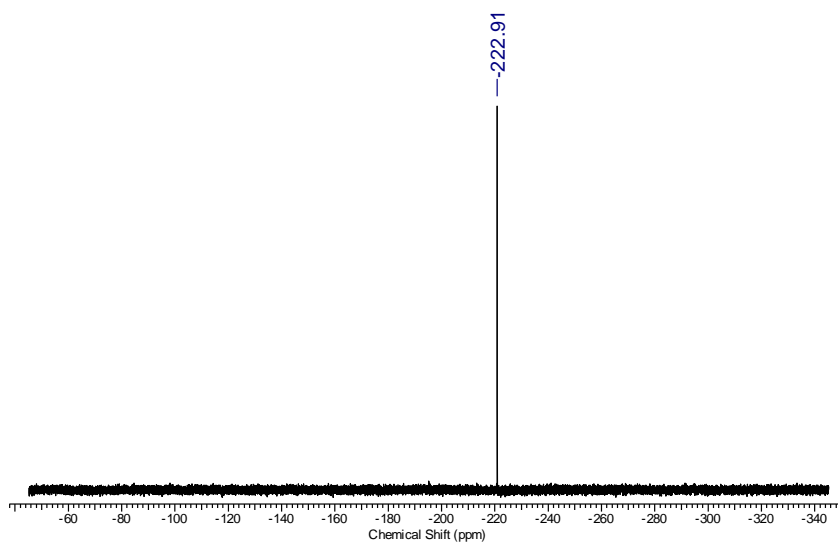


Figure S5.4. ^{19}F $\{^1\text{H}\}$ NMR spectrum of compound F-isoxazoline AuNPs in D_2O .

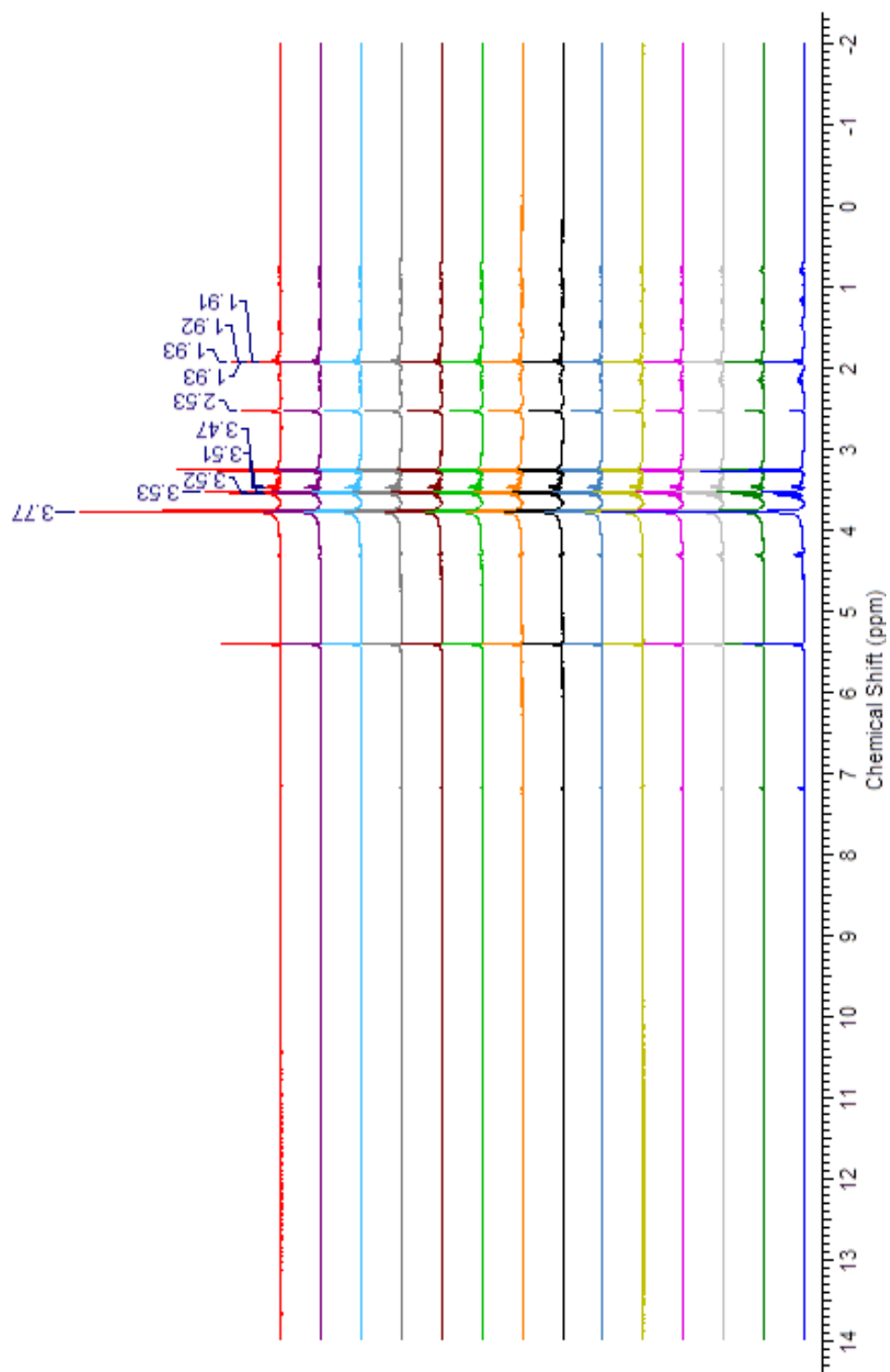


Figure S5.5. ^1H NMR spectra array for a representative kinetic study of SPACC reaction of nitron 6 and BCN 5 to prepare compound 14.

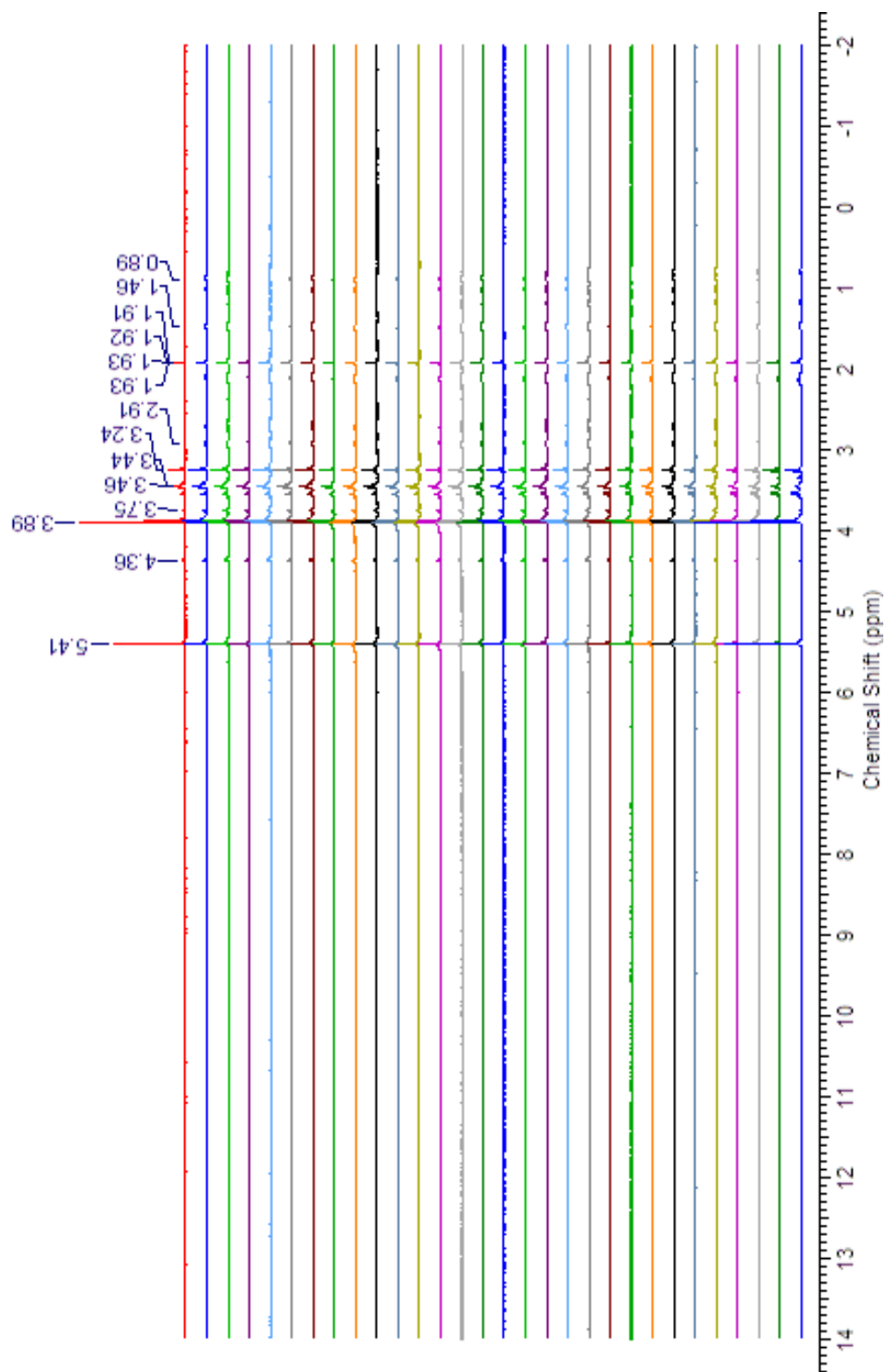


Figure S5.6. ^1H NMR spectra array for a representative kinetic study of SPAAC reaction of azide 7 and BCN 5 to prepare compound 15.

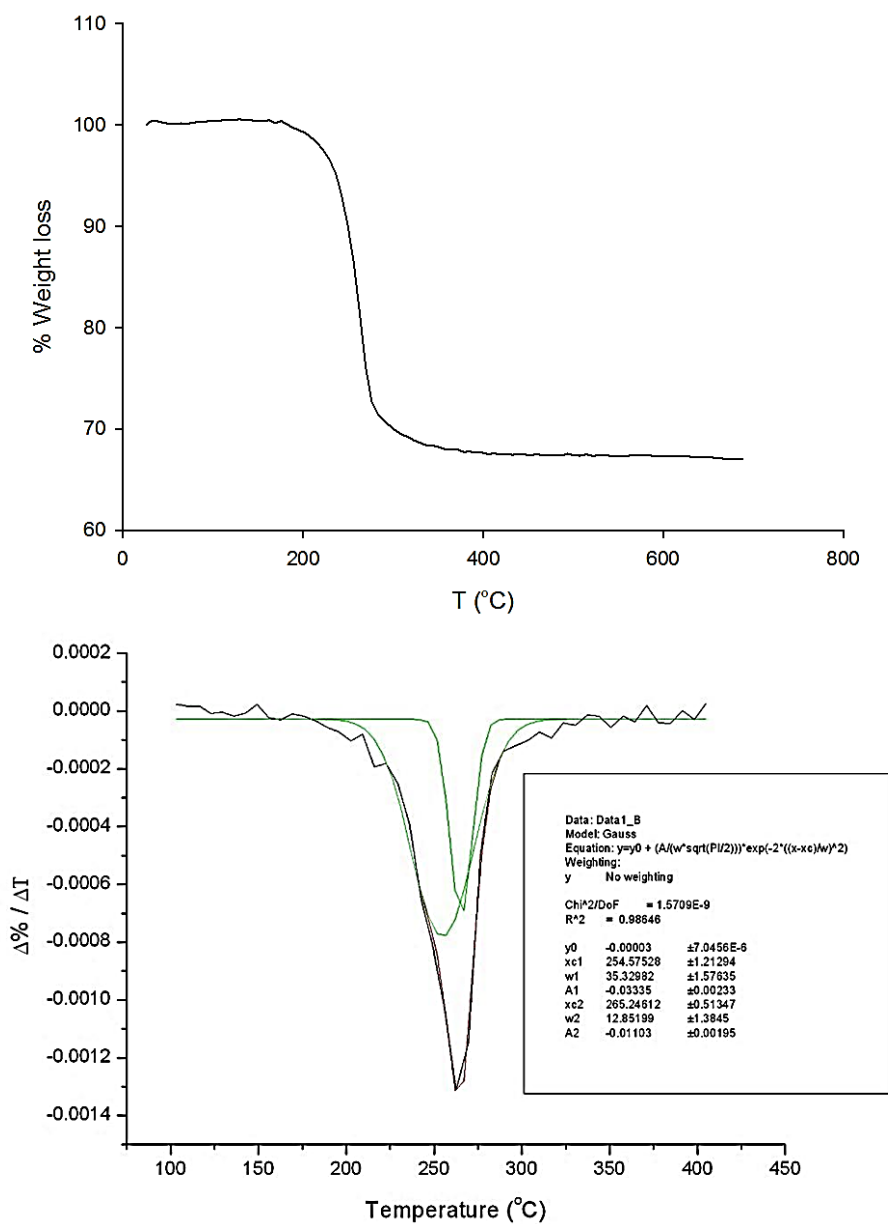


Figure S5.7. TGA (top) and deconvolution of the TGA first derivative curve (bottom) of the Nitron-AuNPs.

Calculation of the nanoparticles raw formula

From the deconvolution of the TGA derivative (see Figure S5.7, bottom) it is possible to calculate the amount (in milligram) of the two ligands (Me-EG₃-SH and Nitron-EG₄-SH) per milligram of Nitron-AuNPs. Having this information and using the following equations we can calculate the raw formula for Nitron-AuNPs.

$$N_{Au} = \frac{\pi \rho d^3 N_A}{6 M_{Au}}$$

ρ = density of face centered cubic (fcc) gold lattice (19.3 g cm⁻³)

d = average diameter of nanoparticles in centimeters (from TEM images)

N_A = Avogadro constant

M_{Au} = mole atomic weight of gold (196.9665 g mol⁻¹)

This is assuming that the AuNPs are spherical and that they are monodispersed.

The total number of ligands (N_L) can be calculated using the following formula:

$$N_L = \frac{N_{Au} M_{Au} M_{TGAOrg}}{(1 - M_{TGAOrg})(MW_1 n_1 + MW_2 n_2)}$$

MW_{TGAOrg} = organic percentage mass loss from TGA

MW_1 = molecular weight of ligand 1 (Me-EG₃-S-)

n_1 = molar percentage of ligand 1 (Me-EG₃-S-)

MW_2 = molecular weight of ligand 2 (Nitron-EG₄-S-)

n_2 = molar percentage of ligand 2 (Nitron-EG₄-S-)

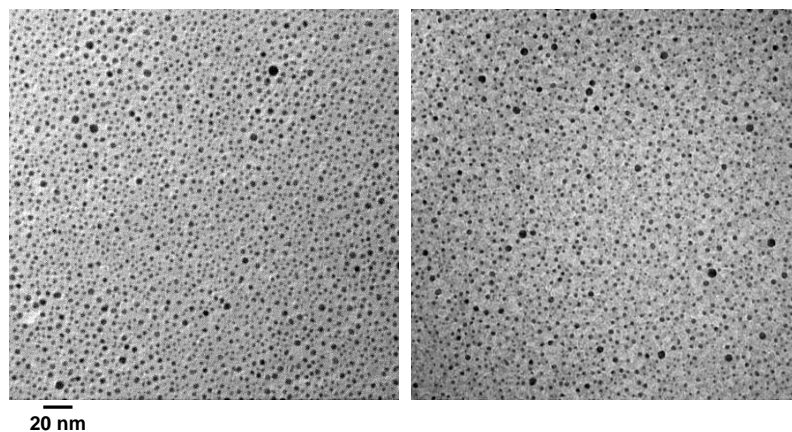


Figure S5.8. TEM images of Nitrone-AuNPs (left) and F-isoxazoline AuNPs (right).

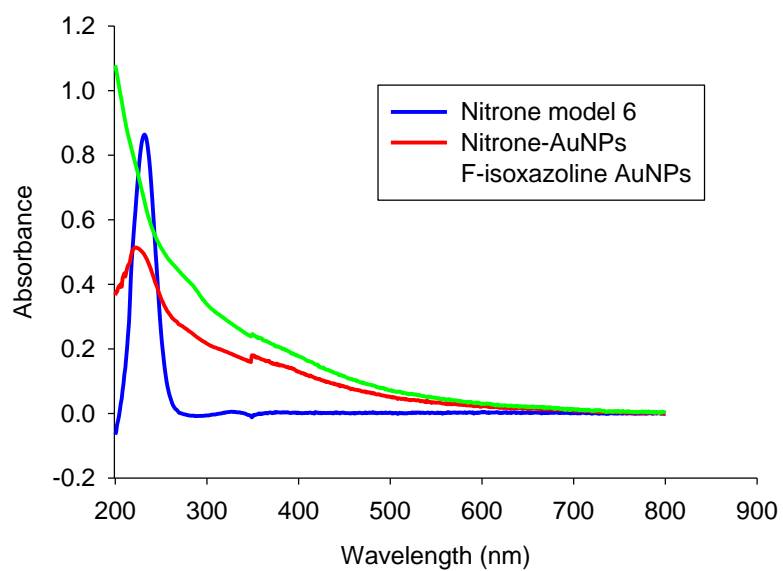


Figure S5.9. UV-vis spectra of compound **6** (blue), Nitrone-AuNPs (dark red), F-isoxazoline AuNPs (green)

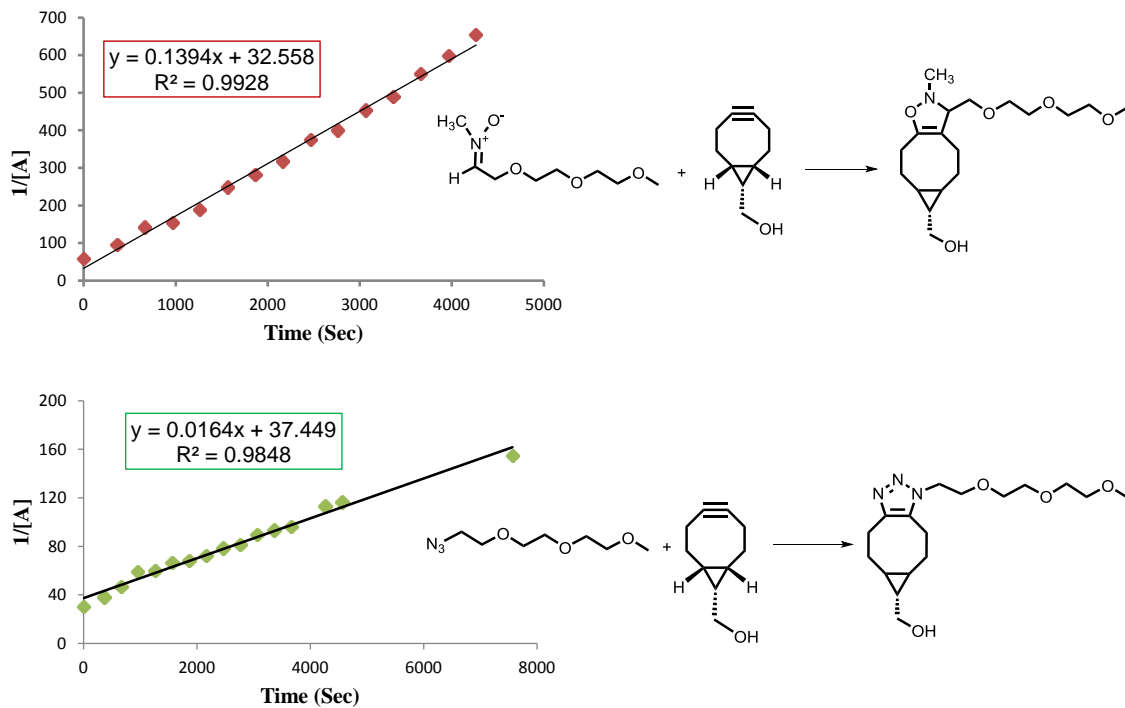


Figure S5.10. Rate plots for the strain-promoted cycloaddition reaction of BCN-5 with nitron 6 (top) and azide 7 (bottom).

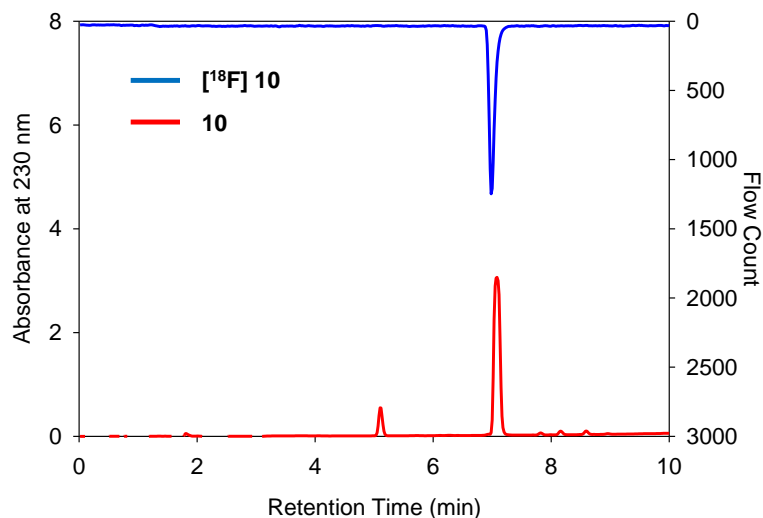


Figure S5.11. HPLC and flow count for compound 10/ [¹⁸F] 10. HPLC condition: Sunfire RP-18 analytical column: 4.6 × 250 mm, 5 μm; mobile phase: acetonitrile (solvent A)/H₂O (solvent B) containing 0.1 % TFA; gradient: solvent A/B from 10/90 at 0 min to 90/10 at 10 min. flow rate: 1.5 mL/min. UV detector: λ_{max}=230 nm (red curve); radioactive detector (blue curve).

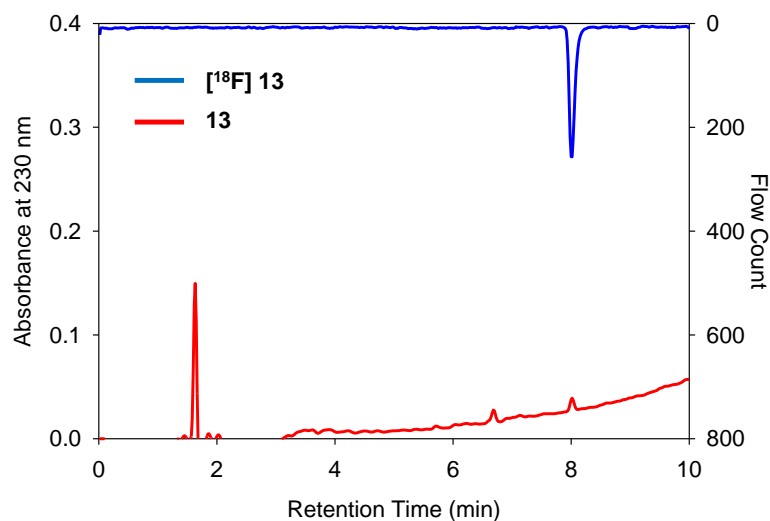


Figure S5.12. HPLC and flow count for compound 13/ [¹⁸F] 13. HPLC condition: Sunfire RP-18 analytical column: 4.6 × 250 mm, 5 μm; mobile phase: acetonitrile (solvent A)/H₂O (solvent B) containing 0.1 % TFA; gradient: solvent A/B from 10/90 at 0 min to 90/10 at 10 min. flow rate: 1.5 mL/min. UV detector: λ_{max}=230 nm (red curve); radioactive detector (blue curve).

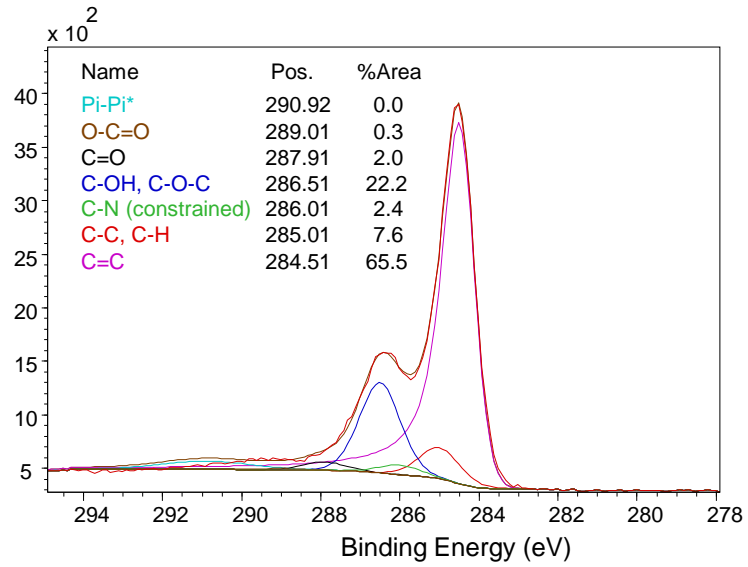


Figure S5.13. High resolution XPS C 1s spectrum of SWCNT-AuNP.

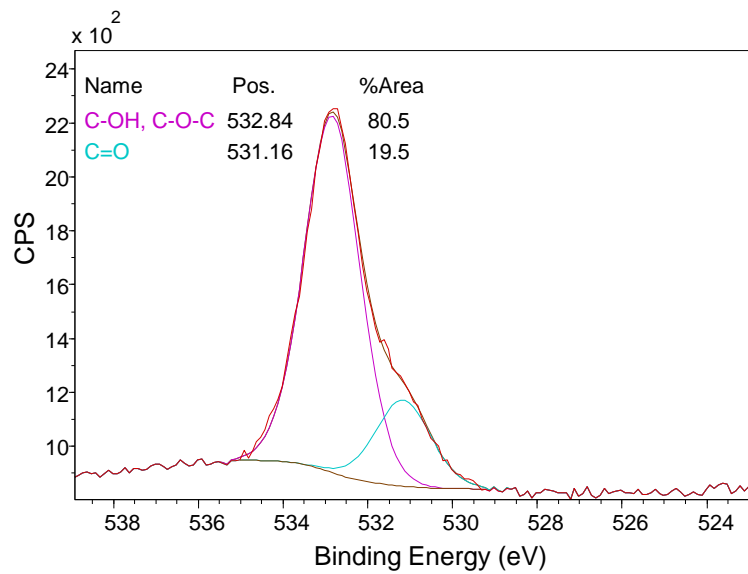


Figure S5.14. High resolution XPS O 1s spectrum of SWCNT-AuNP.

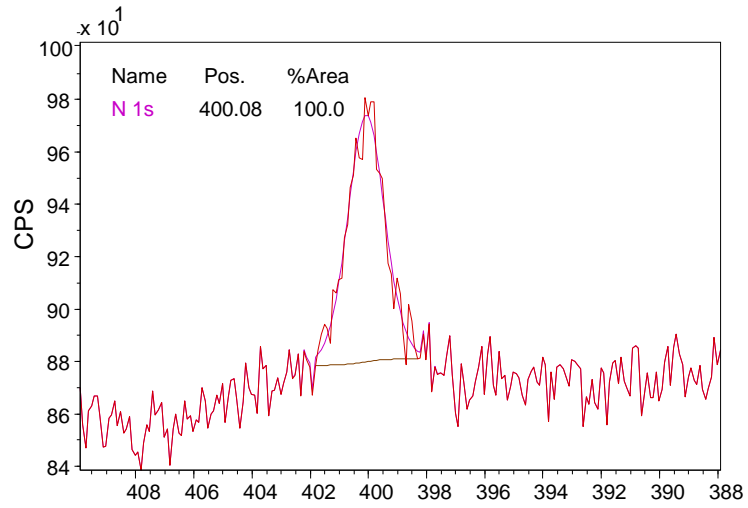


Figure S5.15. High resolution XPS N 1s spectrum of SWCNT-AuNP.

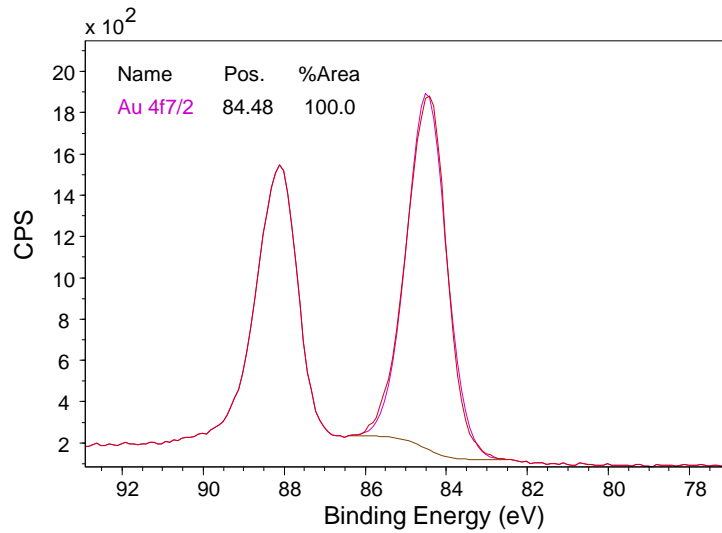


Figure S5.16. High resolution XPS Au 4f spectrum of SWCNT-AuNP.

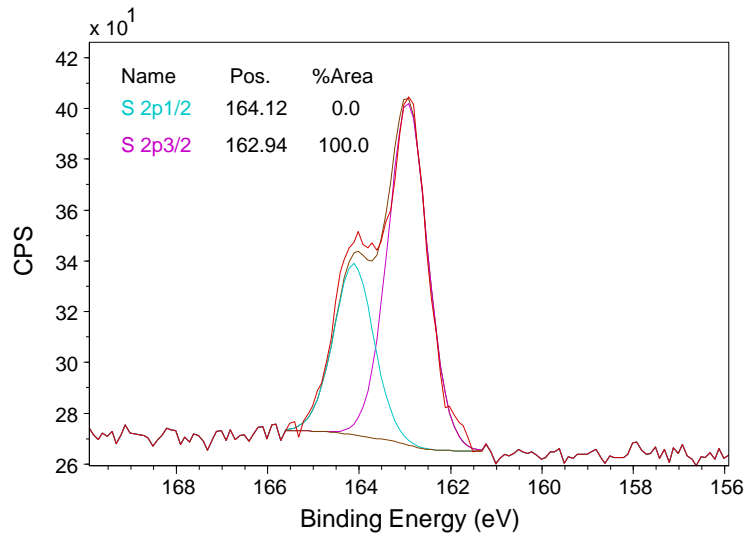


Figure S5.17. High resolution XPS S 1s spectrum of SWCNT-AuNP.

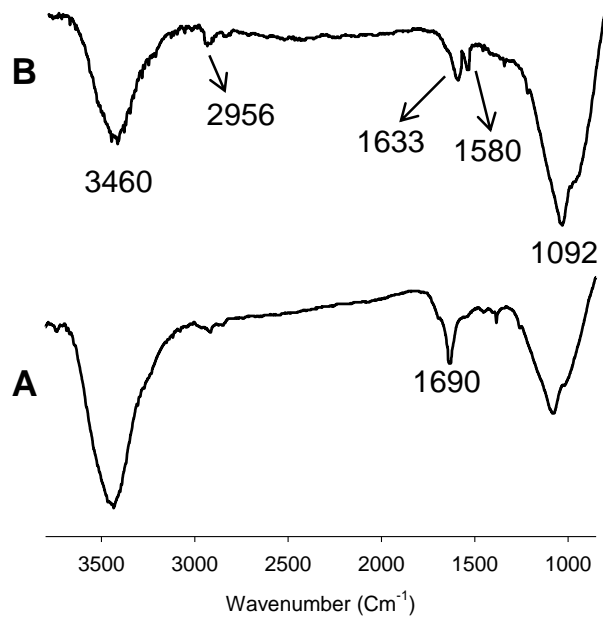


Figure S5.18. IR spectra of A) SWCNT starting material and B) SWCNT-BCN.

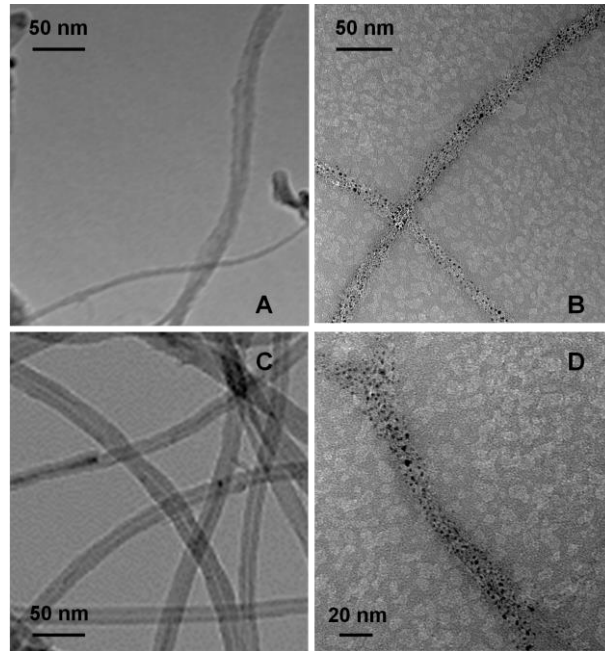


Figure S5.19. TEM images of A) SWCNT-BCN, B) SWCNT-AuNP hybrid, C) control experiment (SWCNT-BCN + Me-EG₃-AuNP), D) SWCNT-AuNP hybrid after 1 hour sonication

Chapter 6

Contributions of the Studies

Due to the ability that surface chemistry has in shaping the macroscopic world, surface modification techniques are being used in a variety of industries ranging from electronics to biomedical. To design target materials for a specific application with control over their chemical and physical properties, general surface modification methods need to be developed. Surface modification strategies can be classified into two main categories: physical and chemical approaches. The use of irreversible chemical bonds to modify the surface of metals, semiconductors, carbon, and other materials produces stable modifying layers and has been growing in popularity in recent years. Based on the existing surface properties of different substrates and nanomaterials, a variety of reactive functional groups can be designed to react with the starting substrates. With the exposed reactive terminal groups on the surface, further chemical reactions can be utilized to assemble different materials so that a novel target material can be constructed. The investigations presented in this dissertation have focused on how photochemically and thermally reactive moieties at the interface can be utilized to further modify the surface of various substrates including cotton, paper, gold nanoparticles (AuNPs) and carbon nanotubes (CNTs).

The initial focus of this research was on developing new photochemical strategies for material surface modification. It has been previously demonstrated by our group that

diazirines can be used as a tether to prepare a range of hybrid materials.¹⁻⁴ In chapter 2, we examined the feasibility of this photochemical approach to prepare hydrophobic surfaces. Inspired by nature, scientists have developed artificial hydrophobic surfaces by tailoring the surface topography of materials. These surfaces have found applications in a variety of settings, including micro fluidic or biomedical devices, and self-cleaning surfaces.⁵⁻⁸ Given that surface modification with low surface energy materials,⁹⁻¹² such as fluorine containing compounds would render them hydrophobic, highly fluorinated phosphonium slats (HFPS) were employed to prepare hydrophobic surfaces on cotton and paper substrates. 3-Aryl-3-(trifluoromethyl) diazirine functionalized HFPSs were synthesized, characterized and utilized as photoinduced carbene precursors for covalent attachment of the HFPS onto cotton/paper to impart hydrophobicity to these surfaces. We showed that irradiation of cotton and paper treated with the diazirine-HFPS leads to robust hydrophobic cotton and paper surfaces with anti-wetting properties. The contact angles of water were estimated to be 139° and 137° for cotton and paper, respectively. In contrast water placed on the untreated or the control samples (those treated with the diazirine-HFPS but not irradiated), was simply absorbed into the surface. Additionally the chemically grafted hydrophobic coating showed high durability towards wash cycles and sonication in organic solvents. Because of the mode of activation to covalently tether the hydrophobic coating, it is amenable to photo-patterning, which was demonstrated macroscopically. Due to the reactivity of carbene intermediate towards various functionalities, this methodology can be used to form robust hydrophobic coatings on a host of materials including glass, CNT, graphene, diamond, other fabrics to name a few.

Functionalization of AuNPs is a key challenge given the broad range of their applications in biology, nanomedicine, optics and catalysis.¹³⁻¹⁵ Because many of these applications are correlated with the nature of the protecting ligand attached to the gold core, developing techniques to prepare nanoparticles with specific functionalities, directly or by carrying out chemical reactions on the protecting shells, is necessary. Among the various approaches for the synthesis of AuNPs with the desired functionality, interfacial reactions of AuNPs have attracted much interest due to their effectiveness and simplicity. Another key factor affecting the utility of AuNPs is their solubility. Despite all their advantages, the solubility of the commonly used alkane thiolate modified AuNPs is limited to a narrow range of organic solvents. The lack of solubility in water or other polar solvents limits their application for modification to materials that are soluble or dispersible in the same solvent medium. Ethylene glycol thioalkylated AuNPs have shown great promise for the synthesis of robust water soluble AuNPs.¹⁶ We have developed a straightforward procedure for the synthesis of small (< 3 nm) water soluble AuNPs through thiol exchange reactions, using triethylene glycol monomethyl ether functionalized AuNPs as the building blocks. Such AuNPs have the added benefit of remaining soluble in a range of organic solvents as well. Furthermore, we demonstrated that having a moiety at the gold interface, which can be thermally or photochemically activated, could be exploited to further modify AuNPs through the subsequent interfacial reaction (chapter 3-5).

It has been previously shown that utilizing AuNPs as macromolecular-type reagents and carrying out organic reactions on the surface monolayer containing suitable terminal

groups is a promising strategy to introduce new functionality. However, the need to perform reactions on AuNPs under relatively mild and low temperature conditions limits the types of thermal reactions that can be performed efficiently and quantitatively in these systems. In that respect, incorporating photo-reactive groups onto the AuNP surface offers flexibility in design and synthesis of nanoparticles in a way that tailor-made materials with vastly different physical properties are accessible in rather a short time and under mild conditions. In chapter 3, dual water and organic solvent soluble 3-Aryl-3-(trifluoromethyl) diazirine functionalized AuNPs were prepared through a place exchange reaction from triethylene glycol monomethyl ether capped AuNPs. These nanoparticles were fully characterized using ^1H and ^{19}F NMR spectroscopy, TEM, TGA and XPS. Irradiation of the diazirine capped AuNPs results in nitrogen extrusion and the formation of a highly reactive carbene that can be utilized to tether the attached AuNPs via insertion into C=C or O-H functionality inherent on various substrates. We demonstrated that photolysis of the diazirine modified AuNPs in the presence of a variety of model carbene scavengers lead to clean and efficient insertion products while maintaining their solubility in polar solvents. We further studied the efficacy of this approach to prepare glyconanoparticles by irradiating the diazirine modified AuNPs in presence of carbohydrates (*e.g.* mannose). These results indicate that one can construct mannose capped AuNPs through photochemical reaction of diazirine, although with only moderate efficiency. This is expected for the photochemical reaction of diazirine in aqueous media, due to the unspecific reaction of the highly reactive carbene with surrounding solvent (*i. e.* water) molecules. However, we believe that this methodology can still be useful for

immobilization of AuNPs on biomolecules as well as other materials under mild conditions in wide range of solvents.

Even though diazirine proved to be a very useful tether for surface modification, because of the high reactivity of the carbene there is no control over the reaction once the carbene is generated upon irradiation of diazirine. In pursuit of alternate approaches that offer more selectivity, we examined the usefulness of “click-type” reactions for AuNP surface modification as they offer selectivity as well as high efficiency under mild reaction conditions.

The maleimide functional group has great potential because it is a small, symmetrical, stable and biocompatible molecule that can be easily functionalized thanks to its nucleophilic nitrogen forming the corresponding *N*-substituted derivatives. In addition, maleimide can undergo a plethora of “click-type” reactions: Michael addition, 1,3-dipolar cycloaddition, and Diels-Alder. These three reactions are desirable because they form stable reaction products under mild reaction conditions and are compatible with water media. Hence, incorporating maleimide group onto the surface of AuNPs will result in a reactive template that can be utilized in Michael addition, Diels Alder and 1,3-dipolar cycloaddition reactions. In chapter 4, we described our efforts towards the synthesis of water soluble maleimide modified AuNPs and their modification of through interfacial cycloaddition reactions. Maleimide terminated triethylene glycol thiolate monolayer-protected AuNPs with a core size of 2.5 ± 0.7 nm were prepared. As discussed in chapter four, maleimide is highly reactive towards nucleophiles and

especially thiols, therefore maleimide functionalized AuNPs cannot be prepared directly. Incorporation of the maleimide functional group onto the AuNP surface was achieved through a protection/deprotection procedure.¹⁷ They were then modified in high yields via 1,3-dipolar cycloaddition and Diels Alder reactions using a variety of nitrones and dienes respectively. The resulting cycloadduct modified AuNPs were characterized using ¹H NMR spectroscopy and were verified by comparison of the spectra to those obtained for the products of the model reactions with the same nitrones and dienes. TEM analysis showed that the reaction conditions did not affect the shape or size of the gold core, suggesting that this is an efficient methodology to modify small water soluble AuNPs under ambient pressure and temperature with high yields and a reasonable reaction time. Our results demonstrate the high potential of these nanoparticles as a platform for cycloaddition reactions with any substrate bearing a diene or nitrone functionality. Due to the AuNPs solubility in both water and a host of organic solvents, the application of these particles is not limited to a narrow range of solvents.

In continuation of our previous studies and in pursuit of efficient AuNP modification strategy that offers faster kinetics, we examined the utility of strain-promoted alkyne-nitrone cycloaddition (SPANC) reactions for such purposes. Strain-promoted cycloaddition reactions are powerful techniques due to their rapid kinetics, chemoselectivity and biocompatibility.¹⁸ Therefore, they can serve as an ideal strategy for surface modification of AuNPs in order to construct AuNP-conjugates for *in vivo* applications or for preparation of hybrid materials. In chapter 5, we prepared novel and versatile water- and organic solvent-soluble nitrone modified AuNPs. These

nanoparticles were then characterized using ^1H NMR and UV-vis spectroscopy, TEM, TGA, and XPS. To showcase their efficacy in biorthogonal SPANC reactions, their reactivity towards model compounds bearing bicyclononyne (BCN) moieties was studied. Quantitative conversion of Nitron-AuNPs to the cycloadduct products was observed in a matter of minutes. Considering that SPANC offers fast kinetics, it can serve as a suitable strategy in radiopharmaceuticals. In chapter five, we demonstrated for the first time that utilizing Interfacial SPANC (i-SPANC) as a novel and efficient conjugation method on AuNPs, ^{18}F radiolabeled AuNPs can be prepared for potential PET imaging applications. Given that nanoparticles allow multivalent attachment of various ligands, a major future application of the above approach is to use nanoparticle platforms for targeted molecular imaging.

The desirable characteristics of SPANC reactions not only make this reaction highly useful in biochemistry, but also provide invaluable opportunities in designing new materials through interfacial reactions. To present the usefulness of SPANC strategy to construct hybrid nanomaterials, we prepared cycloalkyne modified CNTs. It was demonstrated how CNT-AuNP hybrid material can be prepared by simply mixing the CNT and nitron AuNPs through the interfacial SPANC (i-SPANC) reaction.

Overall throughout this thesis, new thermal and photochemical reactions were described which can be utilized to efficiently and quantitatively modify surface of materials including: cotton, paper, AuNPs and CNTs under mild conditions. Photochemical reactions included carbene generation on the monolayer of AuNPs using

irradiation of diazirine precursors. Click-type reactions including Diels Alder, 1,3-dipolar cycloaddition and SPANC reactions were also employed to modify the surface of water soluble AuNPs as well as in preparation of CNT-AuNP hybrid nanomaterials.

References

- 1) Ismaili, H.; Lee, S.; Workentin, M. S. *Langmuir* **2010**, 26, 14958.
- 2) Ismaili, H.; Lagugne-Labarthe, F.; Workentin, M. S. *Chem. Mater.* **2011**, 23, 1519.
- 3) Ismaili, H.; Workentin, M. S. *Chem. Commun.* **2011**, 47, 7788.
- 4) Ismaili, H.; Geng, D.; Kantzas, T. T.; Sun, X.; Workentin, M. S. *Langmuir*, **2011**, 27, 13261.
- 5) Jain, P. K. *Angew. Chem. Int. Ed.* **2014**, 53, 1197.
- 6) Hutchings, G. J.; Brust, M.; Schmidbaur, H. *Chem. Soc. Rev.* **2008**, 37, 1759.
- 7) Corma, A.; Hermenegildo, G. *Chem. Soc. Rev.* **2008**, 37, 2096.
- 8) Tiwari, P.M.; Vig, K.; Dennis, V.A.; Singh, S.R. *Nanomaterials* **2011**, 1, 31.
- 9) Tadanaga, K.; Morinaga, J.; Matsuda, A.; Minami, T. *Chem. Mater.* **2000**, 12, 590.
- 10) Nakajima, A.; Hashimoto, K.; Watanabe, T. *Langmuir* **2000**, 16, 7044.
- 11) Youngblood, J. P.; McCarthy, T. J. *Macromolecules* **1999**, 32, 6800.
- 12) Tindale, J. J.; Ragogna, P. J. *Chem. Commun.* **2009**, 14, 1831

- 13) Hutchings, G. J.; Brust, M.; Schmidbaur, H. *Chem. Soc. Rev.* **2008**, 37, 1759.
- 14) Daniel, M. C.; Astruc, D. *Chem. Rev.* **2004**, 104, 293.
- 15) Stewart, M. E.; Anderton, C. R.; Thompson, L. B.; Maria, J.; Gray, S. K.; Rogers, J. A.; Nuzzo, R. G. *Chem. Rev.* **2008**, 108, 494.
- 16) Foos, E. E.; Snow, A. W.; Twigg, M. E.; Ancona, M. G. *Chem. Mater.* **2002**, 14, 2401.
- 17) Gobbo, P.; Workentin, M. S. *Langmuir* **2012**, 28, 12357.
- 18) McKay, C. S.; Moran, J.; Pezacki, J. P. *Chem. Commun.* **2010**, 46, 931.

Appendix-List of Permissions

ROYAL SOCIETY OF CHEMISTRY LICENSE TERMS AND CONDITIONS

Jun 11, 2015

This is a License Agreement between Sara Ghiassian ("You") and Royal Society of Chemistry ("Royal Society of Chemistry") provided by Copyright Clearance Center ("CCC"). The license consists of your order details, the terms and conditions provided by Royal Society of Chemistry, and the payment terms and conditions.

All payments must be made in full to CCC. For payment instructions, please see information listed at the bottom of this form.

License Number	3646251311137
License date	Jun 11, 2015
Licensed content publisher	Royal Society of Chemistry
Licensed content publication	Chemical Communications (Cambridge)
Licensed content title	Highly fluorinated phosphonium ionic liquids: novel media for the generation of superhydrophobic coatings
Licensed content author	Jocelyn J. Tindale,Paul J. Ragonna
Licensed content date	Mar 6, 2009
Issue number	14
Type of Use	Thesis/Dissertation
Requestor type	academic/educational
Portion	figures/tables/images
Number of figures/tables/images	3
Format	print and electronic
Distribution quantity	5
Will you be translating?	no
Order reference number	None
Title of the thesis/dissertation	Strategies for Photochemical and Thermal Modification of Materials
Expected completion date	Jul 2015
Estimated size	300
Total	0.00 USD

Terms and Conditions

This License Agreement is between {Requestor Name} ("You") and The Royal Society of Chemistry ("RSC") provided by the Copyright Clearance Center ("CCC"). The license consists of your order details, the terms and conditions provided by the Royal Society of Chemistry, and the payment terms and conditions.

RSC / TERMS AND CONDITIONS

INTRODUCTION

The publisher for this copyrighted material is The Royal Society of Chemistry. By clicking “accept” in connection with completing this licensing transaction, you agree that the following terms and conditions apply to this transaction (along with the Billing and Payment terms and conditions established by CCC, at the time that you opened your RightsLink account and that are available at any time at .

LICENSE GRANTED

The RSC hereby grants you a non-exclusive license to use the aforementioned material anywhere in the world subject to the terms and conditions indicated herein. Reproduction of the material is confined to the purpose and/or media for which permission is hereby given.

RESERVATION OF RIGHTS

The RSC reserves all rights not specifically granted in the combination of (i) the license details provided by your and accepted in the course of this licensing transaction; (ii) these terms and conditions; and (iii) CCC’s Billing and Payment terms and conditions.

REVOCAATION

The RSC reserves the right to revoke this license for any reason, including, but not limited to, advertising and promotional uses of RSC content, third party usage, and incorrect source figure attribution.

THIRD-PARTY MATERIAL DISCLAIMER

If part of the material to be used (for example, a figure) has appeared in the RSC publication with credit to another source, permission must also be sought from that source. If the other source is another RSC publication these details should be included in your RightsLink request. If the other source is a third party, permission must be obtained from the third party. The RSC disclaims any responsibility for the reproduction you make of items owned by a third party.

PAYMENT OF FEE

If the permission fee for the requested material is waived in this instance, please be advised that any future requests for the reproduction of RSC materials may attract a fee.

ACKNOWLEDGEMENT

The reproduction of the licensed material must be accompanied by the following acknowledgement:

Reproduced (“Adapted” or “in part”) from {Reference Citation} (or Ref XX) with permission of The Royal Society of Chemistry.

If the licensed material is being reproduced from New Journal of Chemistry (NJC), Photochemical & Photobiological Sciences (PPS) or Physical Chemistry Chemical Physics (PCCP) you must include one of the following acknowledgements:

For figures originally published in NJC:

Reproduced (“Adapted” or “in part”) from {Reference Citation} (or Ref XX) with permission of The Royal Society of Chemistry (RSC) on behalf of the European Society for Photobiology, the European Photochemistry Association and the RSC.

For figures originally published in PPS:

Reproduced (“Adapted” or “in part”) from {Reference Citation} (or Ref XX) with permission of The Royal Society of Chemistry (RSC) on behalf of the Centre National de la Recherche Scientifique (CNRS) and the RSC.

For figures originally published in PCCP:

Reproduced (“Adapted” or “in part”) from {Reference Citation} (or Ref XX) with permission of the PCCP Owner Societies.

HYPERTEXT LINKS

With any material which is being reproduced in electronic form, you must include a hypertext link to the original RSC article on the RSC’s website. The recommended form for the hyperlink is <http://dx.doi.org/10.1039/DOI> suffix, for example in the link <http://dx.doi.org/10.1039/b110420a> the DOI suffix is ‘b110420a’. To find the relevant DOI suffix for the RSC article in question, go to the Journals section of the website and locate the article in the list of papers for the volume and issue of your specific journal. You will find the DOI suffix quoted there.

LICENSE CONTINGENT ON PAYMENT

While you may exercise the rights licensed immediately upon issuance of the license at the end of the licensing process for the transaction, provided that you have disclosed complete and accurate details of your proposed use, no license is finally effective unless and until full payment is received from you (by CCC) as provided in CCC’s Billing and Payment terms and conditions. If full payment is not received on a timely basis, then any license preliminarily granted shall be deemed automatically revoked and shall be void as if never granted. Further, in the event that you breach any of these terms and conditions or any of CCC’s Billing and Payment terms and conditions, the license is automatically revoked and shall be void as if never granted. Use of materials as described in a revoked license, as well as any use of the materials beyond the scope of an unrevoked license, may constitute copyright infringement and the RSC reserves the right to take any and all action to protect its copyright in the materials.

WARRANTIES

The RSC makes no representations or warranties with respect to the licensed material.

INDEMNITY

You hereby indemnify and agree to hold harmless the RSC and the CCC, and their respective officers, directors, trustees, employees and agents, from and against any and all claims arising out of your use of the licensed material other than as specifically authorized pursuant to this licence.

NO TRANSFER OF LICENSE

This license is personal to you or your publisher and may not be sublicensed, assigned, or transferred by you to any other person without the RSC’s written permission.

NO AMENDMENT EXCEPT IN WRITING

This license may not be amended except in a writing signed by both parties (or, in the case of “Other Conditions, v1.2”, by CCC on the RSC’s behalf).

OBJECTION TO CONTRARY TERMS

You hereby acknowledge and agree that these terms and conditions, together with CCC’s

Billing and Payment terms and conditions (which are incorporated herein), comprise the entire agreement between you and the RSC (and CCC) concerning this licensing transaction, to the exclusion of all other terms and conditions, written or verbal, express or implied (including any terms contained in any purchase order, acknowledgment, check endorsement or other writing prepared by you). In the event of any conflict between your obligations established by these terms and conditions and those established by CCC's Billing and Payment terms and conditions, these terms and conditions shall control.

JURISDICTION

This license transaction shall be governed by and construed in accordance with the laws of the District of Columbia. You hereby agree to submit to the jurisdiction of the courts located in the District of Columbia for purposes of resolving any disputes that may arise in connection with this licensing transaction.

LIMITED LICENSE

The following terms and conditions apply to specific license types:

Translation

This permission is granted for non-exclusive world English rights only unless your license was granted for translation rights. If you licensed translation rights you may only translate this content into the languages you requested. A professional translator must perform all translations and reproduce the content word for word preserving the integrity of the article.

Intranet

If the licensed material is being posted on an Intranet, the Intranet is to be password-protected and made available only to bona fide students or employees only. All content posted to the Intranet must maintain the copyright information line on the bottom of each image. You must also fully reference the material and include a hypertext link as specified above.

Copies of Whole Articles

All copies of whole articles must maintain, if available, the copyright information line on the bottom of each page.

Other Conditions

v1.2

Gratis licenses (referencing \$0 in the Total field) are free. Please retain this printable license for your reference. No payment is required.

If you would like to pay for this license now, please remit this license along with your payment made payable to "COPYRIGHT CLEARANCE CENTER" otherwise you will be invoiced within 48 hours of the license date. Payment should be in the form of a check or money order referencing your account number and this invoice number {Invoice Number}.

Once you receive your invoice for this order, you may pay your invoice by credit card.

Please follow instructions provided at that time.

Make Payment To:
Copyright Clearance Center
Dept 001

P.O. Box 843006
Boston, MA 02284-3006

For suggestions or comments regarding this order, contact Rightslink Customer Support:
customercare@copyright.com or +1-855-239-3415 (toll free in the US) or +1-978-646-2777.

Questions? customercare@copyright.com or +1-855-239-3415 (toll free in the US) or +1-978-646-2777.

**ROYAL SOCIETY OF CHEMISTRY LICENSE
TERMS AND CONDITIONS**

Jun 11, 2015

This is a License Agreement between Sara Ghiassian ("You") and Royal Society of Chemistry ("Royal Society of Chemistry") provided by Copyright Clearance Center ("CCC"). The license consists of your order details, the terms and conditions provided by Royal Society of Chemistry, and the payment terms and conditions.

All payments must be made in full to CCC. For payment instructions, please see information listed at the bottom of this form.

License Number	3646260071977
License date	Jun 11, 2015
Licensed content publisher	Royal Society of Chemistry
Licensed content publication	Chemical Communications (Cambridge)
Licensed content title	Covalent diamond-gold nanoscale hybrids via photochemically generated carbenes
Licensed content author	Hossein Ismaili, Mark S. Workentin
Licensed content date	Jun 3, 2011
Volume number	47
Issue number	27
Type of Use	Thesis/Dissertation
Requestor type	academic/educational
Portion	figures/tables/images
Number of figures/tables/images	3
Format	print and electronic
Distribution quantity	5
Will you be translating?	no
Order reference number	None
Title of the thesis/dissertation	Strategies for Photochemical and Thermal Modification of Materials
Expected completion date	Jul 2015
Estimated size	300
Total	0.00 USD

Terms and Conditions

This License Agreement is between {Requestor Name} ("You") and The Royal Society of Chemistry ("RSC") provided by the Copyright Clearance Center ("CCC"). The license consists of your order details, the terms and conditions provided by the Royal Society of Chemistry, and the payment terms and conditions.

RSC / TERMS AND CONDITIONS

INTRODUCTION

The publisher for this copyrighted material is The Royal Society of Chemistry. By clicking “accept” in connection with completing this licensing transaction, you agree that the following terms and conditions apply to this transaction (along with the Billing and Payment terms and conditions established by CCC, at the time that you opened your RightsLink account and that are available at any time at .

LICENSE GRANTED

The RSC hereby grants you a non-exclusive license to use the aforementioned material anywhere in the world subject to the terms and conditions indicated herein. Reproduction of the material is confined to the purpose and/or media for which permission is hereby given.

RESERVATION OF RIGHTS

The RSC reserves all rights not specifically granted in the combination of (i) the license details provided by your and accepted in the course of this licensing transaction; (ii) these terms and conditions; and (iii) CCC’s Billing and Payment terms and conditions.

REVOCAION

The RSC reserves the right to revoke this license for any reason, including, but not limited to, advertising and promotional uses of RSC content, third party usage, and incorrect source figure attribution.

THIRD-PARTY MATERIAL DISCLAIMER

If part of the material to be used (for example, a figure) has appeared in the RSC publication with credit to another source, permission must also be sought from that source. If the other source is another RSC publication these details should be included in your RightsLink request. If the other source is a third party, permission must be obtained from the third party. The RSC disclaims any responsibility for the reproduction you make of items owned by a third party.

PAYMENT OF FEE

If the permission fee for the requested material is waived in this instance, please be advised that any future requests for the reproduction of RSC materials may attract a fee.

ACKNOWLEDGEMENT

The reproduction of the licensed material must be accompanied by the following acknowledgement:

Reproduced (“Adapted” or “in part”) from {Reference Citation} (or Ref XX) with permission of The Royal Society of Chemistry.

If the licensed material is being reproduced from New Journal of Chemistry (NJC), Photochemical & Photobiological Sciences (PPS) or Physical Chemistry Chemical Physics (PCCP) you must include one of the following acknowledgements:

For figures originally published in NJC:

Reproduced (“Adapted” or “in part”) from {Reference Citation} (or Ref XX) with permission of The Royal Society of Chemistry (RSC) on behalf of the European Society for Photobiology, the European Photochemistry Association and the RSC.

For figures originally published in PPS:

Reproduced (“Adapted” or “in part”) from {Reference Citation} (or Ref XX) with permission of The Royal Society of Chemistry (RSC) on behalf of the Centre National de la Recherche Scientifique (CNRS) and the RSC.

For figures originally published in PCCP:

Reproduced (“Adapted” or “in part”) from {Reference Citation} (or Ref XX) with permission of the PCCP Owner Societies.

HYPERTEXT LINKS

With any material which is being reproduced in electronic form, you must include a hypertext link to the original RSC article on the RSC’s website. The recommended form for the hyperlink is <http://dx.doi.org/10.1039/DOI suffix>, for example in the link <http://dx.doi.org/10.1039/b110420a> the DOI suffix is ‘b110420a’. To find the relevant DOI suffix for the RSC article in question, go to the Journals section of the website and locate the article in the list of papers for the volume and issue of your specific journal. You will find the DOI suffix quoted there.

LICENSE CONTINGENT ON PAYMENT

While you may exercise the rights licensed immediately upon issuance of the license at the end of the licensing process for the transaction, provided that you have disclosed complete and accurate details of your proposed use, no license is finally effective unless and until full payment is received from you (by CCC) as provided in CCC’s Billing and Payment terms and conditions. If full payment is not received on a timely basis, then any license preliminarily granted shall be deemed automatically revoked and shall be void as if never granted. Further, in the event that you breach any of these terms and conditions or any of CCC’s Billing and Payment terms and conditions, the license is automatically revoked and shall be void as if never granted. Use of materials as described in a revoked license, as well as any use of the materials beyond the scope of an unrevoked license, may constitute copyright infringement and the RSC reserves the right to take any and all action to protect its copyright in the materials.

WARRANTIES

The RSC makes no representations or warranties with respect to the licensed material.

INDEMNITY

You hereby indemnify and agree to hold harmless the RSC and the CCC, and their respective officers, directors, trustees, employees and agents, from and against any and all claims arising out of your use of the licensed material other than as specifically authorized pursuant to this licence.

NO TRANSFER OF LICENSE

This license is personal to you or your publisher and may not be sublicensed, assigned, or transferred by you to any other person without the RSC’s written permission.

NO AMENDMENT EXCEPT IN WRITING

This license may not be amended except in a writing signed by both parties (or, in the case of “Other Conditions, v1.2”, by CCC on the RSC’s behalf).

OBJECTION TO CONTRARY TERMS

You hereby acknowledge and agree that these terms and conditions, together with CCC's Billing and Payment terms and conditions (which are incorporated herein), comprise the entire agreement between you and the RSC (and CCC) concerning this licensing transaction, to the exclusion of all other terms and conditions, written or verbal, express or implied (including any terms contained in any purchase order, acknowledgment, check endorsement or other writing prepared by you). In the event of any conflict between your obligations established by these terms and conditions and those established by CCC's Billing and Payment terms and conditions, these terms and conditions shall control.

JURISDICTION

This license transaction shall be governed by and construed in accordance with the laws of the District of Columbia. You hereby agree to submit to the jurisdiction of the courts located in the District of Columbia for purposes of resolving any disputes that may arise in connection with this licensing transaction.

LIMITED LICENSE

The following terms and conditions apply to specific license types:

Translation

This permission is granted for non-exclusive world English rights only unless your license was granted for translation rights. If you licensed translation rights you may only translate this content into the languages you requested. A professional translator must perform all translations and reproduce the content word for word preserving the integrity of the article.

Intranet

If the licensed material is being posted on an Intranet, the Intranet is to be password-protected and made available only to bona fide students or employees only. All content posted to the Intranet must maintain the copyright information line on the bottom of each image. You must also fully reference the material and include a hypertext link as specified above.

Copies of Whole Articles

All copies of whole articles must maintain, if available, the copyright information line on the bottom of each page.

Other Conditions

v1.2

Gratis licenses (referencing \$0 in the Total field) are free. Please retain this printable license for your reference. No payment is required.

If you would like to pay for this license now, please remit this license along with your payment made payable to "COPYRIGHT CLEARANCE CENTER" otherwise you will be invoiced within 48 hours of the license date. Payment should be in the form of a check or money order referencing your account number and this invoice number {Invoice Number}.

Once you receive your invoice for this order, you may pay your invoice by credit card.

Please follow instructions provided at that time.

Make Payment To:
Copyright Clearance Center

Dept 001
P.O. Box 843006
Boston, MA 02284-3006

For suggestions or comments regarding this order, contact Rightslink Customer Support:
customer@copyright.com or +1-855-239-3415 (toll free in the US) or +1-978-646-2777.

Questions? customer@copyright.com or +1-855-239-3415 (toll free in the US) or +1-978-646-2777.



RightsLink®

Home

Account Info

Help



ACS Publications
Most Trusted. Most Cited. Most Read.

Title: Covalently Assembled Gold Nanoparticle-Carbon Nanotube Hybrids via a Photoinitiated Carbene Addition Reaction

Author: Hossein Ismaili, François Lagugné-Labarthet, Mark S. Workentin

Publication: Chemistry of Materials

Publisher: American Chemical Society

Date: Mar 1, 2011

Copyright © 2011, American Chemical Society

Logged in as:

Sara Ghiassian

Account #:

3000927211

LOGOUT

PERMISSION/LICENSE IS GRANTED FOR YOUR ORDER AT NO CHARGE

This type of permission/license, instead of the standard Terms & Conditions, is sent to you because no fee is being charged for your order. Please note the following:

- Permission is granted for your request in both print and electronic formats, and translations.
- If figures and/or tables were requested, they may be adapted or used in part.
- Please print this page for your records and send a copy of it to your publisher/graduate school.
- Appropriate credit for the requested material should be given as follows: "Reprinted (adapted) with permission from (COMPLETE REFERENCE CITATION). Copyright (YEAR) American Chemical Society." Insert appropriate information in place of the capitalized words.
- One-time permission is granted only for the use specified in your request. No additional uses are granted (such as derivative works or other editions). For any other uses, please submit a new request.

If credit is given to another source for the material you requested, permission must be obtained from that source.

BACK

CLOSE WINDOW

Copyright © 2015 Copyright Clearance Center, Inc. All Rights Reserved. [Privacy statement](#). [Terms and Conditions](#). Comments? We would like to hear from you. E-mail us at customercare@copyright.com



RightsLink®

Home

Account Info

Help



ACS Publications
Most Trusted. Most Cited. Most Read.

Title: Light-Activated Covalent Formation of Gold Nanoparticle–Graphene and Gold Nanoparticle–Glass Composites

Author: Hossein Ismaili, Dongsheng Geng, Andy Xueliang Sun, et al

Publication: Langmuir

Publisher: American Chemical Society

Date: Nov 1, 2011

Copyright © 2011, American Chemical Society

Logged in as:

Sara Ghiassian

Account #:

3000927211

LOGOUT

PERMISSION/LICENSE IS GRANTED FOR YOUR ORDER AT NO CHARGE

This type of permission/license, instead of the standard Terms & Conditions, is sent to you because no fee is being charged for your order. Please note the following:

- Permission is granted for your request in both print and electronic formats, and translations.
- If figures and/or tables were requested, they may be adapted or used in part.
- Please print this page for your records and send a copy of it to your publisher/graduate school.
- Appropriate credit for the requested material should be given as follows: "Reprinted (adapted) with permission from (COMPLETE REFERENCE CITATION). Copyright (YEAR) American Chemical Society." Insert appropriate information in place of the capitalized words.
- One-time permission is granted only for the use specified in your request. No additional uses are granted (such as derivative works or other editions). For any other uses, please submit a new request.

If credit is given to another source for the material you requested, permission must be obtained from that source.

BACK

CLOSE WINDOW

Copyright © 2015 [Copyright Clearance Center, Inc.](#) All Rights Reserved. [Privacy statement.](#) [Terms and Conditions.](#) Comments? We would like to hear from you. E-mail us at customer@copyright.com



RightsLink®

Home

Account Info

Help



ACS Publications
Most Trusted. Most Cited. Most Read.

Title: A Photochemical Method for Patterning the Immobilization of Ligands and Cells to Self-Assembled Monolayers

Author: W. Shannon Dillmore, Muhammad N. Yousaf, Milan Mrksich

Publication: Langmuir

Publisher: American Chemical Society

Date: Aug 1, 2004

Copyright © 2004, American Chemical Society

Logged in as:
Sara Ghiassian
Account #:
3000927211

LOGOUT

PERMISSION/LICENSE IS GRANTED FOR YOUR ORDER AT NO CHARGE

This type of permission/license, instead of the standard Terms & Conditions, is sent to you because no fee is being charged for your order. Please note the following:

- Permission is granted for your request in both print and electronic formats, and translations.
- If figures and/or tables were requested, they may be adapted or used in part.
- Please print this page for your records and send a copy of it to your publisher/graduate school.
- Appropriate credit for the requested material should be given as follows: "Reprinted (adapted) with permission from (COMPLETE REFERENCE CITATION). Copyright (YEAR) American Chemical Society." Insert appropriate information in place of the capitalized words.
- One-time permission is granted only for the use specified in your request. No additional uses are granted (such as derivative works or other editions). For any other uses, please submit a new request.

If credit is given to another source for the material you requested, permission must be obtained from that source.

BACK

CLOSE WINDOW

Copyright © 2015 Copyright Clearance Center, Inc. All Rights Reserved. [Privacy statement](#). [Terms and Conditions](#). Comments? We would like to hear from you. E-mail us at customercare@copyright.com



RightsLink®

Home

Account Info

Help



ACS Publications
Most Trusted. Most Cited. Most Read.

Title: 1,3-Dipolar Cycloaddition in Polymer Synthesis. 1. Polyadducts with Flexible Spacers Derived from Bis(N-methylnitron)s and Bis(N-phenylmaleimide)s

Author: Lyudmyla Vretik, Helmut Ritter

Publication: Macromolecules

Publisher: American Chemical Society

Date: Aug 1, 2003

Copyright © 2003, American Chemical Society

Logged in as:

Sara Ghiassian

Account #:

3000927211

LOGOUT

PERMISSION/LICENSE IS GRANTED FOR YOUR ORDER AT NO CHARGE

This type of permission/license, instead of the standard Terms & Conditions, is sent to you because no fee is being charged for your order. Please note the following:

- Permission is granted for your request in both print and electronic formats, and translations.
- If figures and/or tables were requested, they may be adapted or used in part.
- Please print this page for your records and send a copy of it to your publisher/graduate school.
- Appropriate credit for the requested material should be given as follows: "Reprinted (adapted) with permission from (COMPLETE REFERENCE CITATION). Copyright (YEAR) American Chemical Society." Insert appropriate information in place of the capitalized words.
- One-time permission is granted only for the use specified in your request. No additional uses are granted (such as derivative works or other editions). For any other uses, please submit a new request.

If credit is given to another source for the material you requested, permission must be obtained from that source.

BACK

CLOSE WINDOW

Copyright © 2015 Copyright Clearance Center, Inc. All Rights Reserved. [Privacy statement](#). [Terms and Conditions](#). Comments? We would like to hear from you. E-mail us at customercare@copyright.com

**JOHN WILEY AND SONS LICENSE
TERMS AND CONDITIONS**

Jun 11, 2015

This Agreement between Sara Ghiassian ("You") and John Wiley and Sons ("John Wiley and Sons") consists of your license details and the terms and conditions provided by John Wiley and Sons and Copyright Clearance Center.

License Number	3646261330533
License date	Jun 11, 2015
Licensed Content Publisher	John Wiley and Sons
Licensed Content Publication	Angewandte Chemie International Edition
Licensed Content Title	Gold in a Metallic Divided State—From Faraday to Present-Day Nanoscience
Licensed Content Author	Peter P. Edwards, John Meurig Thomas
Licensed Content Date	Jun 11, 2007
Pages	7
Type of use	Dissertation/Thesis
Requestor type	University/Academic
Format	Print and electronic
Portion	Figure/table
Number of figures/tables	3
Original Wiley figure/table number(s)	Fig 7
Will you be translating?	No
Title of your thesis / dissertation	Strategies for Photochemical and Thermal Modification of Materials
Expected completion date	Jul 2015
Expected size (number of pages)	300
Requestor Location	Sara Ghiassian 1116 Richamond St London, ON N6A 5B7 Canada Attn: Sara Ghiassian
Billing Type	Invoice
Billing Address	Sara Ghiassian 1116 Richamond St London, ON N6A 5B7

Canada
Attn: Sara Ghiassian

Total

0.00 USD

[Terms and Conditions](#)

TERMS AND CONDITIONS

This copyrighted material is owned by or exclusively licensed to John Wiley & Sons, Inc. or one of its group companies (each a "Wiley Company") or handled on behalf of a society with which a Wiley Company has exclusive publishing rights in relation to a particular work (collectively "WILEY"). By clicking accept in connection with completing this licensing transaction, you agree that the following terms and conditions apply to this transaction (along with the billing and payment terms and conditions established by the Copyright Clearance Center Inc., ("CCC's Billing and Payment terms and conditions"), at the time that you opened your Rightslink account (these are available at any time at <http://myaccount.copyright.com>).

Terms and Conditions

- The materials you have requested permission to reproduce or reuse (the "Wiley Materials") are protected by copyright.
- You are hereby granted a personal, non-exclusive, non-sub licensable (on a stand-alone basis), non-transferable, worldwide, limited license to reproduce the Wiley Materials for the purpose specified in the licensing process. This license is for a one-time use only and limited to any maximum distribution number specified in the license. The first instance of republication or reuse granted by this licence must be completed within two years of the date of the grant of this licence (although copies prepared before the end date may be distributed thereafter). The Wiley Materials shall not be used in any other manner or for any other purpose, beyond what is granted in the license. Permission is granted subject to an appropriate acknowledgement given to the author, title of the material/book/journal and the publisher. You shall also duplicate the copyright notice that appears in the Wiley publication in your use of the Wiley Material. Permission is also granted on the understanding that nowhere in the text is a previously published source acknowledged for all or part of this Wiley Material. Any third party content is expressly excluded from this permission.
- With respect to the Wiley Materials, all rights are reserved. Except as expressly granted by the terms of the license, no part of the Wiley Materials may be copied, modified, adapted (except for minor reformatting required by the new Publication), translated, reproduced, transferred or distributed, in any form or by any means, and no derivative works may be made based on the Wiley Materials without the prior permission of the respective copyright owner. You may not alter, remove or suppress in any manner any copyright, trademark or other notices displayed by the Wiley Materials. You may not license, rent, sell, loan, lease, pledge, offer as security, transfer or assign the Wiley Materials on a stand-alone basis, or any of the rights granted to you hereunder to any other person.
- The Wiley Materials and all of the intellectual property rights therein shall at all times remain the exclusive property of John Wiley & Sons Inc, the Wiley Companies, or

their respective licensors, and your interest therein is only that of having possession of and the right to reproduce the Wiley Materials pursuant to Section 2 herein during the continuance of this Agreement. You agree that you own no right, title or interest in or to the Wiley Materials or any of the intellectual property rights therein. You shall have no rights hereunder other than the license as provided for above in Section 2. No right, license or interest to any trademark, trade name, service mark or other branding ("Marks") of WILEY or its licensors is granted hereunder, and you agree that you shall not assert any such right, license or interest with respect thereto.

- NEITHER WILEY NOR ITS LICENSORS MAKES ANY WARRANTY OR REPRESENTATION OF ANY KIND TO YOU OR ANY THIRD PARTY, EXPRESS, IMPLIED OR STATUTORY, WITH RESPECT TO THE MATERIALS OR THE ACCURACY OF ANY INFORMATION CONTAINED IN THE MATERIALS, INCLUDING, WITHOUT LIMITATION, ANY IMPLIED WARRANTY OF MERCHANTABILITY, ACCURACY, SATISFACTORY QUALITY, FITNESS FOR A PARTICULAR PURPOSE, USABILITY, INTEGRATION OR NON-INFRINGEMENT AND ALL SUCH WARRANTIES ARE HEREBY EXCLUDED BY WILEY AND ITS LICENSORS AND WAIVED BY YOU
- WILEY shall have the right to terminate this Agreement immediately upon breach of this Agreement by you.
- You shall indemnify, defend and hold harmless WILEY, its Licensors and their respective directors, officers, agents and employees, from and against any actual or threatened claims, demands, causes of action or proceedings arising from any breach of this Agreement by you.
- IN NO EVENT SHALL WILEY OR ITS LICENSORS BE LIABLE TO YOU OR ANY OTHER PARTY OR ANY OTHER PERSON OR ENTITY FOR ANY SPECIAL, CONSEQUENTIAL, INCIDENTAL, INDIRECT, EXEMPLARY OR PUNITIVE DAMAGES, HOWEVER CAUSED, ARISING OUT OF OR IN CONNECTION WITH THE DOWNLOADING, PROVISIONING, VIEWING OR USE OF THE MATERIALS REGARDLESS OF THE FORM OF ACTION, WHETHER FOR BREACH OF CONTRACT, BREACH OF WARRANTY, TORT, NEGLIGENCE, INFRINGEMENT OR OTHERWISE (INCLUDING, WITHOUT LIMITATION, DAMAGES BASED ON LOSS OF PROFITS, DATA, FILES, USE, BUSINESS OPPORTUNITY OR CLAIMS OF THIRD PARTIES), AND WHETHER OR NOT THE PARTY HAS BEEN ADVISED OF THE POSSIBILITY OF SUCH DAMAGES. THIS LIMITATION SHALL APPLY NOTWITHSTANDING ANY FAILURE OF ESSENTIAL PURPOSE OF ANY LIMITED REMEDY PROVIDED HEREIN.
- Should any provision of this Agreement be held by a court of competent jurisdiction to be illegal, invalid, or unenforceable, that provision shall be deemed amended to achieve as nearly as possible the same economic effect as the original provision, and the legality, validity and enforceability of the remaining provisions of this Agreement shall not be affected or impaired thereby.
- The failure of either party to enforce any term or condition of this Agreement shall not constitute a waiver of either party's right to enforce each and every term and condition

of this Agreement. No breach under this agreement shall be deemed waived or excused by either party unless such waiver or consent is in writing signed by the party granting such waiver or consent. The waiver by or consent of a party to a breach of any provision of this Agreement shall not operate or be construed as a waiver of or consent to any other or subsequent breach by such other party.

- This Agreement may not be assigned (including by operation of law or otherwise) by you without WILEY's prior written consent.
- Any fee required for this permission shall be non-refundable after thirty (30) days from receipt by the CCC.
- These terms and conditions together with CCC's Billing and Payment terms and conditions (which are incorporated herein) form the entire agreement between you and WILEY concerning this licensing transaction and (in the absence of fraud) supersedes all prior agreements and representations of the parties, oral or written. This Agreement may not be amended except in writing signed by both parties. This Agreement shall be binding upon and inure to the benefit of the parties' successors, legal representatives, and authorized assigns.
- In the event of any conflict between your obligations established by these terms and conditions and those established by CCC's Billing and Payment terms and conditions, these terms and conditions shall prevail.
- WILEY expressly reserves all rights not specifically granted in the combination of (i) the license details provided by you and accepted in the course of this licensing transaction, (ii) these terms and conditions and (iii) CCC's Billing and Payment terms and conditions.
- This Agreement will be void if the Type of Use, Format, Circulation, or Requestor Type was misrepresented during the licensing process.
- This Agreement shall be governed by and construed in accordance with the laws of the State of New York, USA, without regards to such state's conflict of law rules. Any legal action, suit or proceeding arising out of or relating to these Terms and Conditions or the breach thereof shall be instituted in a court of competent jurisdiction in New York County in the State of New York in the United States of America and each party hereby consents and submits to the personal jurisdiction of such court, waives any objection to venue in such court and consents to service of process by registered or certified mail, return receipt requested, at the last known address of such party.

WILEY OPEN ACCESS TERMS AND CONDITIONS

Wiley Publishes Open Access Articles in fully Open Access Journals and in Subscription journals offering Online Open. Although most of the fully Open Access journals publish open access articles under the terms of the Creative Commons Attribution (CC BY) License only, the subscription journals and a few of the Open Access Journals offer a choice of Creative Commons Licenses: Creative Commons Attribution (CC-BY) license [Creative](#)

[Commons Attribution Non-Commercial \(CC-BY-NC\) license](#) and [Creative Commons Attribution Non-Commercial-NoDerivs \(CC-BY-NC-ND\) License](#). The license type is clearly identified on the article.

Copyright in any research article in a journal published as Open Access under a Creative Commons License is retained by the author(s). Authors grant Wiley a license to publish the article and identify itself as the original publisher. Authors also grant any third party the right to use the article freely as long as its integrity is maintained and its original authors, citation details and publisher are identified as follows: [Title of Article/Author/Journal Title and Volume/Issue. Copyright (c) [year] [copyright owner as specified in the Journal]. Links to the final article on Wiley's website are encouraged where applicable.

The Creative Commons Attribution License

The [Creative Commons Attribution License \(CC-BY\)](#) allows users to copy, distribute and transmit an article, adapt the article and make commercial use of the article. The CC-BY license permits commercial and non-commercial re-use of an open access article, as long as the author is properly attributed.

The Creative Commons Attribution License does not affect the moral rights of authors, including without limitation the right not to have their work subjected to derogatory treatment. It also does not affect any other rights held by authors or third parties in the article, including without limitation the rights of privacy and publicity. Use of the article must not assert or imply, whether implicitly or explicitly, any connection with, endorsement or sponsorship of such use by the author, publisher or any other party associated with the article.

For any reuse or distribution, users must include the copyright notice and make clear to others that the article is made available under a Creative Commons Attribution license, linking to the relevant Creative Commons web page.

To the fullest extent permitted by applicable law, the article is made available as is and without representation or warranties of any kind whether express, implied, statutory or otherwise and including, without limitation, warranties of title, merchantability, fitness for a particular purpose, non-infringement, absence of defects, accuracy, or the presence or absence of errors.

Creative Commons Attribution Non-Commercial License

The [Creative Commons Attribution Non-Commercial \(CC-BY-NC\) License](#) permits use, distribution and reproduction in any medium, provided the original work is properly cited and is not used for commercial purposes.(see below)

Creative Commons Attribution-Non-Commercial-NoDerivs License

The [Creative Commons Attribution Non-Commercial-NoDerivs License \(CC-BY-NC-ND\)](#) permits use, distribution and reproduction in any medium, provided the original work is properly cited, is not used for commercial purposes and no modifications or adaptations are made. (see below)

Use by non-commercial users

For non-commercial and non-promotional purposes, individual users may access, download, copy, display and redistribute to colleagues Wiley Open Access articles, as well as adapt, translate, text- and data-mine the content subject to the following conditions:

- The authors' moral rights are not compromised. These rights include the right of "paternity" (also known as "attribution" - the right for the author to be identified as such) and "integrity" (the right for the author not to have the work altered in such a way that the author's reputation or integrity may be impugned).
- Where content in the article is identified as belonging to a third party, it is the obligation of the user to ensure that any reuse complies with the copyright policies of the owner of that content.
- If article content is copied, downloaded or otherwise reused for non-commercial research and education purposes, a link to the appropriate bibliographic citation (authors, journal, article title, volume, issue, page numbers, DOI and the link to the definitive published version on **Wiley Online Library**) should be maintained. Copyright notices and disclaimers must not be deleted.
- Any translations, for which a prior translation agreement with Wiley has not been agreed, must prominently display the statement: "This is an unofficial translation of an article that appeared in a Wiley publication. The publisher has not endorsed this translation."

Use by commercial "for-profit" organisations

Use of Wiley Open Access articles for commercial, promotional, or marketing purposes requires further explicit permission from Wiley and will be subject to a fee. Commercial purposes include:

- Copying or downloading of articles, or linking to such articles for further redistribution, sale or licensing;
- Copying, downloading or posting by a site or service that incorporates advertising with such content;
- The inclusion or incorporation of article content in other works or services (other than normal quotations with an appropriate citation) that is then available for sale or licensing, for a fee (for example, a compilation produced for marketing purposes, inclusion in a sales pack)
- Use of article content (other than normal quotations with appropriate citation) by for-profit organisations for promotional purposes
- Linking to article content in e-mails redistributed for promotional, marketing or educational purposes;
- Use for the purposes of monetary reward by means of sale, resale, licence, loan, transfer or other form of commercial exploitation such as marketing products
- Print reprints of Wiley Open Access articles can be purchased from:

corporatesales@wiley.com

Further details can be found on Wiley Online Library
<http://olabout.wiley.com/WileyCDA/Section/id-410895.html>

Other Terms and Conditions:

v1.9

Questions? customercare@copyright.com or +1-855-239-3415 (toll free in the US) or
+1-978-646-2777.

**JOHN WILEY AND SONS LICENSE
TERMS AND CONDITIONS**

Jun 11, 2015

This Agreement between Sara Ghiassian ("You") and John Wiley and Sons ("John Wiley and Sons") consists of your license details and the terms and conditions provided by John Wiley and Sons and Copyright Clearance Center.

License Number	3646261055499
License date	Jun 11, 2015
Licensed Content Publisher	John Wiley and Sons
Licensed Content Publication	Angewandte Chemie International Edition
Licensed Content Title	Protein Modification by Strain-Promoted Alkyne–Nitrone Cycloaddition
Licensed Content Author	Xinghai Ning,Rinske P. Temming,Jan Dommerholt,Jun Guo,Daniel B. Ania,Marjoke F. Debets,Margreet A. Wolfert,Geert-Jan Boons,Floris L. van Delft
Licensed Content Date	Mar 23, 2010
Pages	4
Type of use	Dissertation/Thesis
Requestor type	University/Academic
Format	Print and electronic
Portion	Figure/table
Number of figures/tables	3
Original Wiley figure/table number(s)	Scheme 2
Will you be translating?	No
Title of your thesis / dissertation	Strategies for Photochemical and Thermal Modification of Materials
Expected completion date	Jul 2015
Expected size (number of pages)	300
Requestor Location	Sara Ghiassian 1116 Richmond St London, ON N6A 5B7 Canada Attn: Sara Ghiassian
Billing Type	Invoice
Billing Address	Sara Ghiassian 1116 Richmond St

London, ON N6A 5B7
Canada
Attn: Sara Ghiassian

Total 0.00 USD

[Terms and Conditions](#)

TERMS AND CONDITIONS

This copyrighted material is owned by or exclusively licensed to John Wiley & Sons, Inc. or one of its group companies (each a "Wiley Company") or handled on behalf of a society with which a Wiley Company has exclusive publishing rights in relation to a particular work (collectively "WILEY"). By clicking accept in connection with completing this licensing transaction, you agree that the following terms and conditions apply to this transaction (along with the billing and payment terms and conditions established by the Copyright Clearance Center Inc., ("CCC's Billing and Payment terms and conditions"), at the time that you opened your Rightslink account (these are available at any time at <http://myaccount.copyright.com>).

Terms and Conditions

- The materials you have requested permission to reproduce or reuse (the "Wiley Materials") are protected by copyright.
- You are hereby granted a personal, non-exclusive, non-sub licensable (on a stand-alone basis), non-transferable, worldwide, limited license to reproduce the Wiley Materials for the purpose specified in the licensing process. This license is for a one-time use only and limited to any maximum distribution number specified in the license. The first instance of republication or reuse granted by this licence must be completed within two years of the date of the grant of this licence (although copies prepared before the end date may be distributed thereafter). The Wiley Materials shall not be used in any other manner or for any other purpose, beyond what is granted in the license. Permission is granted subject to an appropriate acknowledgement given to the author, title of the material/book/journal and the publisher. You shall also duplicate the copyright notice that appears in the Wiley publication in your use of the Wiley Material. Permission is also granted on the understanding that nowhere in the text is a previously published source acknowledged for all or part of this Wiley Material. Any third party content is expressly excluded from this permission.
- With respect to the Wiley Materials, all rights are reserved. Except as expressly granted by the terms of the license, no part of the Wiley Materials may be copied, modified, adapted (except for minor reformatting required by the new Publication), translated, reproduced, transferred or distributed, in any form or by any means, and no derivative works may be made based on the Wiley Materials without the prior permission of the respective copyright owner. You may not alter, remove or suppress in any manner any copyright, trademark or other notices displayed by the Wiley Materials. You may not license, rent, sell, loan, lease, pledge, offer as security, transfer or assign the Wiley Materials on a stand-alone basis, or any of the rights granted to you hereunder to any other person.
- The Wiley Materials and all of the intellectual property rights therein shall at all times

remain the exclusive property of John Wiley & Sons Inc, the Wiley Companies, or their respective licensors, and your interest therein is only that of having possession of and the right to reproduce the Wiley Materials pursuant to Section 2 herein during the continuance of this Agreement. You agree that you own no right, title or interest in or to the Wiley Materials or any of the intellectual property rights therein. You shall have no rights hereunder other than the license as provided for above in Section 2. No right, license or interest to any trademark, trade name, service mark or other branding ("Marks") of WILEY or its licensors is granted hereunder, and you agree that you shall not assert any such right, license or interest with respect thereto.

- NEITHER WILEY NOR ITS LICENSORS MAKES ANY WARRANTY OR REPRESENTATION OF ANY KIND TO YOU OR ANY THIRD PARTY, EXPRESS, IMPLIED OR STATUTORY, WITH RESPECT TO THE MATERIALS OR THE ACCURACY OF ANY INFORMATION CONTAINED IN THE MATERIALS, INCLUDING, WITHOUT LIMITATION, ANY IMPLIED WARRANTY OF MERCHANTABILITY, ACCURACY, SATISFACTORY QUALITY, FITNESS FOR A PARTICULAR PURPOSE, USABILITY, INTEGRATION OR NON-INFRINGEMENT AND ALL SUCH WARRANTIES ARE HEREBY EXCLUDED BY WILEY AND ITS LICENSORS AND WAIVED BY YOU
- WILEY shall have the right to terminate this Agreement immediately upon breach of this Agreement by you.
- You shall indemnify, defend and hold harmless WILEY, its Licensors and their respective directors, officers, agents and employees, from and against any actual or threatened claims, demands, causes of action or proceedings arising from any breach of this Agreement by you.
- IN NO EVENT SHALL WILEY OR ITS LICENSORS BE LIABLE TO YOU OR ANY OTHER PARTY OR ANY OTHER PERSON OR ENTITY FOR ANY SPECIAL, CONSEQUENTIAL, INCIDENTAL, INDIRECT, EXEMPLARY OR PUNITIVE DAMAGES, HOWEVER CAUSED, ARISING OUT OF OR IN CONNECTION WITH THE DOWNLOADING, PROVISIONING, VIEWING OR USE OF THE MATERIALS REGARDLESS OF THE FORM OF ACTION, WHETHER FOR BREACH OF CONTRACT, BREACH OF WARRANTY, TORT, NEGLIGENCE, INFRINGEMENT OR OTHERWISE (INCLUDING, WITHOUT LIMITATION, DAMAGES BASED ON LOSS OF PROFITS, DATA, FILES, USE, BUSINESS OPPORTUNITY OR CLAIMS OF THIRD PARTIES), AND WHETHER OR NOT THE PARTY HAS BEEN ADVISED OF THE POSSIBILITY OF SUCH DAMAGES. THIS LIMITATION SHALL APPLY NOTWITHSTANDING ANY FAILURE OF ESSENTIAL PURPOSE OF ANY LIMITED REMEDY PROVIDED HEREIN.
- Should any provision of this Agreement be held by a court of competent jurisdiction to be illegal, invalid, or unenforceable, that provision shall be deemed amended to achieve as nearly as possible the same economic effect as the original provision, and the legality, validity and enforceability of the remaining provisions of this Agreement shall not be affected or impaired thereby.
- The failure of either party to enforce any term or condition of this Agreement shall not

constitute a waiver of either party's right to enforce each and every term and condition of this Agreement. No breach under this agreement shall be deemed waived or excused by either party unless such waiver or consent is in writing signed by the party granting such waiver or consent. The waiver by or consent of a party to a breach of any provision of this Agreement shall not operate or be construed as a waiver of or consent to any other or subsequent breach by such other party.

- This Agreement may not be assigned (including by operation of law or otherwise) by you without WILEY's prior written consent.
- Any fee required for this permission shall be non-refundable after thirty (30) days from receipt by the CCC.
- These terms and conditions together with CCC's Billing and Payment terms and conditions (which are incorporated herein) form the entire agreement between you and WILEY concerning this licensing transaction and (in the absence of fraud) supersedes all prior agreements and representations of the parties, oral or written. This Agreement may not be amended except in writing signed by both parties. This Agreement shall be binding upon and inure to the benefit of the parties' successors, legal representatives, and authorized assigns.
- In the event of any conflict between your obligations established by these terms and conditions and those established by CCC's Billing and Payment terms and conditions, these terms and conditions shall prevail.
- WILEY expressly reserves all rights not specifically granted in the combination of (i) the license details provided by you and accepted in the course of this licensing transaction, (ii) these terms and conditions and (iii) CCC's Billing and Payment terms and conditions.
- This Agreement will be void if the Type of Use, Format, Circulation, or Requestor Type was misrepresented during the licensing process.
- This Agreement shall be governed by and construed in accordance with the laws of the State of New York, USA, without regards to such state's conflict of law rules. Any legal action, suit or proceeding arising out of or relating to these Terms and Conditions or the breach thereof shall be instituted in a court of competent jurisdiction in New York County in the State of New York in the United States of America and each party hereby consents and submits to the personal jurisdiction of such court, waives any objection to venue in such court and consents to service of process by registered or certified mail, return receipt requested, at the last known address of such party.

WILEY OPEN ACCESS TERMS AND CONDITIONS

Wiley Publishes Open Access Articles in fully Open Access Journals and in Subscription journals offering Online Open. Although most of the fully Open Access journals publish open access articles under the terms of the Creative Commons Attribution (CC BY) License only, the subscription journals and a few of the Open Access Journals offer a choice of

Creative Commons Licenses:: Creative Commons Attribution (CC-BY) license [Creative Commons Attribution Non-Commercial \(CC-BY-NC\) license](#) and [Creative Commons Attribution Non-Commercial-NoDerivs \(CC-BY-NC-ND\) License](#). The license type is clearly identified on the article.

Copyright in any research article in a journal published as Open Access under a Creative Commons License is retained by the author(s). Authors grant Wiley a license to publish the article and identify itself as the original publisher. Authors also grant any third party the right to use the article freely as long as its integrity is maintained and its original authors, citation details and publisher are identified as follows: [Title of Article/Author/Journal Title and Volume/Issue. Copyright (c) [year] [copyright owner as specified in the Journal]. Links to the final article on Wiley's website are encouraged where applicable.

The Creative Commons Attribution License

The [Creative Commons Attribution License \(CC-BY\)](#) allows users to copy, distribute and transmit an article, adapt the article and make commercial use of the article. The CC-BY license permits commercial and non-commercial re-use of an open access article, as long as the author is properly attributed.

The Creative Commons Attribution License does not affect the moral rights of authors, including without limitation the right not to have their work subjected to derogatory treatment. It also does not affect any other rights held by authors or third parties in the article, including without limitation the rights of privacy and publicity. Use of the article must not assert or imply, whether implicitly or explicitly, any connection with, endorsement or sponsorship of such use by the author, publisher or any other party associated with the article.

For any reuse or distribution, users must include the copyright notice and make clear to others that the article is made available under a Creative Commons Attribution license, linking to the relevant Creative Commons web page.

To the fullest extent permitted by applicable law, the article is made available as is and without representation or warranties of any kind whether express, implied, statutory or otherwise and including, without limitation, warranties of title, merchantability, fitness for a particular purpose, non-infringement, absence of defects, accuracy, or the presence or absence of errors.

Creative Commons Attribution Non-Commercial License

The [Creative Commons Attribution Non-Commercial \(CC-BY-NC\) License](#) permits use, distribution and reproduction in any medium, provided the original work is properly cited and is not used for commercial purposes.(see below)

Creative Commons Attribution-Non-Commercial-NoDerivs License

The [Creative Commons Attribution Non-Commercial-NoDerivs License](#) (CC-BY-NC-ND) permits use, distribution and reproduction in any medium, provided the original work is properly cited, is not used for commercial purposes and no modifications or adaptations are made. (see below)

Use by non-commercial users

For non-commercial and non-promotional purposes, individual users may access, download, copy, display and redistribute to colleagues Wiley Open Access articles, as well as adapt, translate, text- and data-mine the content subject to the following conditions:

- The authors' moral rights are not compromised. These rights include the right of "paternity" (also known as "attribution" - the right for the author to be identified as such) and "integrity" (the right for the author not to have the work altered in such a way that the author's reputation or integrity may be impugned).
- Where content in the article is identified as belonging to a third party, it is the obligation of the user to ensure that any reuse complies with the copyright policies of the owner of that content.
- If article content is copied, downloaded or otherwise reused for non-commercial research and education purposes, a link to the appropriate bibliographic citation (authors, journal, article title, volume, issue, page numbers, DOI and the link to the definitive published version on **Wiley Online Library**) should be maintained. Copyright notices and disclaimers must not be deleted.
- Any translations, for which a prior translation agreement with Wiley has not been agreed, must prominently display the statement: "This is an unofficial translation of an article that appeared in a Wiley publication. The publisher has not endorsed this translation."

Use by commercial "for-profit" organisations

Use of Wiley Open Access articles for commercial, promotional, or marketing purposes requires further explicit permission from Wiley and will be subject to a fee. Commercial purposes include:

- Copying or downloading of articles, or linking to such articles for further redistribution, sale or licensing;
- Copying, downloading or posting by a site or service that incorporates advertising with such content;
- The inclusion or incorporation of article content in other works or services (other than normal quotations with an appropriate citation) that is then available for sale or licensing, for a fee (for example, a compilation produced for marketing purposes, inclusion in a sales pack)
- Use of article content (other than normal quotations with appropriate citation) by for-profit organisations for promotional purposes
- Linking to article content in e-mails redistributed for promotional, marketing or educational purposes;
- Use for the purposes of monetary reward by means of sale, resale, licence, loan, transfer or other form of commercial exploitation such as marketing products
- Print reprints of Wiley Open Access articles can be purchased from:

corporatesales@wiley.com

Further details can be found on Wiley Online Library
<http://olabout.wiley.com/WileyCDA/Section/id-410895.html>

Other Terms and Conditions:

v1.9

Questions? customercare@copyright.com or +1-855-239-3415 (toll free in the US) or
+1-978-646-2777.

**NRC RESEARCH PRESS LICENSE
TERMS AND CONDITIONS**

Jun 11, 2015

This is a License Agreement between Sara Ghiassian ("You") and NRC Research Press ("NRC Research Press") provided by Copyright Clearance Center ("CCC"). The license consists of your order details, the terms and conditions provided by NRC Research Press, and the payment terms and conditions.

All payments must be made in full to CCC. For payment instructions, please see information listed at the bottom of this form.

License Number	3646270027637
License date	Jun 11, 2015
Licensed content publisher	NRC Research Press
Licensed content publication	Canadian Journal of Chemistry
Licensed content title	Synthesis of small water-soluble diazirine-functionalized gold nanoparticles and their photochemical modification
Licensed content author	Sara Ghiassian, Mark C. Biesinger, Mark S. Workentin
Licensed content date	Jan 1, 2015
Volume number	93
Issue number	1
Type of Use	Thesis/Dissertation
Requestor type	Author (original work)
Format	Print and electronic
Portion	Full article
Order reference number	None
Title of your thesis / dissertation	Strategies for Photochemical and Thermal Modification of Materials
Expected completion date	Jul 2015
Estimated size(pages)	300
Total	0.00 USD
Terms and Conditions	

General Terms & Conditions

Permission is granted upon the requester's compliance with the following terms and conditions:

1. A credit line will be prominently placed in your product(s) and include: for books the author, book title, editor, copyright holder, year of publication; for journals the author, title of article, title of journal, volume number, issue number, and the inclusive pages. The credit line must include the following wording: "© 2008 Canadian Science Publishing or its licensors. Reproduced with permission," except when an author of an original article published in 2009

or later is reproducing his/her own work.

2. The requester warrants that the material shall not be used in any manner that may be derogatory to the title, content, or authors of the material or to Canadian Science Publishing, including but not limited to an association with conduct that is fraudulent or otherwise illegal.
3. Permission is granted for the term (for Books/CDs-Shelf Life; for Internet/Intranet-In perpetuity; for all other forms of print-the life of the title) and purpose specified in your request. Once term has expired, permission to renew must be made in writing.
4. Permission granted is nonexclusive, and is valid throughout the world in English and the languages specified in your original request. A new permission must be requested for revisions of the publication under current consideration.
5. Canadian Science Publishing cannot supply the requester with the original artwork or a "clean copy."
6. If the Canadian Science Publishing material is to be translated, the following lines must be included: The authors, editors, and Canadian Science Publishing are not responsible for errors or omissions in translations.

v1.4

Questions? customercare@copyright.com or +1-855-239-3415 (toll free in the US) or +1-978-646-2777.



RightsLink®

Home

Account Info

Help



ACS Publications
Most Trusted. Most Cited. Most Read.

Title: Photoinduced Carbene Generation from Diazirine Modified Task Specific Phosphonium Salts To Prepare Robust Hydrophobic Coatings
Author: Sara Ghiassian, Hossein Ismaili, Brett D. W. Lubbock, et al
Publication: Langmuir
Publisher: American Chemical Society
Date: Aug 1, 2012
Copyright © 2012, American Chemical Society

Logged in as:
Sara Ghiassian
Account #:
3000927211

LOGOUT

PERMISSION/LICENSE IS GRANTED FOR YOUR ORDER AT NO CHARGE

This type of permission/license, instead of the standard Terms & Conditions, is sent to you because no fee is being charged for your order. Please note the following:

- Permission is granted for your request in both print and electronic formats, and translations.
- If figures and/or tables were requested, they may be adapted or used in part.
- Please print this page for your records and send a copy of it to your publisher/graduate school.
- Appropriate credit for the requested material should be given as follows: "Reprinted (adapted) with permission from (COMPLETE REFERENCE CITATION). Copyright (YEAR) American Chemical Society." Insert appropriate information in place of the capitalized words.
- One-time permission is granted only for the use specified in your request. No additional uses are granted (such as derivative works or other editions). For any other uses, please submit a new request.

BACK

CLOSE WINDOW

Copyright © 2015 Copyright Clearance Center, Inc. All Rights Reserved. [Privacy statement](#). [Terms and Conditions](#). Comments? We would like to hear from you. E-mail us at customer care@copyright.com

**JOHN WILEY AND SONS LICENSE
TERMS AND CONDITIONS**

Aug 10, 2015

This Agreement between Sara Ghiassian ("You") and John Wiley and Sons ("John Wiley and Sons") consists of your license details and the terms and conditions provided by John Wiley and Sons and Copyright Clearance Center.

License Number	3685460579539
License date	Aug 10, 2015
Licensed Content Publisher	John Wiley and Sons
Licensed Content Publication	European Journal of Organic Chemistry
Licensed Content Title	Water-Soluble Maleimide-Modified Gold Nanoparticles (AuNPs) as a Platform for Cycloaddition Reactions
Licensed Content Author	Sara Ghiassian, Pierangelo Gobbo, Mark S. Workentin
Licensed Content Date	Jul 20, 2015
Pages	1
Type of use	Dissertation/Thesis
Requestor type	Author of this Wiley article
Format	Electronic
Portion	Full article
Will you be translating?	No
Title of your thesis / dissertation	Strategies for photochemical and thermal modification of materials
Expected completion date	Aug 2015
Expected size (number of pages)	300
Requestor Location	Sara Ghiassian 1116 Richmond St London, ON N6A 5B7 Canada Attn: Sara Ghiassian
Billing Type	Invoice
Billing Address	Sara Ghiassian 1116 Richmond St London, ON N6A 5B7 Canada Attn: Sara Ghiassian
Total	0.00 CAD
Terms and Conditions	

TERMS AND CONDITIONS

This copyrighted material is owned by or exclusively licensed to John Wiley & Sons, Inc. or one of its group companies (each a "Wiley Company") or handled on behalf of a society with which a Wiley Company has exclusive publishing rights in relation to a particular work (collectively "WILEY"). By clicking accept in connection with completing this

licensing transaction, you agree that the following terms and conditions apply to this transaction (along with the billing and payment terms and conditions established by the Copyright Clearance Center Inc., ("CCC's Billing and Payment terms and conditions"), at the time that you opened your Rightslink account (these are available at any time at <http://myaccount.copyright.com>).

Terms and Conditions

- The materials you have requested permission to reproduce or reuse (the "Wiley Materials") are protected by copyright.
- You are hereby granted a personal, non-exclusive, non-sub licensable (on a stand-alone basis), non-transferable, worldwide, limited license to reproduce the Wiley Materials for the purpose specified in the licensing process. This license is for a one-time use only and limited to any maximum distribution number specified in the license. The first instance of republication or reuse granted by this licence must be completed within two years of the date of the grant of this licence (although copies prepared before the end date may be distributed thereafter). The Wiley Materials shall not be used in any other manner or for any other purpose, beyond what is granted in the license. Permission is granted subject to an appropriate acknowledgement given to the author, title of the material/book/journal and the publisher. You shall also duplicate the copyright notice that appears in the Wiley publication in your use of the Wiley Material. Permission is also granted on the understanding that nowhere in the text is a previously published source acknowledged for all or part of this Wiley Material. Any third party content is expressly excluded from this permission.
- With respect to the Wiley Materials, all rights are reserved. Except as expressly granted by the terms of the license, no part of the Wiley Materials may be copied, modified, adapted (except for minor reformatting required by the new Publication), translated, reproduced, transferred or distributed, in any form or by any means, and no derivative works may be made based on the Wiley Materials without the prior permission of the respective copyright owner. You may not alter, remove or suppress in any manner any copyright, trademark or other notices displayed by the Wiley Materials. You may not license, rent, sell, loan, lease, pledge, offer as security, transfer or assign the Wiley Materials on a stand-alone basis, or any of the rights granted to you hereunder to any other person.
- The Wiley Materials and all of the intellectual property rights therein shall at all times remain the exclusive property of John Wiley & Sons Inc, the Wiley Companies, or their respective licensors, and your interest therein is only that of having possession of and the right to reproduce the Wiley Materials pursuant to Section 2 herein during the continuance of this Agreement. You agree that you own no right, title or interest in or to the Wiley Materials or any of the intellectual property rights therein. You shall have no rights hereunder other than the license as provided for above in Section 2. No right, license or interest in any trademark, trade name, service mark or other branding ("Marks") of WILEY or its licensors is granted hereunder, and you agree that you shall not assert any such right, license or interest with respect thereto.
- NEITHER WILEY NOR ITS LICENSORS MAKES ANY WARRANTY OR REPRESENTATION OF ANY KIND TO YOU OR ANY THIRD PARTY, EXPRESS, IMPLIED OR STATUTORY, WITH RESPECT TO THE MATERIALS OR THE ACCURACY OF ANY INFORMATION CONTAINED IN THE MATERIALS, INCLUDING, WITHOUT LIMITATION, ANY IMPLIED WARRANTY OF MERCHANTABILITY, ACCURACY, SATISFACTORY QUALITY, FITNESS FOR A

PARTICULAR PURPOSE, USABILITY, INTEGRATION OR NON-INFRINGEMENT AND ALL SUCH WARRANTIES ARE HEREBY EXCLUDED BY WILEY AND ITS LICENSORS AND WAIVED BY YOU

- WILEY shall have the right to terminate this Agreement immediately upon breach of this Agreement by you.
- You shall indemnify, defend and hold harmless WILEY, its Licensors and their respective directors, officers, agents and employees, from and against any actual or threatened claims, demands, causes of action or proceedings arising from any breach of this Agreement by you.
- IN NO EVENT SHALL WILEY OR ITS LICENSORS BE LIABLE TO YOU OR ANY OTHER PARTY OR ANY OTHER PERSON OR ENTITY FOR ANY SPECIAL, CONSEQUENTIAL, INCIDENTAL, INDIRECT, EXEMPLARY OR PUNITIVE DAMAGES, HOWEVER CAUSED, ARISING OUT OF OR IN CONNECTION WITH THE DOWNLOADING, PROVISIONING, VIEWING OR USE OF THE MATERIALS REGARDLESS OF THE FORM OF ACTION, WHETHER FOR BREACH OF CONTRACT, BREACH OF WARRANTY, TORT, NEGLIGENCE, INFRINGEMENT OR OTHERWISE (INCLUDING, WITHOUT LIMITATION, DAMAGES BASED ON LOSS OF PROFITS, DATA, FILES, USE, BUSINESS OPPORTUNITY OR CLAIMS OF THIRD PARTIES), AND WHETHER OR NOT THE PARTY HAS BEEN ADVISED OF THE POSSIBILITY OF SUCH DAMAGES. THIS LIMITATION SHALL APPLY NOTWITHSTANDING ANY FAILURE OF ESSENTIAL PURPOSE OF ANY LIMITED REMEDY PROVIDED HEREIN.
- Should any provision of this Agreement be held by a court of competent jurisdiction to be illegal, invalid, or unenforceable, that provision shall be deemed amended to achieve as nearly as possible the same economic effect as the original provision, and the legality, validity and enforceability of the remaining provisions of this Agreement shall not be affected or impaired thereby.
- The failure of either party to enforce any term or condition of this Agreement shall not constitute a waiver of either party's right to enforce each and every term and condition of this Agreement. No breach under this agreement shall be deemed waived or excused by either party unless such waiver or consent is in writing signed by the party granting such waiver or consent. The waiver by or consent of a party to a breach of any provision of this Agreement shall not operate or be construed as a waiver of or consent to any other or subsequent breach by such other party.
- This Agreement may not be assigned (including by operation of law or otherwise) by you without WILEY's prior written consent.
- Any fee required for this permission shall be non-refundable after thirty (30) days from receipt by the CCC.
- These terms and conditions together with CCC's Billing and Payment terms and conditions (which are incorporated herein) form the entire agreement between you and WILEY concerning this licensing transaction and (in the absence of fraud) supersedes all prior agreements and representations of the parties, oral or written. This Agreement may not be amended except in writing signed by both parties. This Agreement shall be binding upon and inure to the benefit of the parties' successors, legal representatives, and authorized assigns.

- In the event of any conflict between your obligations established by these terms and conditions and those established by CCC's Billing and Payment terms and conditions, these terms and conditions shall prevail.
- WILEY expressly reserves all rights not specifically granted in the combination of (i) the license details provided by you and accepted in the course of this licensing transaction, (ii) these terms and conditions and (iii) CCC's Billing and Payment terms and conditions.
- This Agreement will be void if the Type of Use, Format, Circulation, or Requestor Type was misrepresented during the licensing process.
- This Agreement shall be governed by and construed in accordance with the laws of the State of New York, USA, without regards to such state's conflict of law rules. Any legal action, suit or proceeding arising out of or relating to these Terms and Conditions or the breach thereof shall be instituted in a court of competent jurisdiction in New York County in the State of New York in the United States of America and each party hereby consents and submits to the personal jurisdiction of such court, waives any objection to venue in such court and consents to service of process by registered or certified mail, return receipt requested, at the last known address of such party.

WILEY OPEN ACCESS TERMS AND CONDITIONS

Wiley Publishes Open Access Articles in fully Open Access Journals and in Subscription journals offering Online Open. Although most of the fully Open Access journals publish open access articles under the terms of the Creative Commons Attribution (CC BY) License only, the subscription journals and a few of the Open Access Journals offer a choice of Creative Commons Licenses:: Creative Commons Attribution (CC-BY) license [Creative Commons Attribution Non-Commercial \(CC-BY-NC\) license](#) and [Creative Commons Attribution Non-Commercial-NoDerivs \(CC-BY-NC-ND\) License](#). The license type is clearly identified on the article.

Copyright in any research article in a journal published as Open Access under a Creative Commons License is retained by the author(s). Authors grant Wiley a license to publish the article and identify itself as the original publisher. Authors also grant any third party the right to use the article freely as long as its integrity is maintained and its original authors, citation details and publisher are identified as follows: [Title of Article/Author/Journal Title and Volume/Issue. Copyright (c) [year] [copyright owner as specified in the Journal]. Links to the final article on Wiley's website are encouraged where applicable.

The Creative Commons Attribution License

The [Creative Commons Attribution License \(CC-BY\)](#) allows users to copy, distribute and transmit an article, adapt the article and make commercial use of the article. The CC-BY license permits commercial and non-commercial re-use of an open access article, as long as the author is properly attributed.

The Creative Commons Attribution License does not affect the moral rights of authors, including without limitation the right not to have their work subjected to derogatory treatment. It also does not affect any other rights held by authors or third parties in the article, including without limitation the rights of privacy and publicity. Use of the article must not assert or imply, whether implicitly or explicitly, any connection with, endorsement or sponsorship of such use by the author, publisher or any other party associated with the article.

For any reuse or distribution, users must include the copyright notice and make clear to others that the article is made available under a Creative Commons Attribution license, linking to the relevant Creative Commons web page.

To the fullest extent permitted by applicable law, the article is made available as is and without representation or warranties of any kind whether express, implied, statutory or otherwise and including, without limitation, warranties of title, merchantability, fitness for a particular purpose, non-infringement, absence of defects, accuracy, or the presence or absence of errors.

Creative Commons Attribution Non-Commercial License

The [Creative Commons Attribution Non-Commercial \(CC-BY-NC\) License](#) permits use, distribution and reproduction in any medium, provided the original work is properly cited and is not used for commercial purposes.(see below)

Creative Commons Attribution-Non-Commercial-NoDerivs License

The [Creative Commons Attribution Non-Commercial-NoDerivs License](#) (CC-BY-NC-ND) permits use, distribution and reproduction in any medium, provided the original work is properly cited, is not used for commercial purposes and no modifications or adaptations are made. (see below)

Use by non-commercial users

For non-commercial and non-promotional purposes, individual users may access, download, copy, display and redistribute to colleagues Wiley Open Access articles, as well as adapt, translate, text- and data-mine the content subject to the following conditions:

- The authors' moral rights are not compromised. These rights include the right of "paternity" (also known as "attribution" - the right for the author to be identified as such) and "integrity" (the right for the author not to have the work altered in such a way that the author's reputation or integrity may be impugned).
- Where content in the article is identified as belonging to a third party, it is the obligation of the user to ensure that any reuse complies with the copyright policies of the owner of that content.
- If article content is copied, downloaded or otherwise reused for non-commercial research and education purposes, a link to the appropriate bibliographic citation (authors, journal, article title, volume, issue, page numbers, DOI and the link to the definitive published version on **Wiley Online Library**) should be maintained. Copyright notices and disclaimers must not be deleted.
- Any translations, for which a prior translation agreement with Wiley has not been agreed, must prominently display the statement: "This is an unofficial translation of an article that appeared in a Wiley publication. The publisher has not endorsed this translation."

Use by commercial "for-profit" organisations

Use of Wiley Open Access articles for commercial, promotional, or marketing purposes requires further explicit permission from Wiley and will be subject to a fee. Commercial purposes include:

- Copying or downloading of articles, or linking to such articles for further

redistribution, sale or licensing;

- Copying, downloading or posting by a site or service that incorporates advertising with such content;
- The inclusion or incorporation of article content in other works or services (other than normal quotations with an appropriate citation) that is then available for sale or licensing, for a fee (for example, a compilation produced for marketing purposes, inclusion in a sales pack)
- Use of article content (other than normal quotations with appropriate citation) by for-profit organisations for promotional purposes
- Linking to article content in e-mails redistributed for promotional, marketing or educational purposes;
- Use for the purposes of monetary reward by means of sale, resale, licence, loan, transfer or other form of commercial exploitation such as marketing products
- Print reprints of Wiley Open Access articles can be purchased from:
corporatesales@wiley.com

Further details can be found on Wiley Online Library <http://olabout.wiley.com/WileyCDA/Section/id-410895.html>

Other Terms and Conditions:

v1.9

Questions? customercare@copyright.com or +1-855-239-3415 (toll free in the US) or +1-978-646-2777.

Curriculum Vitae

Sara Ghiassian

Department of Chemistry
The University of Western Ontario

EDUCATION

- **Ph.D. in Organic Chemistry**, University of Western Ontario, London, ON, Canada (2010-present)
- **M.Sc. in Organic Chemistry**, Sharif University of Technology, Tehran, Iran (2008-2010)
- **B.Sc in Chemistry (*with Honours*)**, Sharif University of Technology, Tehran, Iran (2003-2007)

RELEVANT WORK EXPERIENCE

- **Graduate Research Assistant**, Department of Chemistry, University of Western Ontario (2010-Present)
- **Teaching Assistant**, Department of Chemistry, University of Western Ontario (2010-Present)
 - Laboratory Teaching Assistant for Organic Chemistry for Life Sciences
 - Laboratory Teaching Assistant for Organic Chemistry of Biological Molecules
 - Tutorial Teaching Assistant for Organic Chemistry
- **Graduate Research Assistant**, Department of Chemistry, Sharif University of Technology (2008-2010)

AWARDS AND SCHOLORSHIPS

- Western Graduate Research Scholarship (WGRS), (2011-Present)
- International Graduate Student Scholarship (2010-2014)

SELECTED PUBLICATIONS

Articles in Peer-Reviewed Journals

1. "Nitrene Modified Gold Nanoparticles: Synthesis, Characterization and Their Potential for the Development of ^{18}F -Labeled PET Probes" **S. Ghiassian**, A. Nazemi, L. Yu, L. G. Luyt, and M. S. Workentin, in preparation.
2. "Strain-Promoted Alkyne-Nitrene Cycloaddition (i-SPAN) for the Preparation of Hybrid Materials" **S. Ghiassian**, A. Nazemi, E. R. Gillies, and M. S. Workentin, in preparation.
3. "Water-Soluble Maleimide Modified Gold Nanoparticles (AuNPs) as a Platform for Cycloaddition Reactions" **S. Ghiassian**, P. Gobbo, and M. S. Workentin, accepted to *Eur. J. Org. Chem.* DOI: 10.1002/ejoc.201500685.
4. "Synthesis of Small Water-Soluble Diazirine-Functionalized Gold Nanoparticles and Their Photochemical Modification" **S. Ghiassian**, M. C. Biesinger, and M. S. Workentin, *Can. J. Chem.* 93, 98-105 (2014).
5. "Electrochemistry of Robust Gold Nanoparticle-Glassy Carbon Hybrids Generated Using a Patternable Photochemical Approach" P. Gobbo, **S. Ghiassian**, M. Hesari, K. G. Stamplecoskie, N. Kazemi-Zanjani, F. Lagugné-Labarthe, and M. S. Workentin, *J. Mater. Chem.* 22, 23971-23980 (2012).
6. "Photoinduced Carbene Generation from Diazirine Modified Task Specific Phosphonium Salts to Prepare Robust Hydrophobic Coatings" **S. Ghiassian**, H. Ismaili, B. D. W. Lubbock, J. W. Dube, P. J. Ragogna, and M. S. Workentin, *Langmuir* 28, 12326-12333 (2012).
7. "Heterogeneously Catalysed Strecker-Type Reactions Using Supported Co(II) Catalysts: Microwave vs. Conventional Heating" F. Rajabi, S. Nourian, **S. Ghiassian**, A. M. Balu, M. R. Saidi, J. C. Serrano-Ruiz, R. Luque, *Green Chem.* 13, 3282-3289 (2011).
8. "Efficient Co(II) Heterogeneously Catalysed Synthesis of α -Aminonitriles at Room Temperature via Strecker-Type Reactions, F. Rajabi, **S. Ghiassian**, M. R. Saidi, *Green Chem.* 12, 1349-1352 (2010).

Conference Proceedings and Presentations: (Presenting author in bold)

1. Rapid and Efficient Gold Nanoparticle Modification Using Interfacial Strain Promoted Alkyne-Nitrene Cycloaddition (i-SPAN) Reaction, **S. Ghiassian**, A.

- Nazemi, P. Gobbo, L. Yu, E. R. Gillies, L. G. Luyt, M. S. Workentin, 42nd Physical Organic Mini-Symposium (POMS), Hamilton ON, (2014), Oral presentation.
2. Thermal and Photochemical Modification of Small Water Soluble Gold Nanoparticles, **S. Ghiassian** and M. S. Workentin, *97th Canadian Chemistry Conference and Exhibition*, Vancouver, BC, (2014), Oral presentation.
 3. Synthesis of Small Water-Soluble Diazirine-functionalized Gold Nanoparticles for Biological Applications, **S. Ghiassian** and M. S. Workentin, *Surface Canada*, London, ON, (2013), Poster.
 4. Photoinduced Carbene Generation From Diazirine Modified Phosphonium Salts To Prepare Robust Hydrophobic Coatings, **S. Ghiassian**, H. Ismaili, B. D. W. Lubbock, J. W. Dube, P. J. Ragona and M. S. Workentin, *95th Canadian Chemistry Conference and Exhibition*, Calgary, AB, (2012), Oral presentation.
 5. Method to Covalently Functionalize Glassy Carbon Electrode Surfaces With Gold Nanoparticles through Photolysis of Interfacial diazirine Functionalities, **P. Gobbo**, S. Ghiassian, M. Hesari, K. G. Stamplecoskie, N. Kazemi-Zanjani, F. Laguné-Labartheta, and M. S. Workentin, *95th Canadian Chemistry Conference and Exhibition*, Calgary, AB, (2012), Oral presentation.
 6. Photoinduced Carbene Generation From Diazirine Modified Phosphonium Salts To Prepare Robust Hydrophobic Coatings, **S. Ghiassian**, H. Ismaili, B. D. W. Lubbock, J. W. Dube, P. J. Ragona and M. S. Workentin, 39th Physical Organic Mini-Symposium (POMS), London, ON, (2011), Oral presentation.